# Energy efficiency optimisation of wastewater treatment: study of ATAD

Jamie Rojas Hernandez


UNIVERSITY *of* LIMERICK

OLLSCOIL LUIMNIGH

# Energy Efficiency Optimisation of Wastewater Treatment: Study of ATAD

*A thesis submitted for the degree of*

Doctor of Philosophy

*by*

Jaime Rojas Hernandez

University of Limerick

Supervised by Toshko Zhelev

Submitted to the University of Limerick, October, 2011

# Abstract

The aim of this investigation was to minimise the energy requirement of autothermal thermophilic aerobic digestion (ATAD) systems while complying with treatment objectives. Due to the discontinuous, semi-batch nature of the ATAD reaction, these systems have to be optimised via dynamic optimisation. To this end, two dynamic ATAD models were developed: ATM1 and ATM2. These models have the novel and unique feature that they are capable of quantifying the two treatment objectives, i.e., stabilisation and pasteurisation. Thereby, they are also able to determine the minimum energy requirement needed to satisfy legal standards.

Simulation studies were carried out to examine model behaviour of different ATAD systems at start-up and steady state operation. Overall, the behaviour observed in the simulations was in good qualitative agreement with the behaviour of full-scale plants. In an asymptotic analysis of the ATM1 model, the general, qualitative structure of the solution was studied. The structure is composed of a number of regions which are limited by different factors: first by the availability of dissolved oxygen, second by readily biodegradable substrate, and finally by slowly biodegradable substrate. The structure of the solution can explain the qualitative behaviour of respirometric curves of ATAD systems. A global sensitivity analysis was carried out to identify the model parameters with the strongest influence on energy requirement and plant capacity. In this context, it was found that reactor volume, aeration flowrate, reaction time, loading time, and volume replaced after each batch were the most significant parameters. It was also found that the ATAD reaction is generally limited by the stabilisation process. A general relation of inverse proportionality was found between energy requirement and plant capacity, which holds for other wastewater and sludge treatment processes. The potential implications of this finding are yet to be explored. A model assessment of ATM1 was carried out, indicating a good qualitative agreement between data and simulations. Nonetheless, there exists room for improvement in quantitative terms.

The optimisation problem was then formulated within the framework of the direct sequential approach and it was solved for a single-stage (CS1) and a two-stage (CS2) system. After optimisation, their energy requirement had been reduced by 23 and 18%, respectively. An even better solution (with 42% reduction) was found for CS2 by assuming a pre-dewatering stage and treating the remaining sludge in the first-stage reactor. Finally, a tentative framework for dynamic optimisation of ATAD within the direct simultaneous approach was proposed. The optimisation problem was reformulated. Even though the problem was not solved, simulations studies pointed out some of the difficulties of implementing and solving this problem and their potential solutions. In the future, the latter framework shall prove useful for the structural optimisation of ATAD systems.

Optimisation is rarely used in wastewater engineering. Given the high, rising cost of wastewater treatment, optimisation should become the norm for design and operation of wastewater treatment plants.

# Declaration

I, Jaime Rojas Hernandez, hereby declare that this thesis is my own work and effort and that it has not been concurrently submitted in candidature of any other award or degree. Where other sources of information have been used, they have been acknowledged.

Jaime Rojas Hernandez

October 4, 2011

*To all humanity.*

# Acknowledgements

My first thought goes to my family: my parents, my brother, and my sister. They have always been there for me. Unconditionally. Without their care and support I would not be who I am. My love and gratitude go to them.

I am also indebted to my supervisor Toshko Zhelev. He gave me the freedom to pursue my own ideas, always offering supportive and critical advice. I admired his sincerity. He broadened my thinking and encouraged me to engage in collaborative work that, against my initial will and expectations, turned out to be very fruitful. Thank you.

I wish to acknowledge the work of the Master and Final Year Project students that I co-supervised, especially that of Pedro Afanador Castillo and Roberto Loi. Their intensity and our many discussions helped to answer old questions and gave rise to new ones.

I am very grateful to Seamus McMonagle and Tony Pembroke who always found some time to meet me and answer my questions. To Tony Pembroke I also wish to express my heartfelt gratitude for taking the responsibility of organising the *viva voce* examination after Toshko sadly passed away.

I express my gratitude to Edin Omerdic who gave me and other CPI students a series of valuable programming seminars at the beginning of our research. These seminars proved very helpful for my later research.

My thanks go also to Aaron Bojarski. During my stay at UPC in Barcelona, we had the opportunity to work together and to develop several ideas. Our joint work I deem very fruitful.

Over the course of this research, I had the fortune to meet my colleague and friend Elisabet Capon Garcia. Such openness and integrity I have rarely found. Together, we set out to explore some of the most complex issues of process engineering, such as structural optimisation and orthogonal collocation. Even though our joint work is unfinished and has not seen the light, our discussions were the germ of some of the insights presented in this thesis. She also helped me to correct the thesis.

A big thank you goes also to other members of the scientific community (too many to be mentioned) who kindly and keenly replied to my inquisitive emails. Special thanks go to Robert Kovacs, Lorenz T. Biegler, and Julio Banga.

I am very grateful for the continuous support of the operators and engineers at our case study plants, Jairo Gomez (NILSA, Navarra, Spain) and Louie O'Keeffe (Killarney Wastewater Treatment Works, Co. Kerry, Ireland). They provided me with all the data I asked for, and took the time (more than once) to guide me through the plants and explain their functioning in detail. In return, I hope that they will find useful the outcomes of this study.

I also wish to gratefully acknowledge the generous financial support of Charles Parsons Initiative and Science Foundation Ireland. It is my believe and desire that the taxpayer's money that has made this investigation possible has been turned into a valuable contribution. I have made all within my reach to make that happen. This publication has emanated from research conducted with the financial support of Science Foundation of Ireland under Grant No. 06/CP/E007.

# Contents

# List of Figures

# List of Tables

# List of Abbreviations

| | |
|---|---|
| **ASM** | Activated sludge model |
| **ASM1** | Activated sludge model no. 1 |
| **ATAD** | Autothermal thermophilic aerobic digestion |
| **ATM1** | ATAD model no. 1 |
| **ATM2** | ATAD model no. 2 |
| **COD** | Chemical oxygen demand |
| **CS1** | Case study 1 |
| **CS2** | Case study 2 |
| **CVP** | Control vector parameterization |
| **DAE** | Differential-algebraic equation |
| **DO** | Dissolved oxygen |
| **eSS** | Enhanced scatter search |
| **HJB** | Hamilton-Jacobi-Bellman |
| **HRT** | Hydraulic retention time |
| **IAWPRC** | International association on water pollution research and control |
| **IWA** | International water association |
| **MAE** | Mean absolute error |
| **NLP** | Nonlinear programming |

| | |
|---|---|
| **OC** | Orthogonal collocation |
| **ODE** | Ordinary differential equation |
| **ORP** | Oxidation reduction potential |
| **OUR** | Oxygen uptake rate |
| **PCC** | Partial correlation coefficient |
| **PFRP** | Process to further reduce pathogens |
| **PMP** | Pontryagin's minimum principle |
| **RK** | Runge Kutta |
| **SEM** | Scanning electron microscope |
| **SQP** | Sequential quadratic programming |
| **SRC** | Standardised regression coefficient |
| **TS** | Total solids |
| **TVS** | Total volatile solids |
| **VS** | Volatile solids |
| **vvh** | volume of air per volume of sludge per hour |

# Nomenclature

$\alpha, \beta$ Substrate and oxygen transformation coefficients (dimensionless)

$\delta$ Accelerating rate of activation (dimensionless)

$\delta_i, \theta_i$ Dimensionless parameters (dimensionless)

$\dot{m}_{in}, \dot{m}_{out}$ Influent and effluent gravimetric sludge flowrates (kg/day)

$\eta$ Coefficient of heat utilisation (dimensionless)

$\lambda$ Heat production (°C· l/g)

$\mu$ Maximum specific growth rate (1/day)

$\mu_{S,P}$ Activation rate (1/day)

$\nu_{ij}$ Stoichiometric coefficient of process $j$ on component $i$ (dimensionless)

$\rho_j$ Rate of process $j$ (g/(l· day))

$\tau$ Dynamic residence time (days)

$\vec{u}$ Control variable

$A_l, A_g$ Surface area of liquid and gas phase ($m^2$)

$b$ specific decay rate (1/day)

$c_m, c_V$ Gravimetric and volumetric plant capacity (kg/day, $m^3$/day)

$C_P$ Specific heat capacity (kJ/(kg·°C))

$D$ Contact time (days)

$E_m, E_V$ Gravimetric and volumetric energy requirement (kWh/kg, kWh/m$^3$)

$f_P$ Fraction of biomass yielding particulate products (dimensionless)

$f_{COD}$ Conversion factor between COD and VS (g of COD per g of VS)

$H$ Enthalpy of liquid phase (MJ)

$In(\cdot), Ou(\cdot)$ Influent and effluent advective terms

$K_a$ Aerator-specific parameter (1/vv)

$K_O$ Half-velocity constant for $S_O$ (mg/l)

$K_S$ Half-velocity constant for $S_S$ (g/l)

$k_S$ Specific hydrolysis rate (1/day)

$K_w all$ Heat transfer coefficient of reactor walls (kW/(m$^2$·°C))

$K_X$ Half-velocity constant for hydrolysis (dimensionless)

$L$ Lethality (dimensionless)

$L_i$ Latent heat of evaporation (kJ/kg)

$m_{in}$ Mass of influent VS (kg)

$n_b$ Number of consecutive batches (dimensionless)

$n_{q_a}$ Parameterization number for $q_a$ (dimensionless)

$P$ Power of the aeration equipment (kW)

$p_i$ Actual water vapor pressure (mmHg)

$p_{atm}$ Atmospheric pressure (mmHg)

$P_{bio}$ Biological heat generation (kW)

$P_{eq}$ Power of aeration and mixing equipment (kW)

$p_i^{sat}$ Saturation vapor pressure (mmHg)

$P_{mix}$ Heat input through mixing (kW)

$P_{wall}$ Heat lost through reactor walls (kW)

$q_a$ Aeration flowrate (vvh)

$Q_{lat}, Q_s$ Latent and sensible heat of gas stream (kW)

$r_i$ Reaction rate of component $i$ (g/(l· day))

$r_{VS}$ VS reduction (dimensionless)

$S_I$ Inert soluble organic matter (g/l)

$S_O$ Dissolved oxygen (mg/l)

$S_S$ Readily biodegradable substrate (g/l)

$T$ Temperature (°C)

$t_f$ Final time (days)

$t_r$ Reaction time (days)

$t_S, t_P$ Stabilisation and pasteurisation times (days)

$T_{amb}$ Ambient temperature (°C)

$V$ Volume of liquid phase ($m^3$)

$V_{in}$ Volume of influent sludge ($m^3$)

$w$ Specific humidity (kg of water vapor per kg of dry air)

$X_B$ Biomass (g/l)

$X_I$ Inert suspended organic matter (g/l)

$X_P$ Particulate products from decay (g/l)

$X_S$ Slowly biodegradable substrate (g/l)

$X_{B,H,T}$ Heterotrophic thermophilic biomass (g/l)

$X_{B,H}$ Heterotrophic mesophilic biomass (g/l)

$X_{SP}$ Inactive thermophilic biomass (g/l)

$X_{VS}$ VS concentration (g/l)

$Y_H$ Heterotrophic yield (dimensionless)

RH Relative humidity (%)

# Chapter 1

# Introduction

The ever increasing pace of industrialisation over the last two hundred years has led to the present economic climate which is characterised by volatile and soaring oil and electricity prices, the foreseeable depletion of non-renewable energy sources, insecurity of energy supply, and the steady increase of greenhouse gas emissions. In spite of these trends, global energy demand is expected to continue on the rise, with an increase of 20 to 40% over the next 20 years. In the light of this development, it has become evident that measures and steps towards a more sustainable economy ought to be taken. Energy efficiency improvement is such a measure, representing the most effective option to face the current energy and environmental challenges. Improving energy efficiency generally leads to lower electricity consumption, cost savings, a better use of resources, and lower greenhouse gas emissions (European Commission, 2006).

At present, Europe wastes 20% of its energy as a result of inefficiency. In order to realise the energy saving potential, new energy efficient consumption and production patterns have to be pursued. In the particular case of industry, overall potential savings Europe-wide have been estimated at 25% (European Commission, 2006).

The principal interest of the wastewater industry has always been to meet water quality standards in order to keep public trust (Focus on Energy, 2006). Thus, energy considerations have received very little attention. As a result, wastewater treatment plants are hardly ever designed with energy efficiency in mind, even though they tend to be highly energy-intensive and, thus, expensive to operate.

As an example, in the US alone, wastewater treatment plants consume about 2%[1] of the total amount of electricity generated (Batts et al., 1993), and represent the single largest cost to local governments with up to 33% of their total budget (Jones, 1991; M/J Industrial Solutions, 2003; Yonkin et al., 2008). In addition, the energy consumption of wastewater treatment is expected to increase by 30 to 40% in the next 20 to 30 years. Such increase will be due to the introduction of new regulations imposing higher levels of treatment, to higher loads resulting from population growth, and to new technologies which require greater amounts of electricity (such as UV disinfection, autothermal thermophilic aerobic digestion, etc.) (Metcalf & Eddy, 2003).

In the light of these facts, it is surprising that very few efforts have been devoted to optimising the energy efficiency of wastewater treatment processes (e.g., Moles et al., 2003; Fikar et al., 2005; Holenda et al., 2007; Descoins et al., 2010, and references therein). Optimisation is still uncommon in wastewater engineering. Descoins et al. (2010) pointed out that the experts in the field of wastewater treatment have mainly focused on the simulation and prediction of wastewater qualities in order to comply with legal effluent requirements and standards, while the associated energy aspects of the treatments have been widely neglected.

Only recently and in the context mentioned above, design and operation of wastewater treatment plants have started to shift to include a new emphasis on energy efficiency improvement. So far, the operation of wastewater treatment plants has been based on experience and an intuitive approach, and the criterion for good control has been the compliance with effluent standards (Metcalf & Eddy, 2003).

After labor, electricity is the largest operating cost associated with wastewater treatment with 25 to 40% of the total (M/J Industrial Solutions, 2003). In the most common type of wastewater treatment plant, the activated sludge plant, about 50% of this energy is used for aeration (Metcalf & Eddy, 2003). Among the different stages in wastewater treatment, sludge treatment generally accounts for a major fraction of the total energy cost (Barnes et al., 1986). There are three methods

[1]The more conservative figure of 2% comes from the work by Batts et al. (1993) which is referenced by Metcalf & Eddy (2003), while Gellings (1996) suggested 3%, and Jones (1991) estimated this value at ∼8%.

for sludge treatment: incineration, composting, and digestion. This investigation focuses on a sludge treatment process known as autothermal thermophilic aerobic digestion (ATAD). Compared to other sludge treatments, ATAD is seen as a high energy user (Metcalf & Eddy, 2003).

## 1.1 Motivation

ATAD has a history of over 40 years. The first ATAD systems were oxygen-driven, and they were developed during the 1960s in the US (Warakomski et al., 2007). Later on, in the 1970s, air-driven ATAD systems were patented and manufactured in Germany (USEPA, 1990). However and despite decades of development, neither oxygen-driven nor air-driven systems have been optimised in terms of design and operation (Warakomski et al., 2007). In this investigation, only air-driven systems are considered because most available publications on ATAD deal with such systems. Very few studies and data dealing with oxygen-driven systems have been published. Thus, not enough details on oxygen-driven systems are known to us in order to include such systems in this investigation.

As pointed out earlier, compared to other sludge treatment processes, ATAD has been said to be particularly energy-intensive and has found a more limited application (Metcalf & Eddy, 2003; Le, 2006). Conflicting reports in current literature regarding energy efficiency and cost effectiveness of ATAD technology may have contributed to their limited use (Layden et al., 2007b).

A number of experimental findings clearly indicate that the operating conditions of ATAD systems are unexploited:

- *Aeration flowrate.* Conventional systems make use of invariable air supply regardless of the great variations of bacterial activity along the reaction (Scisson, 2003). This design leads to excessive energy consumption (Layden et al., 2007b). Variable speed drives would allow for an optimisation of the hydraulic retention time (HRT) and energy requirement (Kelly and Mavinic, 2003). La-Para and Alleman (1999) concluded that further work is needed in order to determine the best way to accommodate the enormous oxygen uptake rate

(OUR) that characterise the reaction.

- *Reaction time.* Due to operating convenience, batch times are set by the manufacturers to a default 24-hour cycle. Consequently, both stabilisation and pasteurisation levels at the end of the reaction generally exceed legal requirements. These excessively long reaction times result in increased energy requirements. Reducing reaction times while complying with effluent standards could result in lower energy requirements. Other advantages of shorter reaction times would be the avoidance of oxygen-limited conditions, reduction of thermal shock, and greater plant capacities (Csikor et al., 2002).

- *Sludge flowrate.* The sludge flowrate has been found to influence sludge stabilisation as well as the energy requirement (Ponti et al., 1995a,b). In spite of these advantages and because of operating convenience, conventional systems generally make use of one single volume change per day, thus not allowing a complete exploitation of the thermophiles' efficiency (Ponti et al., 1995a).

- *Influent temperature.* Pre-heating of the influent sludge using the heat from the effluent would reduce the thermal shock, and potentially result in shorter reaction times; shorter reaction times would lead in turn to lower energy requirements. In spite of this, very few plants make use of heat integration (Layden et al., 2007b).

In the light of these considerations, several researchers agree on need to identify the optimum operating conditions of ATAD systems (LaPara and Alleman, 1999; Layden et al., 2007a). Nonetheless, there is no study in the available literature devoted to the optimisation of the ATAD reaction.

## 1.2 Thesis Statement

In view of the lack of optimisation and the rudimentary understanding of ATAD systems, the objectives of this investigation are:

- To minimise the energy requirement of air-driven ATAD systems by altering the operating conditions while complying with effluent quality standards.

- To gain insight into the operating, structural, and scheduling factors influencing both energy requirement and plant capacity of ATAD systems through simulation studies.
- To develop a dynamic model of the ATAD reaction to aid in the aforementioned simulation and optimisation tasks.
- To gain insight into the reaction process and its inner workings.
- To pave the way for the structural optimisation of ATAD systems.

## 1.3 Thesis Overview

Chapter 1 introduces the relevance of energy efficiency optimisation of wastewater treatment in general and ATAD in particular. It gives the general reader a succinct account of the motivation and objectives of the present investigation.

Chapter 2 gives a literature-based explanation of the general aspects and stages of wastewater treatment, followed by a more in-depth description of the different aspects of ATAD, such as metabolism, microbiology, treatment objectives, origin, design, operation, as well as its perceived advantages and disadvantages.

In Chapter 3, the motivation and objectives of this work are presented in the light of the background given in Chapter 2.

Chapter 4 concerns the development of two dynamic ATAD models. These models will be instrumental in developing new knowledge about the ATAD reaction, as well as in the formulation and implementation of the optimisation problem.

In Chapter 5, simulation studies are presented concerning the start-up and steady state operation of ATAD systems, along with an asymptotic analysis, a sensitivity analysis to identify the operating conditions with the strongest influence on the energy requirement and plant capacity, and a model assessment and parameter estimation. The findings from the sensitivity analysis will be key to select the most promising optimisation variables.

Chapter 6 deals with the formulation and implementation of the optimisation problem stated above. Two case studies are presented and optimised following the

direct sequential approach. It then goes on to explore and provide a tentative framework for the formulation and implementation of the optimisation problem in terms of a direct simultaneous approach, namely, orthogonal collocation.

Finally, Chapter 7 summarises the main conclusions of this investigation and considers new avenues of research for the future.

# Chapter 2

# Literature Review

## 2.1 The necessity of wastewater treatment

Human activity results in different forms of pollution. One of these forms of pollution is present in wastewater. Whether the nature of wastewater is domestic (e.g., from communities, institutions, commercial complexes) or industrial (e.g., from manufacturing industries), wastewater always contains components in relatively high concentrations which, if discharged untreated, would cause considerable damage to the receiving water bodies. The damage to the receiving water bodies would have, in turn, consequences for the environment and for human health. A number of relevant components of wastewater and their corresponding effects are listed in Table 2.1. Environmental effects include the change in conditions of natural habitats, production of malodorous gases, aesthetic inconveniences, toxicity, and the destruction of entire ecosystems through eutrophication and oxygen depletion. On the other hand, effects on human health include the pollution of watercourses used by communities (e.g., as source of potable or bathing water) and the transmission of water-born diseases (Henze et al., 1990; Horan, 1990). Some of these pollutants are suspected to be carcinogenic, teratogenic, or mutagenic (Barnes et al., 1986). Thus and to protect the environment and human health, wastewater has to be treated in order to reduce the concentration of pollutants to safe levels. So, the main objective of wastewater treatment is to reduce the concentration of dangerous pollutants to safe levels.

Table 2.1: Components of wastewater and their corresponding effects on the environment and human health. Adapted from Henze et al. (1990).

| Component | Of special interest | Effects |
|---|---|---|
| Microorganisms | Pathogenic bacteria, viruses, and worms | Risk when bathing and eating shellfish |
| Biodegradable organic materials | Oxygen depletion in rivers, lakes, and fjords | Destruction of ecosystems |
| Other organic materials | Detergents, pesticides, fat, oil and grease, colouring, solvents, phenol, cyanide | Toxic effect, aesthetic inconveniences, bio-accumulation |
| Nutrients | Nitrogen, phosphorus, ammonia | Eutrophication, oxygen depletion, toxic effect |
| Metals | Hg, Pb, Cd, Cr, Cu, Ni | Toxic effect, bio-accumulation |
| Other inorganic materials | Acids (e.g., hydrogen sulphide, bases) | Corrosion, toxic effect |
| Thermal effects | Hot water | Changing living conditions for flora and fauna |
| Odour and taste | Hydrogen sulphide | Aesthetic inconveniences, toxic effect |
| Radioactive matter | | Toxic effect, bio-accumulation |

Table 2.2: Stages of wastewater treatment. Adapted from Metcalf & Eddy (2003).

| Treatment stage | Description |
|---|---|
| Preliminary | Physical treatment through screening for removal of floating objects and coarse particles |
| Primary | Physical treatment through sedimentation for partial removal of suspended solids |
| Secondary | Biological or chemical treatment for partial removal of organic matter, suspended solids, and nutrients (e.g., nitrogen, phosphorous, etc) |
| Tertiary | Often a combination of physical, chemical, and biological processes to further remove dissolved and suspended solids |

## 2.2 Stages of wastewater treatment

Wastewater treatment plants are designed in such a manner that the treated water will comply with the applicable effluent quality standards. Most plants consist of a number of operations and processes, each of them targeting different wastewater components. These operations and processes form the different stages of wastewater treatment: preliminary, primary, secondary, and tertiary treatment. Table 2.2 lists the different stages with a brief description of their nature and purpose. The most important part of the treatment is the secondary, biological stage, whose performance depends strongly on that of the preliminary and primary stages.

*Preliminary and primary treatment.* It involves the removal of floating objects

and coarse particles (such as rags and grit) and suspended solids from the influent wastewater by means of physical forces. If not removed, some of these objects and particles would damage the mechanical equipment of the later stages through abrasion, deposition, and accumulation. The most common types of physical operation are screening, comminutors, grit removal, and sedimentation. Other more advanced physical operations are packed-bed filters, membrane separation systems, and ammonia stripping. The removed material is often disposed of in landfill sites or through incineration.

*Secondary treatment.* As mentioned above, the secondary stage is often regarded as the most important part of wastewater treatment. This stage may involve the use of chemical and biological processes which aim at reducing the oxygen demand of the wastewater and (in some cases) destroying hazardous microorganisms. Chemical processes are those by which wastewater components are transformed through chemical reactions. The most common types of chemical processes are chemical coagulation, chemical precipitation, chemical disinfection (typically with chlorine), and chemical oxidation. Biological processes are those by which wastewater components are transformed via metabolic activity. The main concept is to use microorganisms (principally bacteria) to degrade or stabilise the organic matter and nutrients present in the wastewater. As per Equation (2.1), the general metabolic reaction involves the oxidation of large organic matter molecules converting them into simple, low-energy compounds and biomass (Metcalf & Eddy, 2003).

$$\begin{aligned} \nu_1(organic\ matter) + \nu_2 O_2 + \nu_3 NH_3 + \nu_4 PO_4^{3-} \rightarrow \\ \nu_5(biomass) + \nu_6 CO_2 + \nu_7 H_2O \end{aligned} \tag{2.1}$$

The symbol $\nu$ represents the stoichiometric coefficient. In this equation, oxygen, ammonia, and phosphate represent the nutrients needed for the microbial metabolic conversion of organic matter (often in the form $C_{18}H_{19}O_9N$) into biomass (i.e., cell tissue), carbon dioxide, and water.

Depending on the nature of the metabolic reaction, biological processes can be

aerobic, anaerobic, anoxic, facultative, or combined. Aerobic processes take place in the presence of oxygen, while anaerobic processes take place in its absence. Anoxic processes take place in the absence of oxygen by converting nitrate nitrogen into nitrogen gas (also known as denitrification). Facultative processes are those in which the microorganisms can convert organic matter in presence *and* absence of oxygen. Combined processes make use of aerobic, anaerobic, and anoxic processes in order to attain a particular treatment objective.

Biological processes can also have different objectives, such as biological nutrient removal, phosphorous removal, organic matter removal, nitrification, and denitrification. Biological nutrient removal refers to the removal of nitrogen and phosphorous. Phosphorous removal refers to the removal of phosphorous through accumulation in the microorganisms and subsequent solids separation. Organic matter removal refers to the removal of organic matter through conversion of organic matter into biomass and several gases. Nitrification is a two-step process in which ammonia is converted first into nitrite and then into nitrate. In the denitrification process, nitrate is converted into nitrogen and other gases.

*Tertiary treatment.* In this stage (also known as advanced treatment), a number of processes and operations are combined to remove suspended and dissolved matter that remains after the secondary treatment. This stage is required when the secondary treatment does not provide a significant reduction of these compounds.

For a comprehensive account of the stages of wastewater treatment, see Metcalf & Eddy (2003).

## 2.3 Sludge treatment

After the primary and secondary stages, the treated wastewater is passed through clarifiers and thickeners in order to separate the water from the solids. The treated water is then disposed of, for example, in a water body, or it might be used for irrigation or for some other beneficial purpose. The solids or *sludge*, i.e., the concentrated residue at the bottom of the tanks, is then diverted to the sludge treatment site.

Table 2.3: Typical chemical composition of untreated and digested sludge. Adapted from Metcalf & Eddy (2003).

| | Untreated primary sludge | | Digested primary sludge | |
|---|---|---|---|---|
| Component | Range | Typical | Range | Typical |
| Total dry solids (TS), % | 5–9 | 6 | 2–5 | 4 |
| Volatile solids (% of TS) | 60–80 | 65 | 30–60 | 40 |
| Grease and fats (% of TS) | 6–30 | | 5–20 | 18 |
| Protein (% of TS) | 20–30 | 25 | 15–20 | 18 |
| Nitrogen (N, % of TS) | 1.5–4 | 2.5 | 1.6–3 | 3 |
| Phosphorous ($P_2O_5$, % of TS) | 0.8–2.8 | 1.6 | 1.5–4 | 2.5 |
| Cellulose (% of TS) | 8–15 | 10 | 8–15 | 10 |
| pH | 5–8 | 6 | 6.5–7.5 | 7 |
| Alkalinity (g/l as $CaCO_3$) | 0.5–1.5 | 0.6 | 2.5–3.5 | 3 |
| Organic acids (g/l as HAc) | 0.2–2 | 0.5 | 0.1–0.6 | 0.2 |
| Energy content (MJ/kg TSS) | 23–29 | 25 | 9–14 | 12 |

The objective of sludge treatment is to reduce the water and organic matter content of the sludge in such a way that it will be rendered suitable for final disposal or reuse.

The treatment, reuse, and disposal of sludge represent the most complex tasks facing the wastewater engineer. This is due to the fact that sludge is the wastewater residue of largest volume. Thus, sludge treatment is often treated separately from the other stages involved in wastewater treatment.

*Sludge composition.* The most important characteristic of sludge is its water and organic matter content. A high concentration of organic matter in an untreated sludge means that it will further degrade, thus posing a potential health and odour risk. Typically, sludge has a water content of 90–99% which is significantly higher than that of the raw influent wastewater, of about 99.97%. The typical chemical composition of untreated and digested primary sludge can be seen in Table 2.3.

### 2.3.1 Sludge treatment methods

In the first step, operations such as thickening, conditioning, dewatering, and drying are employed to reduce the water content of the sludge and, thus, its volume.

The next step is the stabilisation of the sludge, that is, the reduction of the organic matter content of the sludge. The purpose of stabilisation is to generate an end product with the following characteristics: (i) reduced pathogen content, (ii) absence of odours, and (iii) reduced risk of putrefaction. Sludge stabilisation

is employed in the vast majority of wastewater treatment plants. The principal methods to stabilise the sludge are composting and digestion. Incineration is also employed as a means for sludge treatment.

*Incineration.* Incineration consists of the total conversion of organic matter into simple oxidised compounds, such as ash, water, and carbon dioxide through complete combustion. Its advantages include high volume reduction thus decreasing disposal requirements, elimination of pathogens and toxic compounds, and energy recovery potential. Disadvantages include its high capital and operating cost, large emission of greenhouse gases, and production of potentially hazardous end products.

*Composting.* It involves the biological degradation of organic matter connected to the production of humic acid, thus producing a stable end product which can be used as soil conditioner. The process is carried out by bacteria, actinomycetes, and fungi, and it takes place in an enclosed reactor. Bacteria seem to be responsible for heat generation and the degradation of a major part of the organic matter. Due to the thermophilic operating temperatures, enteric microorganisms are eliminated. Composting is considered to be an environmentally friendly and cost-effective treatment.

*Digestion.* It is the decomposition of organic matter through microbial activity. There are three main types of digestion: anaerobic digestion, aerobic digestion, and autothermal thermophilic aerobic digestion. Anaerobic digestion is the biological degradation of organic matter in the absence of oxygen through fermentation processes. This process is often performed in a heated reactor for the production of methane. The process is susceptible to relatively small disturbances of the operating conditions and recovery is slow. Therefore, it requires skilled operation. The end product can be used as soil conditioner.

Aerobic digestion is the biological degradation of organic matter in the presence of oxygen. Its principle is similar to that of the activated sludge process: when organic matter is scarce, the microorganisms consume their own protoplasm in order to generate energy. Cell mass is thus oxidized and converted into ammonia, carbon dioxide, and water. The process usually takes place in an open tank and, thus, at ambient temperature. It is not susceptible to disturbances in the operating

Table 2.4: Degree of attenuation of stabilisation processes. Adapted from Metcalf & Eddy (2003).

| | Degree of attenuation | | |
|---|---|---|---|
| Process | Pathogens | Putrefaction | Odour potential |
| Alkaline stabilisation | Good | Fair | Fair |
| Anaerobic digestion | Fair | Good | Good |
| Aerobic digestion | Fair | Good | Good |
| ATAD | Excellent | Good | Good |
| Composting | Fair | Good | Poor to fair |
| Composting (thermophilic) | Excellent | Good | Poor to fair |

conditions. Due to the energy required for aeration, the process is energy-intensive.

ATAD is similar to aerobic digestion with the exception that the process occurs at thermophilic temperatures. This is achieved by using enclosed, well-insulated reactors and higher aeration levels. The process is not significantly susceptible to disturbances of the operating conditions (especially when compared to other processes, such as thermophilic anaerobic digestion) and it can produce Class A Biosolids. ATAD is energy-intensive due to the high aeration level required to reach and maintain thermophilic temperatures.

A comparison of the performance of stabilisation processes in terms of their attenuation capacity is shown in Table 2.4. ATAD displays, overall, the best performance.

A more detailed description of the available methods for sludge treatment can be found in Metcalf & Eddy (2003).

## 2.4 Energy efficiency and cost of wastewater treatment

The principal interest of the wastewater industry has always been to meet water quality standards in order to keep public trust (Focus on Energy, 2006). Thus, energy considerations have received very little attention. As a result, wastewater treatment plants are hardly ever designed with energy efficiency in mind, even though they tend to be highly energy-intensive and expensive to operate.

As an example, in the US alone, wastewater treatment plants consume about

2%[1] of the total amount of electricity generated (Batts et al., 1993), and represent the single largest cost to local governments with up to 33% of their total budget (Jones, 1991; M/J Industrial Solutions, 2003; Yonkin et al., 2008). In addition, the energy consumption of wastewater treatment is expected to increase by 30 to 40% in the next 20 to 30 years. Such increase will be due to the introduction of new regulations imposing higher levels of treatment, to higher loads resulting from population growth, and to new technologies which require greater amounts of electricity (such as UV disinfection, autothermal thermophilic aerobic digestion, etc.) (Metcalf & Eddy, 2003).

In the light of these facts, it is surprising that very few efforts have been devoted to optimising the energy efficiency of wastewater treatment processes (e.g., Moles et al., 2003; Fikar et al., 2005; Holenda et al., 2007; Descoins et al., 2010, and references therein). Optimisation is still rare in wastewater engineering. Descoins et al. (2010) pointed out that the experts in the field of wastewater treatment have mainly focused on the simulation and prediction of wastewater qualities in order to comply with legal effluent requirements and standards, while the associated energy aspects of the treatments have been widely neglected.

Only recently and in the context mentioned above, design and operation of wastewater treatment plants have started to shift to include a new emphasis on energy efficiency improvement. In general, the operation of wastewater treatment plants has been based on experience and an intuitive approach, and the criterion for good control has been the compliance with effluent standards (Metcalf & Eddy, 2003).

After labor, electricity is the largest operating cost associated with wastewater treatment with 25 to 40% of the total (M/J Industrial Solutions, 2003). In the most common type of wastewater treatment plant, the activated sludge plant, about 50% of this energy is used for aeration (Metcalf & Eddy, 2003). Among the different stages in wastewater treatment, sludge treatment generally accounts for a major fraction of the total energy cost (Barnes et al., 1986).

[1]The more conservative figure of 2% comes from the work by Batts et al. (1993) which is referenced by Metcalf & Eddy (2003), while Gellings (1996) suggested 3%, and Jones (1991) estimated its value at ∼8%.

One of the most energy-intensive sludge treatment processes is autothermal thermophilic aerobic digestion, which represents the focus of this investigation.

## 2.5 Autothermal thermophilic aerobic digestion

ATAD is a sludge treatment process similar to the activated sludge process. ATAD represents a variation of conventional mesophilic and high-purity oxygen aerobic digestion (Metcalf & Eddy, 2003).

### 2.5.1 The ATAD process

#### Metabolism

ATAD involves the decomposition of organic matter in the presence of oxygen through microbial oxidation at thermophilic temperatures (40–70 °C). Through the oxidation process, organic matter is eventually converted into biomass, ammonia, carbon dioxide, and water. However, there is almost no information on the biochemical metabolic pathways that make this reaction possible (Muller et al., 1998).

An important difference between ATAD and other aerobic digestion processes is the high operating temperature which inhibits nitrification. Nonetheless, there is a significant similarity between the biochemistry of ATAD and that of the activated sludge process: as biodegradable organic matter becomes exhausted, the microorganisms start using their own protoplasm as well as cell material released into the environment by cell lysis as source of organic matter in order to obtain energy for cell maintenance and synthesis of new cell material (microbial growth). This phase is called *endogenous respiration*. It is mainly during this phase that the organic matter content of the sludge is reduced. This reduction is known as *endogenous decay*.

While oxygen is plentiful, the oxidation of cell matter into carbon dioxide, water, and nitrogen compounds during the phase of endogenous respiration is ruled by Equation 2.2 and 2.3 (Metcalf & Eddy, 2003).

$$C_5H_7NO_2 + 7\,O_2 \rightarrow 5\,CO_2 + 3\,H_2O + HNO_3 \quad (2.2)$$

$$C_5H_7NO_2 + 5\,O_2 \rightarrow 5\,CO_2 + NH_3 + 2\,H_2O \quad (2.3)$$

The formula $C_5H_7NO_2$ is the conventional representation for cell material originally proposed by Hoover and Porges (1952). During this reaction, ammonia and other nitrogen compounds are produced which are not further broken down due to the inhibition of nitrification. As a result, alkalinity increases and the pH of the sludge will be in the range 8–9. The high concentration of ammonia contributes (often with hydrogen sulphide $H_2S$) to the characteristic smell of the exhaust gas from the reactors.

However, oxygen is generally not plentiful in ATAD reactors; the reason being that oxygen demand usually exceeds oxygen supply with dissolved oxygen concentration falling below detectable levels (Stensel and Coleman, 2000). This is known as microaerophilic or microaerobic conditions. Subject to microaerophilic conditions, proteinaceous cell material, such as peptone, is broken down into volatile fatty acids, for example acetic acid, through the fermentation process described by Equation 2.4 (Chu and Mavinic, 1998).

$$4\,CH_2NH_2COOH + 4\,H_2O \rightarrow 3\,CH_3COOH + 2\,(NH_4)_2CO_3 \quad (2.4)$$

Finally and given enough dissolved oxygen is available, acetic acid will undergo oxidation to produce carbon dioxide and water following Equation 2.5 (Metcalf & Eddy, 2003).

$$CH_3COOH + 2\,O_2 \rightarrow 2\,CO_2 + 2\,H_2O \quad (2.5)$$

The fact that fermentative (and even anaerobic) processes take place, shows that ATAD is not, strictly speaking, an aerobic process. It is a combination of aerobic, fermentative, and anaerobic processes (Kelly and Warren, 1997).

During their digestion, thermophilic microorganisms release vast amounts of

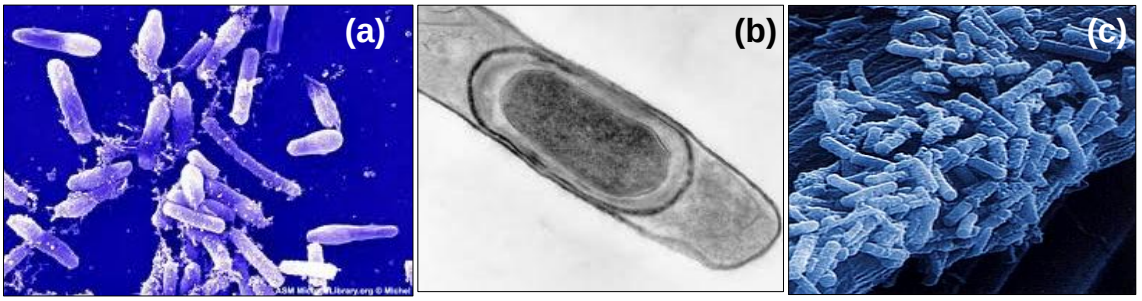


Figure 2.1: SEM micrographs of microorganisms involved in ATAD: (a) thermophilic *Bacillus* (Todar, 2011), (b) *B. licheniformis* (Ehrenreich, 2011), and (c) *B. stearothermophilus* (Holowko, 2011).

metabolic energy in the form of heat thus rising reactors' temperatures to the thermophilic range. To be more precise, about 14 MJ of metabolic energy are released into the environment for each kilogram of oxygen consumed (Gomez et al., 2007). This inefficient metabolism may be one of the main characteristics of the thermophilic community.

### Microbiology

Little is known about the microbiological aspects of ATAD (LaPara and Alleman, 1999). It is generally thought, however, that the dominant microbial population is the thermophilic *Bacillus* spp. such as *B. stearothermophilus* (Sonnleitner and Fiechter, 1983), *Paenibacillus* and Peptostreptococcaceae (Piterina et al., 2008), and *B. licheniformis* and *Brevibacillus* (Ugwuanyi et al., 2008; Li et al., 2009). Yet, in a more recent study, Liu et al. (2010) found the bacteria *Ureibacillus* of Bacillaceae, Hydrogenophilaceae, Thermotogaceae, and Clostridiaceae to be dominant. They also found that there were significant population dynamics during periods of temperature changes; at higher temperatures, the aforementioned dominant groups were selected replacing less temperature-tolerant microorganisms such as Sphingobacteriaceae and the genus *Trichococcus*. Figure 2.1 shows micrographs of some of the microorganisms involved in the ATAD reaction.

Staton et al. (2001) stated that it was unclear whether anaerobic microorganisms would be able to survive and thrive in ATAD reactors. However, recent evidence

shows the presence of anaerobic and even strict anaerobic microorganisms as well as methanogenic activity in ATAD systems (Ugwuanyi et al., 2005; Piterina et al., 2008). This might be due to the prevalence of microaerophilic conditions during the reaction. It is nonetheless unclear what the contribution of these anaerobic populations might be in terms of the stabilisation capacity of ATAD systems. As stated earlier, ATAD is a combination of anaerobic, fermentative, and aerobic processes (Kelly and Warren, 1997).

There is an important difference between the microbiology of ATAD and that of the conventional activated sludge process: nitrifying microorganisms, protozoa, and other life forms are not present (LaPara and Alleman, 1999). The absence of nitrifying microorganisms is due to the high operating temperatures.

### 2.5.2 Treatment objectives

Perhaps the most comprehensive and authoritative standard for the final use or disposal of sewage sludge of domestic origin is United States Environmental Protection Agency (USEPA) 40 CFR Part 503 (USEPA, 1993). This set of regulations establishes, among others, the general requirements in terms of pathogens and vector attraction reduction when treated sludge is intended for land application or surface disposal.

These regulations define two types or qualities of treated sludge or *biosolids*: Class A and Class B Biosolids. These definitions are based on the species and number of pathogens present in the treated sludge, with Class A displaying lower and Class B higher numbers. Class A Biosolids have to meet the more stringent criteria as they can be used as soil conditioner by the general public, as well as in gardens, etc. Class B Biosolids find a more limited use as soil conditioner on agricultural land or alternatively they may be disposed of in landfill.

Under these regulations, ATAD is considered to meet Class A Biosolids standards and to be a process to further reduce pathogens (PFRP). All such processes have to meet the requirements for pathogen reduction as well as vector attraction reduction.

### Pasteurisation

Pathogens are all those microorganisms able to cause disease, such as bacteria, viruses, protozoa, and helminths. They can infect humans and animals in different ways and the level of exposure necessary for infection depends on each specific pathogen and host. In this particular context, the most dangerous pathogens are those from the enteric and urinary systems of humans. They are present in the sludge through feces and urine. Generally, wastewater and sewage sludge contain very high concentrations of pathogens. However, they can only thrive under certain conditions of temperature, pH, etc. Outside of these conditions, they are not able to survive. Treatments for pathogen reduction are based on this fact. Some of these treatments include application of high temperatures, radiation, and chemical disinfectants.

The process by which pathogen numbers are reduced via thermal treatment is termed *pasteurisation*. The applicable pathogen reduction must be attained before or at the same time as vector attraction reduction. This is required in order to prevent the growth of pathogens after reducing vector attraction.

Under 40 CFR 503.32(a)(3), USEPA (1993) establishes that a certain time-temperature relationship has to be satisfied in order to reduce pathogens through thermal treatment. For the particular case of ATAD, this time-temperature relationship, also known as thermal death time, obeys Equation 2.6 and it is displayed in Figure 2.2a:

$$D = \frac{5007000}{10^{0.14 \cdot T}},\ T \geq 50\ ^{\circ}\text{C},\ D \geq 0.021 \text{ days (30 minutes)}, \tag{2.6}$$

where $D$ represents the contact time (days), and $T$ the temperature (°C). Exposing the sludge to the temperature $T$ during the corresponding contact time $D$ ensures that pathogens are reduced below detectable levels. When the right level of exposure has been achieved, the sludge is said to be *pasteurised*.

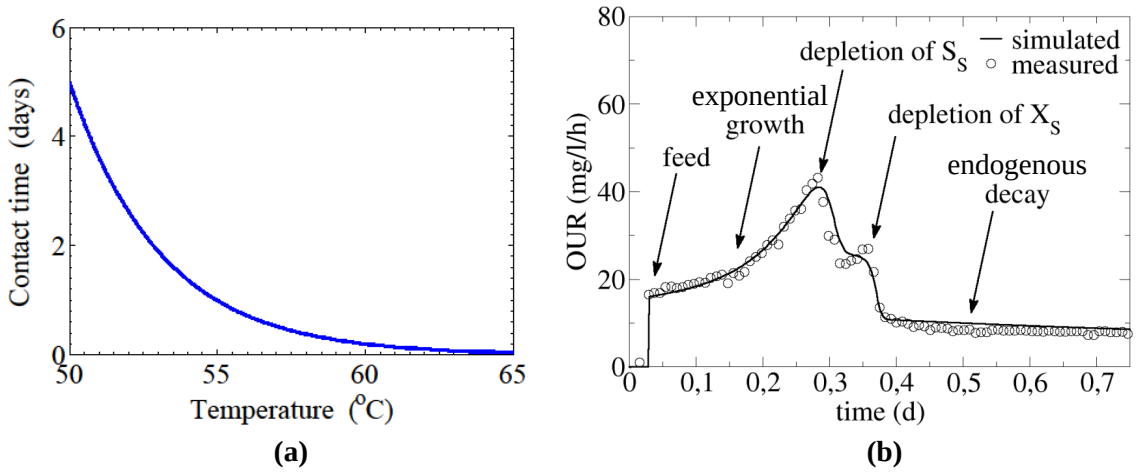


Figure 2.2: (a) Contact time required for pasteurisation as a function of the operating temperature, and (b) evolution of oxygen uptake rate (OUR) in ATAD laboratory-scale reactor (adapted from Kovacs (2007) and Jamniczky-Kaszas (2010)).

### Stabilisation

Vector attraction reduction refers to the reduction of three potential risks: putrescibility of the sludge once it is applied on land, the subsequent growth of pathogens, and the eventual spread of infectious diseases.

When untreated sludge is applied to land, it provides pathogens with sufficient organic matter to grow and thrive. Then, these pathogens might spread and be transmitted to humans by means of other organisms, called "vectors", that are attracted to the sludge as a food source. Examples of vectors are rodents, flies, mosquitoes, etc.

There are two ways to reduce vector attraction. The first is to treat the sludge to a level that will no longer attract vectors. The second consists of placing a barrier between the sludge and the vectors.

When the first option is chosen under 40 CFR 503.33(b)(1), the mass of volatile solids in the sludge has to be reduced by a minimum of 38% with regard to the influent sludge (USEPA, 1993). When this condition is satisfied, the sludge is said to be *stable* or *stabilised*. Once the sludge has been stabilised, it is then less likely to become putrid, the amount of substrate for growth of pathogens has been significantly reduced, and less vectors will be attracted.

As mentioned earlier, the phase during which the organic matter concentration is reduced, is called endogenous decay. It is mostly during this phase that sludge stabilisation is achieved. Figure 2.2b shows the evolution of the OUR in a laboratory-scale ATAD reactor. It can be seen that, after a period of exponential growth, the microorganisms deplete the readily biodegradable organic matter (denoted by $S_S$), and shortly thereafter they also deplete the slowly biodegradable organic matter (denoted $X_S$). Soon after that, microorganisms start consuming their own tissue and that of lysed cells in order to obtain energy, thus entering the phase of endogenous decay. During endogenous decay, proteinaceous cell material is transformed into simple, low-energy compounds (such as $CO_2$, $NH_3$, and water) and lysed, effectively reducing the organic matter concentration of the sludge.

In short, the treatment objectives of ATAD are the pasteurisation and stabilisation of the sludge to the aforementioned levels.

According to what has been seen in the last sections, the principle of the ATAD reaction can be summarised as follows: raw sewage sludge containing relatively high concentrations of organic matter and pathogens is fed into a well-insulated reactor. The sludge is then aerated (with either pure oxygen or air) and mixed for a certain period of time. The thermophilic microorganisms naturally present in the sludge start to feed and grow at the expense of oxygen and organic matter. This effectively reduces the organic matter concentration resulting in sludge stabilisation. During their digestion, the thermophiles release vast amounts of metabolic energy into the environment in form of heat, rising reactors' temperatures to the thermophilic range. These high temperatures are lethal for pathogens. Consequently, pathogen concentrations fall below detectable levels resulting in sludge pasteurisation. Hence, the end product is a stable, pasteurised sludge classified as Class A Biosolids that can be used as soil conditioner without restrictions.

### 2.5.3 Origin, design, and operation of ATAD systems

#### Origin

According to LaPara and Alleman (1999), the original thermophilic aerobic plants evolved accidentally from research conducted during the 1950s, as heat released during mesophilic digestion of high-strength sludge increased reactors' temperatures to the thermophilic range.

Exploratory research on activated sludge systems using pure oxygen started as early as the 1960s (Warakomski et al., 2007). The first such system, developed by the American company *Union Carbide's Linde Division* (now *Mixing and Mass Transfer Technologies LLC*), was patented in 1967. The company built and successfully operated the first experimental full-scale, oxygen-driven system in 1972 in Speedway, Indiana, US (Gyger et al., 2007). To date, the company has built more than 100 oxygen-driven systems.

Initially, it was believed that thermophilic temperatures could only be reached and maintained when using pure oxygen (Matsch and Drnevich, 1977; Gould and Drnevich, 1978). Nonetheless, other developments showed that thermophilic temperatures could also be reached and maintained using air at laboratory and pilot scale (Loll, 1977; Jewell and Kabrick, 1978).

During the late 1970s, the German company *Fuchs Gas- und Wassertechnick GmbH* (now *FUCHS Enprotec GmbH*) successfully built and operated an experimental full-scale, air-driven system consisting of one single stage fed with high-strength sludge which was able to reach and maintain thermophilic temperatures (Layden et al., 2007a). This success lead the company to build the first full-scale, air-driven, municipal ATAD system in 1977 in Vilsbiburg, Germany (USEPA, 1990). The later and prevailing design of this company would be a two-stage system consisting of two reactors in series. They have since built over 80 air-driven ATAD plants worldwide.

Other companies involved in the development and commercialisation of ATAD systems over the last three decades include *Kruger-Fuchs*, *US Filter*, *Air Products*, *Dayton Knight*, *CBI Walker*, and *Thermal Process Systems* (Gyger et al., 2007). Most of these companies deal or manufacture air-driven systems.

Table 2.5: Main design parameters of two-stage ATAD systems. Adapted from USEPA (1990).

| Parameter | Description |
|---|---|
| Reactors | Two stages or more, depending on load; tanks of equal size (typically 100 $m^3$) operated in series; daily semi-batch operation |
| Reactor type | Cylindrical; height-diameter ratio of 0.5–1.0 |
| Sludge type | Primary, secondary activated sludge, trickling filter, gravity or air flotation thickened, mixture of primary and secondary, domestic or industrial origin, manure |
| Feed TS range | 40–60 g/l (4–6 %) |
| Required VSS | $\geq$25 g/l (2.5 %) |
| HRT | 5–6 days |
| Mininum reaction time | 20 hr/stage |
| Temperature and pH | Reactor I: 35–50 °C, pH$\geq$7.2<br>Reactor II: 50–65 °C, pH$\geq$8.0 |
| Aeration flowrate | 4 $m^3$ $m^{-3}$ $hr^{-1}$ (or vvh) |
| Specific power | 85–105 W/$m^3$ of active reactor volume |
| Energy requirement | 9–15 kWh/$m^3$ of sludge |
| Heat potential for recovery | 20–30 kWh/$m^3$ of sludge |

This investigation exclusively concerns air-driven systems because most available publications on ATAD deal with such systems. Publications and data dealing with oxygen-driven systems are scarce and insufficient to include them in this investigation.

### Design and operation

The prevailing design among air-driven ATAD systems is the two-stage design developed by *Fuchs Gas- und Wassertechnick GmbH*. This design is described in detail in USEPA (1990) where it is considered the design standard. For this reason, this design is also going to be considered the standard in this investigation.

Both single- and multiple-stage ATAD systems are in operation. However, over the years, two-stage systems have become the most widely used type. This development may be rooted in the perception that single-stage systems may not be able to achieve the same pasteurisation levels as multiple-stage systems (USEPA, 1990). Nonetheless, single-stage systems do achieve similar volatile solids (VS) reductions as multiple-stage systems.

A summary of the main design parameters of two-stage systems is listed in Table 2.5.

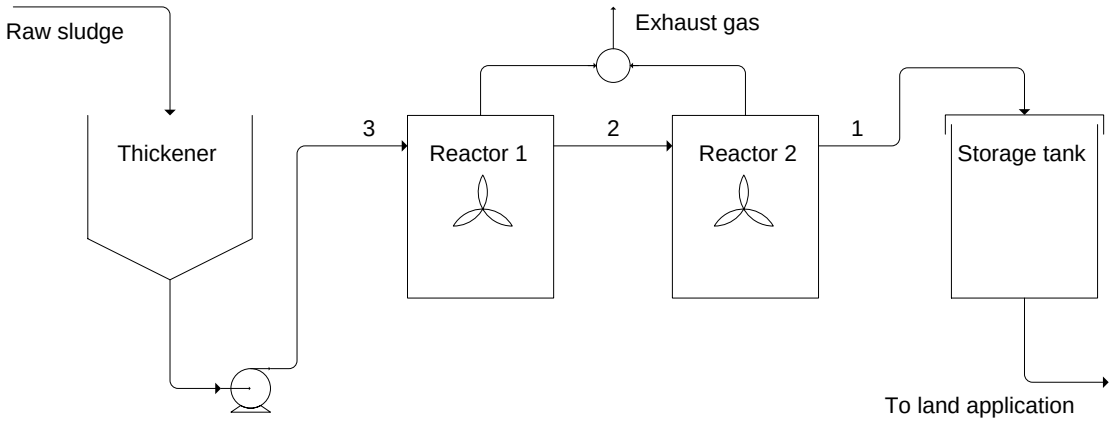


Figure 2.3: Flow diagram of two-stage, semibatch ATAD system. The numbers indicate the reverse order of the streams. Adapted from USEPA (1990).

*Mode of operation.* Two-stage ATAD systems are typically operated in a semi-batch mode. This semi-batch, series mode operated following a reverse-order loading procedure ensures that the treated sludge from the second-stage reactor is not contaminated with raw sludge or partially digested sludge from the first-stage reactor. After a reaction time of 23 hours, aeration and mixing equipment are switched off to give way to a 1-hour loading procedure: a certain volume of treated sludge from the second-stage reactor is transferred into the storage tank; next, the first-stage reactor discharges the same volume of sludge into the second-stage reactor; finally, the same volume of raw sludge is transferred into the first-stage reactor. Figure 2.3 displays the flow diagram of the typical two-stage ATAD system. Stabilisation is greater in the first-stage ($\sim$60%) than in the second-stage reactor ($\sim$40%), as the first-stage reactor is fed with the raw sludge. However, pasteurisation generally takes place in the second-stage reactor due to its higher operating temperatures.

*Sludge pre-thickening.* The feed sludge or influent sludge is usually thickened before digestion through gravity thickening. A total solids (TS) concentration of 4–6% allows the reactors to reach and maintain thermophilic temperatures. About 60% of TS have to be in the form of biodegradable VS in order to sustain the process. Thus, the VS concentration of the influent sludge is a critical parameter: while VS are the subject of the treatment, they are at the same time the driving force or fuel of the process. Influent sludge is commonly a mixture of primary and secondary

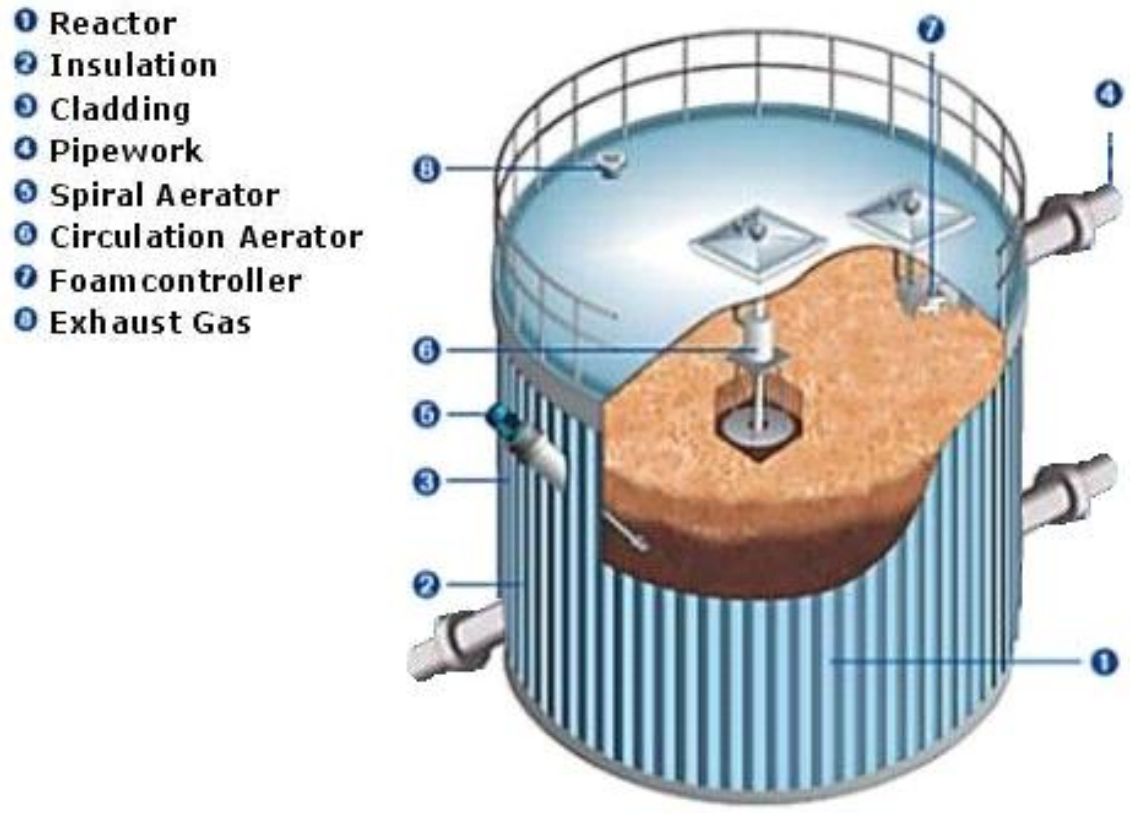


Figure 2.4: Artistic image of *Fuchs* ATAD reactor highlighting its essential parts. Adapted from ISMA (2011).

sludge.

*Reactors.* The reactors are enclosed and cylindrical with a height-diameter ratio of 0.5–1.0, and have a typical volume of 100 $m^3$ each. As a result of the higher reaction rates and lower HRT of ATAD systems, ATAD reactors are significantly smaller (one-sixth to one-half) than those used for other digestion processes (Kelly and Warren, 1997). To reduce the rate of heat loss and prevent temperatures from plummeting, reactors are insulated with a 10-cm-thick layer of mineral wool, and styrene foam. The range of the resulting heat transfer coefficient is 0.3–0.4 W $m^{-2}$ $°C^{-1}$. To protect the insulation, the reactor is then covered with a metallic layer of corrugated steel or aluminium. The reactors are operated with a freeboard of 0.5–1 m. Figure 2.4 displays an artistic image of a typical *Fuchs* ATAD reactor highlighting its most important parts.

*Hydraulic residence time.* The HRT is in the range 5–6 days which corresponds

Table 2.6: Changes in the physico-chemical properties of water at thermophilic temperatures (compared to mesophilic temperatures) and their impact on ATAD treatment. Adapted from LaPara and Alleman (1999) and Layden et al. (2007a).

| Property | Expected change | Impact on ATAD treatment |
|---|---|---|
| Viscosity | Decrease | Improved gas transfer efficiency<br>Improved mixing efficiency<br>Improved rheology for pumping |
| Surface tension | Decrease | Improved gas transfer efficiency<br>Increased tendency for foaming |
| Diffusivity | Increase | Improved gas transfer efficiency<br>Improved mixing efficiency |
| Gas-liquid solubility | Decrease | Reduced transfer efficiency of undersaturated gas (e.g., $O_2$)<br>Increased stripping of supersaturated off-gases (e.g., $CO_2$, $NH_3$, etc.) |
| Solid-liquid solubility | Increase | Higher permissible concentrations of most organics and inorganics<br>Lower solubility of carbonate salts |

to 2.5–3 days in each reactor. The minimum daily reaction time should be 20 hr per reactor. This represents the batch phase during which loading is interrupted, aeration and mixing are resumed, and pathogens and VS concentrations are reduced. The loading process is completed approximately within 30 min per reactor, leading to an average reaction time of 23.5 hr. Changes in the sludge flowrate should not lead to HRT variations greater than 20%.

*Aeration and mixing.* Choosing the right amount of aeration and mixing is another critical parameter when designing an ATAD system. Aeration serves two purposes: providing microorganisms with oxygen and mixing the sludge. Each reactor is equipped with two spiral aerators on opposite sides and at a certain angle thus creating a vertical downward flow. This type of aerators propels the sludge in a spiral, highly turbulent movement. Based on a TS concentration of 2.5–5.0% and an oxygen requirement of 1.42 kg of $O_2$ per kg of VS destroyed, the aeration flowrate is set at 4 $m^3$ $m^{-3}$ $hr^{-1}$ (also vvh, or volume of air per volume of sludge per hour). The specific power input of the aeration equipment is in the range 85–105 $W/m^3$, leading to an energy requirement of 9–15 $kWh/m^3$ of sludge treated.

*Temperature.* The changes in the physico-chemical properties of water at thermophilic temperatures and their impact on the ATAD treatment are displayed in Table 2.6. A decrease in viscosity and surface tension, and an increase in diffusivity

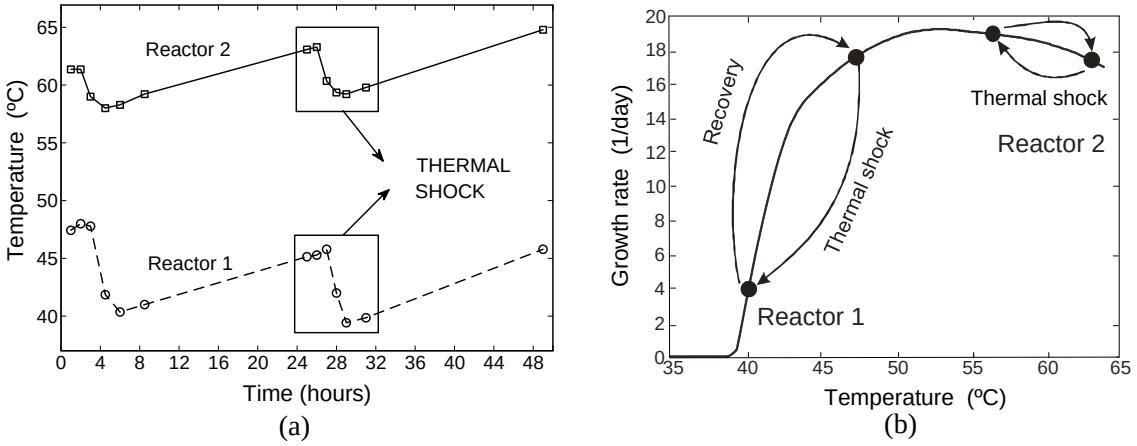


Figure 2.5: (a) Two-day temperature time series showing the effect of the thermal shock in a two-stage ATAD system, and (b) temperature dependence of thermophilic growth rate and effect of thermal shock on both reactors with potential implications for sludge stabilisation and pasteurisation.

result in increased gas transfer efficiency. On the other hand, the decrease of gas-liquid solubility decreases gas transfer efficiency. Hence, it could be expected that these effects offset each other. Vogelaar et al. (2000) confirmed this hypothesis. They found that temperature changes between 20 and 55 °C in tapwater, paper process water, and thermophilic sludge had a negligible effect on the oxygen transfer rate. They concluded that this was due to the counteracting effect of the increasing overall oxygen transfer coefficient against the decreasing oxygen saturation concentration.

As a result of daily reactor loading with a typical 33% displacement of reactor volume, there is a drop in reactors' temperatures, known as *thermal shock* (see Figure 2.5a). The thermal shock in the first-stage reactor is in the range 5–10 °C, while in the second-stage reactor it ranges 4–6 °C. The temperature recovery rate in the first-stage reactor is ∼1 °C/hr and somewhat higher in the second-stage reactor. Temperatures should not fall below 40 °C to prevent biological adaptation problems (see Figure 2.5b), or be higher than 65 °C to avoid resolubilisation of organic matter. As can be seen in Figure 2.5b, the thermal shock might have implications for both sludge stabilisation and pasteurisation due to a decrease of bacterial activity.

Kelly and Warren (1997) suggested that ATAD is not strictly thermophilic, as the first-stage reactor may operate below that range as a result of the thermal

shock. They indicated that one function of the first-stage reactor is to rise the sludge temperature, thus allowing the second-stage reactor to operate consistently in the thermophilic range.

Overall, the temperature profile along the ATAD reaction is mainly determined by the aeration flowrate, influent sludge concentration, reactor insulation, and thickness of the foam layer.

As a result of the high operating temperatures, nitrification is inhibited and the pH depressions observed in nitrifying environments do not take place. Thus, pH does not have to be controlled. Given a raw sludge with a pH of 6.5, the pH in the first-stage reactor would be higher than 7.2, and higher than 8 in the second stage.

*Foam control.* As a result of the strong aeration levels, a foam layer of several centimeters forms on top of the liquid phase. When foam becomes excessive, it may eventually overflow the reactor thus creating an urgent problem. However, this layer has important advantages for the treatment. It creates an extra layer of insulation that lowers the rate of heat loss. It also rises oxidation and stabilisation rates by increasing the area of the gas-liquid interphase. Thus, the foam layer should not be completely removed; rather, it should be kept within adequate levels.

In order to make room for the foam layer, a freeboard of 0.5–1.0 m is used. Each tank is equipped with at least two foam cutters whose function is to break bigger bubbles into smaller ones, thus keeping the foam layer at a desired level.

*Storage and dewatering.* When treated sludge is intended for land application, a minimum storage capacity of 3 months is the norm. This allows enough storage to be available during the time (typically winter) in which sludge cannot be applied to the land. Storage tanks do not require aeration. However, they have a mixing system that operates for about an hour every day. Problems with reactivation of pathogens and odours are not common when the sludge has been properly pasteurised and stabilised.

At some facilities, sludge is dewatered prior to storage. The typical range of TS after dewatering is 6–9%. The hot effluent sludge does not dewater easily immediately after treatment due to thermal convection. Thus, it is more common to wait for the sludge to cool down to ambient temperature before the dewatering process

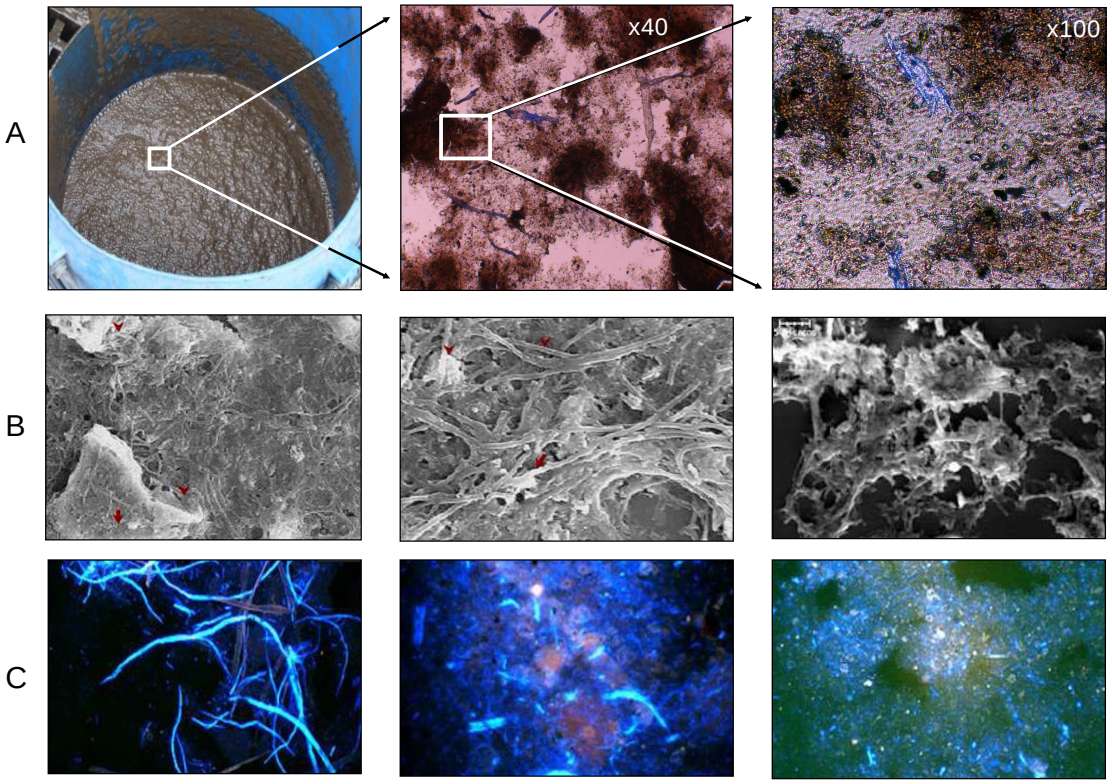


Figure 2.6: *Panel A*. Micrographs of ATAD sludge at different degrees of amplification. *Panel B*. SEM micrographs of ATAD sludge displaying its filamentous nature. *Panel C*. Epifluorescence images illustrating pattern of fibre degradation. Adapted from Piterina et al. (2011).

takes place. Some researchers have indicated that ATAD sludge is very difficult and expensive to dewater due to the disperse growth of floc-forming ATAD microorganisms (LaPara and Alleman, 1999; Scisson, 2003). Figure 2.6 displays photographs of ATAD sludge at different levels of magnification, as well as SEM micrographs and epifluorescence images taken by Piterina et al. (2011).

*Heat integration.* If the raw sludge has an insufficient VS content, the use of heat exchangers could be necessary in order to maintain thermophilic temperatures. In this case, effluent sludge would be used to pre-heat the influent sludge.

Alternatively, the heat from the effluent sludge could also be used to heat the buildings thus reducing the overall running cost of the plant. Very few plants have been reported to make use of heat integration.

Table 2.7: Advantages and disadvantages of ATAD. Adapted from Layden et al. (2007a).

| Advantages | Disadvantages |
|---|---|
| Higher degradation rates and lower sludge yields than anaerobic digestion result in smaller reactor volumes and lower capital cost | High operating cost due to high OUR and aeration level |
| Shorter reaction time and HRT than other digestion processes | Insufficient reaction time |
| Odours are kept inside of enclosed reactors and diverted to gas treatment site | Odours require control and treatment system |
| High levels of pasteurisation and stabilisation can be attained, producing Class A Biosolids | End product often extraordinarily difficult to settle and dewater |
| Process is self-regulating in relation to temperature | Foam control is necessary |
| Very robust and resistant to shock loads and fluctuations of the operating conditions when compared to anaerobic digestion | Inflexible design and invariable air supply |
| Easy to operate, start up, and shut down | |

### 2.5.4 Advantages and disadvantages of ATAD

Table 2.7 summarises the most important advantages and disadvantages of ATAD. Perhaps, its most recognised advantage is the lower capital cost in relation to other digestion processes; this is due to the higher degradation rates resulting in smaller reactor volumes. Sludge yields, reaction times, and HRTs are also lower than in other digestion processes. Another important advantage is the high level of stabilisation and pasteurisation of treated sludge that satisfies the requirements under 40 CFR Part 503 (USEPA, 1993). In doing so, the end product is considered as Class A Biosolids. In fact, when compared to other sludge treatment processes (see Table 2.4), ATAD performs better in terms of stabilisation and pasteurisation. Start-up and shut down of ATAD systems are also much easier and their operation less susceptible to fluctuations of the operating conditions than other digestion processes, especially anaerobic digestion. Additionally, the process does not tend to generate odours because the reactors are enclosed and the gas streams are diverted to a gas treatment facility.

On the other hand, the most important disadvantage is the high energy consumption related to the constant and high aeration levels required to satisfy the enormous oxygen uptake rates. ATAD is said to be highly energy-intensive compared to other sludge treatments (Metcalf & Eddy, 2003; Le, 2006). However, such comparison of

the energy efficiency of different sludge treatment processes seems unsubstantiated, as no such study or information was found in the literature during the course of this investigation. This claim may be based on perception rather than actual research.

Another disadvantage is the extraordinary difficulty and cost involved in settling and dewatering ATAD sludge (often with extremely high polymer doses) (LaPara and Alleman, 1999; Scisson, 2003; Layden et al., 2007a). This can lead to higher volumes of biosolids and hence higher transport cost. Odours and excessive foam have been the cause of operational difficulties in particular instances (Scisson, 2003; Layden et al., 2007a). Additionally, it has been reported at least once that the 23-hr reaction time of two-stage ATAD systems is insufficient and often leads to poor stabilisation and odours (Scisson, 2003). These systems also have the serious drawback of using invariable air supply despite the great changes of bacterial activity along the reaction (Scisson, 2003).

# Chapter 3

# Motivation and Objectives

## 3.1 Motivation

There are conflicting reports in current literature regarding the energy efficiency and cost effectiveness of ATAD systems (Layden et al., 2007b). Le (2006) claims that ATAD is highly energy-intensive, costly, and inefficient relative to other sludge treatment options. Other researchers, however, have stated that ATAD is economically competitive when compared to anaerobic digestion, and even the most economic option for small and medium sized populations (Deeny et al., 1991; Kelly, 1999; Riley and Forster, 2002). This contradictory information may have been the main factor leading to the relatively limited use of this kind of technology. Yet, what we know for sure is that ATAD is a highly energy-intensive process (Metcalf & Eddy, 2003). Despite this fact and over 40 years of technological development, neither air-driven nor oxygen-driven ATAD systems have been optimised (Warakomski et al., 2007). Regarding the standard design described in the previous section, there is a number of issues that clearly indicate that the operating conditions of such systems have been left unexploited:

- *Aeration flowrate.* These systems make use of invariable air supply regardless of the great variations of bacterial activity along the reaction as shown by the OURs (Scisson, 2003). This design can result in insufficient oxygen delivery leading to poor stabilization and odours (Scisson, 2003; Layden et al., 2007a).

Another problem can arise with invariable aeration: is the aeration level designed to satisfy the high OUR period, so will it be oversized for the rest of the reaction (Juteau, 2006); this in turn would result in excessive latent heat loss thus lowering reactors' temperatures (Layden et al., 2007a). More importantly, continuous and invariable aeration likely leads to excessive energy consumption (Layden et al., 2007b). On the other hand, a variable aeration level would allow for an optimisation of the HRT (Kelly and Mavinic, 2003). LaPara and Alleman (1999) concluded that further work is needed to determine the best way to accommodate the enormous OURs of ATAD systems. In other words, more work is necessary to identify the optimal aeration strategy.

- *Reaction time.* Shorter reaction times would lead to the avoidance of oxygen-limited conditions, reduction of the thermal shock, and greater plant capacities (Csikor et al., 2002). Reaction times influence the ultimate product quality in terms of stabilisation and pasteurisation (Ponti et al., 1995a). Nonetheless and due to operating convenience, batch times are set by default to a 24-hour interval. As a result, both stabilisation and pasteurisation levels at the end of the reaction generally exceed legal requirements. These excessively long reaction times result in increased energy requirements. On the other hand, Scisson (2003) claimed that the 23-hr reaction time of two-stage ATAD systems is insufficient and can lead to poor stabilisation and odours. Obviously, there is no consensus on what the optimal reaction time is.

- *Sludge flowrate.* The sludge flowrate has been found to influence sludge stabilisation, with higher frequencies leading to higher sludge oxidation rates due to smaller fluctuations of process conditions (Ponti et al., 1995a). Therefore, continuous operation could display the high degradation potential of ATAD (Ponti et al., 1995b). Further advantages of continuous operation are the avoidance of oxygen-limited conditions, thermal shock reduction, and increased plant capacity (Csikor et al., 2002). But most importantly, the sludge flowrate influences the energy requirement of ATAD (Ponti et al., 1995b). In spite of these advantages and because of operating convenience, ATAD systems generally

make use of one single volume change per day, thus not allowing a complete exploitation of the thermophiles' efficiency (Ponti et al., 1995a).

- *Influent temperature.* Conventional ATAD systems make use of poor temperature regulation sometimes requiring heating and cooling loops (Scisson, 2003). Furthermore, daily loading of the reactors with cold raw sludge results in a thermal shock that significantly decreases reactors' temperatures. The use of heat integration could lead to smaller thermal shocks and lower operating cost, and it could even be necessary if sludge concentrations are not sufficiently high to sustain thermophilic temperatures (USEPA, 1990). Pre-heating the cold influent sludge with the effluent sludge by means of sludge-to-sludge heat exchangers would reduce the thermal shock, and potentially result in shorter HRTs (Layden et al., 2007b); in turn, shorter reaction times would lead to lower energy requirements. A similar effect might be achieved by recovering heat from exhaust gas streams. In spite of this, very few plants have been reported to make use of heat integration (USEPA, 1990; Layden et al., 2007b).

In the light of these considerations, several researchers agree on the need to identify the optimal operating conditions of ATAD systems (LaPara and Alleman, 1999; Layden et al., 2007a). However, as yet there is no single study in the available literature devoted to the optimisation of the ATAD reaction.

## 3.2 Objectives

Given the lack of optimisation and the rudimentary understanding of ATAD systems, the objectives of this investigation are:

- To minimise the energy requirement of air-driven ATAD systems by altering the operating conditions while complying with effluent quality standards.

- To gain insight into the operating, structural, and scheduling factors influencing both energy requirement and plant capacity of ATAD systems through simulation studies.

- To develop a dynamic model of the ATAD reaction to aid in the aforementioned simulation and optimisation tasks.
- To gain insight into the reaction process and its inner workings.
- To pave the way for the structural optimisation of ATAD systems.

# Chapter 4

# Modeling of ATAD

## 4.1 Introduction

For a general introduction to dynamical systems, the reader is referred to Strogatz (2001). The branch of dynamical systems deals with the laws of movement or change in terms of the forces that produce such changes. The word "dynamics" comes from the Greek root "dynamis" meaning "power" or "force". Thus, in terms of the general language, dynamical systems could be thought of as processes compelled by a force of necessity which drives the system into different states. In the case of wastewater treatment, this force is a metabolic one resulting from simultaneous catabolic and anabolic activities that are *necessary* to keep the organism alive. This activity involves, on the one hand, the breakdown of complex molecules into simpler ones while producing energy (catabolism), and, on the other hand, the synthesis of complex cell material from simple molecules (anabolism).

The most widely used model for simulation of activated sludge processes is the Activated Sludge Model No. 1, also known as ASM1, IAWQ model, IAWPRC model, etc. This model was developed in the 1980s by Henze et al. (1987). A more recent account of the whole family of Activated Sludge Models can be found in Henze et al. (2000).

Since its first publication, the ASM1 model has been extensively used as a basis for subsequent developments. It incorporates carbon oxidation, nitrification, and

denitrification. However, before going into the model, it is important to understand the conventional way of presentation of these dynamical models in the field of wastewater treatment. This form of presentation facilitates the understanding of the interplay of kinetic forces underlying these dynamical systems.

Generally, this method of presentation includes the reaction components and the processes involved in the conversion of such components. A *component* is any of the fundamental constituent parts of the overall system that are relevant to the reaction, while a *process* is understood as any action involving changes in the system components. The method then quantifies both kinetics and stoichiometry of the different processes. In this context, kinetics refers to the dependence of process rates on the individual components' concentrations, while stoichiometry quantifies the existing relationship of proportionality between components along these processes.

In order to convey all this information with clarity and brevity, the matrix format suggested by Petersen (1965) is conventionally used. The use and meaning of this format can be illustrated through a simple example.

By considering the growth of heterotrophic microorganisms under aerobic conditions, we can see that two fundamental processes take place: biomass concentration increases as a result of cell growth, and it decreases due to decay. Even though other actions take place, such as oxygen and substrate consumption, these are not deemed to be fundamental processes as they depend ultimately on cell growth and decay. Thus, the simplest model for this particular reaction has to incorporate the concentrations of three components: biomass, dissolved oxygen, and substrate. The matrix format presenting the relevant kinetic and stoichiometric information for this particular reaction can be seen in Table 4.1.

The three system components, biomass $X_B$, substrate $S_S$, and dissolved oxygen $S_O$, are located in the upper row, while the two processes, bacterial growth and decay, are listed in the leftmost column. Following IAWPRC notation, insoluble components are denoted with $X$ and soluble components with $S$ (Grau et al., 1982). The subscripts denote the component, that is, $B$ stands for biomass, $S$ for substrate, and $O$ for oxygen. Each component is assigned an index $i$ which in this simple example takes the values 1 to 3. Kinetic expressions or process rates, denoted by

Table 4.1: Petersen matrix of reaction concerning heterotrophic bacterial growth under aerobic conditions. Adapted from Henze et al. (2000).

| Component $i \rightarrow$<br>Process $j \downarrow$ | 1<br>$X_B$ | 2<br>$S_S$ | 3<br>$S_O$ | Process rate, $\rho_j$<br>($\mathrm{ML^{-3}T^{-1}}$) |
|---|---|---|---|---|
| 1 Growth | 1 | $-\frac{1}{Y}$ | $-\frac{1-Y}{Y}$ | $\mu \frac{S_S}{K_S+S_S} X_B$ |
| 2 Decay | -1 | | -1 | $bX_B$ |
| Observed conversion rates ($\mathrm{ML^{-3}T^{-1}}$) | $r_i = \sum_j r_{ij} = \sum_j \nu_{ij}\rho_j$ | | | |
| Stoichiometric parameters: True growth yield, $Y$ | Biomass($\mathrm{ML^{-3}}$) | Substrate ($\mathrm{ML^{-3}}$) | Oxygen ($\mathrm{ML^{-3}}$) | Kinetic parameters: maximum specific growth rate $\mu$, half-velocity constant $K_S$, specific decay rate $b$ |

$\rho_j$, are found in the rightmost column. The process rate $\rho_1$ states that bacterial growth depends on biomass concentration in a first order manner, while it depends on substrate in a mixed order manner. Similarly, the process rate $\rho_2$ states that bacterial decay depends on biomass concentration in a first order manner. Kinetic parameters are found in the lower right corner of the matrix.

The expressions inside the matrix are the stoichiometric coefficients $\nu_{ij}$ which set the quantitative relationships or proportionalities between the components along the different processes. Blank spaces are understood as having stoichiometric coefficients with value zero. In this example, a certain amount of substrate ($-\frac{1}{Y}$) and oxygen ($-\frac{1-Y}{Y}$) is used to produce a proportional amount of biomass (+1). The stoichiometric coefficients are often defined in such a way that they are expressed in oxygen-equivalent units, that is, as chemical oxygen demand (COD). Additionally, the convention is to express the production of COD as positive and consumption as negative. Oxygen is considered as a negative oxygen demand. Stoichiometric coefficients can be found in the lower left corner of the matrix.

One of the advantages of the Petersen matrix is that it allows to quickly determine the fate of the different components. This can be done by going downwards in any column corresponding to a component. The reaction rate $r_i$ for component $i$ can then be obtained following the sum of products of stoichiometric coefficients and

their corresponding process rates, as shown by Equation 4.1.

$$r_i = \sum_j \nu_{ij} \rho_j \tag{4.1}$$

If no transport (advective) terms are considered, this equation gives the mass balance for component $i$. In our example, the reaction rates for biomass, substrate, and oxygen are given by Equations 4.2, 4.3, and 4.4, respectively.

$$r_{X_B} = \frac{\mu S_S}{K_S + S_S} X_B - b X_B \tag{4.2}$$

$$r_{S_S} = -\frac{1}{Y} \frac{\mu S_S}{K_S + S_S} X_B \tag{4.3}$$

$$r_{S_O} = -\frac{1 - Y}{Y} \frac{\mu S_S}{K_S + S_S} X_B - b X_B \tag{4.4}$$

Note that in this notation $r_i = \dot{x_i} = \frac{dx_i}{dt}$, where $x_i$ is component $i$. That is, $r_{X_B} = \dot{X_B} = \frac{dX_B}{dt}$, and so on.

Even though advective terms have not been accounted for in this example, they are a very important aspect of the physical system as a whole. They represent the system boundary (or "input") and generally determine the time-dependent behaviour of the system in question.

An additional advantage of the Petersen matrix is the possibility to test the continuity of mass within the system. This can be done by moving from the left to the right in any row corresponding to a process. In doing so, the sum of the stoichiometric coefficients in each row must equal zero. In the case of the decay process, any amount of COD in the form of lysed cell material will result in a proportional amount of oxygen being used (remember that the coefficient of oxygen has to be multiplied by $-1$). In the case of the growth process, the amount of biomass COD resulting from growth equals the amount of substrate COD removed from solution plus the proportional amount of oxygen needed for cell synthesis.

### 4.1.1 Activated Sludge Model No. 1

The Activated Sludge Model No. 1 or ASM1 includes a total of 13 variables: seven carbonaceous compounds, four nitrogenous compounds, oxygen, and alkalinity (Henze et al., 1987, 2000).

Organic matter is often subdivided into different categories based on biodegradability and solubility. The non-biodegradable fraction of organic matter is biologically inert, that is, it goes through the reaction without undergoing any change. Inert organic matter can be further subdivided into two subcategories based on its solubility: a soluble and a particulate fraction. Inert soluble organic matter is denoted with $S_I$ and inert suspended organic matter with $X_I$.

The biodegradable fraction of organic matter is also further subdivided into two types: readily biodegradable and slowly biodegradable matter. Readily biodegradable matter $S_S$ is considered to be soluble, while slowly biodegradable matter $X_S$ is considered to be particulate (however, this is not always the case). Readily biodegradable matter is made of simple molecules that are small enough to pass the cell walls. This type of molecules is used by the cell to produce new tissue and to generate energy needed for cell maintenance. On the other hand, slowly biodegradable matter is made of complex molecules that are too large to pass the cell walls and thus need to be broken down first into slowly biodegradable matter. The cells bring about this conversion by releasing enzymes into the extracellular space. This conversion, known as *hydrolysis*, apparently does not require the use of energy.

As the specific hydrolysis rate of slowly biodegradable matter tends to be lower than the half-velocity constant of readily biodegradable matter, hydrolysis is generally the limiting factor for biomass growth (as long as $X_S$ is the only form of substrate present). The hydrolysis rate is higher under aerobic conditions than under anoxic conditions, and it becomes almost zero under anaerobic conditions.

Yet another form of organic matter is in the form of heterotrophic biomass $X_B$ which grows at the expense of readily biodegradable matter. Its growth takes place under both aerobic and anoxic conditions and it gradually ceases as the environment

becomes anaerobic. Biomass concentration decreases as a result of decay which may be due to endogenous metabolism, death, predation, or lysis. Through the process of decay, biomass is transformed into slowly biodegradable matter and another type of inert particulate matter $X_P$ that cannot be degraded by the heterotrophs.

Another kind of matter included in the ASM1 model are the nitrogenous compounds. These, too, can be divided into two categories: biodegradable and non-biodegradable. Non-biodegradable nitrogenous matter is again subdivided into soluble and particulate. However, as the soluble fraction is very low compared to the particulate fraction, it is not included in the model. On the other hand, the biodegradable nitrogenous fraction incorporates ammonia $S_{NH}$, soluble organic nitrogen $S_{ND}$, and particulate organic nitrogen $X_{ND}$. The latter undergoes hydrolysis thus being converted into soluble organic nitrogen. Soluble organic nitrogen is, in turn, transformed into ammonia nitrogen by heterotrophic bacteria. Ammonia nitrogen is then used by heterotrophic bacteria for cell synthesis and by autotrophic nitrifying bacteria as source of energy for cell synthesis and maintenance. Under aerobic conditions, autotrophic bacteria transform ammonia nitrogen into nitrate nitrogen $S_{NO}$; the latter can be used under anoxic conditions by heterotrophic bacteria as electron acceptor eventually producing nitrogen gas. Through the decay of both autotrophs and heterotrophs, particulate organic nitrogen is released into solution which can be hydrolysed, starting the cycle again.

Table 4.2 shows the Petersen matrix of the ASM1 model. The inert components $X_i$ and $S_i$ in columns 1 and 3 do not take part in any conversion as can be seen from their zero value stoichiometric coefficients. Yet they are important for wastewater characterisation as well as for the overall performance of the activated sludge process.

In column 2, it can be seen that the concentration of readily biodegradable matter $S_S$ decreases through both aerobic and anoxic growth of heterotroph bacteria, and increases through hydrolysis of slowly biodegradable organic matter. Conversely, the concentration of slowly biodegradable organic matter $X_S$ decreases through hydrolysis and increases via decay of heterotrophic and autotrophic bacteria.

Columns 5 and 6 stand for the two forms of biomass considered in this model: heterotrophic biomass $X_{B,H}$ and autotrophic biomass $X_{B,A}$. The concentration of

Table 4.2: Petersen matrix of Activated Sludge Model No. 1. Adapted from (Henze et al., 2000).

| $j$ | Component $i$ → Process ↓ | 1 $S_I$ | 2 $S_S$ | 3 $X_I$ | 4 $X_S$ | 5 $X_{B,H}$ | 6 $X_{B,A}$ | 7 $X_P$ | 8 $S_O$ | 9 $S_{NO}$ | 10 $S_{NH}$ | 11 $S_{ND}$ | 12 $X_{ND}$ | 13 $S_{ALK}$ | Process rate, $\rho_j$ |
|---|---|---|---|---|---|---|---|---|---|---|---|---|---|---|---|
| 1 | Aerobic growth of heterotrophs | | $-\frac{1}{Y_H}$ | | | 1 | | | $\frac{Y_H-1}{Y_H}$ | | $-i_{XB}$ | | | $-\frac{i_{XB}}{14}$ | $\mu_H \frac{S_S}{K_S+S_S} \frac{S_O}{K_{O,H}+S_O} X_{B,H}$ |
| 2 | Anoxic growth of heterotrophs | | $-\frac{1}{Y_H}$ | | | 1 | | | | $-\frac{1-Y_H}{2.86Y_H}$ | $-i_{XB}$ | | | $\frac{1-Y_H}{14\cdot 2.86Y_H} - \frac{i_{XB}}{14}$ | $\mu_H \frac{S_S}{K_S+S_S} \frac{K_{O,H}}{K_{O,H}+S_O} \times \frac{S_{NO}}{K_{NO}+S_{NO}} \eta_g X_{B,H}$ |
| 3 | Aerobic growth of autotrophs | | | | | | 1 | | $\frac{Y_A-4.57}{Y_A}$ | $\frac{1}{Y_A}$ | $-i_{XB}-\frac{1}{Y_A}$ | | | $-\frac{i_{XB}}{14} - \frac{1}{7Y_A}$ | $\mu_A \frac{S_{NH}}{K_{NH}+S_{NH}} \times \frac{S_O}{K_{O,A}+S_O} X_{B,A}$ |
| 4 | Decay of heterotrophs | | | | $1-f_P$ | $-1$ | | $f_P$ | | | | | $i_{XB} - f_P i_{XP}$ | | $b_H X_{B,H}$ |
| 5 | Decay of autotrophs | | | | $1-f_P$ | | $-1$ | $f_P$ | | | | | $i_{XB} - f_P i_{XP}$ | | $b_A X_{B,A}$ |
| 6 | Ammonification of soluble organic nitrogen | | | | | | | | | | 1 | $-1$ | | $\frac{1}{14}$ | $k_a S_{ND} X_{B,H}$ |
| 7 | Hydrolysis of entrapped organics | | 1 | | $-1$ | | | | | | | | | | $k_H \frac{X_S/X_{B,H}}{K_X+X_S/X_{B,H}} \times [\frac{S_O}{K_{O,H}+S_O} + \eta_h \frac{K_{O,H}}{K_{O,H}+S_O} \frac{S_{NO}}{K_{NO}+S_{NO}}] \times X_{B,H}$ |
| 8 | Hydrolysis of entrapped organics | | | | | | | | | | | 1 | $-1$ | | $\rho_7 X_{ND}/X_S$ |
| | Observed conversion rates ($ML^{-3}T^{-1}$) | $r_i = \sum_j r_{ij} = \sum_j \nu_{ij}\rho_j$ | | | | | | | | | | | | | Stoichiometric[a] and kinetic[b] parameters |

[a]Stoichiometric parameters: heterotrophic yield $Y_H$, autotrophic yield $Y_A$, fraction of biomass yielding particulate products $f_P$, mass N/Mass COD in biomass $i_{XB}$, mass N/Mass COD in products from biomass $i_{XP}$

[b]Kinetic parameters: heterotrophic growth and decay $\mu_H$, $K_S$, $K_{O,H}$, $K_{NO}$, $b_H$; autotrophic growth and decay $\mu_A$, $K_{NH}$, $K_{O,A}$, $b_A$; correction factor for anoxic growth of heterotrophs $\eta_g$, ammonification $k_a$, hydrolysis $k_h$, $K_X$, correction factor for anoxic hydrolysis $\eta_h$

heterotrophic biomass increases through aerobic and anoxic growth and decreases via decay. Similarly, the concentration of autotrophic biomass increases through aerobic growth and decreases with autotrophic decay.

Column 7 corresponds to the particulate products $X_P$ that result from biomass decay. Its concentration increases with the decay of both heterotrophic and autotrophic bacteria. As this form of matter is not subject to significant bacterial attack, its concentration can only increase and it is thus accumulated in the course of the reaction.

The column 8 represents the concentration of dissolved oxygen (DO) $S_O$ in the sludge. As can be seen from the matrix, it decreases through aerobic growth of heterotrophic and autotrophic bacteria. The advective (transport) terms which result in an increase of DO concentration are not included in the matrix, but they have to be included in the overall mass balance of the system.

Nitrate nitrogen $S_{NO}$ is the other electron acceptor considered in the ASM1 model. Column 9 shows that its concentration increases due to aerobic growth of autotrophic biomass and decreases with anoxic growth of heterotrophic bacteria.

Ammonia nitrogen $S_{NH}$ can be found in column 10. It is assumed to be the combination of ionised ammonium and un-ionised ammonia. The latter, however, has generally a very low concentration. Thus, it is satisfactory to consider exclusively the ammonium fraction. Its concentration increases with the ammonification of soluble organic nitrogen and decreases with the growth of heterotrophs and autotrophs.

Soluble organic nitrogen $S_{ND}$ is represented in column 11. It increases with hydrolysis of entrapped organic nitrogen, whereas it decreases with the ammonification of soluble organic nitrogen. Its particulate counterpart $X_{ND}$ in column 12 is formed via decay and removed through hydrolysis.

The first 12 components of the model are deemed to be essential to accurately simulate carbon oxidation, nitrification, and denitrification in an activated sludge system. Thus, they represent the lowest admissible quantity of variables needed to model these three interconnected processes.

The VS concentration in COD units can be calculated as the summation of the particulate components $X_S$, $X_{B,H}$, $X_{B,A}$, $X_P$, and $X_I$. It can be transformed to VS

units by using an appropriate conversion factor that will be denoted here by $f_{COD}$. Its value will be assumed to be 1.42 g of $O_2$ per g of VS destroyed (USEPA, 1990).

The last variable of the model is the total alkalinity $S_{ALK}$ shown in column 13. Although not essential, its incorporation into the model allows the prediction of changes in pH that could have adverse effects upon the process.

As for the processes which act upon the aforementioned components, four are included in the ASM1 model: biomass growth (aerobic and anoxic; heterotrophic and autotrophic), biomass decay (heterotrophic and autotrophic), ammonification of soluble organic nitrogen, and hydrolysis of entrapped organics. These processes can be found in the leftmost column of the matrix and their respective process rates in the rightmost column.

As pointed out before, biomass is assumed to grow at the expense of readily biodegradable matter. On the other hand, slowly biodegradable matter is taken from suspension and captured in the biofloc. This process is assumed to take place instantaneously. Being trapped in the biofloc, slowly biodegradable matter is transformed into readily biodegradable matter through a set of extracellular reactions carried out by enzymes. This set of reactions, or hydrolysis, results basically in a delay of oxygen uptake. The decay process, in turn, is assumed to transform lysed cell material into inert particulate matter as well as slowly biodegradable matter which can be subsequently hydrolysed, thus re-entering the cycle.

As it can be seen from the process rate expressions, the kinetics of some processes can be limited by low nutrient concentrations. For example, aerobic growth of heterotrophic bacteria in row 1 is limited by the concentration of readily biodegradable matter and DO. This amounts to saying that the growth of aerobic heterotrophic bacteria is inhibited under substrate limitation and/or anaerobic conditions. Or, in other words, aerobic heterotrophic growth will approach zero as the concentration of any of these two nutrients approaches zero. Thus, in some particular cases the reaction might be limited by the concentration of substrate and in other cases by that of DO. Such rate-limiting effect (as it is indeed observed during experiments) is the purpose of the inclusion of the so-called "switching functions" in the model. As consistent COD units have been used for the systems components and mass

Table 4.3: Typical values of stoichiometric and kinetic parameters of ASM1 model at 10 °C and 20 °C. Adapted from Henze et al. (2000).

| Parameter | Unit | Value at 10 °C | Value at 20 °C |
|---|---|---|---|
| *Stoichiometric* | | | |
| $Y_A$ | g cell COD formed (g N oxidised)$^{-1}$ | 0.24 | 0.24 |
| $Y_H$ | g cell COD formed (g COD oxidised)$^{-1}$ | 0.67 | 0.67 |
| $f_P$ | dimensionless | 0.08 | 0.08 |
| $i_{XB}$ | g N(g COD)$^{-1}$ in biomass | 0.086 | 0.086 |
| $i_{XE}$ | g N(g COD)$^{-1}$ in endogenous mass | 0.06 | 0.06 |
| *Kinetic* | | | |
| $\mu_H$ | day$^{-1}$ | 3.0 | 6.0 |
| $K_S$ | g COD m$^{-3}$ | 20.0 | 20.0 |
| $K_{O,H}$ | g $O_2$ m$^{-3}$ | 0.20 | 0.20 |
| $K_{NO}$ | g $NO_3$-N m$^{-3}$ | 0.50 | 0.50 |
| $b_H$ | day$^{-1}$ | 0.20 | 0.62 |
| $\eta_g$ | dimensionless | 0.8 | 0.8 |
| $\eta_h$ | dimensionless | 0.4 | 0.4 |
| $k_h$ | g of $X_S$ in COD (g cell COD $\cdot$ day)$^{-1}$ | 1.0 | 3.0 |
| $K_X$ | g of $X_S$ in COD (g cell COD)$^{-1}$ | 0.01 | 0.03 |
| $\mu_A$ | day$^{-1}$ | 0.3 | 0.8 |
| $K_{NH}$ | g $NH_3$-N m$^{-3}$ | 1.0 | 1.0 |
| $K_{O,A}$ | g $O_2$ m$^{-3}$ | 0.4 | 0.4 |
| $k_a$ | m$^3\cdot$ COD(g$\cdot$day)$^{-1}$ | 0.04 | 0.08 |

continuity is required, the quantity of oxygen consumed equals the amount of new synthesized biomass minus the soluble substrate used for growth. A similar reading and interpretation can be made for the remaining processes and process rate expressions (see Henze et al. (2000)).

The values of most of the stoichiometric and kinetic parameters do not fluctuate greatly for different wastewaters. Table 4.3 displays the typical values of these parameters.

Finally, it is worth considering the most important assumptions under which the model holds and remains a good approximation:

- *Complete sludge mixing.* From this assumption follows the homogeneity of the sludge, and it amounts to saying that any two sub-volumes of sludge within the system will have the same qualities in terms of their components at any given time.

- *Constant temperature.* The model as presented in Table 4.2 and 4.3 assumes constant temperatures. If temperature changes were to be allowed, this would

have to be reflected in the form of kinetic and stoichiometric parameters with an explicit temperature dependence.

- *Constant and neutral pH.*
- *No changes in the nature of organic matter within a given component.*
- *No changes in the nature of the biomass.* The nature of heterotrophic bacteria remains the same and does not experience changes in its diversity with time. This assumption is implied in the fact of having constant kinetic parameters.

### 4.1.2 ATAD models in the literature

Over the last three decades, considerable progress has been made in the field of wastewater modeling and simulation. These efforts have resulted in the family of the so-called Activated Sludge Models (Henze et al., 2000). Nowadays, this family of models sets the standard for wastewater modeling and simulation.

Nonetheless, much less effort has been devoted to the modeling of thermophilic processes, such as ATAD, composting, etc. Generally speaking, these processes have received considerably less attention.

In the particular case of ATAD, the first dynamic model was perhaps that developed by Kambhu and Andrews (1969). This three dimensional model includes the concentration of biodegradable organic matter, the concentration of dissolved oxygen, and temperature. The authors used the model to make practical recommendations; however, the model was not assessed or validated against empirical data.

Given that temperature is one of the critical aspects of the ATAD reaction, several subsequent developments focused on the analysis of the energy balance and its implications (Jewell and Kabrick, 1980; Vismara, 1985; Messenger et al., 1990; LaPara and Alleman, 1999).

However, it was not until relatively recently that dynamic ATAD models were developed based on the standard Activated Sludge Models (Kovacs et al., 2007a; Gomez et al., 2007). These models are extensions of the ASM1 at thermophilic

temperatures.

Gomez et al. (2007) developed a model consisting of a liquid phase and a gas phase which include a total of 22 state variables. Twenty of these variables are mass components. The remaining two variables are the total enthalpy of the liquid phase and that of the the gas phase. Some mass components are defined in both phases to ensure that mass continuity is satisfied. Both phases have their own mass and energy balances. An important drawback of this model is the fact that it uses parameter values from the ASM1 model which are not likely to be valid at thermophilic temperatures.

Kovacs et al. (2007a) developed a simpler model consisting of a single liquid phase which contains a total of nine mass balance components. An important drawback of this model is that it lacks an energy balance. Its lower dimensionality shows that this model only incorporates the essential processes and components. These researchers obtained the values of thermophilic kinetic and stoichiometric parameters and their temperature dependence by fitting experimental data to the model at different temperatures.

## 4.2 Proposed ATAD model ATM1

As stated in Chapter 3, the main objective of this thesis is to optimise the energy efficiency of ATAD systems. For this purpose, a dynamic model of the ATAD reaction is necessary. To this end, however, the aforementioned two models are inadequate in their original form.

The model developed by Gomez et al. (2007) is too complex for our objectives. Such complexity renders the model computationally inefficient. Moreover, most of the variables in this model do not have any effect on the two treatment goals, i.e. stabilisation and pasteurisation. Thus, it seems that such level of complexity is not warranted for the sake of continuity (at least for our particular objective). On the other hand, this model includes a detailed energy balance which most of the other models lack.

The model developed by Kovacs et al. (2007a) lacks an energy balance thus not

allowing the prediction of temperature changes. As temperature has a critical effect on both pasteurisation and stabilisation, this model cannot be used in its original form either. Yet, this model contains the main processes from the ASM1 model affecting stabilisation and pasteurisation, without superfluous variables or processes. It additionally contains the specific values of the kinetic and stoichiometric parameters at thermophilic temperatures.

So, both models have advantages and disadvantages. Thus, it is proposed here to combine the strengths of the two: the mass balances and model parameters from Kovacs et al. (2007a) with the energy balance from Gomez et al. (2007).

In analogy to IWA nomenclature, the resulting ATAD model will be called henceforth ATAD Model No. 1 or ATM1.

### 4.2.1 Mass balance

The conceptual mass balance of the model proposed by Kovacs et al. (2007a), as inherited from the ASM1 model, is that of a cycle of life and death. This cycle, first proposed by Dold et al. (1980), is more commonly known as the death-regeneration concept. One important modification with regard to the ASM1 model is the subdivision of biomass into mesophilic and thermophilic biomass. The other important modification is the inclusion of an activation process of inactive thermophilic biomass.

The conceptual structure of the mass balance is shown in Figure 4.1. It can be seen that the overall structure consists of two life cycles: the mesophilic and the thermophilic cycle. The solid black line corresponds to the mesophilic life cycle. This cycle corresponds to that found in the ASM1 model. It involves three processes: growth of mesophilic biomass at the expense of oxygen and readily biodegradable organic matter; biomass decay resulting in the release of inert particulate products and slowly biodegradable organic matter; and hydrolysis of slowly biodegradable organic matter into readily biodegradable organic matter that can be used for further growth, thus re-entering the cycle. The red dashed line corresponds to the thermophilic life cycle. It can be seen that this cycle involves basically the same processes as the mesophilic cycle with one difference: the activation of thermophilic

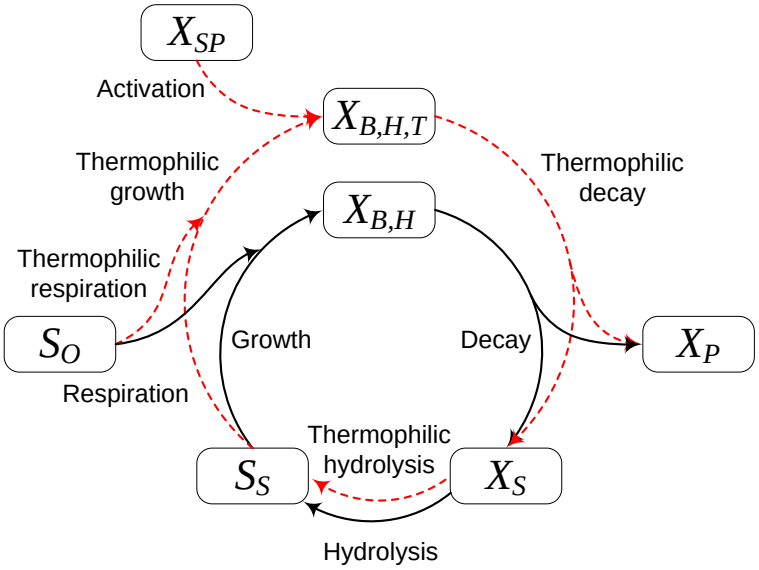


Figure 4.1: Death-regeneration concept (conceptual mass balance) for ATAD reaction consisting of mesophilic (black solid line) and thermophilic (red dashed line) life cycles. Adapted from Kovacs et al. (2007a).

inactive biomass. This activation process, first proposed by Crabb et al. (1975), involves the adaptation of facultative thermophilic bacteria which after a certain period of time become part of the active thermophilic biomass.

Note that the processes of nitrification and denitrification present in the ASM1 model have not been included in this model. This is due to the inhibition of nitrifying bacteria as a result of the high operating temperatures. Hence, the model only considers carbon oxidation.

The reaction rates for the nine mass components can be obtained from the Petersen's matrix shown in Table 4.4.

The values of the mesophilic stoichiometric and kinetic parameters are the same as those from the ASM1 model (except for the specific growth, decay, and hydrolysis rates whose temperature dependence is given below). On the other hand, Kovacs et al. (2007a) describe the temperature dependence of the thermophilic kinetic parameters through modified Arrhenius and Topiwala-Sinclair expressions (Topiwala and Sinclair, 1971). The modification consists of the introduction of a relative, instead of an absolute, scale with a minimum temperature where bacterial activity ceases. This minimum temperature is taken to be 0 °C for mesophilic and 30 °C for

Table 4.4: Petersen matrix of ASM1-based ATM1 model. Adapted from Kovacs et al. (2007a).

| | Component $i \rightarrow$ | 1 | 2 | 3 | 4 | 5 | 6 | 7 | 8 | 9 | |
|---|---|---|---|---|---|---|---|---|---|---|---|
| $j$ | Process $\downarrow$ | $S_I$ | $S_S$ | $X_I$ | $X_S$ | $X_{SP}$ | $X_{B,H}$ | $X_{B,H,T}$ | $X_P$ | $S_O$ | Process rate, $\rho_j$ |
| 1 | Aerobic growth of mesophiles | | $\frac{-1}{Y_H}$ | | | | 1 | | | $\frac{Y_H-1}{Y_H}$ | $\mu_H \frac{S_S}{K_S+S_S} \frac{S_O}{K_O+S_O} X_{B,H}$ |
| 2 | Aerobic growth of thermophiles | | $\frac{-1}{Y_{H,T}}$ | | | | | 1 | | $\frac{Y_{H,T}-1}{Y_{H,T}}$ | $\mu_{H,T} \frac{S_S}{K_{S,T}+S_S} \frac{S_O}{K_{O,T}+S_O} X_{B,H,T}$ |
| 3 | Mesophilic decay | | | | $1-f_P$ | | $-1$ | | $f_P$ | | $b_H X_{B,H}$ |
| 4 | Thermophilic decay | | | | $1-f_{P,T}$ | | | $-1$ | $f_{P,T}$ | | $b_{H,T} X_{B,H,T}$ |
| 5 | Mesophilic hydrolysis | | 1 | | -1 | | | | | | $k_H \frac{X_S/X_{B,H}}{K_X+X_S/X_{B,H}} \frac{S_O}{K_O+S_O} X_{B,H}$ |
| 6 | Thermophilic hydrolysis | | 1 | | -1 | | | | | | $k_{H,T} \frac{X_S/X_{B,H,T}}{K_{X,T}+X_S/X_{B,H,T}} \frac{S_O}{K_{O,T}+S_O} X_{B,H,T}$ |
| 7 | Activation | | | | | -1 | | 1 | | | $\mu_{SP} \frac{S_O}{K_{O,T}+S_O} X_{B,H,T}$ |
| | | Dissolved inert org. matt. | Readily biod. org. matt. | Particulate inert org. matt. | Slowly biod. org. matt. | Inactive biomass | Mesophilic biomass | Active thermophilic biomass | Inert org. matt. from decay | Dissolved oxygen | |

Table 4.5: Parameter values of Arrhenius and Topiwala-Sinclair expressions used in ATM1 model. Adapted from Kovacs et al. (2007a).

| | $T_0$ (°C) | $A$ ($d^{-1}$) | $E_a/R$ (°C) | $B$ ($d^{-1}$) | $E_b/R$ (°C) |
|---|---|---|---|---|---|
| $\mu_H$ | 0 | 73.7 | 42.9 | 201.5 | 135.6 |
| $\mu_{H,T}$ | 30 | 155.4 | 6.1 | 132.8 | 7.7 |
| $b_H$ | 0 | 1075 | 159.9 | -[a] | - |
| $b_{H,T}$ | 30 | 44.9 | 107.9 | - | - |
| $k_h$ | 0 | 42.0 | 45.6 | 12.09 | 363.8 |
| $k_{h,T}$ | 30 | 592 | 201.5 | - | - |
| $\mu_{SP,0}$ | 30 | 1.6 | 24 | 1.7 | 27.3 |
| $\mu_{SP,max}$ | 30 | 157 | 9 | 4197 | 136.8 |

[a]Where $B$ and $E_b/R$ have not been specified, the Arrhenius expression has been used instead of that of Topiwala-Sinclair.

Table 4.6: Remaining stoichiometric and kinetic parameters of thermophilic biomass in ATM1 model. Adapted from Kovacs et al. (2007a).

| Parameter | Description | Value |
|---|---|---|
| *Stoichiometric* | | |
| $Y_{H,T}$ (-) | Thermophilic yield | 0.8 |
| $f_{P,T}$ (-) | Inert fraction of thermophilic biomass | 0.2 |
| *Kinetic* | | |
| $K_{S,T}$ (mgCOD/l) | Half-saturation constant of $S_S$ | $e^{0.13 \cdot T - 2.5}$ |
| $K_{O,T}$ (g/l) | Half-saturation constant of $S_O$ | 0.17 |
| $K_{X,T}$ (-) | Half-saturation constant of hydrolysis | 6.4 |
| $\delta$ (-) | Accelerating rate of activation | 0.5 |

thermophilic parameters. The modified Arrhenius and Topiwala-Sinclair expressions are given by Equations 4.5 and 4.6, respectively:

$$\mu = A \cdot e^{-\frac{E_a}{R(T-T_0)}}, \tag{4.5}$$

$$\mu = A \cdot e^{-\frac{E_a}{R(T-T_0)}} - B \cdot e^{-\frac{E_b}{R(T-T_0)}}, \tag{4.6}$$

where $\mu$ is the maximum specific rate ($d^{-1}$) at temperature $T$ (°C), $A$ and $B$ the Arrhenius constants ($d^{-1}$), $E_a$ and $E_b$ the activation energies ($J \cdot mol^{-1}$), $R$ the ideal gas constant ($J \cdot mol^{-1} \cdot K^{-1}$), and $T$ and $T_0$ the actual and minimum temperatures (°C). The corresponding parameter values for the specific growth, decay, hydrolysis, and activation rates are displayed in Table 4.5. The remaining thermophilic kinetic and stoichiometric parameters are listed in Table 4.6.

As for the activation rate $\mu_{SP}$, it is a function of the time spent under thermophilic conditions and it can be determined as per Equations 4.7 and 4.8:

$$\frac{d\mu_{SP}}{d\tau} = \delta \cdot \mu_{SP}(\mu_{SP,max} - \mu_{SP}), \tag{4.7}$$

$$\mu_{SP}(\tau = 0) = \mu_{SP,0}, \tag{4.8}$$

where $\mu_{SP,0}$ and $\mu_{SP,max}$ represent the minimum and maximum activation rates ($day^{-1}$, see Table 4.5), $\delta$ the rapidity of change of the activation rate (dimensionless, see Table 4.6), and $\tau$ the dynamic residence time (days). The dynamic residence time is an average of the time that inactive thermophiles spend in the system. It can be calculated according to the concept of dynamic solids retention time proposed by Takacs and Patry (2002).

Equation 4.7 is not explicitly dependent on time or any of the model components and it can thus be solved independently, yielding Equation 4.9.

$$\mu_{SP} = \frac{\mu_{SP,max}}{1 + (\frac{\mu_{SP,max}}{\mu_{SP,0}} - 1) \cdot e^{-\delta \cdot \mu_{SP,max} \cdot \tau}} \tag{4.9}$$

From this equation we see the qualitative time-dependent character of the activation rate: activation is slowest immediately after the feed; it then accelerates as time under thermophilic conditions increases, until a maximum value is reached. Kovacs et al. (2007b) suggested that this behavior is due to the enzymatic nature of the activation process: at the beginning of the activation phase, the amount of thermotolerant enzymes synthesized by facultative thermophiles is relatively low. Consequently, activation is slow. As time under thermophilic conditions increases, the amount of thermotolerant enzymes also increases and activation accelerates. Once all the enzymes taking part in the activation process have become thermostable, the activation rate reaches a maximum and it cannot further increase.

As it was the case with the ASM1 model, mass continuity can also be checked by adding the stoichiometric coefficients in Table 4.4 while remembering that oxygen is considered to be negative COD.

The rate of change $r_i$ of component $i$ is then determined by the sum of the reaction and transport terms as shown by

$$r_i = \sum_j \nu_{ij}\rho_j + In(x_i) - Out(x_i), \tag{4.10}$$

where $\nu_{ij}$ is the stoichiometric coefficient of component $i$ along process $j$ (g COD/g COD), $\rho_j$ the rate of process $j$ (g/l·day), and $In(x_i)$ and $Out(x_i)$ the influent and effluent mass flowrates of component $i$ at time $t$ (g/l·day), respectively.

### 4.2.2 Energy balance

As mentioned before, the energy balance proposed in our ATM1 model is a modification of the energy balance presented by Gomez et al. (2007). The latter includes a liquid-solid phase and a gas phase in interaction by means of energy and mass transfer, and each with its corresponding components and energy sinks and sources as shown in Figure 4.2a. The liquid-solid phase has four heat sources: mechanical mixing, flow of influent sludge, biological metabolism, and condensation of water vapor. Conversely, it has three heat sinks: evaporation, flow of effluent sludge, and conduction through the reactor walls. On the other hand, the gas phase has two heat sources, flow of influent gas and evaporation, and two heat sinks, flow of effluent gas and condensation. Gomez et al. (2007) argue that the gas phase has to be considered because the partial pressure of some gases can have an effect on the pH of the sludge.

This argument, however, has two flaws. First, the pH in ATAD systems, contrary to other sludge treatment processes, does *not* vary significantly due to the inhibition of the nitrification process (pH∼7–8, see Table 2.5). Second, there is no evidence that such small changes in the pH of the sludge have any effect on either sludge pasteurisation or stabilisation, the two processes that have to be modeled. For these reasons, the gas phase was excluded from the ATM1 model presented here. Another important reason for the elimination of the gas phase as proposed by Gomez et al. (2007) is that it includes four gaseous components which are irrelevant to the stabilisation and pasteurisation processes to be modeled. Thus, by eliminating

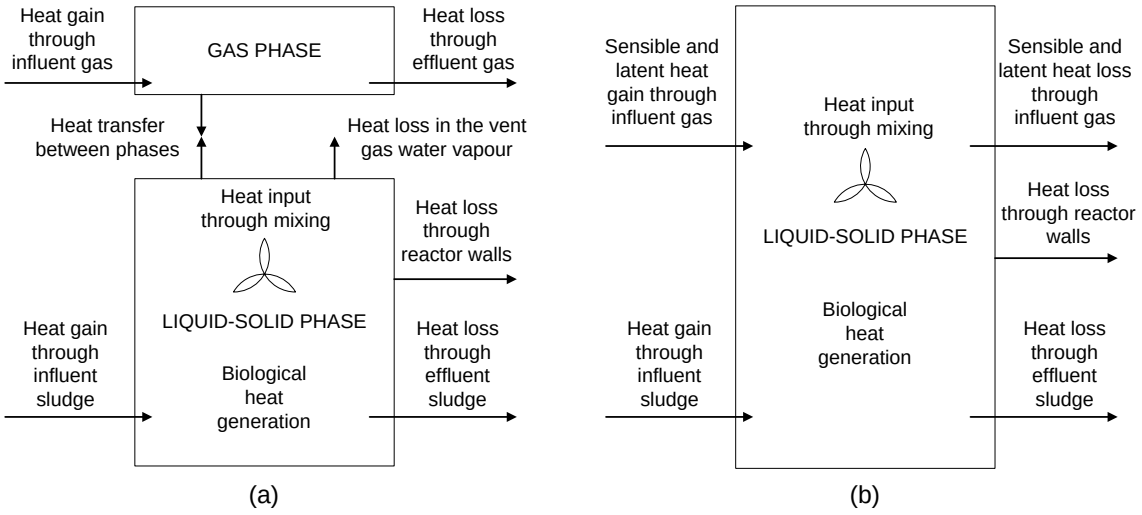


Figure 4.2: Conceptual energy balance of an ATAD reactor as proposed (a) by Gomez et al. (2007), and (b) in our ATM1 model.

the gas phase, these superfluous variables are also eliminated from the model. This simplification results, in turn, in higher computational efficiency when implementing the model.

The conceptual energy balance proposed in our ATM1 model is illustrated in Figure 4.2b. As mentioned before, the main modification from the concept proposed by Gomez et al. (2007) is that it only includes a liquid-solid phase. There are four heat sources: mechanical mixing, biological metabolism, flow of influent sludge, and flow of influent gas. Conversely, there are three heat sinks: conduction through reactor walls, flow of effluent sludge, and flow of effluent gas.

The sludge stream is operated in a semi-batch mode (for just about 1 hour per day) and entails a net loss of sensible heat, while the gas stream is continuous and entails a net loss of both sensible and latent heat. Thus, the gas stream generally represents the greatest heat sink in the system, being around 30% larger than the amount of heat lost through the sludge stream (Warakomski et al., 2007). In this context, it should be noted here that another important drawback of the energy balance proposed by Gomez et al. (2007) is that it does not account for latent heat loss through the gas stream. In our proposed energy balance we have included both sensible and latent heat in the gas stream.

The consideration of the gas stream in the energy balance is, hence, critical. At

first, one may be lead to think that a separate gas phase is necessary in order to account for the gas stream. Nevertheless, this is not really the case. In order to justify the previous statement, let us consider the following two observations made in a full-scale ATAD plant:

1. The gas phase is always saturated with water vapor. In other words, the relative humidity $RH$ of the gas phase is always 100%, i.e. $RH = 1\ \forall t$.

2. The temperature of the gas phase $T_g$ is always equal to the temperature of the liquid phase $T_l$, i.e. $T_g = T_l\ \forall t$.

Based on these observations, it is reasonable to assume the following:

i At any given time $t$, a net latent heat loss through the gas stream will result in an *instantaneous* enthalpy loss in the liquid phase. This follows from observation (1) that the gas phase is permanently saturated with water vapor, despite the fact that the gas stream is constantly replacing saturated gas with non-saturated ambient air; or in other words, because the thermal equilibrium between the gas phase and the liquid phase is established instantaneously. That is, we can assume that the saturation of the influent air takes place *instantaneously*, thus having an immediate effect upon the liquid phase in form of enthalpy loss. Hence, we can write $dH_l/dt \propto Q_{lat}^{in} - Q_{lat}^{out}$, where $H_l$ is the total enthalpy of the liquid phase, and $Q_{lat}^{in}$ and $Q_{lat}^{out}$ the latent heat of the influent and effluent gas stream, respectively.

ii Similarly, at any given time $t$, a net sensible heat loss through the gas stream will result in an *instantaneous* enthalpy loss in the liquid phase. This follows from observation (2) that the temperature of the liquid phase always equals that of the gas phase, despite the fact that air at temperature $T_l$ is constantly being replaced with colder air at ambient temperature. That is, we can assume that the warming up of the influent air takes place *instantaneously*, again having an immediate effect upon the liquid phase in the form of enthalpy loss. Therefore, we can write $dH_l/dt \propto Q_s^{in} - Q_s^{out}$, where $Q_s^{in}$ and $Q_s^{out}$ are the sensible heat of the influent and effluent gas stream, respectively.

In addition, we also assume that mass transfer between phases is negligible. Having said this, there is no need to define a gas phase in order to account for the heat flux due to the gas stream.

On the basis of the previous assumptions, we can now write the energy balance of the liquid phase as

$$\frac{dH}{dt} = In(H) - Out(H) + P_{bio} + P_{mix} + P_{wall} + Q_s^{in} - Q_s^{out} + Q_{lat}^{in} - Q_{lat}^{out}, \quad (4.11)$$

where $H$ is the total enthalpy of the liquid phase (MJ). Note that the index $l$ will not be used any longer as it should be understood that enthalpy and temperature refer to the liquid phase, unless otherwise specified. $In(H)$ and $Out(H)$ represent the sensible heat gain and loss through the sludge stream (kW), respectively, $P_{bio}$ the biological heat generation (kW), $P_{mix}$ the heat input through mixing (kW), and $P_{wall}$ the heat lost due to conduction through the reactor walls (kW). $Q_s^{in}$ and $Q_s^{out}$ are the sensible heat gain and loss through the gas stream (kW), respectively. Finally, $Q_{lat}^{in}$ and $Q_{lat}^{out}$ represent the latent heat gain and loss through the gas stream (kW), respectively.

With exception of $Q_{lat}^{in}$ and $Q_{lat}^{out}$, the expressions of all the other terms in the energy balance have been taken from Gomez et al. (2007).

The sensible heat gain and loss through the sludge stream $In(H)$ and $Out(H)$ can be determined according to

$$In(H) = \dot{m}_{in} \cdot C_P \cdot T_{amb}, \quad (4.12)$$

$$Out(H) = \dot{m}_{out} \cdot C_P \cdot T, \quad (4.13)$$

where $\dot{m}_{in}$ and $\dot{m}_{out}$ are the gravimetric influent and effluent sludge flowrates (kg/day), respectively, $C_P$ the specific heat capacity of water (kJ/kg·°C), and $T_{amb}$ and $T$ the temperatures of the influent sludge (ambient temperature) and the liquid phase (°C), respectively.

The rate of biological heat generation $P_{bio}$ by thermophilic microorganisms is directly proportional to the rate of thermophilic growth $\rho_2$:

$$P_{bio} = Y_{heat} \frac{1 - Y_{H,T}}{Y_{H,T}} \rho_2 V, \tag{4.14}$$

where $Y_{heat}$ is the thermophilic heat yield (MJ/kg $O_2$ consumed), and $V$ the total volume of the liquid phase ($m^3$).

The heat input through mixing $P_{mix}$ is directly proportional to the power of the aeration and mixing equipment $P_{eq}$ (kW) and the coefficient of heat utilisation $\eta$ (dimensionless) as shown in Equation 4.15.

$$P_{mix} = P_{eq} \cdot \eta \tag{4.15}$$

The energy lost in form of conduction through the reactor walls $P_{wall}$ is proportional to the surface area of the liquid and gas phase $A_l$ and $A_g$ ($m^2$), respectively, and to the difference between ambient and sludge temperature:

$$P_{wall} = K_{wall} \cdot (T - T_{amb}) \cdot (A_l + A_g), \tag{4.16}$$

where $K_{wall}$ is the heat transfer coefficient of the reactor walls (kW/($m^2 \cdot$°C)). It is being assumed that the heat transfer coefficients of the gaseous and liquid phases are equal.

The sensible heat gain and loss through the gas stream $Q_s^{in}$ and $Q_s^{out}$ depend on the mass flowrate of influent and effluent air $\dot{m}_{in}^g$ and $\dot{m}_{out}^g$ (kg/day), respectively, as well as the temperature of the sludge and ambient air:

$$Q_s^{in} = \dot{m}_{in}^g \cdot C_P^g \cdot T_{amb}, \tag{4.17}$$

$$Q_s^{out} = \dot{m}_{out}^g \cdot C_P^g \cdot T, \tag{4.18}$$

where $C_P^g$ is the specific heat capacity of air (kW/($m^2 \cdot$°C)).

Finally, the latent heat gain and loss through the gas stream $Q_{lat}^{in}$ and $Q_{lat}^{out}$ can be computed following Equation 4.19 and 4.20, respectively:

$$Q_{lat}^{in} = \dot{m}_{in}^{g} \cdot w_{in} \cdot L_{in}, \tag{4.19}$$

$$Q_{lat}^{out} = \dot{m}_{out}^{g} \cdot w_{out} \cdot L_{out}, \tag{4.20}$$

where $w_{in}$ and $w_{out}$ stand for the specific humidity of the influent and effluent gas (kg of water vapor/kg of dry air), and $L_{in}$ and $L_{out}$ for the latent heat of evaporation of the influent and effluent gas (kJ/kg), respectively.

The specific humidity $w_i$ can then be determined as

$$w_i = \frac{18.015}{2896} \cdot \frac{p_i}{p_{atm} - p_i}, \tag{4.21}$$

$$p_i = RH_i \cdot p_i^{sat} = RH_i \cdot 10^{8.07-(\frac{1730.63}{233.42}-T_i)}, \tag{4.22}$$

where $p_i$ represents the actual water vapor pressure (mmHg), $p_{atm}$ the atmospheric pressure (mmHg), and $p_i^{sat}$ the saturation vapor pressure (mmHg) based on the Antoine equation shown in Equation 4.22.

The latent heat of evaporation $L_i$ is calculated according to

$$L_i = 2501 - 2.361 \cdot T_i. \tag{4.23}$$

Table 4.7 contains a list of the parameters pertaining to the energy balance of the ATM1 model.

## 4.3 Proposed ATAD model ATM2

### 4.3.1 Motivation

The first simulation trials with the ATM1 model showed that this model often requires a significant amount of time for the integration of its ordinary differential equations (ODEs). The optimisation task involves thousands (if not more) of evaluations of the objective function and thus an equal or even higher number of

Table 4.7: Parameters involved in the energy balance of the ATM1 model.

| Parameter[a] | Description | Value |
|---|---|---|
| $C_P$ (J/(g·°C)) | Specific heat capacity of water | 4.1813 |
| $C_P^g$ (J/(g·°C)) | Specific heat capacity of air | 1.012 |
| $T_{amb}$ (°C) | Ambient temperature | 10 |
| $Y_{heat}$ (MJ/kg $O_2$) | Specific heat yield of thermophiles | 13.9 |
| $\dot{m}_{in}^g$ (kg/day) | Mass flowrate of influent air | 9460 |
| $\dot{m}_{out}^g$ (kg/day) | Mass flowrate of effluent air | 8170 |
| $P_{eq}$ (kW) | Power input of equipment | 0.1 |
| $\eta$ (-) | Coefficient of heat utilization | 0.7 |
| $K_{wall}$ (kW/($m^2$·°C)) | Heat transfer coefficient of reactor walls | 0.0115 |
| $p_{atm}$ (mmHg) | Atmospheric pressure | 760 |
| $RH_{in}$ | Relative humidity of influent air | 0.7 |
| $RH_{out}$ | Relative humidity of effluent air | 1 |

[a]The values of $\dot{m}_{in}^g$ and $\dot{m}_{out}^g$ are specified for an aeration flowrate of 4 vvh. The parameters $\dot{m}_{in}^g$, $\dot{m}_{out}^g$, $P_{eq}$, $\eta$, and $K_{wall}$ are in fact case-specific; the values displayed here correspond to those of the standard design in USEPA (1990).

integrations of the ODEs for the different values of the control variables.

In this context, it is clear that a simplified, computationally efficient model of the ATAD reaction is critical and could become even indispensable at some later stage of this research.

As with many biological systems, there is considerable uncertainty in inferring both the functional description of processes and the accuracy of parameterizations when applying laboratory-derived models to the real system. The current models in the wastewater literature are motivated by microbiological and engineering interest and have been devised to incorporate as much as possible of the apparent understanding of underlying processes. As a result, they tend to include a relatively large number of components, processes, and parameters.

This stands in contrast to the paucity of data accessible from ATAD plants in operation: aeration rate and sludge temperature are easily monitored, but data on sludge composition at inlet and outlet and during the course of the batch reaction is typically limited to the total dry weight of solids and the chemical oxygen demand of the volatile solids (by controlled chemical oxidation of the sludge). Volatile solids include the biomass of bacteria in the sludge together with organic growth substrates and metabolically inert organic compounds, so no distinction is made between these

components in the measured data.

The ASM1 and ATM1 models have a relatively large number of components and processes, and consequently many parameters. The motivation for including these in the model is predominantly microbiological, and seems to arise from the urge to include all possible components about which there is some knowledge. However, many of the parameter values are poorly known: they are dependent on the chemical and microbiological make-up of the particular sludge, and therefore typically used as fitting parameters. With such a highly parameterized model, sets of parameter values can be found to fit most data but it is unclear if the model remains reliable in such situations. Applying a parameterized model under different (but physically reasonable) operating conditions may give spurious modeling artifacts. And this may also cause numerical difficulties in attempting any optimisation.

With this in mind, we set out to create a new, simpler ATAD model that would only incorporate the most fundamental processes and components involved in the reaction; a minimal model which should be capable of describing the essential mechanisms of the ATAD process, but ignore issues which (though microbiologically 'known') are not material to the process within the likely range of operating conditions. It is hoped that such a model might describe the process sufficiently accurately while providing a more suitable basis for optimisation. The result of this tentative proposal is the model that we will call here ATAD Model No. 2 or ATM2.

### 4.3.2 Mass and energy balances

Our first assumption is the elimination of mesophilic microorganisms from the model since the mixed sludge is hot enough to render their metabolic activity negligible. The component $X_{B,T}$ stands for the concentration of thermophilic microorganisms in the sludge. Any mesophiles in the influent sludge can effectively be considered as already lysed into additional contributions to substrate and inert compounds.

Secondly, we assume that there is no distinction between the two pools of substrate $S_S$ and $X_S$, and consider a single substrate pool $X$. This is motivated by the urge to simplify to a minimal model, rather than through an assumption that one or other pool may be neglected because it is never rate-limiting under normal

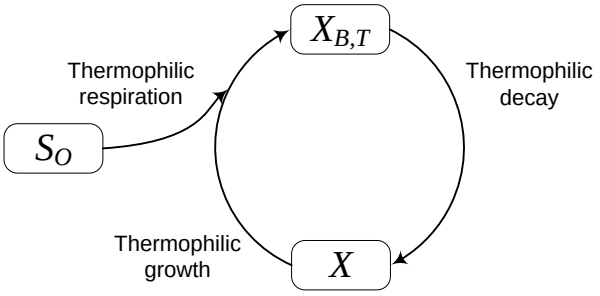


Figure 4.3: Conceptual mass balance of ATM2 model.

operating conditions. The effect of this simplification is obviously greatest after substrate is depleted and becomes limiting: in the ATM2 model, substrate availability for metabolism is directly dependent on biomass decay, while in the ATM1 model it is buffered by the slow substrate reservoir. The size of this effect remains to be demonstrated as well as its importance in relation to achieving treatment objectives.

Thirdly, no particulate products $X_P$ are assumed to form as a result of microbial decay.

The conceptual mass balance of the ATM2 model is therefore greatly simplified, as shown in Figure 4.3. Three components are considered: thermophilic biomass $X_{B,T}$, substrate $X$, and dissolved oxygen $S_O$. The processes are also three: thermophilic respiration, thermophilic growth, and thermophilic decay. In short, microorganisms grow by drawing oxygen and substrate from solution, and die consequently releasing substrate into solution. During their digestion, thermophiles release metabolic energy and rise reactor's temperatures.

During a batch, the reaction is governed by the ordinary differential equations 4.24 to 4.27:

$$\frac{dX_{B,T}}{dt} = G - b(T)X_{B,T}, \tag{4.24}$$

$$\frac{dX}{dt} = -\alpha G + b(T) \cdot (1-f)X_{B,T}, \tag{4.25}$$

$$\frac{dS_O}{dt} = A \cdot (\bar{S_O} - S_O) - \beta G, \tag{4.26}$$

$$\frac{dT}{dt} = \lambda G - h(T), \tag{4.27}$$

where $X_{B,T}$ is the biomass concentration (g/l), $X$ substrate concentration (g/l), $S_O$ oxygen concentration (mg/l), $T$ temperature (°C). The symbol $A$ (1/day) depends on the aeration flowrate $q_a$ (vvh), and its dependency was assumed to be linear as $A = k_a q_a$, where $k_a$ ($\text{vv}^{-1}$) is a case-specific parameter whose value has to be estimated for each particular reactor (Olsson and Newell, 1999). Biomass is assumed here to have a growth rate $G$ given by the dual Michaelis-Menten kinetic expression

$$G = \mu(T)\frac{S_O}{K_O + S_O}\frac{X}{K_X + X}X_{B,T}. \tag{4.28}$$

The biomass is also subject to linear decay with rate constant $b$ which may be temperature-dependent. Growth of biomass is proportional to the substrate and oxygen consumption with the consumption efficiency $1/\alpha$ and $1/\beta$, respectively. Substrate $X$ is also produced as a result of decay of biomass, of which a fraction $(1 - f)$ is recycled as substrate. The VS concentration can be determined as the summation of the particulate components $X_{B,T}$ and $X$.

Dissolved oxygen is replenished through aeration that is subject to the saturation concentration $\bar{S_O}$. The sludge temperature increases at a rate proportional to the biomass growth rate and decreases through heat loss from the reactor. $h(T)$ accounts for heat loss through the reactor walls and via the exhaust gas stream from aeration, as well as heat gained through mechanical mixing. As in the ATM1, the heat loss is dominated by losses through latent heat of evaporation in the exhaust gas stream. The term $h(T)$ can be determined as

$$h(T) = -\frac{P_{mix} + P_{wall} + Q_s^{in} - Q_s^{out} + Q_{lat}^{in} - Q_{lat}^{out}}{V \cdot C_P}, \tag{4.29}$$

where all the terms on the right hand side of the equation have been previously described for the ATM1 model (see Equation 4.15 to 4.20).

The values of the parameters of the ATM2 model are summarised in Table 4.8. While most of these parameters relate to thermophilic metabolism alone, some, such as $\lambda$ and $h$, are in fact case-specific and only a nominal value has been given here.

Table 4.8: Values of parameters in the ATM2 model.

| Parameter | Description | Value |
|---|---|---|
| $K_x$ (g/l) | Half-saturation constant of substrate | 0.1 |
| $K_s$ (mg/l) | Half-saturation constant of oxygen | 0.17 |
| $\mu$ (1/d) | Growth rate | 10 |
| $b$ (1/d) | Decay rate | 5 |
| $f$ (-) | Fraction of not recycled biomass | 0.2 |
| $\alpha$ (-) | Substrate transformation | 1.5 |
| $\beta$ (-) | Oxygen transformation | 0.5 |
| $\lambda$ (°C·l/g) | Heat production | 6.5 |
| $\bar{S_O}$ (mg/l) | Oxygen saturation constant | 10 |

This model describes the batch reaction period from just after a batch intake is mixed into the reactor until batch outflow. The required initial conditions are those of the sludge immediately following mixing of the inflow with the sludge remaining in the reactor from the previous batch, since the reactor volume is only partially replaced at each batch. The pre-existing sludge conditions depend on the history of previous batches in the reactor. With repeated batches of the same type, we expect the batch cycle to settle to a state in which successive batches are identical and the pre-mixing reactor sludge conditions are effectively independent of the initial conditions of the first batch reactor sludge. Provided that influent sludge characteristics and the initial condition of the system are known, the model can be run to simulate successive batches until these settle to a periodic batch cycle.

The linking of successive batches and initial mixing of inflow sludge for each batch can be described by adding advective terms into the ODE system:

$$\frac{X_{B,T}}{dt} = G - bX_{B,T} + Q_\delta \cdot (X_{B,T}^{feed} - X_{B,T}), \tag{4.30}$$

$$\frac{dX}{dt} = -\alpha G + b \cdot (1-f)X_{B,T} + Q_\delta \cdot (X^{feed} - X), \tag{4.31}$$

$$\frac{dS_O}{dt} = A \cdot (\bar{S_O} - S_O) - \beta G + Q_\delta \cdot (S_O^{feed} - S_O), \tag{4.32}$$

$$\frac{dT}{dt} = \lambda G - h + Q_\delta \cdot (T^{feed} - T), \tag{4.33}$$

where we define $Q_\delta$ as

$$Q_\delta = \frac{V_{in}}{V}\delta(t - t_{in}), \tag{4.34}$$

and $\delta(t - t_{in})$ is a Dirac delta function. The volume $V_{in}$ is the total volume replaced after each batch ($m^3$), and $t_{in}$ the loading time (days).

As implied by the Dirac delta function, in this model we consider reactor loading to take place *instantaneously*. By assuming instantaneous reactor loading, there is no need to include the reactor volume $V$ as a state variable. This simplification has the advantage of making the model significantly more efficient in computational terms. On the other hand, it has the limitation that in this form the model does not allow the investigation of the effect of longer loading times upon the process.

## 4.4 Quantification of treatment objectives

As mentioned in Chapter 2 section 2.5.2, the two objectives of the ATAD treatment are the stabilisation and pasteurisation of the sludge.

### 4.4.1 Stabilisation

Stabilisation is defined as the reduction of the VS concentration of the sludge. The purpose of such reduction is to limit the potential of the sludge for vector attraction to a level regarded as being safe for both human health and the environment.

In none of the publications dealing with modeling of ATAD systems it is stated explicitly how the VS concentration was calculated. Hence, it would not be surprising if some authors did so through the summation of all carbonaceous components. Nevertheless, in the standard technical report *Activated Sludge Models ASM1, ASM2, ASM2D and ASM3*, Henze et al. (2000) stated explicitly that the VS concentration is the summation of the particulate carbonaceous components *only*.

We define the VS reduction $r_{VS}$ (dimensionless) at time $t$ as

$$r_{VS}(t) = 1 - \frac{X_{VS}(t)}{X_{VS}^{in}}, \tag{4.35}$$

where $X_{VS}(t)$ is the VS concentration of the sludge in the system at time $t$ (g/l), and $X_{VS}^{in}$ the VS concentration of the influent sludge (g/l).

It was indicated above that the VS concentration has to be reduced, at least, to a certain legally required level by the end of the reaction. This condition can be written as follows:

$$r_{VS}^{min} - r_{VS}(t_f) \leq 0, \tag{4.36}$$

where $t_f$ is the final time of the reaction (days), and $r_{VS}^{min}$ the minimum level of VS reduction required by law (dimensionless). Some countries differ in their regulatory standards. Consequently, the minimum VS reduction $r_{VS}^{min}$ also differs among some of these countries. In the United States, USEPA (1993) under 40 CFR 503.33(b)(1) establishes that this value is 38%. Most European countries have adapted to this code of practice (European Commission, 2000).

We define the minimum time required to satisfy the condition

$$0.38 - r_{VS} \leq 0, \tag{4.37}$$

as the *stabilisation time* $t_S$ (days).

### 4.4.2 Pasteurisation

In this context, pasteurisation is defined as the reduction of the concentration of certain pathogens below detectable levels via heat treatment. This ensures that the sludge will not pose a threat to human health or the environment once it is disposed of in landfill or used as soil conditioner.

ATAD sludge has to be subjected to a certain temperature over a certain period of time in order to be considered as pasteurised. Under 40 CFR 503.32(a)(3), USEPA (1993) establishes that this time-temperature relationship or thermal death time obeys the equation

$$D = \frac{5007000}{10^{0.14 \cdot T}},\ T \geq 50\ ^{\circ}\text{C},\ D \geq 0.021 \text{ days (30 minutes)}, \tag{4.38}$$

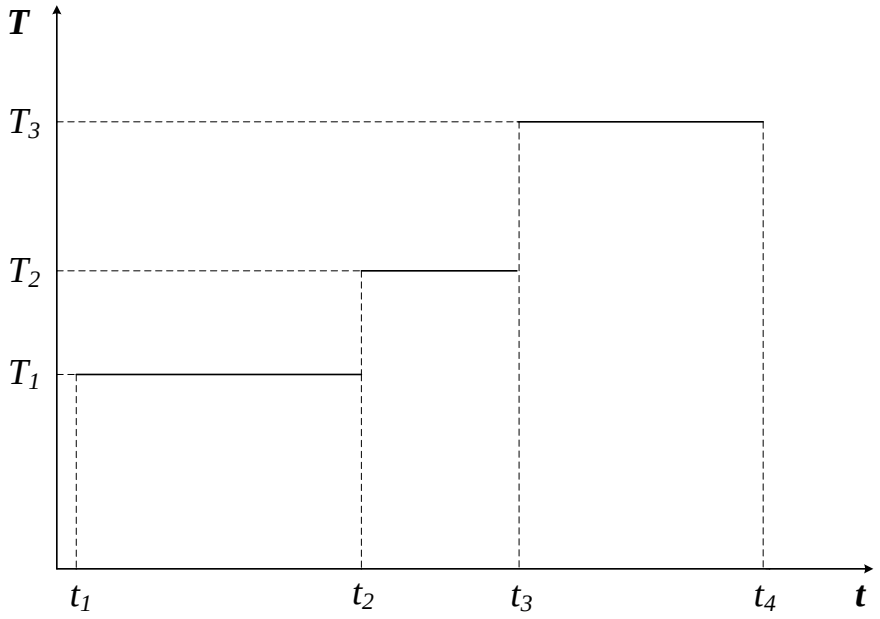


Figure 4.4: Varying temperature profile: How to quantify pasteurisation?

where $D$ represents the contact time (days), and $T$ the temperature (°C). Again, most European countries have adopted these guidelines (European Commission, 2000).

This relationship (Equation 4.38), however, is not sufficient to quantify pasteurisation in ATAD systems under normal operating conditions. The difficulty lies in the fact that this relationship applies to the case of a constant temperature $T$. However, as we have already seen, temperature profiles in ATAD systems generally display significant variations. The question is then, how to quantify pasteurisation under conditions of varying temperatures?

This question can be approached by considering a temperature profile constituted of a finite number of time intervals with constant temperature, as in Figure 4.4. In the first interval of temperature $T_1$, the corresponding contact time will be $D_1$. Analogously, the second and third intervals with temperatures $T_2$ and $T_3$ will have the contact times $D_2$ and $D_3$, respectively. Thus, the question of the quantification of pasteurisation can now be reformulated in a more specific manner: How is it possible to compare the degrees of pasteurisation achieved during time intervals of different length at different temperatures and therefore with different contact times?

The question can be answered by comparing the ratios of total time of exposure

in each interval to its corresponding contact time. For example, in the first interval, the degree of pasteurisation would be given by $\frac{t_2-t_1}{D_1}$. In the same way, the degree of pasteurisation achieved during the second and third intervals would be given by the ratios $\frac{t_3-t_2}{D_2}$ and $\frac{t_4-t_3}{D_3}$. For the $i$-th interval, the degree of pasteurisation would be determined as $\frac{t_{i+1}-t_i}{D_i}$. The ratio itself represents the percentage of pasteurisation achieved during the interval in question. If, for instance, the value of this ratio was 1 for the $i$-th interval, that would mean that the time of exposure $t_{i+1}-t_i$ equals the contact time $D_i$ required to complete pasteurisation. As percentages can be readily compared, it is possible to sum the ratios pertaining to all intervals. The summation of all ratios is defined here as pasteurisation lethality $L$ (dimensionless):

$$L = \sum_{i=1}^{N} \frac{t_{i+1} - t_i}{D_i} = \sum_{i=1}^{N} \frac{\Delta t_i}{D_i}, \tag{4.39}$$

where $N$ is the total number of time intervals. If we allow the length of the intervals to approach zero, i.e. $\Delta t_i \to 0$, then the limit of $L$ is

$$\lim_{\Delta t_i \to 0} L = \sum_{i=1}^{N} \frac{\Delta t_i}{D_i} \to \int_{t_0}^{t_f} \frac{dt}{D(t)}, \tag{4.40}$$

where $t_0$ and $t_f$ are the initial and final time (days), respectively. In this manner, it is possible to use the lethality $L$ as general measure for the degree of pasteurisation irrespective of changes in the operating temperatures. So in the continuous domain the lethality can be expressed as

$$L(t_0, t_f) = \int_{t_0}^{t_f} \frac{dt}{D(t)}. \tag{4.41}$$

No study dealing with modeling of ATAD systems (and perhaps in wastewater engineering more generally) had thus far quantified pasteurisation under conditions of varying temperatures. This is therefore a unique feature of our model. It should be noted though that in other fields, such as food process engineering, this way of quantifying pasteurisation has already been proposed and applied, and it is known as the *General Method* (Toledo, 1994).

The sludge can be considered pasteurised at time $t$ if the following condition is

satisfied:

$$1 - L(t_0, t) \leq 0. \tag{4.42}$$

We define the minimum time required to satisfy this condition as the *pasteurisation time* $t_P$.

The overall reaction time $t_r$ (days) can then be determined as the greatest of the stabilisation and the pasteurisation times following

$$t_r = \max\{t_S, t_P\}, \tag{4.43}$$

and it represents the minimum time needed to satisfy both stabilisation and pasteurisation legal requirements.

## 4.5 Quantification of energy requirement and plant capacity

In this context, the energy requirement represents the amount of energy required to treat a certain amount of sludge or solids. If the energy requirement is measured in relation to the volume of influent sludge undergoing treatment, it is then a volumetric energy requirement (kWh per $m^3$ of sludge treated). But if it is measured in relation to the amount of influent VS undergoing treatment, it is said to be a gravimetric energy requirement (kWh per kg of VS treated).

In some studies, the volumetric energy requirement has been preferred (for example, Ponti et al. (1995a,b)). There is, nonetheless, a clear drawback when using the volumetric measure: it refers to the quantity of sludge being treated but not to the concentration of VS in the influent. However, it is the *solids* in the sludge that are the actual target of the treatment and not the sludge in itself (i.e., mainly water). The problem that arises with the volumetric measure can be brought out more clearly by considering the following hypothetical situation: a given quantity of sludge $V_{in}$ requires an amount of energy $E$ for treatment, and the batch time is

kept constant at 1 day (like in conventional ATAD systems); if the influent VS concentration is varied within a certain range over a number of successive batches, the volumetric energy requirement would not be able to record any changes, as it can do so only through variations in the volume of influent sludge. This problem does not arise if we use the gravimetric energy requirement, as it considers, by definition, the concentration of VS in the influent sludge. We thus consider the gravimetric magnitude to be a more adequate measure for energy consumption than its volumetric counterpart.

For this reason, we chose to use the gravimetric energy requirement as the main measure of energy consumption in this study. Therefore, it should be understood that, from now onwards, whenever the term "energy requirement" is employed on its own, it refers to the gravimetric energy requirement. In spite of this, the volumetric energy requirement will be also investigated in some contexts.

We define the gravimetric and volumetric energy requirements $E_m$ (kWh/kg) and $E_V$ (kWh/m$^3$) according to the equations

$$E_m = \frac{1}{m_{in}} \int_{t_0}^{t_f} P(t) \cdot dt, \tag{4.44}$$

$$E_V = \frac{1}{V_{in}} \int_{t_0}^{t_f} P(t) \cdot dt, \tag{4.45}$$

where $m_{in}$ is the mass of total VS in the influent sludge (kg), $V_{in}$ the volume of influent sludge (m$^3$), $P$ the power of the aeration equipment (kW), and $t_f$ the final time of the reaction (h). If the aeration level is constant (as in conventional ATAD reactors), then the power $P$ is also constant and Equation 4.44 and 4.45 obviously yield

$$E_m = \frac{P \cdot t_f}{m_{in}}, \tag{4.46}$$

$$E_V = \frac{P \cdot t_f}{V_{in}}. \tag{4.47}$$

For a given set of operating conditions, the minimum energy requirement is

achieved when the final time $t_f$ equals the reaction time $t_r$ (see Equation 4.43). It should be emphasised that the ability to determine the minimum energy requirement of the process is a unique feature of our model. This is due to its ability to quantify stabilisation and pasteurisation and thereby to determine the minimum reaction time $t_r$ needed to satisfy legal requirements. The reaction time and thus the minimum energy requirement and the maximum plant capacity are implicit functions of the operating conditions. This implicit dependence lies in the fact that the reaction time is determined by either the pasteurisation or the stabilisation time (see Equation 4.43) which are, in turn, implicit functions of the operating conditions.

Gravimetric and volumetric plant capacities $c_m$ (kg/day) and $c_V$ ($m^3$/day) are defined as

$$c_m = \frac{m_{in}}{t_f}, \tag{4.48}$$

$$c_V = \frac{V_{in}}{t_f}. \tag{4.49}$$

# Chapter 5

# Simulation Studies

This chapter covers a set of numerical analyses, comprising a study of start-up and steady state simulations, an asymptotic analysis, a sensitivity analysis, and a model assessment and parameter estimation. Before proceeding to these analyses, we will consider the two full-scale ATAD plants that will serve as case studies for the aforementioned analyses as well as later on for the optimisation problem.

## 5.1 Case studies

### 5.1.1 Case study 1 (CS1): single-stage system

This single-stage reactor system is located in Tudela (Navarra, Spain). The facility, with a population equivalent of 43,000, was built in 2001 and is the property of the state-owned company *Navarra de Infraestructuras Locales, S.A.* (NILSA). Treated sludge is generally used as soil conditioner for agricultural purposes.

The type of sludge treated in this ATAD facility is a mix of sludge from the primary and secondary stages of wastewater treatment. Prior to treatment, the sludge is thickened via sedimentation in settling tanks or clarifiers. The typical values of TS and VS concentrations after pre-thickening range 45–60 g/l and 30–35 g/l, respectively.

The 350-$m^3$ reactor was built with reinforced concrete and is fully enclosed. To prevent excessive heat loss through the walls, it is covered with an insulating layer


Figure 5.1: Photograph of (a) single-stage ATAD system CS1, and (b) Venturi jet aerator. Adapted from Gomez et al. (2007) and Gomez (2007).

which in turn is protected with a cover made of stainless steel. The overall heat transfer coefficient of the wall is 25 kJ/°C·m$^2$·day. The reactor has a cylindrical geometry with an inner height of 6.5 m and an inner diameter of 9.25 m. A distance of at least 1.5 m has to be left as freeboard in order to handle the formation of foam. The photograph in Figure 5.1a shows the outer appearance of the reactor.

The reactor is operated in a discontinuous, semi-batch mode. The overall batch cycle has a duration of 24 h: the first step has a duration of 15–30 min and it consists of the displacement of a certain volume of treated sludge from the reactor into the storage tank; during the second step, which has the same duration, the reactor is filled with same volume of raw sludge from the feed tank; the third and last step lasts for 23 to 23.5 h and it involves the aeration and agitation of the sludge for the reaction to take place. This sequence then repeats in the same order.

The HRT typically ranges 7 to 12 days. With a typical working volume of 300 m$^3$, it follows that the sludge flowrate is in the range 25–45 m$^3$/day.

The operating temperatures of the reactor oscillate within the interval 50–70 °C.

The aeration system consists of two Venturi jet pumps that mix sludge and air and forcefully rush the mix horizontally at the bottom of the reactor, thus creating a highly turbulent environment. The Venturi effect of these devices has the advantage that it increases the oxygen transfer efficiency (Gomez, 2007). This is a result of

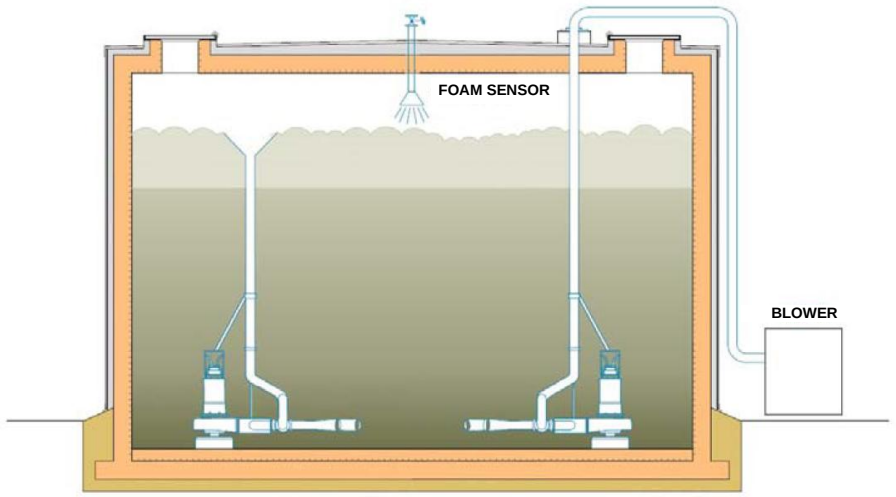


Figure 5.2: Longitudinal cross section of CS1 reactor system with Venturi aeration system. Adapted from Gomez et al. (2007) and Gomez (2007).

subjecting the mix of sludge and air to increased pressure in the converging inlet nozzle. A photograph of the aeration device is shown in Figure 5.1b. Each of these aeration devices is equipped with a 15-kW pump. One jet pumps a mix of outside air with sludge, while the other pumps a mix of air from the gas phase of the reactor with foam as illustrated by Figure 5.2.

This configuration is said to have a number of advantages such as increasing oxygen transfer efficiency through recirculation of air from the gas phase of the reactor, minimising energy losses (both in terms of latent and sensible heat) through the exhaust gas stream, and controlling the formation and thickness of the foam layer.

The engines of the Venturi aerators are fully submerged in the sludge. Thus, all dissipated heat contributes to increasing the temperature of the sludge.

The aeration system produces air flowrates that range between 0.8 and 1.4 vvh. Within this interval, the relationship between power $P$ (kW) and aeration flowrate $q_a$ (vvh) is given by the equation $P = 6 \cdot q_a + 28$. We assume that the same relationship between $P$ and $q_a$ holds when extrapolating from the aeration flowrate interval [0.8,1.4].

The installed specific power in the reactor is thus 100–120 W/m$^3$. For an influent VS concentration of 35 g/l, a replaced volume of 30 m$^3$, and an aeration flowrate of

Table 5.1: Structural and operating parameters of CS1. Adapted from Gomez et al. (2007) and Gomez (2007).

| Parameter | Description |
|---|---|
| Population equivalent | 43,000 |
| Operation mode | Single 300-$m^3$ reactor operated in semi-batch mode following reverse-order loading pattern |
| Reactor type | Geometry: cylindrical; height: 6.5 m; diameter: 9.25 m; heat transfer coefficient of reactor walls: 25 kJ/°C·$m^2$·day |
| Sludge type | Primary and secondary sludge pre-thickened in settling tanks; all sludge from municipal origin |
| Feed TS range | 45–60 g/l |
| Feed VS range | 30–35 g/l |
| HRT | 7–12 days |
| Sludge flowrate | 30–40 $m^3$/day |
| Minimum reaction time | 20 hr operating in batch mode |
| Temperature | 50–70 °C |
| Aeration flowrate | 0.8–1.4 vvh |
| Specific power | 100–120 W/$m^3$ of sludge |
| Energy requirement | 0.72 kWh/kg of VS treated |

0.8 vvh, the corresponding energy requirement is 0.72 kWh/kg.

A summary of the main structural and operating parameters of CS1 is listed in Table 5.1.

### 5.1.2 Case study 2 (CS2): two-stage system

This two-stage ATAD system is located in Killarney (Co. Kerry, Ireland) and is the property of the local authority, the Kerry County Council. It has a population equivalent of 14,000. However, Killarney is a renowned tourist resort and during the summer months the population can rise up to 50,000. For this reason, the ATAD plant (which treats most of the sludge from the region) is equipped with two independent trains of two reactors in series. Usually, only one train is required to cope with the typical winter load. It is only during one or two summer months that the second train is brought into operation in order to cope with the increased load.

The ATAD facility was designed and built according to the standard design developed by the German company *Fuchs GmbH* and described above in section 2.5.3. This plant has, however, a unique, distinctive characteristic that will be discussed later. A photograph of the two trains of reactors can be seen in Figure 5.3a. Treated sludge is generally collected by local farmers and spread on agricultural


Figure 5.3: Photographs of (a) CS2 system with two independent trains of two reactors in series, and (b) storage tanks and collection of treated sludge by local farmer.

land to fertilize the soil (see Figure 5.3b).

The source of sludge are the primary and secondary stages of wastewater treatment. Prior to the ATAD treatment, primary and secondary sludge are settled in a clarifier. After settling, the TS concentration is generally about 20 g/l and the VS concentration about 15 g/l. For some, as yet, unknown reason the sludge does not settle any further. According to the manufacturer these concentrations are not sufficiently high to allow the reactor to reach and maintain thermophilic temperatures. Thus, the operator further thickens the sludge by mixing it with a polymer in a belt press. This addition of polymer is the distinctive characteristic mentioned above. It has a very important impact on the energy requirement of the treatment as will be shown later. After this operation, the sludge consistently reaches a TS concentration of 60 g/l and a VS concentration of 40 g/l.

Each reactor is completely enclosed with a total volume of 110 $m^3$ and a working volume of 100 $m^3$. Their geometry is also cylindrical with a total inner height of 3 m, a working height of 2.73 m, and an inner diameter of 6.83 m. About 0.3 m distance is left as freeboard to control the thickness of the foam layer with the aid of foam cutters that are installed on the upper part of the reactor. The reactors are built with carbon steel and furnished with an inner coal-tar-based layer. Additionally, to prevent excessive heat losses, the reactors have an insulating coating cover which is protected and decorated with a metallic skin of corrugated steel. The resulting heat transfer coefficient of the reactor wall is 35 kJ/°C·$m^2$·day.

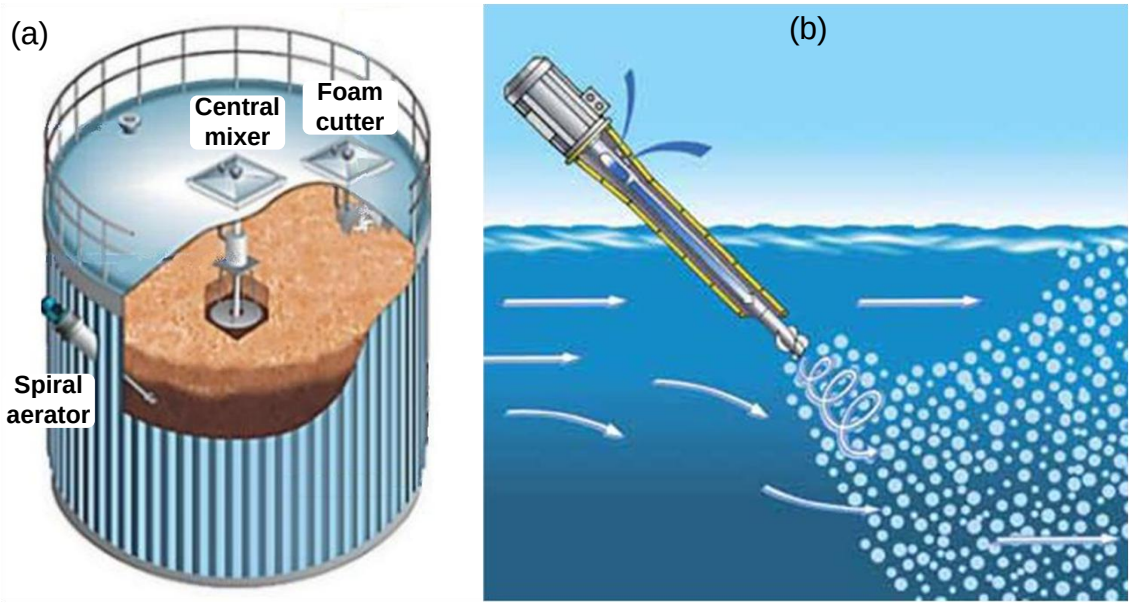


Figure 5.4: Artistic images of (a) CS2 ATAD reactor with detail of spiral aerator, central mixer, and foam cutter, and (b) detail of Fuchs spiral ejector creating fine bubble aeration with high turbulence and strong directional current. Adapted from ISMA (2011) and FUCHS (2011).

The system is operated in the semi-batch mode described in section 2.5.3 (see page 23).

The HRT is in the range 6–10 days. With a total volume of 200 $m^3$, the sludge flowrate ranges between 20 and 35 $m^3$/day. The high sludge flowrates correspond to the high-season summer months while typical values of 20–25 $m^3$/day apply to the rest of the year.

The aeration system of each reactor consists of two side-mounted, near-surface spiral ejectors (see Figure 5.4a). The ejectors are located in opposite sides of the reactor. They provide fine bubble aeration, high turbulence, and strong directional current as illustrated in Figure 5.4b. In contrast to the aeration devices of CS1, the ejectors of CS2 propel only air. The aeration flowrate in the first-stage reactor has a value of 4 vvh with a power of 11 kW while in the second-stage reactor it is 3 vvh and 9 kW. Thus, when extrapolating, we assume that the equation $P_1 = \frac{11}{4} q_a^1$ holds for the first-stage and $P_2 = \frac{9}{3} q_a^2$ for the second-stage, where $P_1$ and $P_2$ are the power (kW) and $q_a^1$ and $q_a^2$ the aeration flowrate (vvh) of the first- and second-stage reactors, respectively.

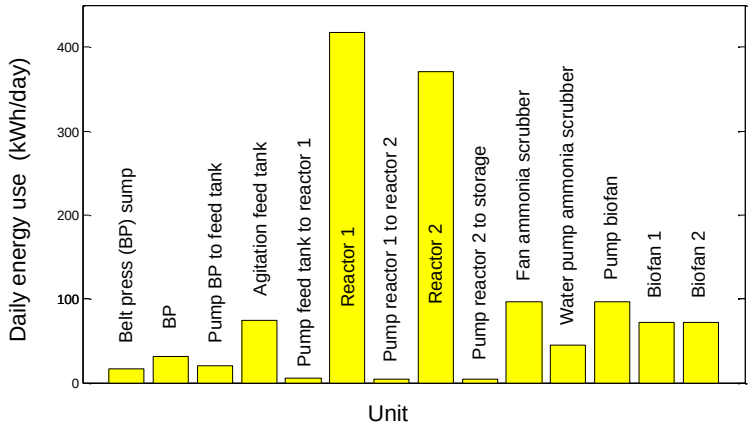


Figure 5.5: Energy breakdown of ATAD facility CS2. Most of the energy (between 60 and 75% of the total, depending on the season) is consumed in the reactors.

Considering only the aeration devices, the specific power of the system is 100 W/m$^3$. For a typical winter day with a sludge flowrate of 25 m$^3$/day, a reaction time of 23 h, a VS concentration of 15 g/l, and a total power of 20 kW, the energy requirement of CS2 is 1.22 kWh/kg of VS treated. Note that here the value of the VS concentration has been taken as 15 and not 40 g/l. That is, it is the concentration before thickening the sludge with polymer that counts. This is due to the fact that the actual contribution of the sludge in terms of solids is the VS concentration before the addition of polymer. If the 40 g/l of solids were entirely contributed by the sludge, then the energy requirement would be 0.46 kWh/kg. This profound impact on the energy requirement is the reason why the addition of polymer is such a bad solution.

Figure 5.5 shows the energy breakdown of CS2. The first units relate to the pre-thickening of the sludge, followed by the feed tank, the first-stage and second-stage reactors, and the gas treatment (removal of ammonia is achieved in the ammonia scrubber and removal of hydrogen sulfide in the bio filter or biofan). It is evident from the breakdown that most of the energy used daily to operate the plant is spent on the reactors (between 60 and 75%, depending on the season). Some of this energy is consumed by the foam cutters and the central mixer, but most of it ($\sim$60%) is used by the spiral aerators. This reinforces the idea that focusing on aeration when trying to minimise the energy requirement of ATAD systems is the best strategy.

Table 5.2: Structural and operating parameters of CS2.

| Parameter | Description |
|---|---|
| Population equivalent | 14,000–50,000 |
| Operation mode | Two trains of two 100-$m^3$ reactors in series operated in semi-batch mode following a reverse-order loading pattern |
| Reactor type | Geometry: cylindrical; height: 3 m; diameter: 6.83 m; heat transfer coefficient of reactor walls: 35 kJ/°C·$m^2$·day |
| Sludge type | Primary and secondary sludge pre-thickened in settling tanks and by means of addition of polymer; all sludge from municipal origin |
| Feed TS range | 20 g/l before and 60 g/l after addition of polymer |
| Feed VS range | 15 g/l before and 40 g/l after addition of polymer |
| HRT | 6–10 days |
| Sludge flowrate | 20–25 $m^3$/day |
| Minimum reaction time | 23 hr per stage |
| Temperature | Reactor 1: 35–50 °C; Reactor 2: 50–70 °C; |
| Aeration flowrate | Reactor 1: 3 vvh; Reactor 2: 4 vvh |
| Specific power | 100 W/$m^3$ of sludge |
| Energy requirement | 1.22 kWh/kg of VS treated |

Another strategy that has considerable potential is the shortening of the reaction time. In doing so, not only aeration energy would be saved but also energy used by the foam cutters, mixing, and gas treatment, all of which are nearly continuous processes.

A summary of the most important design and operating parameters of CS2 is listed in Table 5.2.

## 5.2 Start-up and steady state simulations

As a first step toward verifying the behavior and dynamics of the ATM1 model presented in Chapter 4, a study of simulations of the systems CS1 and CS2 at different conditions will be carried out. In particular, the first interest is to simulate the behavior of these systems during start-up and later at steady state. The different conditions under which these simulations will be examined refer to varying ambient temperatures and influent VS concentrations. These two parameters have been selected because they are, according to experience, the ones that exert the strongest influence on the processes of stabilisation and pasteurisation of the sludge. It should be noted that ambient temperature determines the temperature of the air used for

aeration, that of the influent sludge, and the initial temperature of the reactor.

Ambient temperature will be given the values 10 and 20 °C; these values correspond approximately to those of the winter and summer conditions, respectively. The influent VS concentration will take the values 20 and 40 g/l, corresponding respectively to a rather diluted sludge and a sludge under normal conditions. Generally, it has been thought that sludge with a VS concentration of less than 25 g/l would not allow the reactor to reach and consistently operate at thermophilic temperatures (USEPA, 1990). The remaining operating parameters of CS1 and CS2, such as the aeration flowrate, reaction time, etc, will be given the values specified in Table 5.1 and 5.2, respectively.

### 5.2.1 Start-up simulations

We will begin by examining the start-up of CS1. Figure 5.6 displays the non-dimensional concentrations (i.e., the original concentrations divided by their corresponding initial value), the temperature of the reactor, the DO concentration, the OUR, the VS reduction, and the pasteurisation lethality for an ambient temperature of 10 °C and an influent VS concentration of 40 g/l for CS1. It should be noted that the distribution of VS in terms of the system components is the same for the influent sludge and the initial condition of the system. This underlies the assumption that the content of the reactor at the beginning of the first batch has the same characteristics as the influent sludge. In other words, before the first batch begins, the reactor is loaded in its integrity with influent sludge. The initial condition of the system is

$$S_S = 10 \text{ g/l},\ X_P = 6 \text{ g/l},\ X_S = 21 \text{ g/l},\ X_{SP} = 3.5 \text{ g/l},\ X_{BHT} = 1.5 \text{ g/l}.$$

Under these conditions, the system is limited by the availability of oxygen while readily biodegradable substrate is relatively plentiful. Both temperature and concentrations lie within the expected range of values. The concentrations reach the steady state (i.e., cyclic or periodic operation) after 40 or 45 batches while the temperature

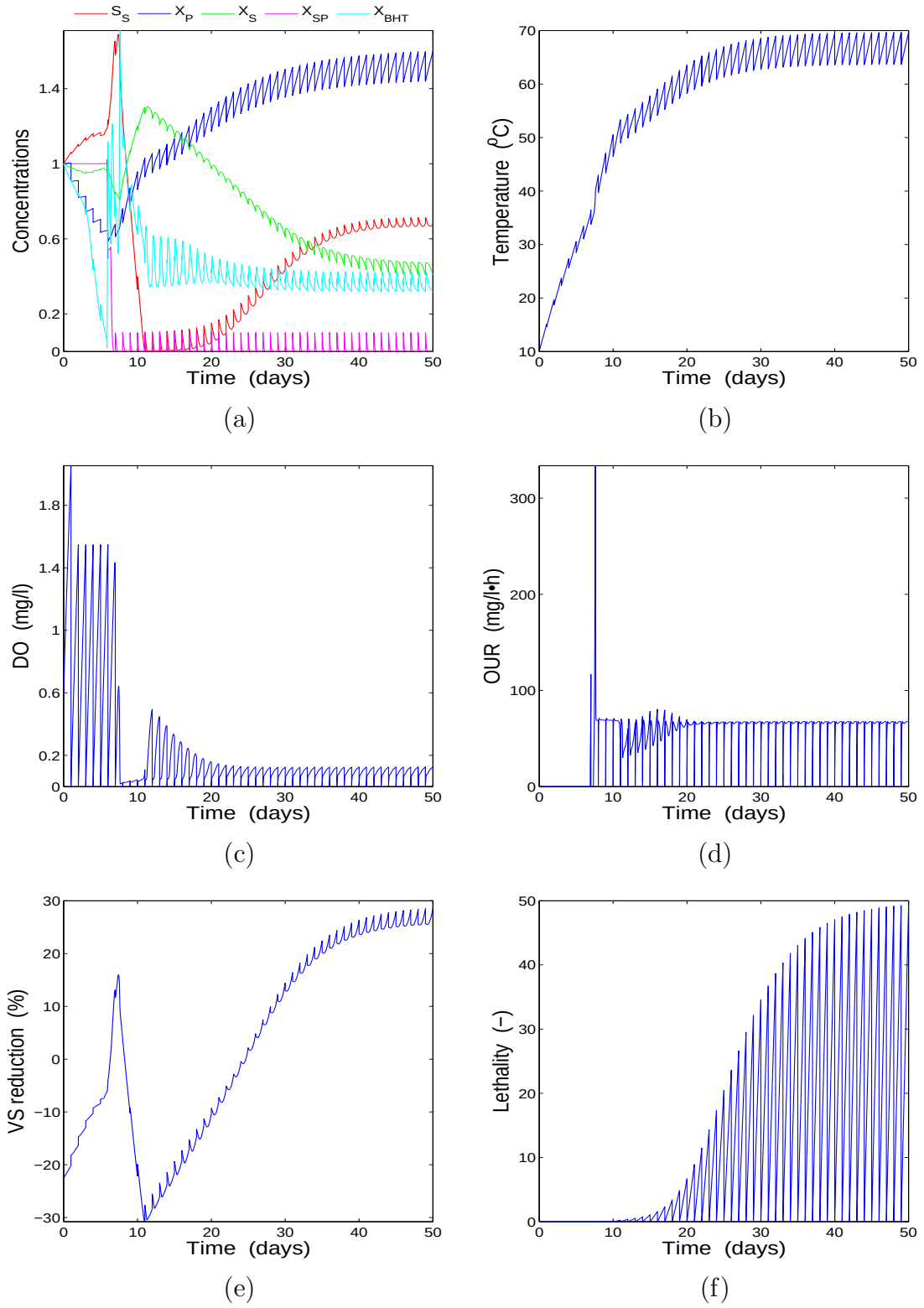


Figure 5.6: Start-up simulation of single-stage system CS1 at an ambient temperature of 10 °C and influent VS concentration of 40 g/l: (a) non-dimensional concentrations, (b) temperature, (c) dissolved oxygen, (d) OUR, (e) VS reduction, and (f) pasteurisation lethality.

does so after just 30 batches. The VS reduction achieved after a transient of 40 to 45 batches is ∼30%. This value is lower than the minimum degree of stabilisation required to satisfy the standard for Class A Biosolids; nonetheless, some full-scale two-stage plants operating at values as low as 25% have been reported (USEPA, 1990). Scisson (2003) suggested that the low degree of stabilisation of some systems is the result of short reaction times or insufficient oxygen delivery, or both. Thus, he suggested that the next generation of ATAD systems should be operated with longer reaction times and increased oxygen supply. Indeed, it could be argued that the level of aeration of CS1 (just 1 vvh in our simulation) is too low to achieve greater VS reductions while operating the system with a reaction time of 23 hr or 1 day. Lethality, on the other hand, exceeds pasteurisation requirements by almost 50 times. This is due to the high operating temperatures. Both VS reduction and pasteurisation lethality reach steady state after 40 to 45 batches.

Figure 5.7 shows the same variables for an ambient temperature of 20 °C, an influent VS concentration of 40 g/l, and the same initial condition for CS1. The process is still oxygen-limited while the availability of substrate is even higher than in the previous figure. The temperatures are also higher than in the previous case leading to increased lethality values. The VS reduction is ∼40% slightly exceeding the legal requirement, which is in good agreement with full-scale experience. An interesting observation is that the two treatment objectives are thus positively affected by higher ambient temperatures, that is, when comparing Figure 5.6 and 5.7. Another interesting observation is that higher ambient temperatures also lead to shorter transient conditions, with ∼20 batches for the temperature, ∼30 for the lethality, and ∼40 for the concentrations and VS concentration.

In Figure 5.8, we see that for an ambient temperature of 10 °C and a VS concentration of 20 g/l the system does not reach the minimum temperature of 50 °C required for pasteurisation. Thus, neither stabilisation nor pasteurisation achieves the minimum legal requirement. This is in agreement with the experimental observation mentioned above, that concentrations below 25 g/l do not generally allow a consistent operation at thermophilic temperatures (USEPA, 1990). It can also be seen that under these conditions the process is substrate-limited, with DO reaching

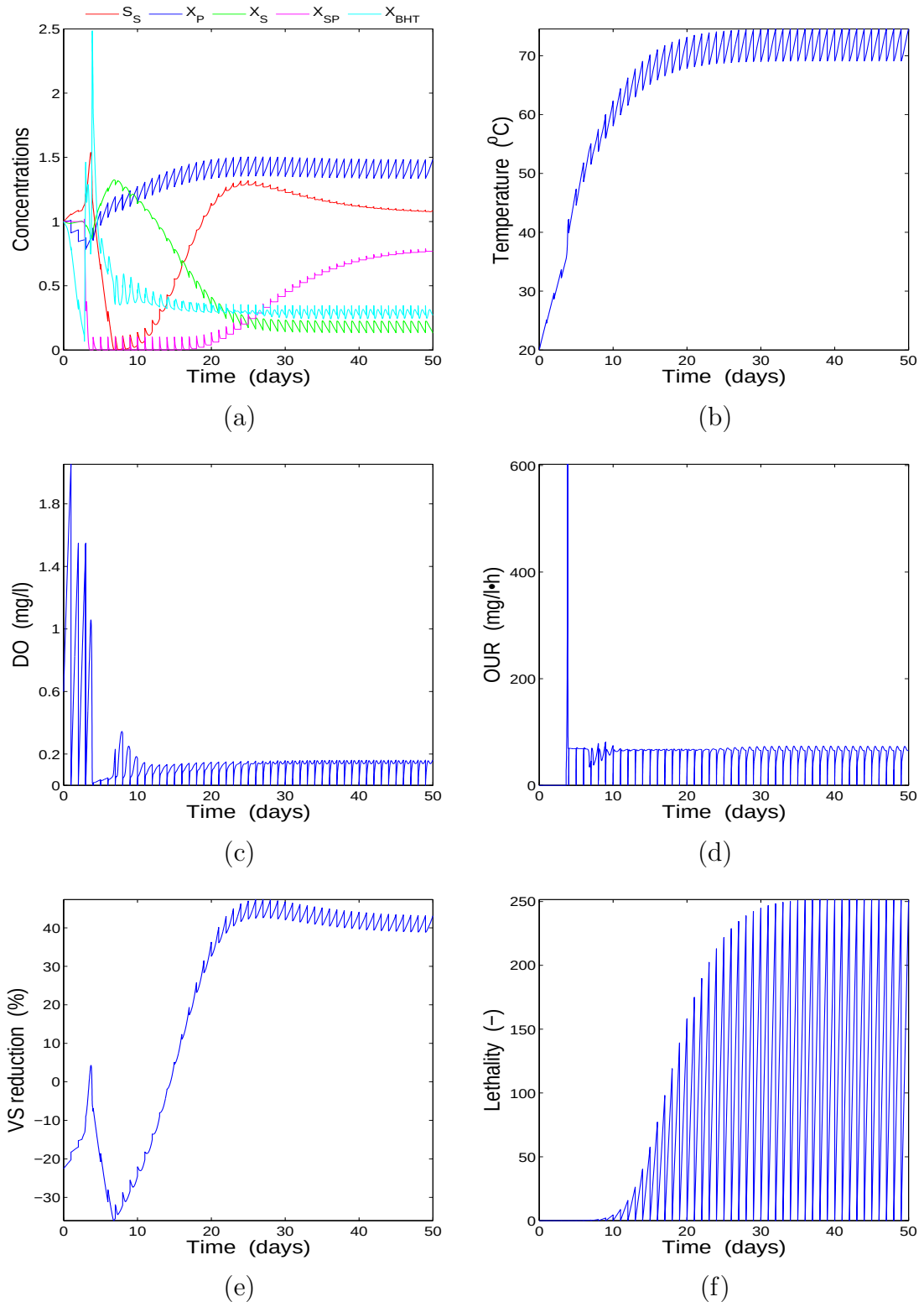


Figure 5.7: Start-up simulation of single-stage system CS1 at an ambient temperature of 20 °C and influent VS concentration of 40 g/l: (a) non-dimensional concentrations, (b) temperature, (c) dissolved oxygen, (d) OUR, (e) VS reduction, and (f) pasteurisation lethality.

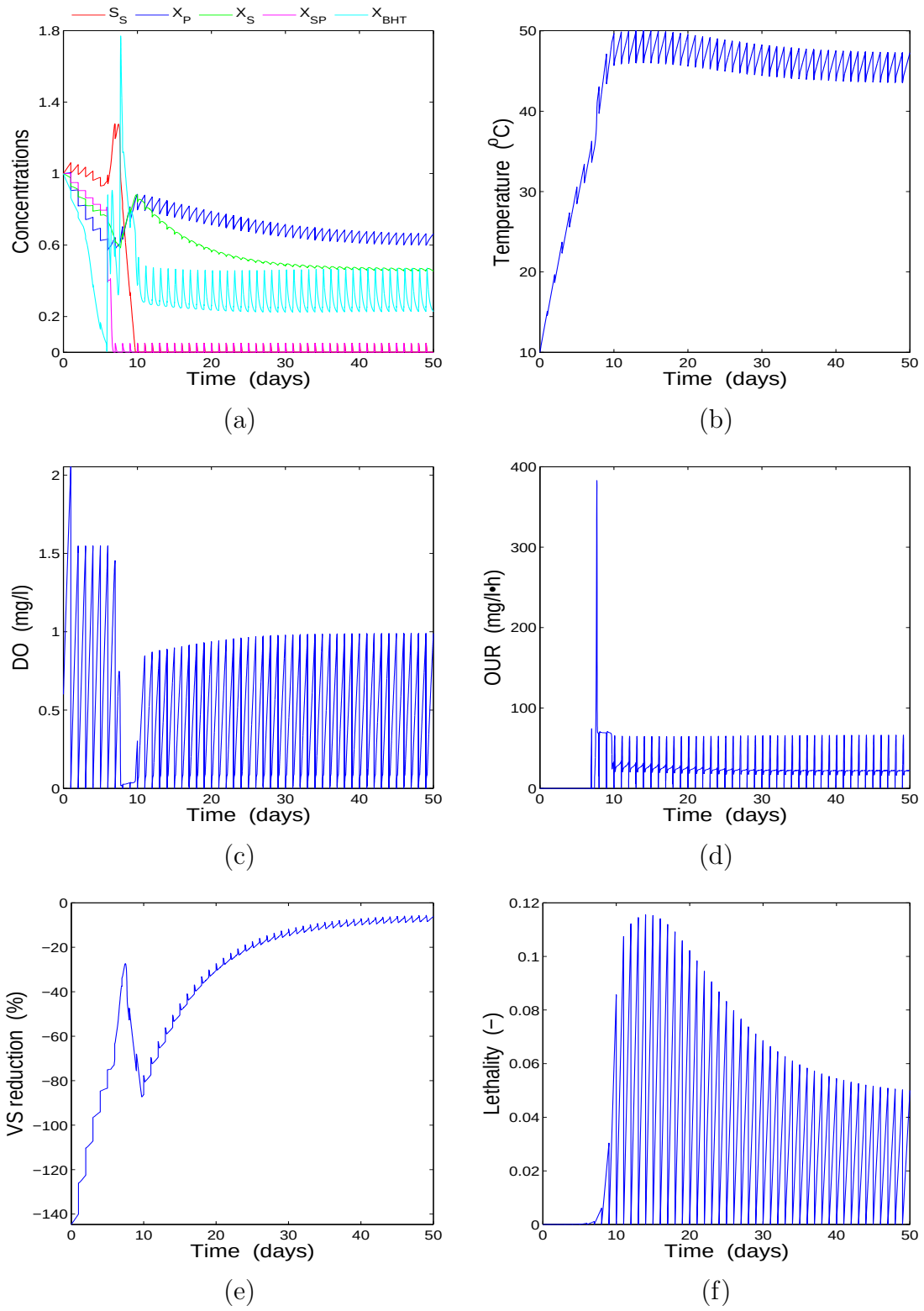


Figure 5.8: Start-up simulation of single-stage system CS1 at an ambient temperature of 10 °C and influent VS concentration of 20 g/l: (a) non-dimensional concentrations, (b) temperature, (c) dissolved oxygen, (d) OUR, (e) VS reduction, and (f) pasteurisation lethality.

values as high as 1 mg/l. The transient has a duration of 40 batches.

Figure 5.9 corresponds to a VS concentration of 20 g/l and an ambient temperature of 20 °C. It shows that, given a higher ambient temperature, a concentration of 20 g/l can be sufficient to reach pasteurisation temperatures (i.e., ≥50 °C). This result challenges the notion that concentrations lower than 25 g/l can under no circumstances sustain the process in the thermophilic temperature range. This implies that, if the nature of the sludge is such that it does not allow pre-thickening above 25 g/l, then heat integration would be a potential solution that would allow the system to operate consistently in the thermophilic temperature range. Under these conditions, the process is substrate-limited (as can be seen in Figure 5.9a) while the DO reaches a concentration of 0.5 mg/l. The VS reduction is relatively high (∼30%) and the lethality exceeds the requirements by approximately 40 times. The transient has in this case a duration of ∼30 batches for the concentrations and VS reduction and ∼40 batches for the temperature and lethality.

By comparing the last four figures pertaining to CS1, it is possible to make the following qualitative observation: higher ambient temperatures lead to shorter durations of the transient conditions and higher degrees of stabilisation and pasteurisation, whereas higher influent VS concentrations lead to higher durations of transient conditions as well as higher degrees of stabilisation and pasteurisation.

The previous simulations also show that single-stage systems are capable of satisfying legal pasteurisation requirements. This result contradicts the notion that single-stage systems are not able to reduce pathogens to the same extent as two-stage or multiple-stage systems (USEPA, 1990).

Let us now proceed to examine the start-up simulations of CS2. Figure 5.10 displays the simulation corresponding to an influent VS concentration of 40 g/l and an ambient temperature of 10 °C. The initial condition of the concentrations in the first- and second-stage reactor respectively is

$$S_S^1 = 4 \text{ g/l},\ X_P^1 = 5 \text{ g/l},\ X_S^1 = 19 \text{ g/l},\ X_{SP}^1 = 7 \text{ g/l},\ X_{BHT}^1 = 3 \text{ g/l},$$

$$S_S^2 = 0.5 \text{ g/l},\ X_P^2 = 5 \text{ g/l},\ X_S^2 = 9 \text{ g/l},\ X_{SP}^2 = 2 \text{ g/l},\ X_{BHT}^2 = 3 \text{ g/l}.$$

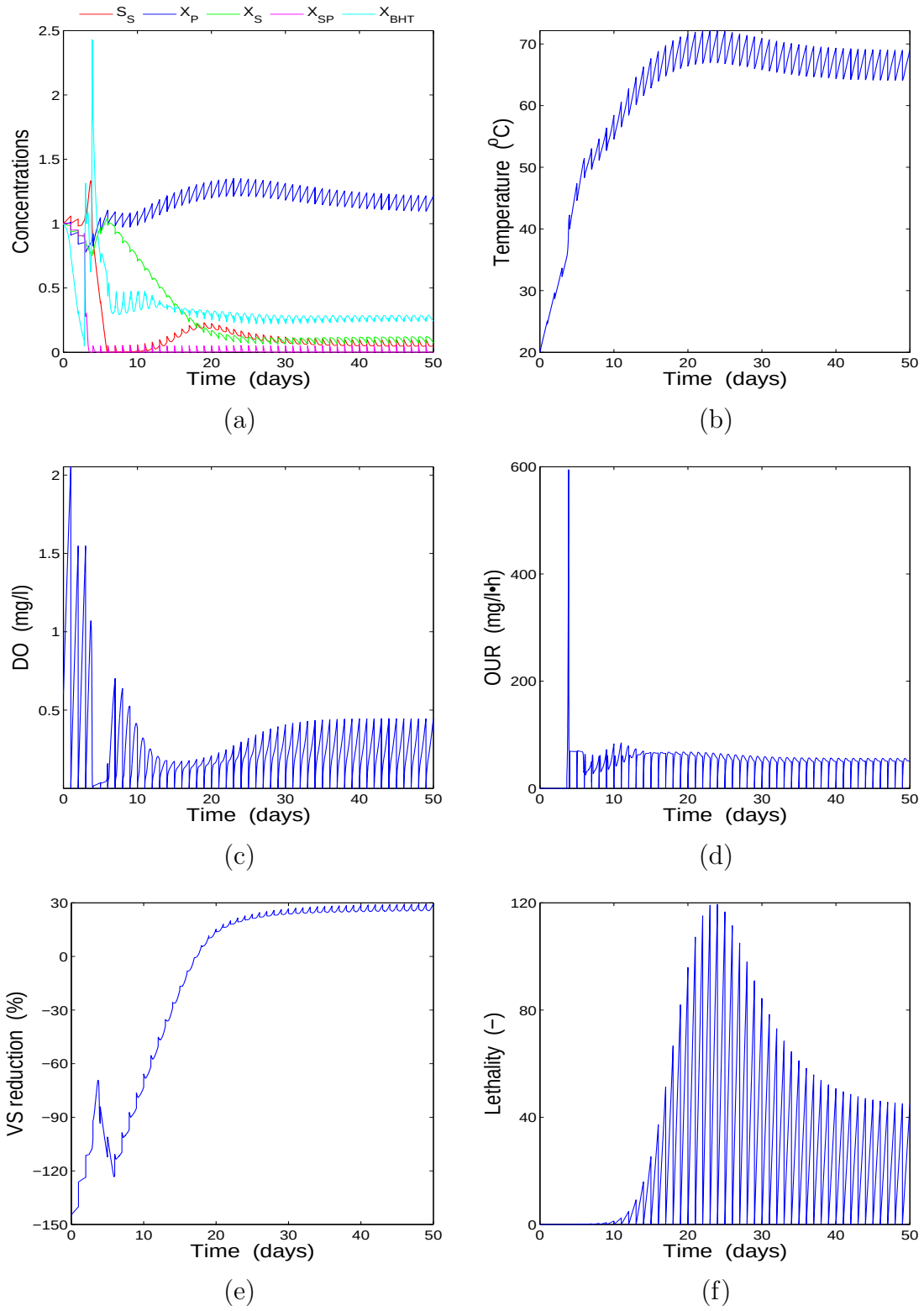


Figure 5.9: Start-up simulation of single-stage system CS1 at an ambient temperature of 20 °C and influent VS concentration of 20 g/l: (a) non-dimensional concentrations, (b) temperature, (c) dissolved oxygen, (d) OUR, (e) VS reduction, and (f) pasteurisation lethality.

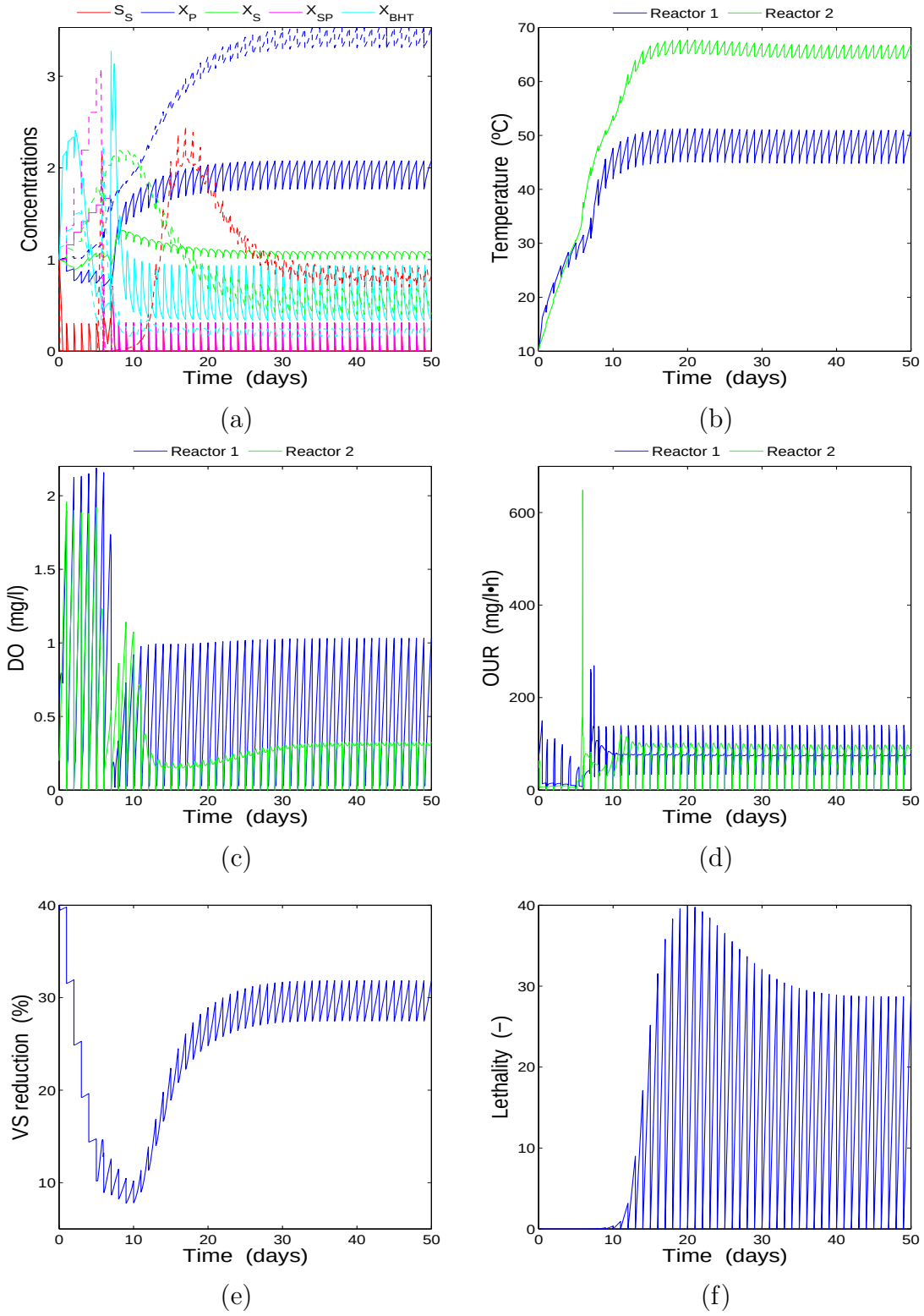


Figure 5.10: Start-up simulation of two-stage system CS2 at an ambient temperature of 10 °C and influent VS concentration of 40 g/l: (a) non-dimensional concentrations (solid lines: reactor 1; dashed lines: reactor 2), (b) temperatures, (c) dissolved oxygen, (d) OURs, (e) VS reduction, and (f) pasteurisation lethality.

The process is substrate-limited in both first-stage and second-stage reactors, and DO is relatively plentiful with concentrations ranging between 0.5 and 1 mg/l. Both concentrations and temperatures are in the range of values that would be expected for this kind of system. Stabilisation takes place predominantly in the first stage, whereas pasteurisation is attained in the second. The first is due to the fact that both VS concentration and the aeration flowrate are higher in the first-stage reactor, and the second due to the higher temperatures in the second-stage reactor. The overall degree of stabilisation achieved at equilibrium is ∼30% which is common (though closer to the lower boundary) in this kind of systems (USEPA, 1990). Lethality is ∼30 times higher than demanded by law. The transient has a duration of ∼30 batches for the VS reduction and about 15 to 20 batches in the case of temperature.

In Figure 5.11 (VS concentration 40 g/l and ambient temperature 20 °C), the reaction is once more limited by the availability of readily biodegradable substrate with relatively high concentrations of DO. Interestingly, the higher ambient temperature has led the temperature profiles of the two reactors to be much closer to each other in terms of values. The first-stage reactor reaches pasteurisation temperatures and those of the second stage are only slightly higher. This is due to the marked scarcity of substrate in the second stage which sets an important limitation on the amount of heat produced. Both treatment objectives have been positively affected by the higher ambient temperature (when compared to the previous figure) with a degree of stabilisation of 35% and a lethality of ∼40. The transient of VS reduction has considerably decreased to 15 to 20 batches.

Under the conditions of Figure 5.12 (VS concentration 20 g/l, ambient temperature 10 °C), it is no surprise that the process is substrate-limited, nor that DO is so high. What is surprising though is that, in spite of the lack of substrate, the system has sufficient "fuel" to allow the second reactor to reach temperatures in excess of 50 °C and attain some degree of pasteurisation (although quite low). It is also surprising that the degree of stabilisation is as high as ∼20% with a transient of 25 to 30 batches.

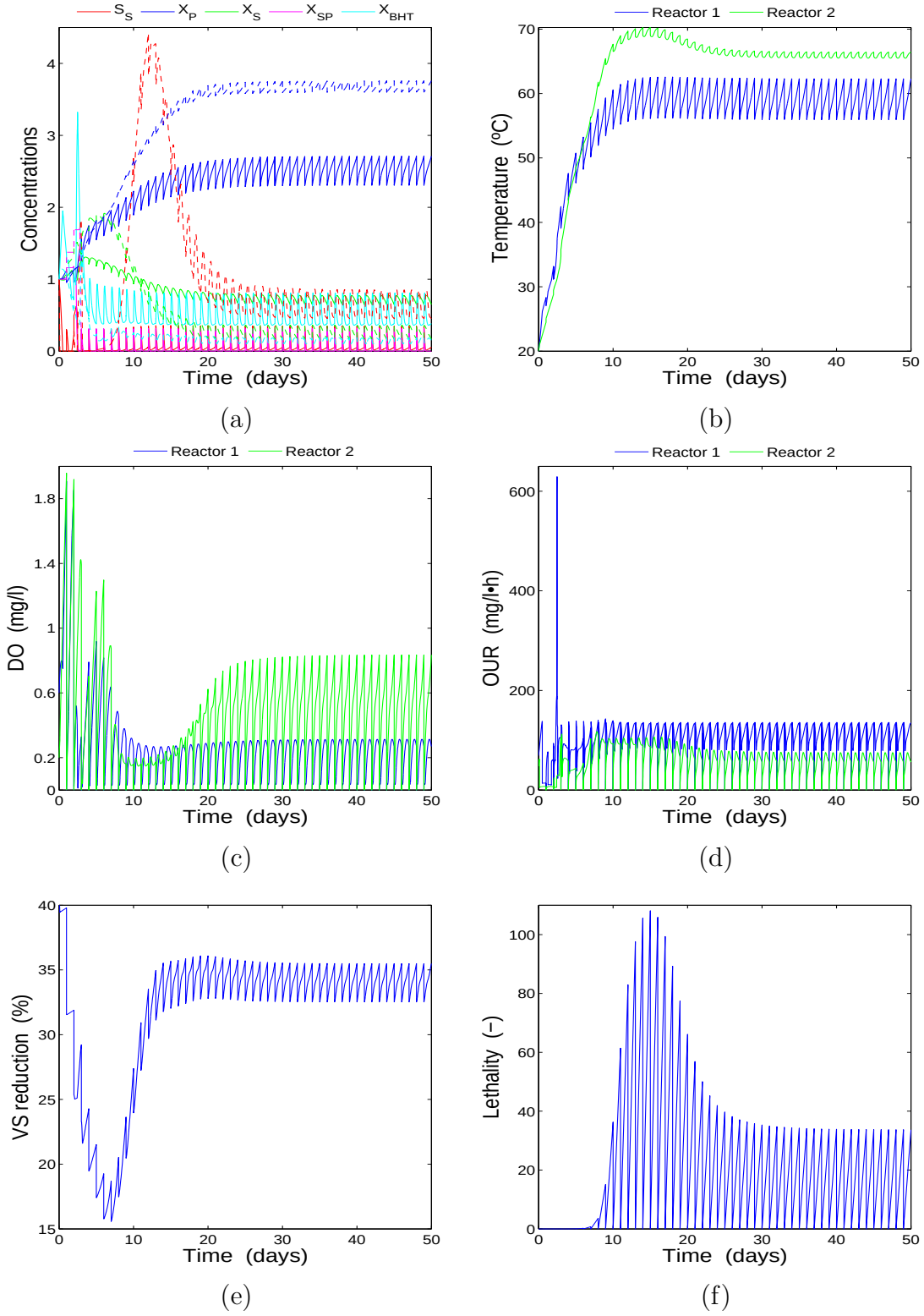


Figure 5.11: Start-up simulation of two-stage system CS2 at an ambient temperature of 20 °C and influent VS concentration of 40 g/l: (a) non-dimensional concentrations (solid lines: reactor 1; dashed lines: reactor 2), (b) temperatures, (c) dissolved oxygen, (d) OURs, (e) VS reduction, and (f) pasteurisation lethality.

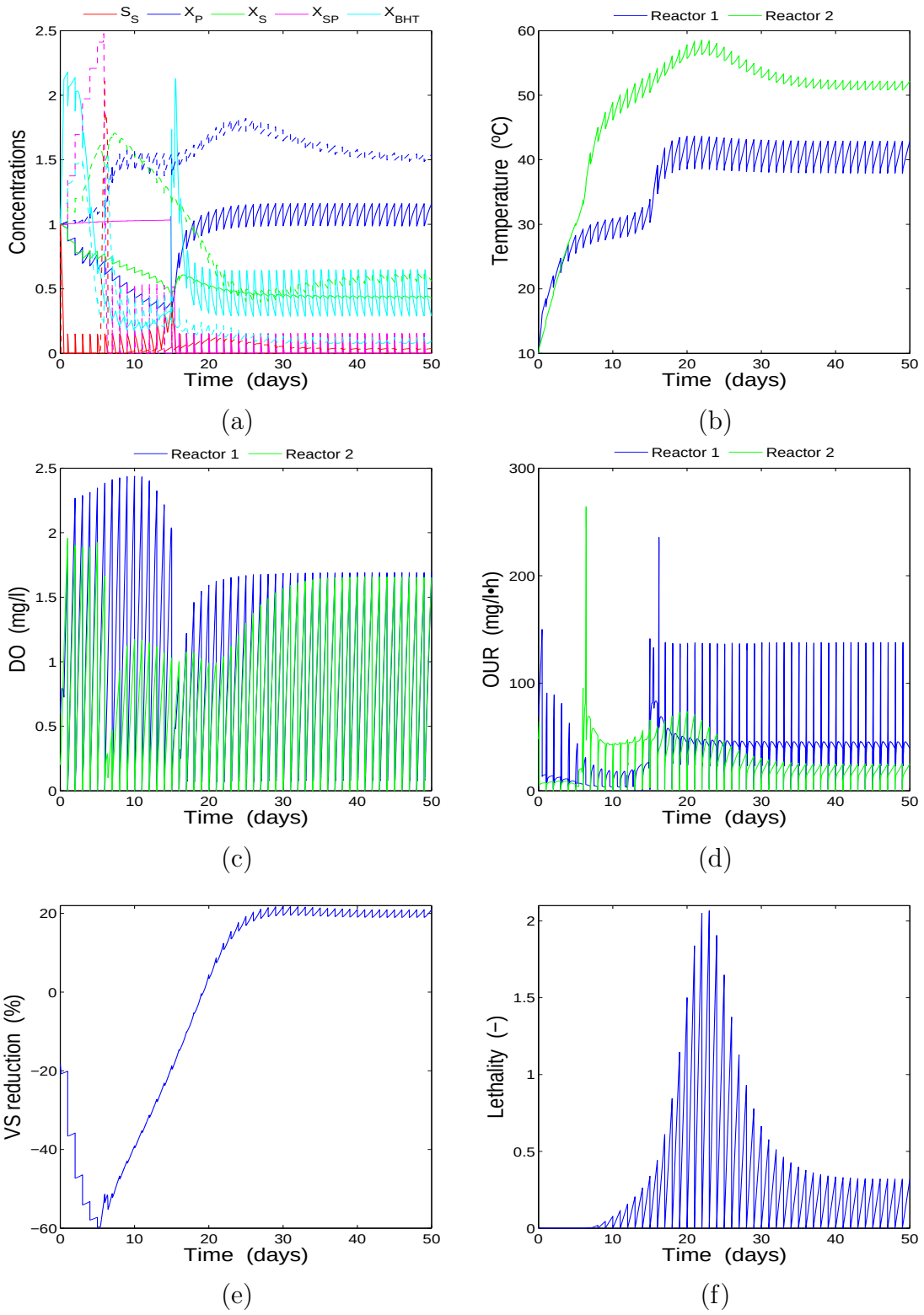


Figure 5.12: Start-up simulation of two-stage system CS2 at an ambient temperature of 10 °C and influent VS concentration of 20 g/l: (a) non-dimensional concentrations (solid lines: reactor 1; dashed lines: reactor 2), (b) temperatures, (c) dissolved oxygen, (d) OURs, (e) VS reduction, and (f) pasteurisation lethality.

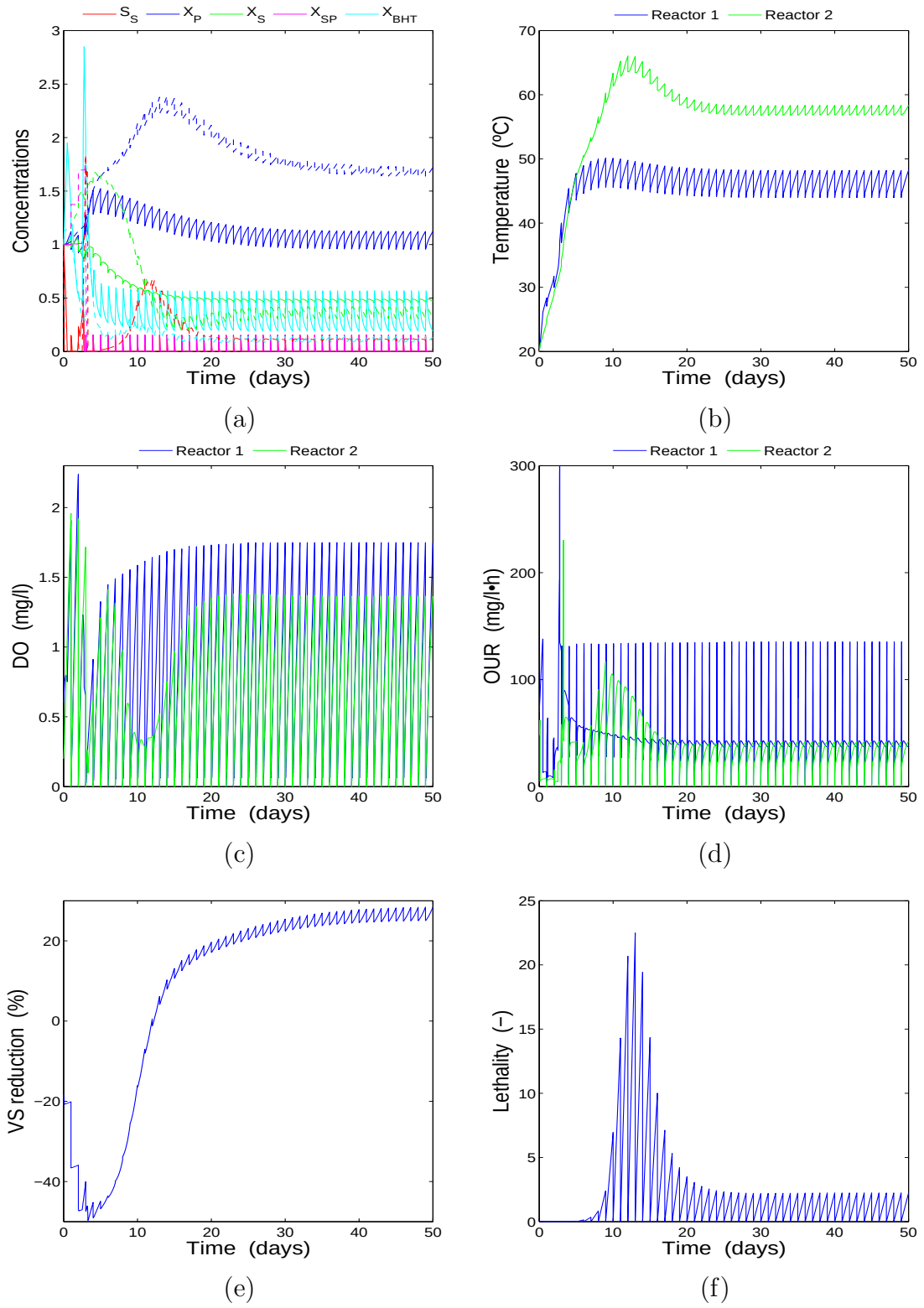


Figure 5.13: Start-up simulation of two-stage system CS2 at an ambient temperature of 20 °C and influent VS concentration of 20 g/l: (a) non-dimensional concentrations (solid lines: reactor 1; dashed lines: reactor 2), (b) temperatures, (c) dissolved oxygen, (d) OURs, (e) VS reduction, and (f) pasteurisation lethality.

In Figure 5.13 (VS concentration 20 g/l, ambient temperature 20 °C), the reaction is substrate-limited with high DO levels. The higher ambient temperature allows the second reactor to attain temperatures close to 60 °C leading to lethalities twice higher than legally required. VS reduction is also positively affected by the higher ambient temperature with ∼30%. The transient has a duration of 35 batches. As it was found for CS1, a VS concentration of 20 g/l can thus be sufficient to attain and sustain thermophilic operation but only as long as ambient temperature is not too low. As it was pointed out before, this result contradicts the statement that VS concentrations have to be in excess of 25 g/l to guarantee thermophilic operation (USEPA, 1990).

A comparison of the last four figures belonging to CS2 leads to a similar observation as for CS1: higher ambient temperatures and higher influent VS concentrations result in increased degrees of stabilisation and pasteurisation. As for the duration of the transient, though, it is not possible to make an unambiguous statement.

### 5.2.2 Steady state simulations

In this section, we will examine in more detail the behaviour of CS1 under steady state conditions. By "steady state", we mean here cyclic or periodic operation, that is, that the time profile of the state variables of a given batch is identical to that of its preceding and following batches. The model ATM1 will be used for these simulations.

First, we will consider the steady state of the system under the four different conditions studied in the previous section; that is, the conditions of influent VS concentration and ambient temperature. Figure 5.14 shows the evolution of the system under the aforementioned conditions during three consecutive 1-day batches. To avoid confusion, the individual carbonaceous components, both particulate and soluble, have been added together resulting in the total VS (TVS) concentration. It can be easily seen that increasing ambient temperature or influent VS concentration leads to higher temperature profiles, and higher degrees of pasteurisation and stabilisation. Thus, this plot makes the qualitative observation mentioned in the previous section more intuitive and easy to grasp. It serves, in a way, as a simple

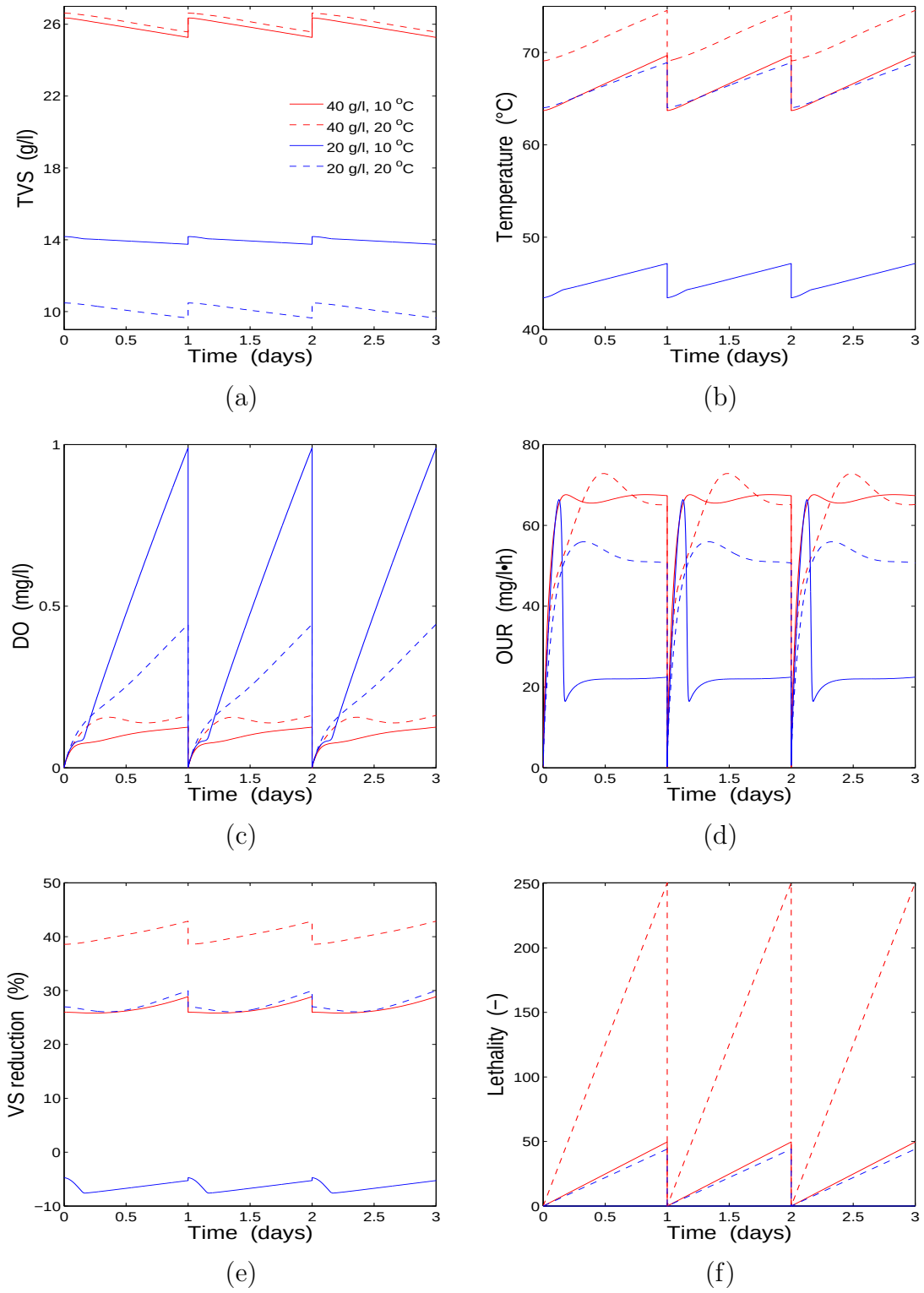


Figure 5.14: Steady state simulation of single-stage system CS1 at different ambient temperatures and influent VS concentrations: (a) TVS, (b) temperatures, (c) dissolved oxygen, (d) OUR, (e) VS reduction, and (f) pasteurisation lethality.

form of sensitivity analysis.

The effect of rising ambient temperature and influent VS concentration on the temperature profile and the overall stabilisation and pasteurisation processes can be understood as being due to an increase of bacterial activity. This interpretation or hypothesis can be backed by the graph of the OUR in Figure 5.14d (as the OUR is considered as a main measure of metabolic activity). It shows that such increases of ambient temperature and VS concentration can bring about significant changes in the level of oxygen uptake by the microorganisms. By comparing the integrals of the OUR at different conditions, it is possible to say that increases in both influent VS concentration and ambient temperature tend in turn to increase bacterial activity. However, increases in ambient temperature only cause significant increases in the OUR at low influent VS concentrations; as VS concentration increases, the effect of higher ambient temperatures on the OUR diminishes and even becomes negative. It is also possible to say that the influent VS concentration had a stronger influence on bacterial activity than did ambient temperature. This reinforces the notion of the influent VS concentration as a critical parameter to be taken into account for both design and operation of ATAD systems.

In section 4.2.1, we discussed the qualitative behaviour and transformations of the mass components of the system which are illustrated in the death-regeneration life cycle illustrated by Figure 4.1. Now we are in a better position to examine this behaviour in a quantitative way by looking at a representative example of system dynamics. Figure 5.15 displays the evolution of the most important system components for the particular case of CS1 with an influent VS concentration of 40 g/l and an ambient temperature of 10 °C. The relatively high concentration of substrate $S_S$ and the low level of DO indicates that the reaction is oxygen-limited under these conditions. The two kinds of substrate $S_S$ and $X_S$ decrease for most of the time. Let us remember that $X_S$ increases as a result of cell lyses and decreases through hydrolysis, while $S_S$ increases as a result of hydrolysis and decreases with biomass growth. In this manner, it can be said that the period of decreasing substrate $S_S$ is likely due to biomass growth outweighing hydrolysis, whereas the opposite applies for the period of increasing concentration. The particulate products from decay $X_P$ show

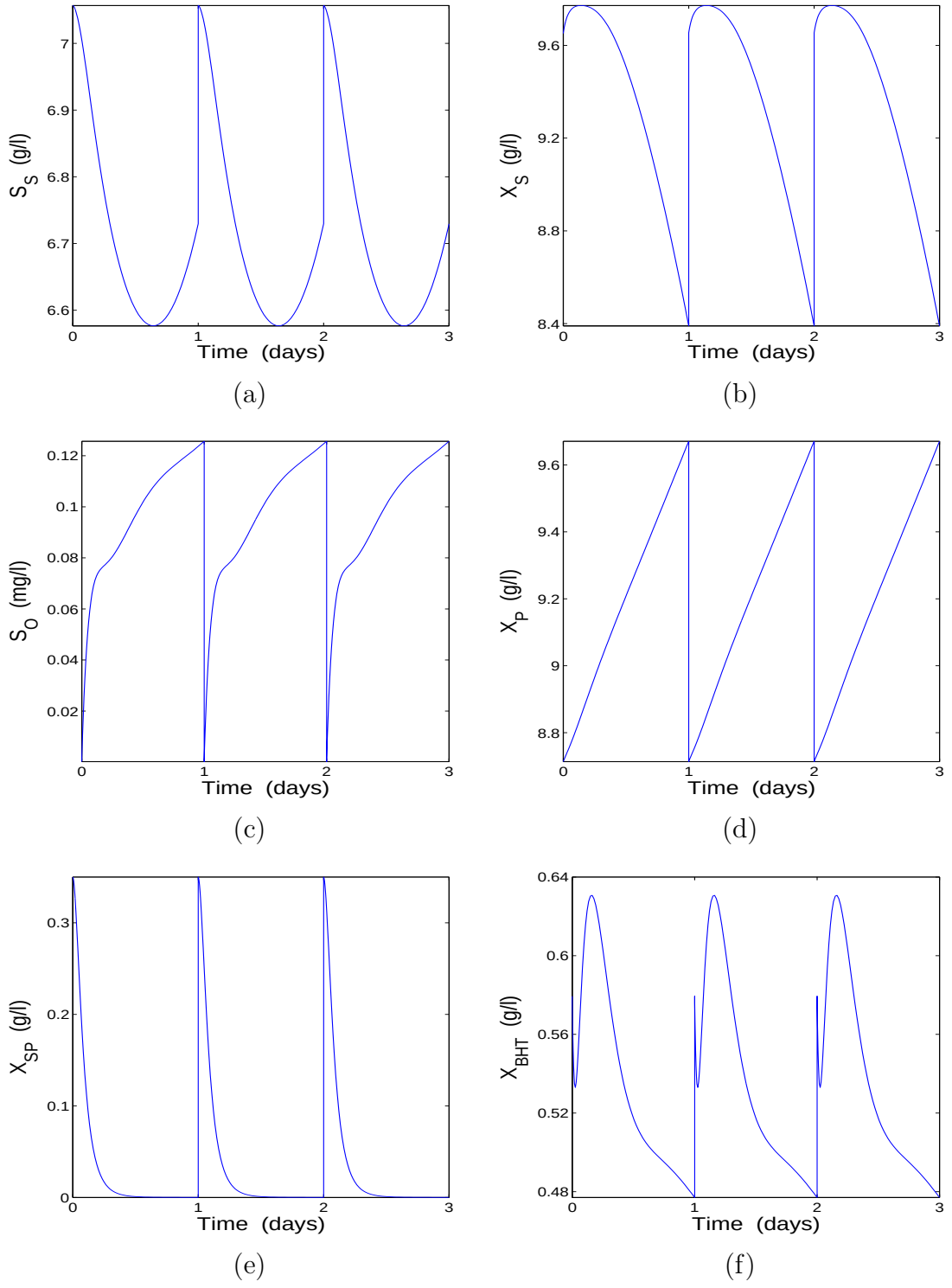


Figure 5.15: Steady state simulation of single-stage system CS1 at ambient temperature of 10 °C and influent VS concentration of 40 g/l over a time period of three 1-day batches: (a) readily biodegradable substrate $S_S$, (b) slowly biodegradable substrate $X_S$, (c) dissolved oxygen $S_o$, (d) particulate products from decay $X_P$, (e) inactive thermophilic biomass $X_{SP}$, and (f) thermophilic biomass $X_{BHT}$.

a steady increase. Their concentration is only affected by the process of cell decay and, as they do not undergo any further transformations, they can only accumulate in the course of the reaction. Inactive thermophilic biomass $X_{SP}$ is assumed to exist in the influent sludge in the form of spores. Thus, its concentration increases suddenly after loading. Then, the spores adapt to the favorable thermophilic conditions in a matter of hours and they transform into active thermophilic biomass $X_{BHT}$. The rapid biomass growth observed after loading is a result of the quick adaptation of the sporulated thermophilic microorganisms. After this period of exponential growth, active biomass experiences a clear and steady decrease. This fast decrease in biomass concentration shows that, under these conditions, cell lysis predominates over biomass growth.

## 5.3 Asymptotic analysis

This section concerns the asymptotic analysis of the ATM1 model. This analysis will allow us to study the behaviour of the system for certain limiting cases. This kind of study is useful in that it helps to determine the terms that dominate the system dynamics under such limiting cases. The ATM1 model described in section 4.2 tracks the evolution of ten variables: nine mass components and the temperature of the system (or its corresponding enthalpy). For simplicity, we disregard the temperature dependence here, and so do not display an equation for the temperature. We set constant values for the model parameters and choose these values for reactor operation at 50 °C. We also neglect the effect of thermophilic activation, on the basis that it occurs rapidly at the start of the batch reaction, and so do not consider inactive biomass $X_{\mathrm{SP}}$ in the model. Reactor-specific parameters correspond to CS1.

Under these assumptions, the governing equations of the ATM1 model are

$$
\begin{aligned}
\frac{dS_{\rm S}}{dt} &= -\frac{1}{Y_{\rm H}}\mu_{\rm H}\frac{S_{\rm S}}{K_{\rm S}+S_{\rm S}}\frac{S_{\rm O}}{K_{\rm O}+S_{\rm O}}X_{\rm BH} - \frac{1}{Y_{\rm HT}}\mu_{\rm HT}\frac{S_{\rm S}}{K_{\rm ST}+S_{\rm S}}\frac{S_{\rm O}}{K_{\rm OT}+S_{\rm O}}X_{\rm BHT} \\
&\quad + k_{\rm H}\frac{X_{\rm S}}{K_{\rm X}X_{\rm BH}+X_{\rm S}}\frac{S_{\rm O}}{K_{\rm O}+S_{\rm O}}X_{\rm BH} + k_{\rm HT}\frac{X_{\rm S}}{K_{\rm XT}X_{\rm BHT}+X_{\rm S}}\frac{S_{\rm O}}{K_{\rm OT}+S_{\rm O}}X_{\rm BHT}, \\
\frac{dX_{\rm S}}{dt} &= b_{\rm H}(1-f_{\rm P})X_{\rm BH} + b_{\rm HT}(1-f_{\rm PT})X_{\rm BHT} - k_{\rm H}\frac{X_{\rm S}}{K_{\rm X}X_{\rm BH}+X_{\rm S}}\frac{S_{\rm O}}{K_{\rm O}+S_{\rm O}}X_{\rm BH} \\
&\quad - k_{\rm HT}\frac{X_{\rm S}}{K_{\rm XT}X_{\rm BHT}+X_{\rm S}}\frac{S_{\rm O}}{K_{\rm OT}+S_{\rm O}}X_{\rm BHT}, \\
\frac{dX_{\rm BH}}{dt} &= \mu_{\rm H}\frac{S_{\rm S}}{K_{\rm S}+S_{\rm S}}\frac{S_{\rm O}}{K_{\rm O}+S_{\rm O}}X_{\rm BH} - b_{\rm H}X_{\rm BH}, \\
\frac{dX_{\rm BHT}}{dt} &= \mu_{\rm HT}\frac{S_{\rm S}}{K_{\rm ST}+S_{\rm S}}\frac{S_{\rm O}}{K_{\rm OT}+S_{\rm O}}X_{\rm BHT} - b_{\rm HT}X_{\rm BHT}, \\
\frac{dS_{\rm O}}{dt} &= -\frac{(1-Y_{\rm H})}{Y_{\rm H}}\mu_{\rm H}\frac{S_{\rm S}}{K_{\rm S}+S_{\rm S}}\frac{S_{\rm O}}{K_{\rm O}+S_{\rm O}}X_{\rm BH} \\
&\quad - \frac{(1-Y_{\rm HT})}{Y_{\rm HT}}\mu_{\rm HT}\frac{S_{\rm S}}{K_{\rm ST}+S_{\rm S}}\frac{S_{\rm O}}{K_{\rm OT}+S_{\rm O}}X_{\rm BHT} + k_a q_a(\bar{S_{\rm O}}-S_{\rm O}), \\
\frac{dX_{\rm P}}{dt} &= f_{\rm P}k_{\rm H}\frac{X_{\rm S}}{K_{\rm X}X_{\rm BH}+X_{\rm S}}\frac{S_{\rm O}}{K_{\rm O}+S_{\rm O}}X_{\rm BH} + f_{\rm PT}k_{\rm HT}\frac{X_{\rm S}}{K_{\rm XT}X_{\rm BHT}+X_{\rm S}}\frac{S_{\rm O}}{K_{\rm OT}+S_{\rm O}}X_{\rm BHT}.
\end{aligned}
\tag{5.1}
$$

The value of the parameters appearing in the model under the specified temperature of 50 °C are shown in Table 5.3. We see that the first five of these equations can be solved independently of the sixth, and so we do not display the equation for the particulate products from decay $X_{\rm P}$ again.

We model the operation of the single-stage system CS1 for one batch, and so solve $5.1_1$ – $5.1_5$ subject to the initial condition

$$
S_{\rm S} = S_{\rm S}^o,\ X_{\rm S} = X_{\rm S}^o,\ X_{\rm BH} = X_{\rm BH}^o,\ X_{\rm BHT} = X_{\rm BHT}^o,\ S_{\rm O} = S_{\rm O}^o \quad \text{at} \quad t = 0. \tag{5.2}
$$

For the illustrative numerical results used in the current analysis, we take

$$
S_{\rm S}^o = 5\ \text{g/l},\ X_{\rm S}^o = 15\ \text{g/l},\ X_{\rm BH}^o = 1\ \text{g/l},\ X_{\rm BHT}^o = 1\ \text{g/l},\ S_{\rm O}^o = 10\ \text{mg/l}.
$$

We scale the system of ordinary differential equations by choosing

Table 5.3: Values of the parameters of the ATM1 model at a constant temperature of 50 °C.

| Symbol | Description | Value | Unit |
|---|---|---|---|
| $K_{\mathrm{S}}$ | Mesophilic half saturation constant for $S_{\mathrm{S}}$ | 0.02 | g/l |
| $K_{\mathrm{O}}$ | Mesophilic half saturation constant for $S_{\mathrm{O}}$ | $2 \cdot 10^{-4}$ | g/l |
| $K_{\mathrm{ST}}$ | Thermophilic half saturation constant for $S_{\mathrm{S}}$ | 0.03 | g/l |
| $K_{\mathrm{OT}}$ | Thermophilic half saturation constant for $S_{\mathrm{O}}$ | $2 \cdot 10^{-4}$ | g/l |
| $S_{\mathrm{O}}$ | Oxygen saturation concentration | $5 \cdot 10^{-3}$ | g/l |
| $\mu_{\mathrm{H}}$ | Maximum growth rate of $X_{\mathrm{BH}}$ | 16.8 | 1/day |
| $\mu_{\mathrm{HT}}$ | Maximum growth rate of $X_{\mathrm{BHT}}$ | 24.3 | 1/day |
| $b_{\mathrm{H}}$ | Decay rate of mesophiles | 43 | 1/day |
| $b_{\mathrm{HT}}$ | Decay rate of thermophiles | 5.2 | 1/day |
| $k_{\mathrm{H}}$ | Maximum mesophilic hydrolysis rate | 10 | 1/day |
| $k_{\mathrm{HT}}$ | Maximum thermophilic hydrolysis rate | 9.2 | 1/day |
| $k_a q_a$ | Oxygen mass transfer coefficient | 1000 | 1/day |
| $Y_{\mathrm{H}}$ | Mesophilic yield | 0.6 | – |
| $Y_{\mathrm{HT}}$ | Thermophilic yield | 0.6 | – |
| $f_{\mathrm{P}}$ | Inert fraction of mesophilic biomass | 0.3 | – |
| $f_{\mathrm{PT}}$ | Inert fraction of thermophilic biomass | 0.3 | – |
| $K_{\mathrm{X}}$ | Half saturation constant for mesophilic hydrolysis | 0.03 | – |
| $K_{\mathrm{XT}}$ | Half saturation constant for thermophilic hydrolysis | 0.03 | – |

$$t \sim t_{\mathrm{batch}},\ S_{\mathrm{S}} \sim S_{\mathrm{S}}^{o},\ X_{\mathrm{S}} \sim X_{\mathrm{S}}^{o},\ X_{\mathrm{BH}} \sim X_{\mathrm{BH}}^{o},\ X_{\mathrm{BHT}} \sim X_{\mathrm{BHT}}^{o},\ S_{\mathrm{O}} \sim S_{\mathrm{O}}^{o},$$

where $t_{\mathrm{batch}} = 1$ day. With this choice of scaling, the dimensionless form for equations $5.1_1$ – $5.1_5$ with the initial condition 5.2 is given by

$$\begin{aligned}
\frac{dS_{\mathrm{S}}}{dt} &= -\delta_1 \frac{S_{\mathrm{S}}}{\delta_2 + S_{\mathrm{S}}} \frac{S_{\mathrm{O}}}{\delta_3 + S_{\mathrm{O}}} X_{\mathrm{BH}} - \delta_4 \frac{S_{\mathrm{S}}}{\delta_5 + S_{\mathrm{S}}} \frac{S_{\mathrm{O}}}{\delta_6 + S_{\mathrm{O}}} X_{\mathrm{BHT}} \\
&\quad + \delta_7 \frac{X_{\mathrm{S}}}{\delta_8 X_{\mathrm{BH}} + X_{\mathrm{S}}} \frac{S_{\mathrm{O}}}{\delta_3 + S_{\mathrm{O}}} X_{\mathrm{BH}} + \delta_9 \frac{X_{\mathrm{S}}}{\delta_{10} X_{\mathrm{BHT}} + X_{\mathrm{S}}} \frac{S_{\mathrm{O}}}{\delta_6 + S_{\mathrm{O}}} X_{\mathrm{BHT}}, \\
\frac{dX_{\mathrm{S}}}{dt} &= \delta_{11} X_{\mathrm{BH}} + \delta_{12} X_{\mathrm{BHT}} - \delta_{13} \frac{X_{\mathrm{S}}}{\delta_8 X_{\mathrm{BH}} + X_{\mathrm{S}}} \frac{S_{\mathrm{O}}}{\delta_3 + S_{\mathrm{O}}} X_{\mathrm{BH}} \\
&\quad - \delta_{14} \frac{X_{\mathrm{S}}}{\delta_{10} X_{\mathrm{BHT}} + X_{\mathrm{S}}} \frac{S_{\mathrm{O}}}{\delta_6 + S_{\mathrm{O}}} X_{\mathrm{BHT}}, \\
\frac{dX_{\mathrm{BH}}}{dt} &= \delta_{15} \frac{S_{\mathrm{S}}}{\delta_2 + S_{\mathrm{S}}} \frac{S_{\mathrm{O}}}{\delta_3 + S_{\mathrm{O}}} X_{\mathrm{BH}} - \delta_{16} X_{\mathrm{BH}}, \\
\frac{dX_{\mathrm{BHT}}}{dt} &= \delta_{17} \frac{S_{\mathrm{S}}}{\delta_5 + S_{\mathrm{S}}} \frac{S_{\mathrm{O}}}{\delta_6 + S_{\mathrm{O}}} X_{\mathrm{BHT}} - \delta_{18} X_{\mathrm{BHT}}, \\
\frac{dS_{\mathrm{O}}}{dt} &= -\delta_{19} \frac{S_{\mathrm{S}}}{\delta_2 + S_{\mathrm{S}}} \frac{S_{\mathrm{O}}}{\delta_3 + S_{\mathrm{O}}} X_{\mathrm{BH}} - \delta_{20} \frac{S_{\mathrm{S}}}{\delta_5 + S_{\mathrm{S}}} \frac{S_{\mathrm{O}}}{\delta_6 + S_{\mathrm{O}}} X_{\mathrm{BHT}} + \delta_{21} \left(\delta_{22} - S_{\mathrm{O}}\right),
\end{aligned} \tag{5.3}$$

subject to the initial condition

$$S_{\mathrm{S}} = 1,\ X_{\mathrm{S}} = 1,\ X_{\mathrm{BH}} = 1,\ X_{\mathrm{BHT}} = 1,\ S_{\mathrm{O}} = 1 \quad \text{at} \quad t = 0,$$

where the definition of, and values for, the non-dimensional parameters $\delta_i$ ($1 \leq i \leq 22$) are given in Table 5.4.

Table 5.4: Dimensionless parameters of the ATM1 model.

| Symbol | Description | Value |
|---|---|---|
| $\delta_1$ | $\mu_{\mathrm{H}} t_{\mathrm{batch}} X^o_{\mathrm{BH}} / (Y_{\mathrm{HT}} S^o_{\mathrm{S}})$ | 5.60 |
| $\delta_2$ | $K_{\mathrm{S}} / S^o_{\mathrm{S}}$ | $4 \cdot 10^{-3}$ |
| $\delta_3$ | $K_{\mathrm{O}} / S^o_{\mathrm{O}}$ | 0.2 |
| $\delta_4$ | $\mu_{\mathrm{HT}} t_{\mathrm{batch}} X^o_{\mathrm{BHT}} / (Y_{\mathrm{HT}} S^o_{\mathrm{S}})$ | 8.10 |
| $\delta_5$ | $K_{\mathrm{ST}} / S^o_{\mathrm{S}}$ | $6 \cdot 10^{-3}$ |
| $\delta_6$ | $K_{\mathrm{OT}} / S^o_{\mathrm{O}}$ | 0.2 |
| $\delta_7$ | $k_{\mathrm{H}} t_{\mathrm{batch}} X^o_{\mathrm{BH}} / S^o_{\mathrm{S}}$ | 2.0 |
| $\delta_8$ | $K_{\mathrm{X}} X^o_{\mathrm{BH}} / X^o_{\mathrm{S}}$ | $2 \cdot 10^{-3}$ |
| $\delta_9$ | $(k_{\mathrm{HT}} t_{\mathrm{batch}})\,(X^o_{\mathrm{BHT}} / S^o_{\mathrm{S}})$ | 1.84 |
| $\delta_{10}$ | $K_{\mathrm{XT}} X^o_{\mathrm{BHT}} / X^o_{\mathrm{S}}$ | $2 \cdot 10^{-3}$ |
| $\delta_{11}$ | $(1 - f_{\mathrm{P}}) b_{\mathrm{H}} t_{\mathrm{batch}} X^o_{\mathrm{BH}} / X^o_{\mathrm{S}}$ | 2.01 |
| $\delta_{12}$ | $(1 - f_{\mathrm{PT}}) b_{\mathrm{HT}} t_{\mathrm{batch}} X^o_{\mathrm{BHT}} / X^o_{\mathrm{S}}$ | 0.25 |
| $\delta_{13}$ | $k_{\mathrm{H}} t_{\mathrm{batch}} X^o_{\mathrm{BH}} / X^o_{\mathrm{S}}$ | 0.67 |
| $\delta_{14}$ | $k_{\mathrm{HT}} t_{\mathrm{batch}} X^o_{\mathrm{BHT}} / X^o_{\mathrm{S}}$ | 0.61 |
| $\delta_{15}$ | $\mu_{\mathrm{H}} t_{\mathrm{batch}}$ | 16.8 |
| $\delta_{16}$ | $b_{\mathrm{H}} t_{\mathrm{batch}}$ | 43.0 |
| $\delta_{17}$ | $\mu_{\mathrm{HT}} t_{\mathrm{batch}}$ | 24.3 |
| $\delta_{18}$ | $b_{\mathrm{HT}} t_{\mathrm{batch}}$ | 5.2 |
| $\delta_{19}$ | $(1 - Y_{\mathrm{H}}) \mu_{\mathrm{H}} t_{\mathrm{batch}} X^o_{\mathrm{BH}} / (Y_{\mathrm{H}} S^o_{\mathrm{O}})$ | $11.2 \cdot 10^3$ |
| $\delta_{20}$ | $(1 - Y_{\mathrm{HT}}) \mu_{\mathrm{HT}} t_{\mathrm{batch}} X^o_{\mathrm{BHT}} / (Y_{\mathrm{HT}} S^o_{\mathrm{O}})$ | $16.2 \cdot 10^3$ |
| $\delta_{21}$ | $k_a q_a t_{\mathrm{batch}}$ | $10^3$ |
| $\delta_{22}$ | $\bar{S_{\mathrm{O}}} / S^o_{\mathrm{O}}$ | 5.0 |

In Figure 5.16, we show the solution to the system of equations 5.3 for the parameter values listed in Table 5.4. It is noteworthy from the parameter values chosen that the readily biodegradable material is depleted over a period of approximately one half of a day while the slowly biodegradable material is not completely removed until approximately five days later. During the first half of the first day with $S_{\mathrm{S}} \neq 0$, the rate of the reaction is limited by the availability of dissolved oxygen whose concentration is extremely low. After $S_{\mathrm{S}}$ is depleted, the rate of the reaction is limited by the availability of substrate and the concentration of dissolved oxygen increases abruptly. It is during this period of scarcity of substrate (the endogenous phase) that the amount of VS in the sludge is reduced and the sludge is stabilised. Over this period, the rate of the reaction is also limited by the hydrolysis rate. As it

can be seen, $S_S$ does not increase over time due to the fact that it is consumed faster by the biomass than it is generated through hydrolysis. Endogenous decay increases markedly after the slowly biodegradable substrate $X_S$ is depleted. When this happens, biomass concentration plummets and the dissolved oxygen concentration reaches its saturation value. We should note, however, that some of the parameter values used are uncertain, and that they can depend on temperature and time, as well as other factors, such as the character of the influent sludge and the reactor system. Since we have assumed the parameter values to be fixed, the limitations of such an approach are clear. Notwithstanding, our goal in this section is to gain some insight into aspects of the ATM1 model in particular and the ATAD reaction in general, rather than attempting to model a particular reactor system in detail.

What is most important in the solution displayed by Figure 5.16 is its general qualitative structure. In most cases, ATAD systems show this kind of behaviour in which the reaction is first oxygen-limited (while substrate is available) and then substrate-limited, finishing with a period of endogenous respiration and decay. Similar results were first obtained by Gomez et al. (2007). The duration of each of these phases or regions, and the particular quantitative relations between the state variables depend on several factors, such as the initial conditions, system inputs, reactor-specific parameters, etc. Nevertheless, according to our experience, the qualitative structure of the solution is generally the same under most of these conditions. Experimental research has also demonstrated that this behaviour corresponds to that of actual ATAD reaction (Kovacs, 2007; Jamniczky-Kaszas, 2010). For example, this behaviour can explain, at least qualitatively, the respirometric curve in Figure 2.2b.

As mentioned above, under normal ATAD operating conditions a relatively high temperature is maintained in the reactor. Commonly, the temperature after adding a new inflow batch and mixing remains higher than the mesophilic temperature range, and hence the metabolic activity associated to mesophilic microorganisms is rendered unimportant. We can therefore neglect the mesophilic variable in the model and set $X_{BH} = 0$. The system of equations 5.3 then reduces to

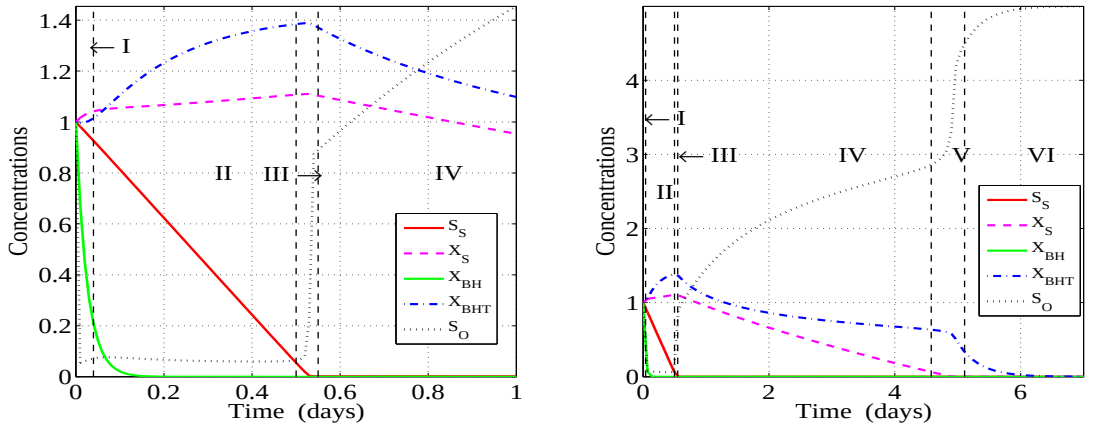


(a) (b)

Figure 5.16: (a) Plot of the solution to system of equations 5.3 over one day and for the parameter values displayed in Table 5.4. (b) The same solution as in (a) plotted over one week. Over this period of time, slowly biodegradable substrate is removed and dissolved oxygen reaches its saturation value.

$$
\begin{aligned}
\frac{dS_{\mathrm{S}}}{dt} &= -\delta_4 \frac{S_{\mathrm{S}}}{\delta_5 + S_{\mathrm{S}}} \frac{S_{\mathrm{O}}}{\delta_6 + S_{\mathrm{O}}} X_{\mathrm{BHT}} + \delta_9 \frac{X_{\mathrm{S}}}{\delta_{10} X_{\mathrm{BHT}} + X_{\mathrm{S}}} \frac{S_{\mathrm{O}}}{\delta_6 + S_{\mathrm{O}}} X_{\mathrm{BHT}}, \\
\frac{dX_{\mathrm{S}}}{dt} &= \delta_{12} X_{\mathrm{BHT}} - \delta_{14} \frac{X_{\mathrm{S}}}{\delta_{10} X_{\mathrm{BHT}} + X_{\mathrm{S}}} \frac{S_{\mathrm{O}}}{\delta_6 + S_{\mathrm{O}}} X_{\mathrm{BHT}}, \\
\frac{dX_{\mathrm{BHT}}}{dt} &= \delta_{17} \frac{S_{\mathrm{S}}}{\delta_5 + S_{\mathrm{S}}} \frac{S_{\mathrm{O}}}{\delta_6 + S_{\mathrm{O}}} X_{\mathrm{BHT}} - \delta_{18} X_{\mathrm{BHT}}, \\
\frac{dS_{\mathrm{O}}}{dt} &= -\delta_{20} \frac{S_{\mathrm{S}}}{\delta_5 + S_{\mathrm{S}}} \frac{S_{\mathrm{O}}}{\delta_6 + S_{\mathrm{O}}} X_{\mathrm{BHT}} + \delta_{21} \left(\delta_{22} - S_{\mathrm{O}}\right), \\
S_{\mathrm{S}} &= 1,\ X_{\mathrm{S}} = 1,\ X_{\mathrm{BHT}} = 1,\ S_{\mathrm{O}} = 1 \quad \text{at} \quad t = 0.
\end{aligned}
\tag{5.4}
$$

Figure 5.17 displays the numerical solutions of the system of equations 5.4 for the parameter values given in Table 5.4. Comparing these with the solutions given in Figure 5.16, one notes that there is good qualitative agreement and reasonable quantitative agreement, as would be expected.

Motivated by the relevant parameter values listed in Table 5.4, we denote

$$\delta_5 = \varepsilon,\ \delta_{10} = \theta_1 \varepsilon,\ \delta_{20} = \theta_2/\varepsilon,\ \delta_{21} = \theta_3/\varepsilon,$$

where $\theta_1, \theta_2, \theta_3 = \mathcal{O}(1)$, and consider the limit $\varepsilon \to 0$. This limit corresponds to a case where biomass growth is not dependent on $S_{\mathrm{S}}$, i.e., biomass growth is

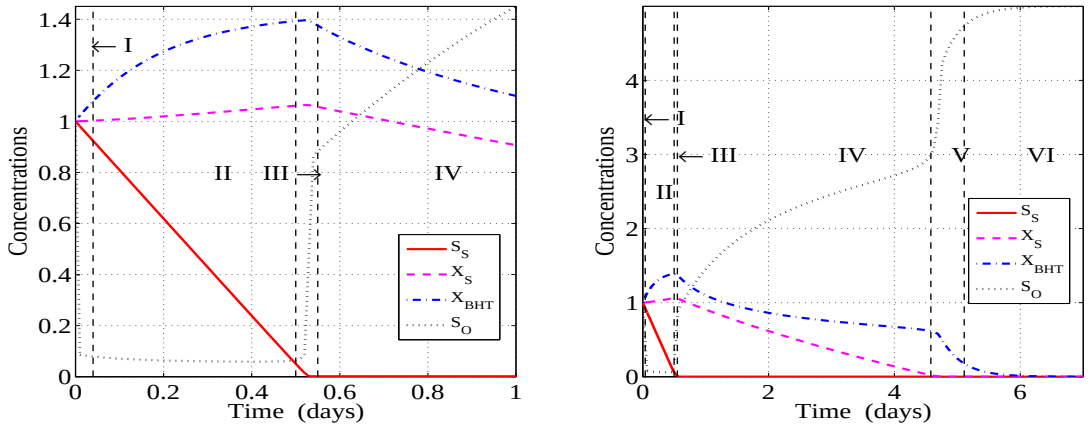


(a) (b)

Figure 5.17: (a) Plot of the solution to system of equations 5.4 over one day for the parameter values displayed in Table 5.4. (b) The same solution as in (a) plotted over one week. The asymptotic regions for $\varepsilon \to 0$ are indicated.

not inhibited by the absence of substrate. For reference, it is worth re-displaying equations 5.4 now in terms of the parameter $\varepsilon$

$$
\begin{aligned}
\frac{dS_{\mathrm{S}}}{dt} &= -\delta_4 \frac{S_{\mathrm{S}}}{\varepsilon + S_{\mathrm{S}}} \frac{S_{\mathrm{O}}}{\delta_6 + S_{\mathrm{O}}} X_{\mathrm{BHT}} + \delta_9 \frac{X_{\mathrm{S}}}{\theta_1 \varepsilon X_{\mathrm{BHT}} + X_{\mathrm{S}}} \frac{S_{\mathrm{O}}}{\delta_6 + S_{\mathrm{O}}} X_{\mathrm{BHT}}, \\
\frac{dX_{\mathrm{S}}}{dt} &= \delta_{12} X_{\mathrm{BHT}} - \delta_{14} \frac{X_{\mathrm{S}}}{\theta_1 \varepsilon X_{\mathrm{BHT}} + X_{\mathrm{S}}} \frac{S_{\mathrm{O}}}{\delta_6 + S_{\mathrm{O}}} X_{\mathrm{BHT}}, \\
\frac{dX_{\mathrm{BHT}}}{dt} &= \delta_{17} \frac{S_{\mathrm{S}}}{\varepsilon + S_{\mathrm{S}}} \frac{S_{\mathrm{O}}}{\delta_6 + S_{\mathrm{O}}} X_{\mathrm{BHT}} - \delta_{18} X_{\mathrm{BHT}}, \\
\varepsilon \frac{dS_{\mathrm{O}}}{dt} &= -\theta_2 \frac{S_{\mathrm{S}}}{\varepsilon + S_{\mathrm{S}}} \frac{S_{\mathrm{O}}}{\delta_6 + S_{\mathrm{O}}} X_{\mathrm{BHT}} + \theta_3 \left(\delta_{22} - S_{\mathrm{O}}\right), \\
S_{\mathrm{S}} &= 1, \; X_{\mathrm{S}} = 1, \; X_{\mathrm{BHT}} = 1, \; S_{\mathrm{O}} = 1 \quad \text{at} \quad t = 0.
\end{aligned}
\tag{5.5}
$$

The limit $\varepsilon \to 0$ is singular, and the asymptotic structure is indicated in Figure 5.17. We now briefly discuss some of the asymptotic regions (time-scales) arising.

### 5.3.1 Region I, $t = \mathcal{O}(\varepsilon)$

The very short initial time-scale, which is visible in Figure 5.17a and Figure 5.17b, although barely visible in Figure 5.17b, appears at $t = \mathcal{O}(\varepsilon)$ and marks a region of rapid change in the dissolved oxygen concentration. We rescale $t = \varepsilon \hat{t}$, and at leading order we have

$$S_{\mathrm{S}} \sim 1,\ X_{\mathrm{S}} \sim 1,\ X_{\mathrm{BHT}} \sim 1,$$

and pose $S_{\mathrm{O}} \sim S_{\mathrm{O}}^{\mathrm{I}}(\hat{t})$, to obtain

$$\frac{dS_{\mathrm{O}}^{\mathrm{I}}}{d\hat{t}} = -\theta_2 \frac{S_{\mathrm{O}}^{\mathrm{I}}}{\delta_6 + S_{\mathrm{O}}^{\mathrm{I}}} + \theta_3 \left(\delta_{22} - S_{\mathrm{O}}^{\mathrm{I}}\right),$$

where

$$S_{\mathrm{O}}^{\mathrm{I}} = 1 \text{ at } \hat{t} = 0,$$

and $dS_{\mathrm{O}}^{\mathrm{I}}/d\hat{t} \to 0$, $S_{\mathrm{O}}^{\mathrm{I}} \to \rho_1$ as $\hat{t} \to \infty$, with $\rho_1$ given by

$$\rho_1 = \frac{1}{2}\left(\delta_{22} - \delta_6 - \frac{\theta_2}{\theta_3} + \sqrt{\left(\delta_{22} - \delta_6 - \frac{\theta_2}{\theta_3}\right)^2 + 4\delta_{22}\delta_6}\right).$$

For the parameter values given in Table 5.4, $\rho_1 = 0.087$, which is in good agreement with the numerical solution displayed in Figure 5.17a. We have to note that $\rho_1 > 1$ is also possible, so that the dissolved oxygen is not necessarily depleted over this time-scale; the competing effects of aeration and oxygen consumption by the biomass enter at leading order here.

### 5.3.2 Region II, $t = \mathcal{O}(1)$ and $t < t_{\mathrm{s}}$

For $t = \mathcal{O}(1)$ and $t < t_{\mathrm{s}}$, where $t_{\mathrm{s}}$ is the moment in which the availability of $S_{\mathrm{S}}$ becomes a limiting factor in the further growth of the biomass, we pose

$$S_{\mathrm{S}} \sim S_{\mathrm{S}}^{\mathrm{II}}(t), X_{\mathrm{S}} \sim X_{\mathrm{S}}^{\mathrm{II}}(t), X_{\mathrm{BHT}} \sim X_{\mathrm{BHT}}^{\mathrm{II}}(t), S_{\mathrm{O}} \sim S_{\mathrm{O}}^{\mathrm{II}}(t),$$

for $\varepsilon \to 0$, to obtain

$$
\begin{aligned}
\frac{dS_{\mathrm{S}}^{\mathrm{II}}}{dt} &= -\left(\delta_4 - \delta_9\right) \frac{S_{\mathrm{O}}^{\mathrm{II}}}{\delta_6 + S_{\mathrm{O}}^{\mathrm{II}}} X_{\mathrm{BHT}}^{\mathrm{II}}, \\
\frac{dX_{\mathrm{S}}^{\mathrm{II}}}{dt} &= \delta_{12} X_{\mathrm{BHT}}^{\mathrm{II}} - \delta_{14} \frac{S_{\mathrm{O}}^{\mathrm{II}}}{\delta_6 + S_{\mathrm{O}}^{\mathrm{II}}} X_{\mathrm{BHT}}^{\mathrm{II}}, \\
\frac{dX_{\mathrm{BHT}}^{\mathrm{II}}}{dt} &= \delta_{17} \frac{S_{\mathrm{O}}^{\mathrm{II}}}{\delta_6 + S_{\mathrm{O}}^{\mathrm{II}}} X_{\mathrm{BHT}}^{\mathrm{II}} - \delta_{18} X_{\mathrm{BHT}}^{\mathrm{II}}, \\
\theta_2 \frac{S_{\mathrm{O}}^{\mathrm{II}}}{\delta_6 + S_{\mathrm{O}}^{\mathrm{II}}} X_{\mathrm{BHT}}^{\mathrm{II}} &= \theta_3 \left(\delta_{22} - S_{\mathrm{O}}^{\mathrm{II}}\right).
\end{aligned}
\tag{5.6}
$$

We do not pursue to solve the system of equations 5.6 here, and confine ourselves instead to considering the system's qualitative behavior. It is clear that in this region biomass growth is not limited by the availability of $S_{\mathrm{S}}$, and that hydrolysis is not limited by the availability of $X_{\mathrm{S}}$. However, both biomass growth and hydrolysis do depend on the available dissolved oxygen here.

From Equation $5.6_1$, it is clear that $dS_{\mathrm{S}}^{\mathrm{II}}/dt \leq 0$ for $\delta_4 > \delta_9$, or, in dimensional terms, $\mu_{\mathrm{HT}}/Y_{\mathrm{HT}} > k_{\mathrm{HT}}$. This corresponds to the case of $S_{\mathrm{S}}$ being consumed faster by the biomass than it is generated via hydrolysis. We restrict our discussion here to this case. For this case, there is $t_{\mathrm{S}} = \mathcal{O}(1)$ such that $S_{\mathrm{S}}^{\mathrm{II}}(t_{\mathrm{S}}) = 0$, and this indicates a region that we will discuss next.

### 5.3.3 Region III, $t^* = \mathcal{O}(1)$

This time-scale corresponds to $t^* = \mathcal{O}(1)$ where $t = t_{\mathrm{S}} + \varepsilon t^*$, and gives the location of a region where the availability of $S_{\mathrm{S}}$ becomes a limiting factor in the further growth of the biomass. Also, the oxygen concentration undergoes a rapid change over this time-scale. In our numerical solutions (see Fig. 5.17b), $t = t_{\mathrm{S}}$ gives the time when the biomass $X_{\mathrm{BHT}}$ achieves its maximum. For $t^* = \mathcal{O}(1)$, we have

$$
X_{\mathrm{S}} \sim X_{\mathrm{S}}^{\mathrm{II}}(t_{\mathrm{S}}),\ X_{\mathrm{BHT}} \sim X_{\mathrm{BHT}}^{\mathrm{II}}(t_{\mathrm{S}}),
$$

where both these quantities are determined as part of the solution to the leading order problem in Region II. In $t^* = \mathcal{O}(1)$, we pose

$$S_{\mathrm{S}} \sim \varepsilon S_{\mathrm{S}}^{\mathrm{III}}(t^*),\ S_{\mathrm{O}} \sim S_{\mathrm{O}}^{\mathrm{III}}(t^*),$$

to obtain

$$\begin{aligned}
\frac{dS_{\mathrm{S}}^{\mathrm{III}}}{dt^*} &= -\delta_4 \frac{S_{\mathrm{S}}^{\mathrm{III}}}{1+S_{\mathrm{S}}^{\mathrm{III}}} \frac{S_{\mathrm{O}}^{\mathrm{III}}}{\delta_6 + S_{\mathrm{O}}^{\mathrm{III}}} X_{\mathrm{BHT}}^{\mathrm{II}}(t_{\mathrm{S}}) + \delta_9 \frac{S_{\mathrm{O}}^{\mathrm{III}}}{\delta_6 + S_{\mathrm{O}}^{\mathrm{III}}} X_{\mathrm{BHT}}^{\mathrm{II}}(t_{\mathrm{S}}), \\
\frac{dS_{\mathrm{O}}^{\mathrm{III}}}{dt^*} &= -\theta_2 \frac{S_{\mathrm{S}}^{\mathrm{III}}}{1+S_{\mathrm{S}}^{\mathrm{III}}} \frac{S_{\mathrm{O}}^{\mathrm{III}}}{\delta_6 + S_{\mathrm{O}}^{\mathrm{III}}} X_{\mathrm{BHT}}^{\mathrm{II}}(t_{\mathrm{S}}) + \theta_3 \left(\delta_{22} - S_{\mathrm{O}}^{\mathrm{III}}\right).
\end{aligned} \tag{5.7}$$

As $t^* \to \infty$, $dS_{\mathrm{S}}^{\mathrm{III}}/dt^* \to 0$, $dS_{\mathrm{O}}^{\mathrm{III}}/dt^* \to 0$, $S_{\mathrm{S}}^{\mathrm{III}} \to \rho_2$, $S_{\mathrm{O}}^{\mathrm{III}} \to \rho_3$, where

$$\rho_2 = \frac{\delta_9}{\delta_4 - \delta_9},$$

(recall that we are considering $\delta_4 > \delta_9$ here), and

$$\rho_3 = \frac{1}{2}\left[\delta_{22} - \delta_6 - \frac{\theta_2}{\theta_3}\frac{\delta_9}{\delta_4} X_{\mathrm{BHT}}^{\mathrm{II}}(t_{\mathrm{S}}) + \sqrt{\left(\delta_{22} - \delta_6 - \frac{\theta_2}{\theta_3}\frac{\delta_9}{\delta_4} X_{\mathrm{BHT}}^{\mathrm{II}}(t_{\mathrm{S}})\right)^2 + 4\delta_{22}\delta_6}\right].$$

These predictions are in good agreement with the numerical solution displayed in Fig. 5.17a.

### 5.3.4 Region IV, $t = \mathcal{O}(1), t_{\mathbf{s}} < t < t_{\mathbf{x}}$

This is the time-scale over which most of the $X_{\mathrm{S}}$ is degraded. In this region, we have

$$S_{\mathrm{S}} \sim \varepsilon \frac{\delta_9}{\delta_4 - \delta_9},$$

and we have $X_{\mathrm{S}}, X_{\mathrm{BHT}}, S_{\mathrm{O}} = \mathcal{O}(1)$. For brevity, we do not display or discuss the leading order equations here, and simply note that there is a $t_{\mathrm{X}} = \mathcal{O}(1)$ such that $X_{\mathrm{S}}(t_{\mathrm{X}}) = 0$, which determines the time when the availability of $X_{\mathrm{S}}$ first becomes a limiting factor for hydrolysis.

We omit discussion of Regions V and VI, other than to give their locations and the scalings. This is because typical batch times are in the order of 1 day

and the behavior of the regions V and VI cannot be observed in these short times. Consequently, these regions are of no practical relevance (as, for example, all the biomass dies out). Region V is located at $t^\dagger = \mathcal{O}(1)$, where $t = t_\mathrm{X} + \varepsilon t^\dagger$, and in which $S_\mathrm{S}, X_\mathrm{S} = \mathcal{O}(\varepsilon)$, $X_\mathrm{BHT}, S_\mathrm{O} = \mathcal{O}(1)$. Region VI is at $t = \mathcal{O}(1), t > t_\mathrm{X}$ and here we also have $S_\mathrm{S}, X_\mathrm{S} = \mathcal{O}(\varepsilon)$, $X_\mathrm{BHT}, S_\mathrm{O} = \mathcal{O}(1)$.

## 5.4 Sensitivity analysis

In this section, we will study the impact of model parameters (model inputs) in ATM1 upon the energy requirement, plant capacity, stabilisation time, and pasteurisation time (model outputs) of an ATAD system. The system in question conforms to the characteristics of the first-stage reactor of CS2.

The first part of the sensitivity analysis studies the effect of all possible model inputs on the aforementioned model outputs. Model inputs include kinetic, stoichiometric, and thermodynamic parameters, initial conditions, influent characteristics, reactor-specific parameters, operating conditions, and reactor volume. The effect of all inputs will be studied regardless of whether these inputs can be influenced in practice. The objective of this part of the analysis is to identify all possible model parameters with a significant influence on the energy requirement and on the other relevant outputs.

The second part of the analysis studies exclusively the effect of the operating conditions (model inputs) upon the same model outputs. The operating conditions include the reaction time, aeration flowrate, influent temperature, loading time, and the volume replaced after each batch. This part of the study thus emphasises only the effect of those parameters that are practically tunable during operation. The objective is to identify the operating conditions with the strongest impact on the energy requirement, and, in this way, to select the most promising optimisation variables.

### 5.4.1 Global sensitivity analysis: all *versus* all

As mentioned above, this section will study the effect of all possible model inputs upon all considered model outputs.

The local sensitivity analysis studies the effect of inputs on outputs in an isolated manner and each at a time, i.e. changing first one input, then the second, and so on. On the other hand, in the global sensitivity analysis, all inputs are changed simultaneously (Saltelli et al., 2004). In doing so, every correlation between inputs and outputs will have a certain degree of uncertainty associated with the changes caused by the other inputs. Local methods can be very informative and tend to work better for relatively simple models. They are a good first step in model analysis, but they are insufficient when the model in question is complex and nonlinear. Global methods are used to obtain more detailed information about model behaviour and to fully characterize nonlinearities.

The ATM1 model is highly nonlinear due, in part, to the switching functions, the multiplication of variables, and the temperature dependence of some parameters. Apart from this, there is a strong feedback between several components; for instance, higher biomass growth results in higher release of metabolic energy and higher temperature, and higher temperatures in turn affect biomass growth. In this way, the evolution of the system is oftentimes not easily predictable or intuitive. Given the high nonlinearity of the model, we decided to perform a global sensitivity analysis.

The global sensitivity analysis can be thought of as the study of input-output model relationships under uncertainty. In order to measure the degree of uncertainty for each input-output relationship, different uncertainty metrics have been proposed in the literature. What follows is a brief account of the relevant uncertainty metrics that will be used in this analysis.

**Uncertainty metrics**[1]

**Classical statistics** Given $n_s$ scenarios, $n_{in}$ input variables $x_h$, and $n_{out}$ output variables $y_l$, the mean or expected value $E(y_l)$ and variance $V(y_l)$ can be computed as

$$E(y_l) = \bar{y}_l = \sum_{i=1}^{n_s} \frac{y_{il}}{n_s}, \tag{5.8}$$

$$V(y_l) = \sigma_{y_l}^2 = \frac{1}{n_s} \sum_{i=1}^{n_s} (y_{il} - \bar{y})^2. \tag{5.9}$$

The standard deviation $\sigma_{y_l}$ is then calculated as the square root of the variance, and the coefficient of variation $CV_{y_l}$ is defined as

$$\sigma_{y_l} = \sqrt{V(y_l)}, \tag{5.10}$$

$$CV_{y_l} = \frac{\sigma_{y_l}}{\bar{y}_l}. \tag{5.11}$$

The size of the confidence interval $CI(\bar{y}_l)$ for the mean $\bar{y}_l$ can be expressed as

$$CI(\bar{y}_l) = [\bar{y}_l - t_{(n_s-1,0975)}\sigma_{y_l}, \bar{y}_l + t_{(n_s-1,0975)}\sigma_{y_l}], \tag{5.12}$$

where $t_{(n_s-1,0975)}$ is the Student-t distribution value for $n_s - 1$ degrees of freedom, which makes the probability be 0.975. The former is based on the assumption of a normal distribution for the errors and 95% coverage of the confidence interval, as described by Law and Kelton (1999).

It is always important to compare the estimated results from sampling runs and the results without uncertainty. If mean and the value without uncertainty coincide, it is a clear result of symmetrical distributions being used for the input parameters (Heijungs and Klejin, 2001). With regards to the coefficient of variation, values below 10% suggest resonable certain results.

[1]This introductory section has been adapted from Bojarski (2010).

**Linear-regression-based metrics** These metrics are based on the linear correlation defined by

$$\hat{y}_l = b_{l0} + \sum_{h=1}^{n_{in}} b_{lh} x_h + \epsilon_i \qquad \forall l = 1, ..., n_{out}. \tag{5.13}$$

An important relation connected to the concept of regression is the model coefficient of determination $R^2_{y_l}$ for output variable $y_l$ which is commonly defined as

$$R^2_{y_l} = \frac{\sum_{f=1}^{n_s} (\hat{y}_{lf} - \bar{y_l})^2}{\sum_{f=1}^{n_s} (y_{lf} - \bar{y_l})^2} \qquad \forall l = 1, ..., n_{out}. \tag{5.14}$$

The closer $R^2_{y_l}$ is to unity, the better the regression model results $\hat{y}_{lf}$ fit the actual model realisations $y_{lf}$. This point is important, given that the validity of regression-based metrics depends on the degree to which the regression model fits the data.

The standardised regression coefficient (SRC) requires the standardisation of input variables and output results which is performed by subtracting the mean value ($\bar{x_h}$, $\bar{y_l}$) and normalising its value by dividing it by the variable's standard deviation $(\sigma_{x_h}, \sigma_{y_l})$[2]. The SRC represents a relation between the $n_{in}$ uncertain input variables $x_h$ and the $n_{out}$ output variables $y_l$, as given by

$$\frac{y_l - \bar{y_l}}{\sigma_{y_l}} = \sum_{h=1}^{n_{in}} SRC_{lh} \frac{x_h - \bar{x_h}}{\sigma_{x_h}} \qquad \forall l = 1, ..., n_{out}. \tag{5.15}$$

A value of $SRC_{lh}$ close to zero indicates that the output variable $y_l$ is not correlated to input variable $x_h$. Additionally, the sign of $SRC_{lh}$ indicates the qualitative kind of relation between input and output: a positive $SRC_{lh}$ indicates that increments of the input variable $x_h$ result in an increase of the output variable $y_l$; the opposite behaviour applies when the $SRC_{lh}$ is negative.

On the other hand, the partial correlation coefficient (PCC) is calculated by

[2]Standardising the data set makes the measurements of different lengths comparable, i.e., the importance of the different measurements does not depend on the scale (Haardle and Hlavka, 2007).

performing several regressions which include or not the input variable under consideration. In this sense, a PCC shows how much each input variable affects the behaviour of the output variables, by performing two separate regressions: the first one considering all input variables, and the second without the subject input variable. The PCC is defined as

$$PCC_{hl}^2 = \frac{\sum_{f=1}^{n_s} (y_{lf} - \widehat{y_{lf}^{\sim x_h}})^2 - \sum_{f=1}^{n_s} (y_{lf} - \widehat{y_{lf}^{full}})^2}{\sum_{f=1}^{n_s} (y_{lf} - \widehat{y_{lf}^{\sim x_h}})^2} \quad (5.16)$$

$$\forall l = 1, ..., n_{out}; h = 1, ..., n_{in},$$

where $\widehat{y_{lf}^{\sim x_h}}$ represents the estimation of the $y_l$ variable value using a regression that does not include input variable $x_h$, while $\widehat{y_{lf}^{full}}$ represents the $y_l$ variable value estimated using a regression that considers all input variables.

### Results

For this analysis, a simple Monte Carlo sampling was adopted. A total of 3000 scenarios were generated using MATLAB©'s random uniform and normal number generator functions. The probability distribution function for each parameter was selected based on previous information regarding those parameters. The energy requirements and plant capacity (both volumetric and gravimetric), and pasteurisation and stabilisation times were examined as model outputs, while all input parameters were studied.

As shown in Table 5.5, initial system enthalpy $H_0$ and reactor volume $V$ are the most significant factors with regard to $t_P$ due to their high PCC and SRC values. The behaviour of $H_0$ is logical due to the fact that a higher initial enthalpy would lead to a higher temperature profile, resulting in a higher degree of pasteurisation and shorter pasteurisation time. Whenever pasteurisation is limiting, shorter pasteurisation times would result in lower energy requirements. This qualitative behaviour is reflected by the SRC values, and is consistent with the suggestion made by Layden et al. (2007b) that sludge pre-heating could potentially lead to shorter hydraulic retention times and lower energy requirements. A possible reason behind

Table 5.5: SRC and PCC values for the most significant input variables.

| Input Variable | | $t_S$ | $t_P$ | $E_m$ | $c_m$ | $E_v$ | $c_v$ |
|---|---|---|---|---|---|---|---|
| *SRC values* | | | | | | | |
| Var. 1 | $V$ (m$^3$) | 0 | **0.18** | -0.05 | -0.09 | -0.05 | -0.1 |
| Var. 7 | $X_{s0}$ (g/l) | **0.19** | 0.01 | 0.16 | 0.02 | 0.16 | 0.02 |
| Var. 11 | $H_0$ (MJ) | -0.01 | **-0.21** | -0.05 | 0.1 | -0.05 | 0.1 |
| Var. 21 | $q_a$ (vvh) | 0.02 | -0.02 | 0.09 | 0.01 | 0.09 | 0.01 |
| Var. 85 | $f_{COD}$ (gCOD/gVS) | **0.28** | 0.04 | **0.31** | -0.05 | **0.24** | -0.05 |
| *PCC values* | | | | | | | |
| Var. 1 | $V$ (m$^3$) | 0 | **0.19** | 0.06 | **0.1** | 0.06 | **0.1** |
| Var. 7 | $X_{s0}$ (g/l) | **0.2** | 0.01 | **0.17** | 0.02 | **0.17** | 0.02 |
| Var. 11 | $H_0$ (MJ) | 0.01 | **0.21** | 0.05 | **0.1** | 0.05 | **0.1** |
| Var. 21 | $q_a$ (vvh) | 0.02 | 0.02 | **0.1** | 0.01 | **0.1** | 0.01 |
| Var. 85 | $f_{COD}$ (gCOD/gVS) | **0.29** | 0.04 | **0.32** | 0.05 | **0.24** | 0.05 |

the correlation between $V$ and $t_P$ is that increasing reactor volume would increase the surface area of the reactor and thus the amount of heat escaping via conduction through the walls. This, in turn, would lead to lower temperature profiles and longer pasteurisation times. This interpretation is consistent with the work of Ponti et al. (1995a) who found experimentally that increased reactor volume correlates with decreasing biological activity and increased energy requirements. This consistency with the experimental work of Ponti et al. (1995a) may, however, be purely coincidental. Their correlation may be due to incomplete reactor mixing: the bigger the reactor, the worse the mixing and the more inhomogeneous the DO distribution.

In the case of $t_S$, the most significant variables are the initial concentration of slowly biodegradable substrate $X_{s0}$ and the conversion factor between volatile solids and chemical oxygen demand $f_{COD}$. This result is also intuitive in that rising the value of $X_{s0}$ would increase the amount of VS to be degraded, and, in consequence, this would require longer time to satisfy stabilisation requirements (as long as hydrolysis is the limiting process of the reaction, which is generally the case). On the other hand, increasing $f_{COD}$ for a constant aeration level would increase the amount of oxygen needed for the oxidation of a given quantity of VS; this also would increase the time required to satisfy stabilisation requirements and thus the energy requirements.

Finally, the aeration flowrate $q_a$ displays a significant positive correlation with

$E_m$ and $E_v$, as indicated by its SRC and PCC values. The mechanism behind this correlation is probably the first-order dependence of the energy requirements upon $q_a$ (see Equation 4.44 and 4.45). This positive correlation supports the hypothesis made by Layden et al. (2007b) that a constant level of aeration is likely to lead to excessive energy use.

Overall, the signs of the SRCs show that the qualitative behaviour of the model is consistent with the expected trends for such input parameter changes. The regression coefficient $R^2$ is very low for all the performed regressions with values of $\sim$0.15. In spite of this, the SRC and PCC values allowed us to distinguish the most significant variables.

Figure 5.18 displays the scatter plots of reactor volume and initial reactor temperature (proportional to $H_0$) against the different model outputs. The initial reactor temperature correlates in a negative way with pasteurisation and stabilisation times and the specific energy requirements, and in a positive way with the specific plant capacity. The reactor volume shows the opposite behaviour.

The fact that the initial reactor temperature and the initial concentration of slowly biodegradable substrate appear as significant variables is the result of evaluating the stabilisation and pasteurisation constraints based on one single batch. Consequently, such results correspond to transient solutions and not to periodic ones. To overcome this problem, in the next section, the constraints will be evaluated based on the last batch of $n_b$ successive batches. In spite of this drawback, the correlations found in this part of the analysis are intuitive, logical, and consistent with other studies.

### 5.4.2 Global sensitivity analysis: operating conditions

This part of the sensitivity analysis studies exclusively the effect of the operating conditions upon model outputs. This emphasis is due to the need to identify the parameters with the strongest impact on the energy requirement, as such parameters would be the most promising optimisation variables.

As in the previous section, a Monte Carlo sampling was adopted with 3000

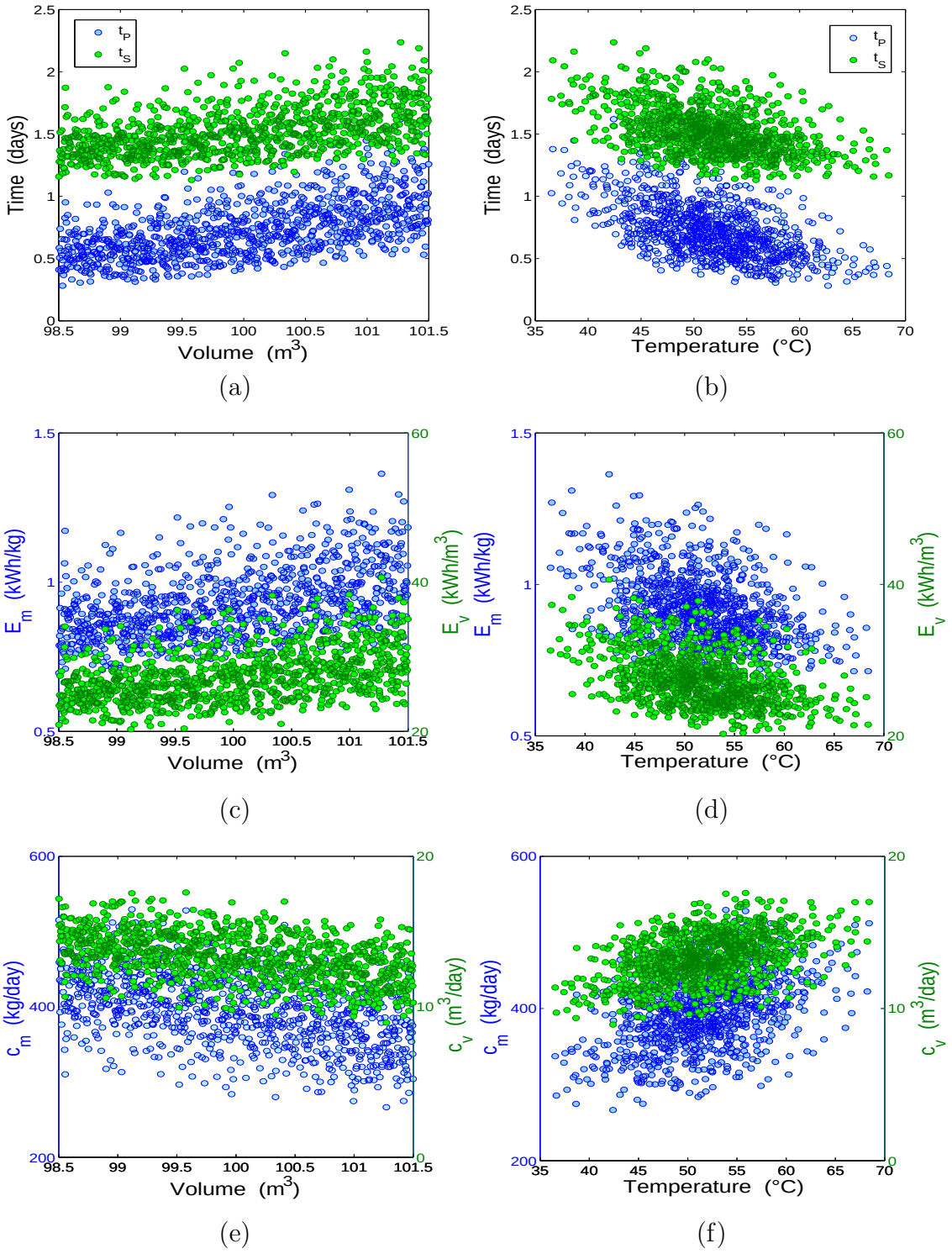


Figure 5.18: Scatter plots from sensitivity analysis: effect of reactor volume and initial reactor temperature on (a)-(b) pasteurisation and stabilisation times, (c)-(d) specific energy requirements, and (e)-(f) specific plant capacity.

scenarios generated with a uniform random distribution and a random normal distribution. To surmount the problem of transient solutions found in the previous part of the analysis, a total of $n_b$ consecutive batches are calculated for a given set of operating conditions; the reaction time is then the one corresponding to the last batch. Choosing a high value for $n_b$ ensures that all solutions obtained are periodic or cyclic. Experience has shown that a value in the range 10–20 generally satisfies the periodicity requirement without incurring an unacceptable computational burden. Hence, the value chosen was 20.

The considered operating conditions include the reaction time, aeration flowrate, influent temperature, loading time, and the volume replaced after each batch. As the number of model inputs is so small, there is no need to calculate SRCs and PCCs. Instead, it is more instructive to present all the relevant scatter plots and to discuss them one by one.

Figure 5.19 shows the impact of the operating conditions upon the energy requirement. Figures 5.19a displays the effect of the aeration flowrate. As it was shown in the previous section by the SRC and PCC values, the aeration flowrate correlates positively with $E_m$. The red line corresponds to the linear fit between the two variables. The scattering of points may make it more difficult for the bare eye to recognize this relation without the aid of the regression line. For this reason, Figure 5.19b was displayed, showing the same relation but for a different simulation in which the volume replaced after each batch (see Figure 5.19e) was not varied. In this graph, the relation between the two variables is evident without the aid of regression. The need to "switch off" the quantity of volume replaced is due to its overshadowing dominance over the other variables. It is unclear, though, why in Figure 5.19b the relation between the aeration flowrate and $E_m$ behaves in such unexpected radial manner. The conclusion is that higher, constant rates of aeration lead to higher energy requirements. This supports the suggestion made by Layden et al. (2007b) that constant aeration flowrates are likely to result in excessive energy use.

Figure 5.19c shows the positive correlation between the reaction time (see Equation 4.43) and the energy requirement. This finding is consistent with experimental

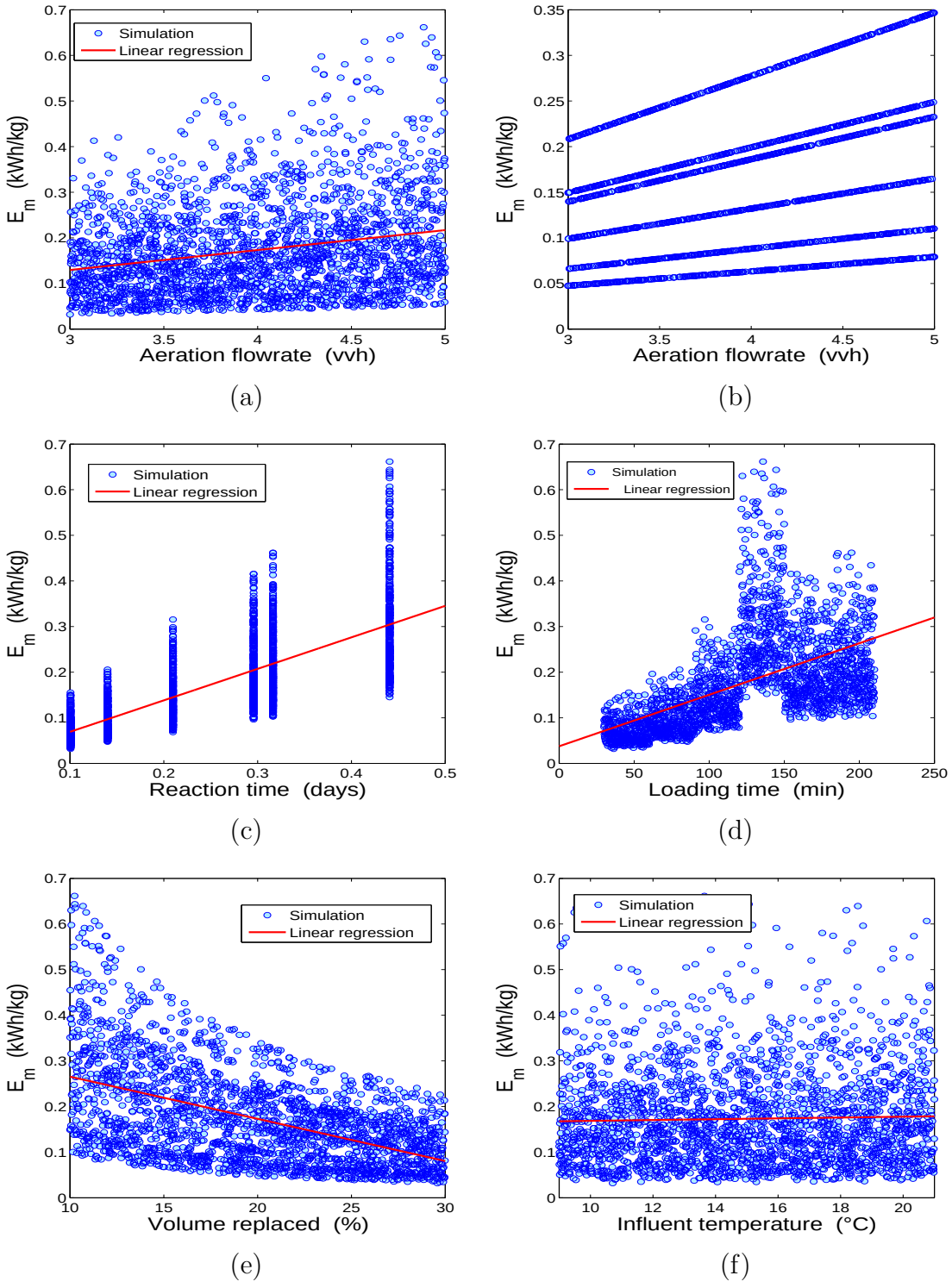


Figure 5.19: Scatter plots from sensitivity analysis. Impact of operating conditions on energy requirement: (a) Aeration flowrate with and (b) without changes of the quantity of volume replaced after each batch, (c) reaction time, (d) loading time, (e) percentage of volume replaced after each batch, and (f) influent temperature.

studies conducted by Ponti et al. (1995b) that show that shorter HRTs and higher frequencies of volume changes correlate with lower energy requirements. From a mathematical point of view, it may seem clear that the energy requirement should exhibit this kind of dependence on the reaction time given their relation in Equation 4.46. Nevertheless, this conclusion is not straightforward, considering that the reaction time is an implicit function of all other operating conditions including the aeration flowrate. And from Equation 4.46, it is clear that $E_m \sim q_a \cdot t_r(q_a)$. Thus, it is not possible to say *a priori* that an increase of $t_r$ would increase $E_m$, as any increase of $t_r$ might be caused by a counteracting change in the aeration flowrate that could offset the effect of $t_r$. That is to say, the relation observed in Figure 5.19c could not have been forecasted given the implicit dependence of $t_r$ on $q_a$.

In Figure 5.19d, longer loading times lead to higher energy requirements. A possible explanation for this behaviour is that longer loading times would lead to lower substrate availability at any given time over the loading period. Lower substrate availability would lead to higher decay rates and lower growth rates, resulting in overall lower concentrations of biomass. Lower biomass concentrations imply lower sludge oxidation rates and this, in turn, longer stabilisation times and (as long as stabilisation is limiting, i.e., $t_r = t_S$) longer reaction times. Obviously, the result of longer reaction times would be higher energy requirements. Interestingly, this finding contradicts the notion that longer loading times could be preferable to avoid oxygen-limited conditions and reduce the thermal shock, thus resulting in smaller fluctuations of process conditions and potentially in shorter reaction times and lower energy requirements.

The percentage of reactor volume replaced after each batch correlates in a negative manner with the energy requirement, as seen in Figure 5.19e. This relation is probably due to the dependence $E_m \sim 1/m_{in}$ (see Equation 4.46) with $m_{in} \sim V_{in}$, so that $E_m \sim 1/V_{in}$. The fact that this inverse proportionality prevails in spite of the fluctuations of the other operating conditions shows that $V_{in}$ is a dominating factor which can outweigh the effect of the aeration flowrate and the reaction time. Another viable explanation for this behaviour is that higher $V_{in}$ values result in higher sludge oxidation rates, as pointed out by Ponti et al. (1995a); higher oxidation rates

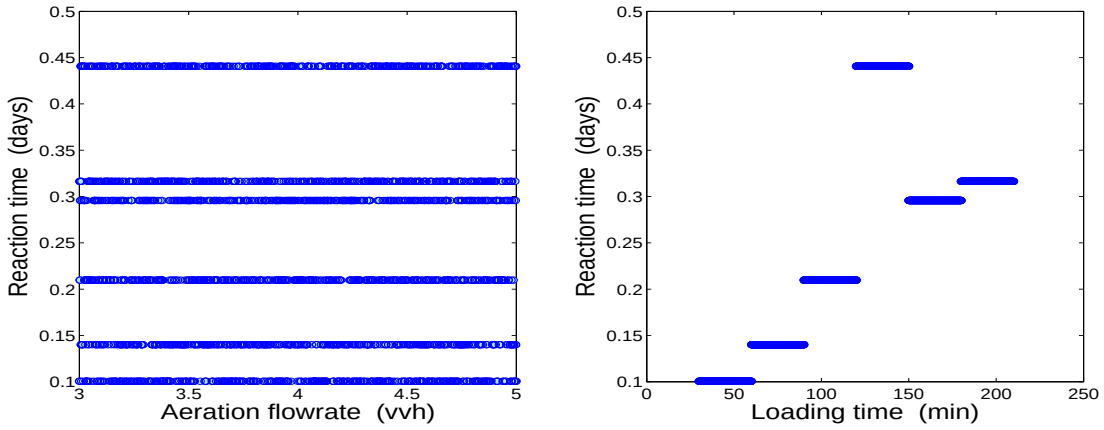


(a) (b)

Figure 5.20: Effect of operating conditions on reaction time: (a) aeration flowrate, and (b) loading time.

could then result in shorter reaction times and lower energy requirements.

Finally, the influent sludge temperature displays a negligible effect on $E_m$ (Figure 5.19f). At first, this can appear surprising, as the temperature does have a direct influence on the biomass growth rate through the temperature-dependent kinetic parameters. However, the biomass growth rate is more likely to be limited by the extremely low DO concentrations rather than by temperature. This finding contradicts the suggestion made by Layden et al. (2007b) that sludge pre-heating could lead to shorter HRTs which in turn would lead to lower energy requirements. Nonetheless, this could indeed happen if, for example, the reaction time was limited by the pasteurisation process (i.e., $t_r = t_P$); however, this is not generally the case.

At this stage, we can thus conclude that the most promising optimisation variables (that is, the operating conditions with the strongest influence on the energy requirement) are the aeration flowrate, reaction time, loading time, and volume replaced. The influent temperature displayed a negligible influence on $E_m$ and can hence be ruled out.

Let us now consider the effect of the aeration flowrate, volume replaced, loading time, and influent temperature on the reaction time. Figure 5.20a displays the effect of the aeration flowrate. As it can be seen, there is no visible correlation between the two variables. However, this does not mean that there is no correlation. There might

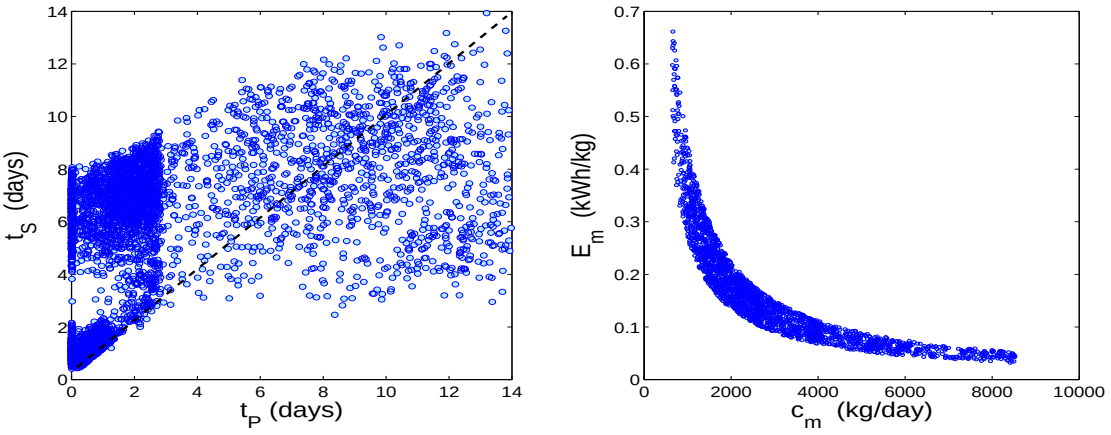


(a) (b)

Figure 5.21: Scatter plots displaying (a) stabilisation versus pasteurisation time, and (b) plant capacity against energy requirement. The first plot shows that the reaction tends to be limited by the stabilisation process, and the second that the relation between plant capacity and energy requirement obeys a law of inverse proportionality.

be a correlation concealed as a result of such disparate data. On the other hand, if there was no correlation, this would make sense of the explanation suggested above for the correlation between $t_r$ and $E_m$: if the dependence of $t_r$ on $q_a$ is negligible, that is, if they are decoupled, then $E_m$ can only depend on $t_r$ in a linear manner regardless of $q_a$. The volume replaced and the influent temperature did not display either a visible effect on the reaction time. Surprisingly, only the loading time was found to have a clear effect on $t_r$, as shown in Figure 5.20b. This positive correlation makes sense of the explanation for the correlation between the loading time and $E_m$ proposed above.

An interesting insight is gained by looking at Figure 5.21a, displaying the stabilisation versus pasteurisation time for the 3000 scenarios. It turns out that in more than 85% of these scenarios the reaction is limited by the stabilisation process, i.e., $t_S > t_P$ and $t_r = t_S$. This means that the ATAD reaction is generally limited by stabilisation and only under relatively few conditions by pasteurisation. To our knowledge, this insight has never been reported before in the available literature.

Yet another interesting insight can be gained by considering Figure 5.21b which plots the plant capacity against the energy requirement for the different sets of operating conditions. As can be readily seen, the two variables correlate in a negative

manner. The kind of correlation seems to correspond to an inverse proportionality. The reason behind this kind of correlation can be traced back to the very definition of these two variables. Considering the definitions for a constant level of aeration (see Equation 4.46 and 4.48), we see that $E_m \sim 1/x$ and $c_m \sim x$, where $x = m_{in}/t_f$, so that $E_m \sim 1/c_m$. In this way, it becomes clear that this inverse proportionality is ingrained in, and derivative from, the very definition of $E_m$ and $c_m$. What is highly significant is the generality of this relation: this definition of $E_m$ and $c_m$ is not confined to ATAD, but it applies (in one form or another) to *all* treatment processes, that is, to all wastewater and sludge treatments, whether continuous or discontinuous. Thus, the inverse proportionality should hold for all these processes as well. An indication that this is the case is found in Burton (1996) and Metcalf & Eddy (2003) who, with the aid of empirical data, found a similar relation for activated sludge, activated sludge with nitrification and filtration, and trickling filters. In terms of the general language, this insight indicates that the sets of operating conditions leading to energy efficient regions of the graph also lead to high-capacity regions. Or, in other words, energy efficient solutions are also high-capacity solutions. Conversely, energy inefficient solutions are low-capacity solutions. More work should be carried out to unearth the full implications of this relation.

Finally, let us consider the effect of the operating conditions on the plant capacity $c_m$. We have just seen that the energy requirement is inversely proportional to plant capacity; it is, therefore, reasonable to expect that some of the dependencies of $E_m$ on the operating conditions should be mirrored by $c_m$ in an inverted manner. Figure 5.22a shows that the aeration flowrate has no visible effect on the plant capacity. This is the only dependence that is not mirrored by $c_m$ with regard to $E_m$. This is probably due to the fact that, unlike in the case of the energy requirement, plant capacity does not depend on the aeration flowrate in a first-order manner (see Equation 4.46 and 4.48, where $P \sim q_a$). As for the reaction time, loading time, and the volume replaced, their correlations are the opposite as in the case of $E_m$ (see Figure 5.22b–d). Furthermore, the form of the dependence of $c_m$ on the reaction time and the volume replaced can be deduced from, and explained through, the definition of plant capacity. The qualitative dependence of $c_m$ on the loading

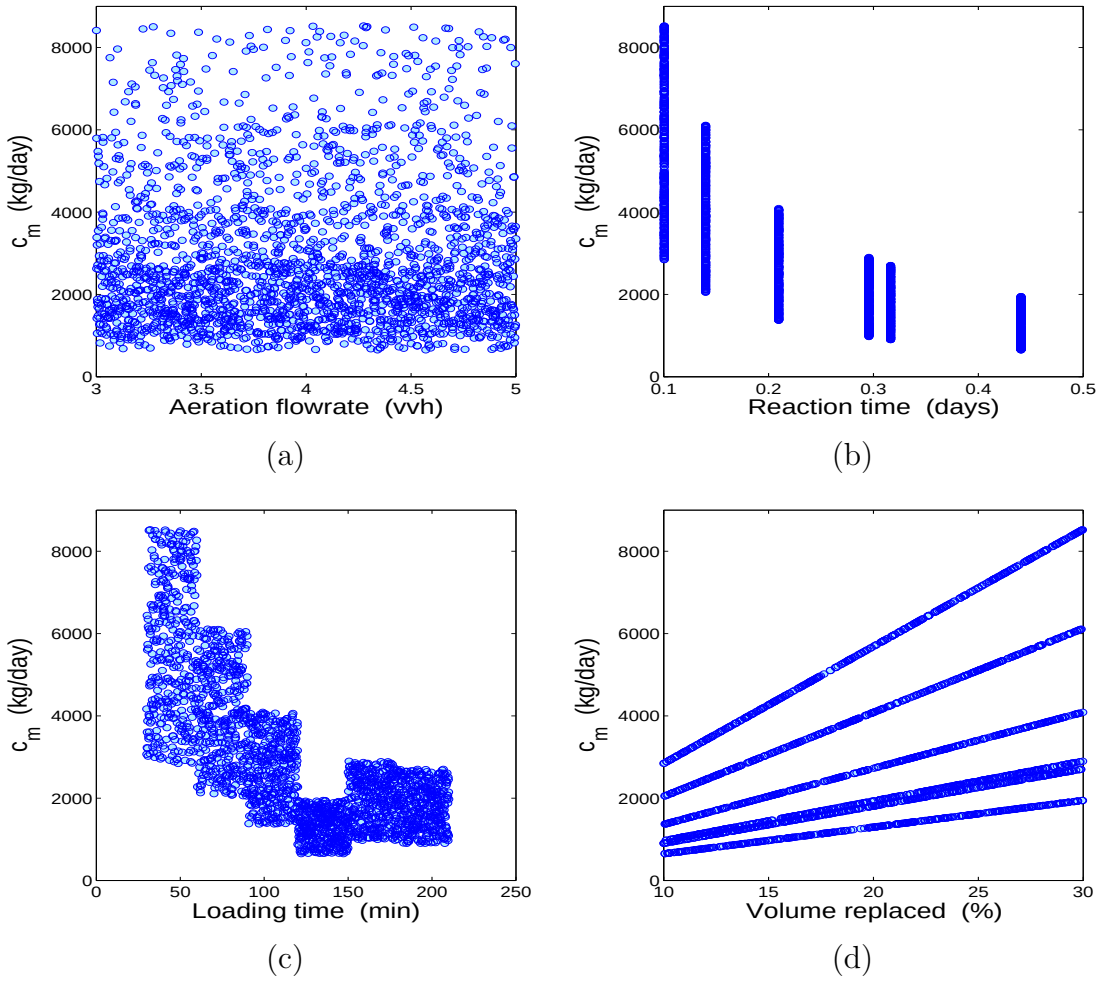


Figure 5.22: Scatter plots displaying effect of operating conditions on the plant capacity: (a) aeration flowrate, (b) reaction time, (c) loading time, and (d) volume replaced. The influent temperature is not displayed because, like the aeration flowrate, it has no influence on plant capacity.

time can be explained in a similar way as it was done with $E_m$ (i.e., through its influence on the reaction time), but considering that $c_m$ is inversely proportional to the reaction time. The influent temperature has been left out, as, like in the case of the aeration flowrate, it has no visible effect on plant capacity.

## 5.5 Model assessment and parameter estimation

A critical part of any modeling effort is model validation. As a preliminary step toward validating the ATAD models presented in this thesis, in this section we shall assess the ATM1 model.

For clarity, it may be useful to review the fundamental concepts of *code verification* and *model validation*, before applying them to our particular case study. According to Boehm (1981) and Blottner (1990), code verification and model validation can be concisely and respectively defined as "solving the equations right" and "solving the right equations". In other words, verification is about the correct implementation of the model, while validation is about using the right model. Verification is a mathematical exercise in which the code author makes sure that the model has been implemented correctly and to a satisfactory degree of approximation. Thus, verification is a purely mathematical activity that is independent from whether the considered model bears any relation to the physical system of interest. It is, hence, an exercise in mathematics regardless of the science or engineering behind it. Validation, on the other hand, consists of evaluating the degree of correspondence between the mathematical model and the physical system it abstracts. It is thus an exercise in science or engineering.

*Verification.* Following Roache (1998), code verification means that the author has to choose what differential equations and boundary conditions are going to be solved, and doing so to a reasonable order of accuracy and consistency; that is, when a certain measure of discretization (such as the step size or mesh increment) goes to zero, the discrete solution obtained through integration should converge to the exact continuous solution.

*Validation.* It is often defined as the assessment of the degree of accuracy of a model over a range of parameters and within its domain of applicability to correctly represent the behaviour of the physical system under consideration, thus determining whether the right model was used (Mehta, 1995). Some definitions of validation also include the specification and use of performance metrics (Tsang, 1991).

In this spirit, the modeling aspects of code verification pertaining to our case study were already specified in Chapter 4. In addition, it should be noted that the code was implemented in the MATLAB© platform and the differential equations were integrated using the stiff solver *ode15s* and *ode45*.

We will now address the validation of the ATM1 model for the CS1 and CS2 case studies in some detail. As performance metric, the mean absolute error (MAE)

was chosen. The reason for this choice is that the most common nonlinear metrics, such as the mean squared error, have the disadvantage of weighing large errors more heavily than smaller ones. Model simulations were fitted, via minimisation of the MAE, to data from the two case-study plants by tuning the value of the important case-specific parameter $K_a$.

According to Olsson and Newell (1999), the value of this parameter has to be determined for each particular aeration device and facility. Given the uncertainty with regard to its value and the great impact that this parameter has on model outputs, it was selected for parameter estimation. The parameter $K_a$ appears in the differential equation for DO when the advective or transport term due to aeration is considered:

$$r_{S_O} = \sum \nu_{ij}\rho_j + A \cdot (\overline{S} - S_O), \tag{5.17}$$

where the first term represents the reaction term and the second one the advective term resulting from aerating the sludge. The parameter $A$ ($\mathrm{h}^{-1}$) is a function of the aeration flowrate $q_a$ (vvh) and can be formulated in several ways. In our case, we have assumed a first-order dependence, following $A = K_a q_a$, where $K_a$ ($\mathrm{vv}^{-1}$) is the case-specific parameter whose value has to be determined.

In the case of CS1, a 21-day time series of temperature and VS concentration was used to fit the model and estimate $K_a$. Figure 5.23a and 5.23b show respectively the MAEs for prediction of temperature and VS concentration at different $K_a$ values. A clear difference between the two prediction errors is that $\mathrm{MAE_T}$ is far more sensitive to changes of $K_a$ than $\mathrm{MAE_{VS}}$. It can also be seen that the minimum of $\mathrm{MAE_T}$ lies at $K_a = 5.4$ $\mathrm{vv}^{-1}$, while that of $\mathrm{MAE_{VS}}$ is at 4.8 $\mathrm{vv}^{-1}$. As a compromise, the value 5 $\mathrm{vv}^{-1}$ was taken as the optimum. Figure 5.23c and 5.23d display the simulations of the temperature and VS time series for the optimal $K_a$ value. It can be seen that there is a reasonable qualitative agreement (i.e., regarding value ranges and overall tendencies) in the two cases, even though there is still room for improvement in quantitative terms.

In the case of CS2, a 5-day temperature time series was used to fit the model and

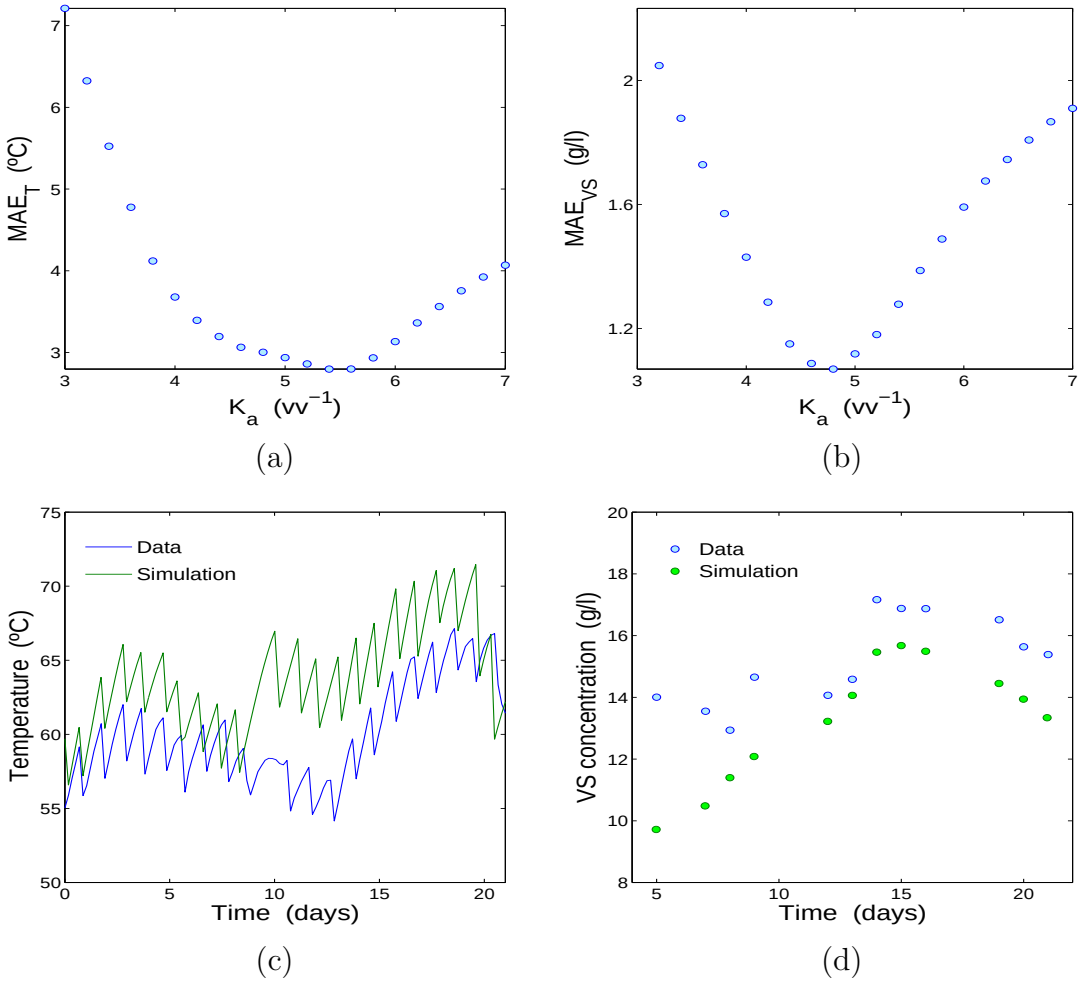


Figure 5.23: Assessment of ATM1 model through CS1 data and estimation of $K_a$: MAE for prediction of (a) temperature and (b) VS concentration at different $K_a$ values, and simulation of (c) temperature and (d) VS concentration time series for optimal $K_a$ value of 5 $vv^{-1}$.

estimate the value of $K_a$. No data was available regarding VS concentration. Figure 5.24a shows $MAE_T$ at different $K_a$ values. As in the previous case, the function is highly sensitive to changes of $K_a$. The minimum of the function is found for a value at 3.5 $vv^{-1}$. Figure 5.24b displays the simulation of the temperature time series for the optimal $K_a$ value. Again, qualitative agreement is reasonable though some quantitative differences can be seen. The better quantitative agreement when compared to CS1 (see Figure 5.23c) either in terms of the performance metric or as can be readily seen by the unaided eye lies, at least partially, in the fact that the operating conditions in this case are not subject to such strong fluctuations.

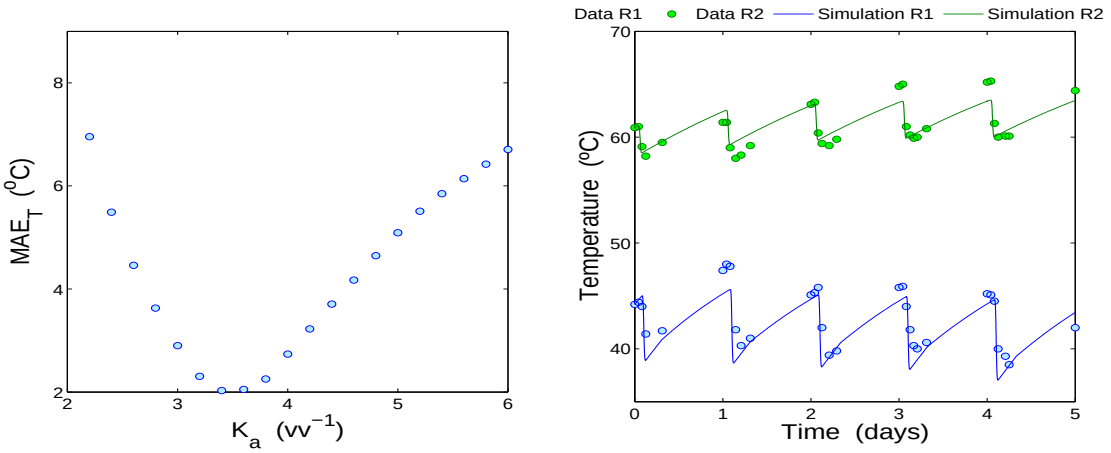


(a) (b)

Figure 5.24: Assessment of ATM1 model through CS2 data and estimation of $K_a$: (a) MAE for prediction of temperature, and (b) simulation of temperature time series for optimal $K_a$ value of 3.5 $vv^{-1}$.

It is important to note here that, while some wastewater treatment models (e.g., the ASM family) have been in existence and undergone a constant process of validation for over 30 years, dynamic ATAD models have less than 5 years of development. Thus, present ATAD models are still at a relatively early stage of development, and should be seen as platforms for yet further development. It is also important to note that the available data regarding ATAD operation is extremely scarce. Higher quality and more quantity of data should be published if these models are to be further validated.

# Chapter 6

# Optimisation

As stated in Chapter 3, the main objective of this study is to minimise the energy requirement of ATAD systems while complying with treatment objectives. This problem obviously falls within the realm of optimisation. Due to its discontinuous, semi-batch nature, ATAD has to be optimised via dynamic optimisation. The present chapter will give an introduction to dynamic optimisation, its general mathematical framework and formulation, and the different approaches that are available to solve this kind of problems. It will then present the general formulation for the minimisation of the energy requirement of an ATAD system, which will be implemented and solved for CS1 and CS2 following the direct sequential approach. Finally, it will provide a tentative framework for the optimisation of ATAD systems following the direct simultaneous approach. The latter shall prove very useful in future work for the structural optimisation of ATAD systems, due to its superior computational efficiency.

## 6.1 Introduction

Dynamic optimisation, also referred to as *optimal control*, originated from the work of the Russian mathematician Lev Pontryagin, and it is a generalisation of the calculus of variations (Pontryagin, 1964). The need for this kind of methodology arose during the 1950s in the field of aeronautical and astronautical engineering, in order to control and stabilise the trajectory of space shuttles crossing the atmosphere.

These fields continue to amass the largest number of publications when it comes to the use of this methodology (Biegler, 2007).

In the field of process engineering, this methodology has been used for the optimal design and operation of batch processes. Typical examples are the optimal operation of bioreactors and fermenters (Cuthrell and Biegler, 1989; Riascos and Pinto, 2004), reactive distillation (Sargent and Sullivan, 1979; Sorensen et al., 1996), crystallisation (Lang et al., 1998), polymerisation reactors (Jang and Lin, 1991; Flores et al., 2005), or batch distillation systems (Mujtaba and Macchietto, 1997; Furlonge et al., 1999). Two recent reviews on the use of dynamic optimisation in (bio)process engineering can be found in Banga et al. (2003) and Bonvin et al. (2003).

In the context of wastewater treatment, the use of this methodology has been far more limited. Most of the few available publications in this area are fairly recent, focusing on the minimisation of the energy requirement of alternated activated sludge processes (Moles et al., 2003; Fikar et al., 2005; Holenda et al., 2007; Descoins et al., 2010).

The advantages of using optimisation are well documented, and the gains are often significant. However, from an industrial perspective, the use of dynamic optimisation for batch and semi-batch processes is still rare. Generally, industrial batch processes are operated following experimental conditions which are then improved by the operators according to anecdotal evidence and experience (Bonvin et al., 2003).

## 6.2 Fundamentals of dynamic optimisation[1]

The verb "to optimise" comes from the Latin root *optimus* meaning "best". This meaning implies the notion of *choice*. Thus, the germ or original idea behind this methodology is *to choose the best of all possibilities*.

In the mathematical realm of optimisation, distinctions are made among the different kinds of optimisation problems. One such distinction arises when considering the factor of time. When time is not relevant to the system and problem of interest,

[1]This introductory section has been partly adapted from Chiang (1992).

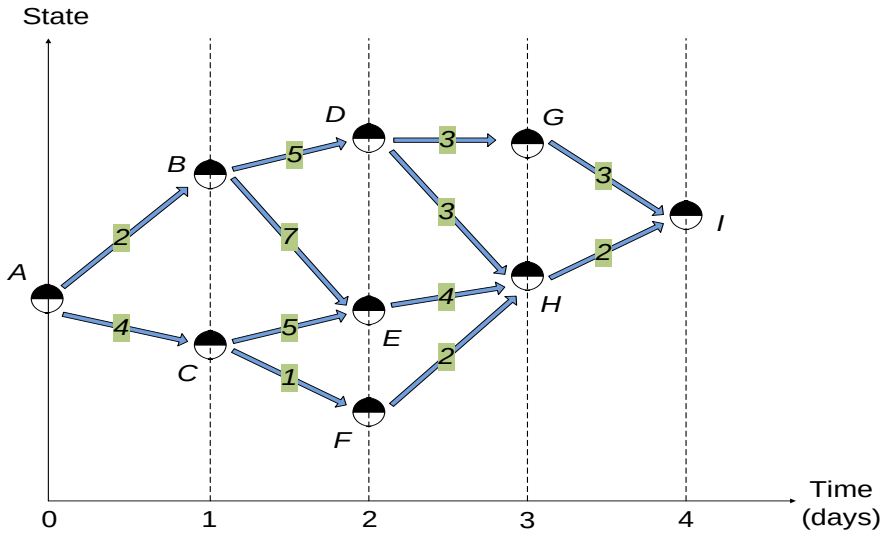


Figure 6.1: Example of dynamic optimisation in the discrete time domain. The optimal pathway is *ACFHI*. Adapted from Chiang (1992).

then the problem is said to be one of *static optimisation*. A typical problem of this kind is to maximise the flowrate of a continuous chemical process, such as distillation. If, on the contrary, time *is* relevant to the problem at hand, then it is said to be a problem of *dynamic optimisation*. A common example would be to maximise the profit of a batch pharmaceutical plant for the production of specialty chemicals. Generally, the former kind of problems is found in the literature far more frequently than the latter.

Hence, the salient feature of dynamic optimisation is the fact that the optimisation process takes place *in time*. To illustrate what it means to optimise in time, let us consider a simple example. A chemical plant has to transform a certain chemical $A$, the raw material, into another chemical $I$, the end product, by means of a series of chemical reactions. Each reaction ($AB$, $AC$, etc.) has a duration of 1 day and incurs a different cost. The problem facing the plant manager is that he does not know which pathway of chemical reactions is best to minimise the cost of transforming $A$ into $I$. Figure 6.1 illustrates this situation with the whole set of chemical states (circles $A$, $B$, $C$, etc.), reactions between states (arrows), and the corresponding cost of each reaction (number over each arrow). After the first choice has been made the first day (say, reaction $AC$), another choice has to be made the second day (say, $CE$), and so on, until reaching the end product $I$. Each pathway will have a

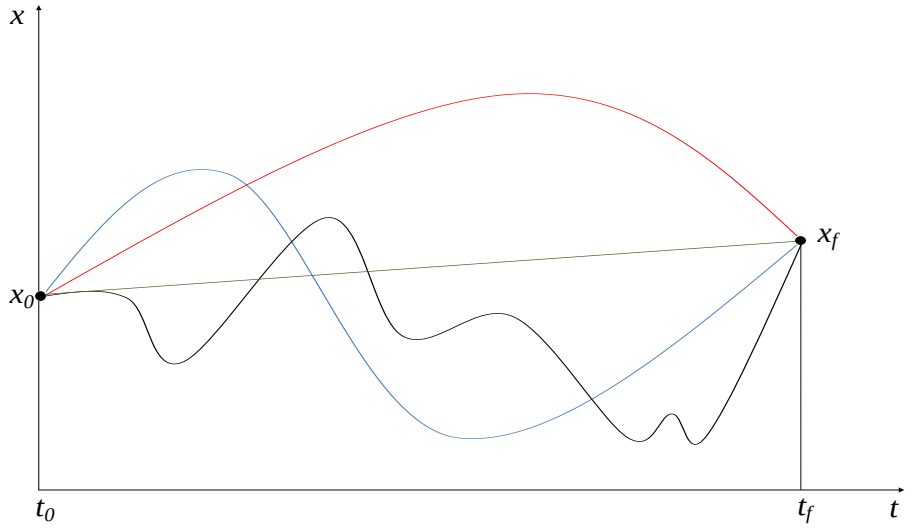


Figure 6.2: Different paths between two arbitrary points in the continuous time domain. Adapted from Chiang (1992).

different cost. After considering all possible pathways, it is clear that the best or optimal pathway is *ACFHI* with a total cost of 9. In this way, it becomes clear that optimisation is a problem of *choosing the best of all possibilities*. Yet, this example also reveals an important fact of dynamic optimisation: the optimal solution is not generally found by selecting the current best choice at every point in time. In other words, the shortsighted approach of choosing whatever seems best at each moment regardless of preceding or subsequent choices does not usually result in the best or optimal solution. As a counterexample against this shortsighted approach, note that it would have lead us to choose the pathway *ABDGI* with total cost of 13 or *ABDHI* with 12, which are clearly not optimal. That is, the "goodness" of a certain choice cannot be judged in isolation from its previous and subsequent choices. It is rather the *whole set of choices* that determine the "goodness" of the solution.

The previous example illustrated the philosophy of dynamic optimisation in the discrete time domain. Now, we will briefly review how the same concept works in the continuous time domain. The main difference is now that the values of the variables time $t$ and state $x$ are to be taken from the set of real numbers $\mathbb{R}$. Therefore, between two contiguous points of time $t_1$ and $t_2$ and their corresponding states $x_1$ and $x_2$ there is always an infinite number of stages through which the system has to go. These trajectories between two arbitrary points are known as *paths*. Figure

6.2 shows several paths between two such arbitrary points $x_0$ and $x_f$. Imagine now that the surface represents a mountainous territory and that we are trying to carry certain goods from point $(t_0, x_0)$ to $(t_f, x_f)$. It then becomes obvious that every path will incur a different cost for oil consumption and that every path will, depending on the topography of the territory, have a different cost.

From what we have seen so far, it is clear that any kind of dynamic optimisation problem includes the following elements, regardless of whether it is formulated in the discrete or continuous time domain:

1. a generally fixed *starting point* and sometimes a fixed *terminal point*,
2. a group of *feasible paths* between the starting and terminal points,
3. a group of *path values* corresponding to each path and representing their *performance indices*, and
4. an *optimisation criterion*, that is, the minimisation or maximisation of the performance index by choosing the optimal path.

It is important to note here that the relation between any path and its corresponding performance index or path value is a special type of function. Therefore, it is given the name *functional*, thus differentiating it from the common function $f$ that associates scalar elements of a set $X$ with scalar elements of another set $Y$ (i.e., $f : X \to Y$). Instead, a functional associates a *curve* or *vector* with a scalar. This type of function is central to the concept of calculus of variations. To indicate that a functional $J$ is dependent on an entire curve or vector $x(t)$, the notation $J[x(t)]$ or $J[x]$ is commonly used. Figure 6.3 illustrates the mapping between different curves $x_{\mathrm{I}}(t)$, $x_{\mathrm{II}}(t)$, and $x_{\mathrm{III}}(t)$ and their corresponding path values $J_{\mathrm{I}}$, $J_{\mathrm{II}}$, and $J_{\mathrm{III}}$.

It is also important to note that the starting and terminal points can be either fixed or free. These possibilities define different types of optimisation problems. When the terminal time is given and the terminal state is free, it is a *fixed-time problem*. If, on the contrary, the terminal time is free and the terminal state fixed, it is a *fixed-endpoint problem*. In the more flexible type of problem, neither the

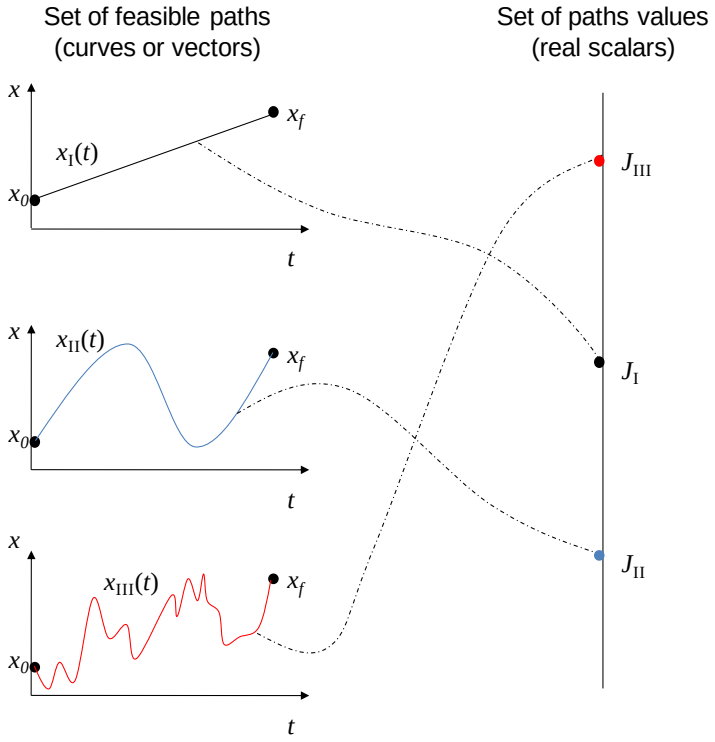


Figure 6.3: Functional: mapping between curves and scalars. Adapted from Chiang (1992).

terminal time nor the terminal state is fixed. In this case, it is known as *terminal-curve problem*, and the terminal state is usually bound to the terminal time through a constraint $x_f = g(t_f)$. Thus, in such case there are not two but one single degree of freedom. The three types of problems are illustrated in Figure 6.4.

So far we have only given attention to two types of variables: the time $t$ and the states $\vec{x}(t)$. However, in dynamic optimisation problems there is one additional kind of variable involved: the control variable $\vec{u}(t)$. This variable is central to the problem and its practical implications, due to the fact that state variables are not directly controllable. It is rather the control variable that allows us to have an influence on the state variables and the state and fate of the system as a whole. The control variables determine the state of the system and its change. For this reason, they are the actual instrument of optimisation; state variables occupy a secondary role in the optimisation problem, for they are derivative from $\vec{u}(t)$.

Once the control variables are given, the state variables can be derived through the *state equation*,

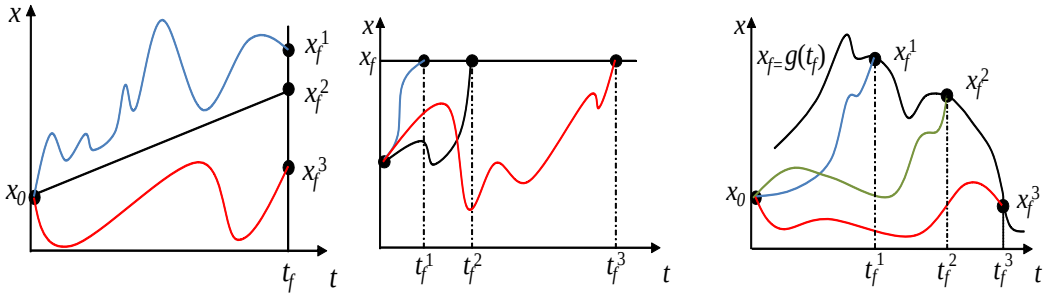


(a) (b) (c)

Figure 6.4: Typical types of problems in dynamic optimisation: (a) fixed-time problem, (b) fixed-endpoint problem, and (c) terminal-curve problem. Adapted from Chiang (1992).

$$\vec{f}(\dot{\vec{x}}(t), \vec{x}(t), \vec{u}(t), t) = \vec{0}. \tag{6.1}$$

The optimal path $\vec{u}^*(t)$ is defined as the curve that minimises (or maximises) the cost functional $J[\vec{x}(t), \vec{u}(t)]$. Once this optimal control path has been found, the optimal state path $\vec{x}^*(t)$ can be derived from the state equation. Let us define the Lagrangian $\mathcal{L}$ as the function that assigns values to the infinitesimal arcs constituting any given path, and $\Phi$ as a function that assigns a certain endpoint cost that depends exclusively on the final state of the system. Then, the cost functional $J$ can be defined as

$$J[\vec{x}(t), \vec{u}(t)] = \int_{t_0}^{t_f} \mathcal{L}[\dot{\vec{x}}(t), \vec{x}(t), \vec{u}(t), t]dt + \Phi[\vec{x}(t_f), \vec{u}(t_f)]. \tag{6.2}$$

Finally, there is another important element pertaining to dynamic optimisation problems: *constraints*. Most problems contain a number of algebraic constraints that place restrictions on the movement of the control and state variables. Some constraints involve only state variables, while some others involve both state and control variables. There are two types of algebraic constraints: *equality* and *inequality constraints*. Obviously, equality constraints are the most restrictive ones. Additionally, some constraints are only active at the terminal point of the path, and are thus named *terminal constraints*. Paths that do not satisfy all the present constraints are said to be *infeasible*, and *feasible* otherwise.

### 6.2.1 General formulation

In terms of the general language, the problem formulation of dynamic optimisation consists of finding the control histories that optimise a given performance index (say, the cost, productivity, or profit) subject to certain constraints. In the mathematical language, this optimisation problem is formulated as the search for the control profiles $\vec{u}^*(t)$ and free terminal time $t_f^*$ that minimise the cost functional $J[\vec{x}(t), \vec{u}(t)]$, subject to a set of dynamic and algebraic constraints:

$$\min_{\vec{u}(t), t_f} J[\vec{x}(t), \vec{u}(t)] = \int_{t_0}^{t_f} \mathcal{L}[\vec{x}(t), \vec{u}(t), t]dt + \Phi[\vec{u}(t_f)], \tag{6.3}$$

subject to

$$\begin{aligned}
\vec{f}(\dot{\vec{x}}(t), \vec{x}(t), \vec{u}(t), t) &= \vec{0}, && (6.4)\\
\vec{x}(t_0) &= \vec{x}_0, && (6.5)\\
\vec{g}(\vec{x}(t), \vec{u}(t)) &= \vec{0}, && (6.6)\\
\vec{h}(\vec{x}(t), \vec{u}(t)) &\leq \vec{0}, && (6.7)\\
\vec{u}_{min} \leq \vec{u}(t) &\leq \vec{u}_{max}, && (6.8)
\end{aligned}$$

where Equation 6.4 is the *dynamic constraint*, that is, the state equations that govern the system dynamics (discussed above; see Equation 6.1); Equation 6.5 is their corresponding initial condition. Equation 6.6 and 6.7 are the algebraic path constraints, with the former representing the equality and the latter the inequality constraints. In practice, the need to include this kind of constraints may arise from safety, environmental, efficiency, quality, or economic reasons. Finally, Equation 6.8 stands for the control boundaries. Equations 6.3 to 6.8 set the general mathematical formalism for any dynamic optimisation problem, whose elements have been described above in some detail.

The solution of the above optimisation problem is given by the optimal trajectories of controls $\vec{u}^*(t)$ and states $\vec{x}^*(t)$, the optimal terminal time $t_f^*$, and the optimal value $J^*$ of the cost functional. If the optimal trajectories of the control variables are

only dependent on time, that is, $\vec{u}^* = \vec{u}^*(t)$, and thus determined at the initial time, the problem is said to be *open loop*. If, however, they are dependent on both time and the state variables, i.e., $\vec{u}^* = \vec{u}^*(\vec{x}(t), t)$, the problem is then said to be *closed loop*. The latter case means that the optimal control trajectories can be changed whenever new information is available regarding the present state of the system.

The problem formulation given by the set of equations 6.3–6.8, also known as the *direct formulation*, can be reformulated within the framework of Pontryagin's Minimum Principle (PMP) in which the Hamiltonian $\mathcal{H}$, instead of the scalar functional $J$, is minimised. Alternatively, the problem can also be reformulated following the framework of Hamilton-Jacobi-Bellman (HJB) in terms of the scalar value function $V$ and the HJB partial differential equation, which has to be solved by finding the minimal value of $V$. Both PMP and HJB formulations are known as *indirect formulations*, because they require a complete reformulation of the original problem. One notable disadvantage of indirect formulations is that the problem can be extremely difficult to solve when active path constraints are present. PMP represents only a necessary condition for optimality, while HJB is a sufficient condition. An elucidating review on the different formulations and their corresponding approaches can be found in Bonvin et al. (2003).

In this work, we shall concern ourselves exclusively with the direct formulation and its corresponding approaches. The reason for this choice is the arduous and time-consuming task of reformulating the original problem, as well as the fact that our particular problem may include, in one form or another, active path constraints.

### 6.2.2 Direct methods: sequential and simultaneous approaches[2]

There are two direct approaches for the solution of problem 6.3–6.8: the sequential and the simultaneous approach. The sequential approach solves the problem in terms of continuous state variables $\vec{x}(t)$ and discretized control variables $\vec{u}(t)$. The simultaneous approach, also known as *orthogonal collocation* or *direct transcription*,

[2]This introductory section has been partly adapted from Bonvin et al. (2003).

solves the problem by discretizing both states and controls. Another important difference is that in the sequential approach the integration of the state equations takes place explicitly, whereas in the case of the simultaneous approach the integration is done in an implicit manner.

**Sequential approach**

In this approach, only the control variables $\vec{u}(t)$ are used as optimisation variables. For any given vector $\vec{u}(t)$, the set of differential equations is integrated explicitly, and the functional $J$ and path constraints $\vec{g}$ and $\vec{h}$ are evaluated. Because the differential equations are satisfied at every iteration of the optimisation, the sequential approach is considered a *feasible-path approach*. The following are the steps involved in this approach:

1. Parameterization of control variables in a finite number $n$ of intervals. For the terminal time problem, the terminal time $t_f$ has to be considered as one of the optimisation variables. The control variables are typically approximated through piecewise polynomials or piecewise-constant intervals. Are the time intervals of the piecewise-constant approximation of equal size, so the approach receives the name of control vector parameterezation (CVP) (see, for example, Ray, 1981; Edgar and Himmelblau, 1988).

2. Selection of initial value for optimisation variables.

3. Integration of state equations and evaluation of functional $J$ and path constraints $\vec{g}$ and $\vec{h}$.

4. Computation of the new values for the optimisation variables through an algorithm. Steps 3 and 4 should be repeated until functional $J$ has been minimised. For a set of efficient and robust algorithms, see Banga et al. (2005) or Egea et al. (2010).

The greatest advantage of the sequential approach is that it is simple and straightforward. On the other hand, its most noticeable disadvantage is that Step 3 tends to be highly time-consuming. This is because the state equations (Equation 6.4) are

explicitly and accurately integrated at every iteration, even when the control vector is far from the optimum.

An important advantage of CVP is that it is easy to implement. Nevertheless, it can be slow when it comes to evaluating the path constraints due to the accurate integration of the differential equations. Another drawback is that the quality of the optimal solution $J^*$ depends on the parameterization of the control variables.

### Simultaneous approach

To avoid the time-consuming Step 3 in the sequential approach, the simultaneous approach involves the approximation of the state equations through the introduction of the so-called *residual*, whose elements are forced to be zero. In doing so, the state equations are solved in an implicit way, and not through an explicit and accurate integration of the differential equations at every iteration. Therefore, this approach is far more efficient than the previous one on a computational basis. Generally, the state equations are satisfied only once, namely, at the optimal solution. Consequently, this is called an *infeasible-path approach*. The main difference with regard to the sequential approach is that the optimisation is performed in the entire space of discretized control *and* state variables.

The time period of interest $[t_0, t_f]$ is broken into a number of intervals, known as *finite elements*, and the state equations are only studied at the roots of the orthogonal polynomials, known as *collocation points*. Both finite elements and collocation points are central to orthogonal collocation and have a considerable effect on the optimisation process. Usually, as the mesh of finite elements and collocation points becomes rougher (that is, worse) the optimisation results become better. Careful attention is therefore called for, in order to avoid (apparently) good solutions that are, in fact, highly inaccurate. The tradeoff between approximation and optimisation has been studied by Srinivasan et al. (1995), who concluded that the accuracy could be improved by including an additional accuracy constraint or by increasing the number of collocation points.

The steps involved in this approach are:

1. Parameterization of control and state variables by means of piecewise polynomials (typically the orthogonal Legendre polynomials). The final time $t_f$ should be considered as one of the optimisation variables.

2. Discretisation of state equations. The time instants at which the state equations should be evaluated are commonly taken to be the Legendre or Radau roots. Through the above parameterization and discretization, the dynamic optimisation problem becomes a common nonlinear programming (NLP) problem.

3. Selection of initial value for optimisation variables.

4. Iterative algorithmic solution of NLP problem until functional has been minimised.

Most NLP problems arising from the above procedure contain a large number of optimisation variables. Therefore, efficient algorithms should be employed in their solution. Some of these algorithms include sequential quadratic programming (SQP), reduced-space SQP, interior-point approach, and conjugate gradient methods (Biegler, 1984; Renfro et al., 1987; Cervantes and Biegler, 1998; Biegler et al., 2002).

## 6.3 Problem formulation for a generic ATAD system

Within the framework of the direct sequential approach, the free-terminal-time problem of the minimisation of the energy requirement for a generic ATAD system can be formulated as

$$\min_{\vec{u}(t),t_f} E_m[\vec{u}(t)] = \frac{1}{m_{in}} \int_{t_0}^{t_f} P[\vec{u}(t)]dt, \tag{6.9}$$

subject to

$$\vec{f}(\dot{\vec{x}}(t), \vec{x}(t), \vec{u}(t), t) = \vec{0}, \tag{6.10}$$

$$\vec{x}(t_0) = \vec{x}_0, \tag{6.11}$$

$$0.38 - r_{VS}(t_f) \leq 0, \tag{6.12}$$

$$1 - L(t_f) \leq 0, \tag{6.13}$$

$$\vec{u}_{min} \leq \vec{u}(t) \leq \vec{u}_{max}, \tag{6.14}$$

where 6.9 represents the optimisation criterion, 6.10 the dynamic constraint (that is, the ATM1 model) and 6.11 its initial condition, 6.12 the algebraic inequality constraint for stabilisation, 6.13 the algebraic inequality constraint for pasteurisation, and 6.14 the boundary conditions for the control variables.

The stabilisation and pasteurisation constraints 6.12 and 6.13 enforce that at least the minimum legal requirements for sludge stabilisation and pasteurisation are achieved by the end of the reaction, effectively rendering infeasible all paths that do not satisfy them. Note that these inequality constraints are only active at the terminal time $t_f$.

The development of the ATM1 model in Chapter 4 was due to the need to account for the system dynamics in constraint 6.10. The quantification of the treatment objectives, on the other hand, was necessary to specify the algebraic inequality constraints 6.12 and 6.13, and the specific energy requirement $E_m$ defines the cost functional to be minimised in 6.9.

Thus, the development of the ATM1 model, the quantification of stabilisation and pasteurisation, and the unambiguous definition of the energy requirement, accomplished in previous chapters, now pave the way for the dynamic optimisation of ATAD systems.

## 6.4 Optimisation results for CS1

The problem posed by equations 6.9 to 6.14 was implemented in the MATLAB© platform following the direct sequential CVP approach, and it was solved for the

single-stage system CS1 by means of the enhanced scatter search (eSS) algorithm developed by Egea et al. (2009). This evolutionary metaheuristic is a global search method that alternates with local search algorithms to refine the best solutions. The global search algorithm is an enhanced version of scatter search, while the local search algorithm used here is *fmincon*, a gradient-based SQP algorithm that finds the minimum closest to the starting point. The eSS algorithm thus offers a good compromise between diversification and intensification.

The control variables chosen here are the aeration flowrate and the final time. The loading time and the volume replaced were not considered because they require the reactor volume as one of the state variables; this, in turn, would entail a considerable computational burden, apart from making the optimisation process unstable. Therefore, the reactor volume is not considered as a state variable and reactor loading is assumed to take place *instantaneously*. The lower and upper boundaries for the aeration flowrate are 0.8 vvh and 10 vvh, respectively. By choosing such a high upper boundary, we ensure that the algorithm will have the freedom to search in a wide area of the control space. The lower boundary is the same as currently in the plant and unequal to zero, as this would create anaerobic conditions inside of the reactor (with its associated problems, such as odours). The lower and upper boundaries of the final time are 0.7 and 2 days, respectively. The lower boundary is justified by the fact that the maximum sludge production in the plant is ∼45 $m^3$/day; and considering that replaced volume in the optimisation is assumed to be 45 $m^3$, the minimum final time should not be lower than ∼0.7 days in order to stay within the actual range of sludge production of the plant. The upper boundary was chosen high enough to allow a broad area of the control space to be explored.

It is important to specify that, for each iteration within the optimisation and for each control vector $\vec{u}$, a total of $n_b$ consecutive batches are calculated. The objective functional $E_m$ and the constraints are then evaluated based on the last batch in the series. This was done to ensure that optimal solutions are periodic or quasi-periodic (and far away from the transient period). The value of $n_b$ was chosen as 10, as experience has shown that this is generally enough to obtain periodicity, while it does not impose an excessive computational burden.

The parameterization or discretization parameter $n_{q_a}$ specifies the number of elements or intervals in which the aeration flowrate is discretized. In the present optimisation, the value of the $n_{q_a}$ was chosen as 10. Note that within each element or interval the aeration flowrate is given a constant value.

The control vector $\vec{u}$ therefore consists of the first $n_{q_a}$ components specifying the value of the aeration flowrate in each interval, followed by the final time. In this way, there are a total of $n_{q_a} + 1$ elements in the control vector.

Let us now briefly recall that under usual operating conditions the CS1 plant is operated with a batch time of 1 day, a sludge flowrate of 30 $m^3$/day, a VS influent concentration of 35 g/l, and a constant aeration flowrate of $\sim$1 vvh. The corresponding energy requirement is 0.72 kWh/kg of VS treated (see section 5.1.1).

Figure 6.5 shows the optimal trajectories for state and control variables as well as VS reduction and pasteurisation lethality. Both substrate and dissolved oxygen concentrations are quite low. However, it is not easy to say which one of the two limitations outweighs the other. As for the other concentrations, they behave in the usual way. The temperature increases approximately 10 °C during the reaction, which is slightly higher than under normal conditions; the difference is probably due to the higher aeration flowrates. The aeration flowrate takes values that are considerably higher (up to 7.5 vvh) than the usual ones of the plant. As expected, it can also be seen that the dynamics of both OUR and dissolved oxygen are responses to changes in the aeration flowrate. The qualitative behaviour of the aeration flowrate is such that it commences at higher values and it decreases gradually until reaching the lower boundary. An interesting feature of this solution is its biological plausibility: at the beginning of the batch the substrate concentration is higher and so is the need for oxygen, in order to oxidise the plentiful organic matter; in order to match the high oxygen demand, the aeration flowrate has to be higher at the beginning of the reaction. As time passes and substrate is gradually consumed, the demand for oxygen decreases and so does the aeration flowrate. Thus, this qualitative optimal profile makes sense of the underlying biological system. This result shows that the optimal behaviour of the aeration flowrate is far from invariable, as it is typically

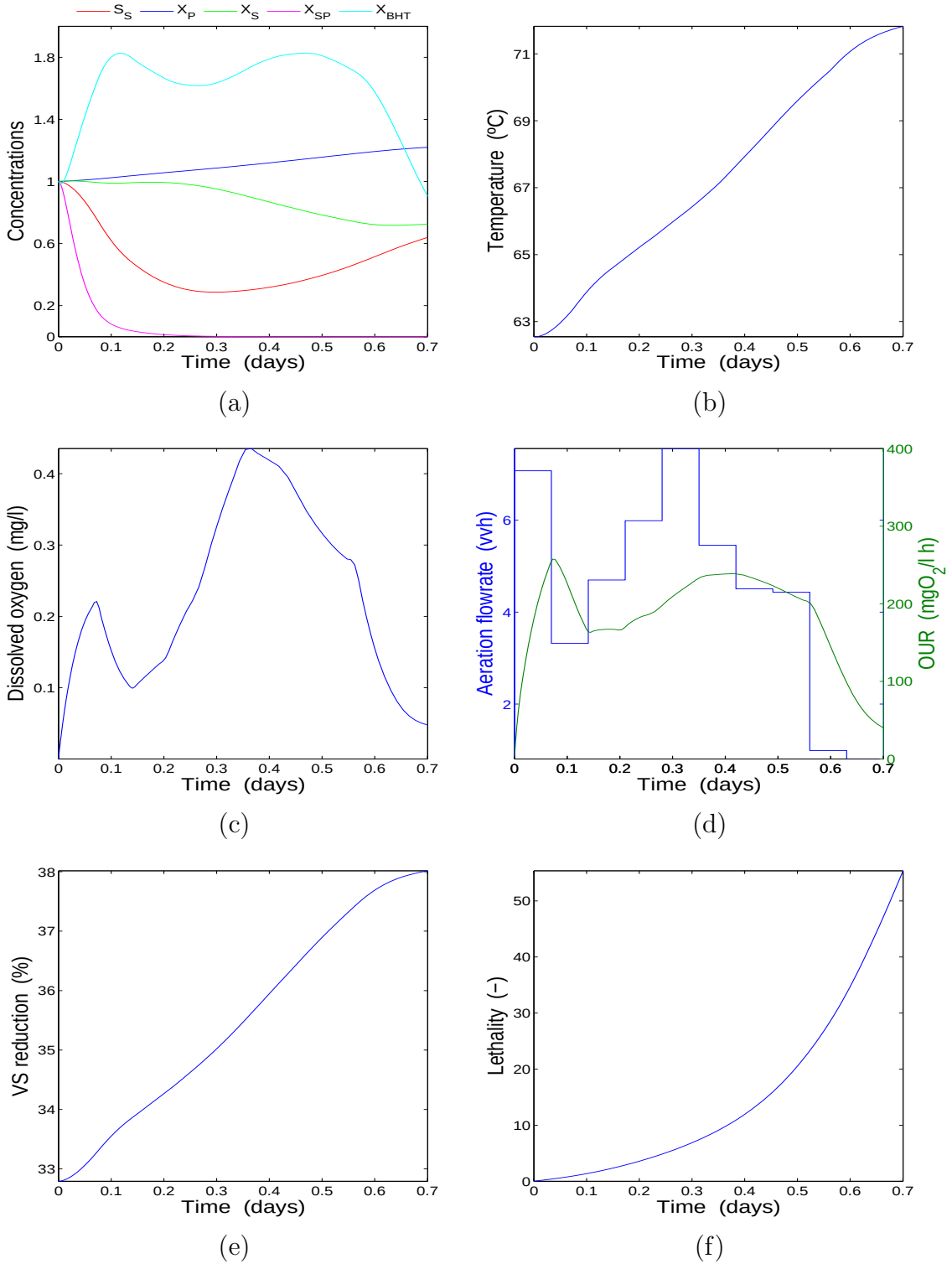


Figure 6.5: Optimisation results for CS1: optimal profiles of (a) concentrations (initial condition: $S_S = 1.5$ g/l, $X_P = 7.2$ g/l, $X_S = 9$ g/l, $X_{SP} = 0.5$ g/l, $X_{BHT} = 0.8$ g/l), (b) temperature, (c) dissolved oxygen, (d) aeration flowrate and OUR, (e) VS reduction, and (f) pasteurisation lethality ($n_b = 10$, $n_{q_a} = 10$). The optimal energy requirement is 0.55 kWh/kg, corresponding to a reduction of 23%.

found in conventional ATAD systems. At this stage, it can thus be seen that exploiting the aeration flowrate as an additional degree of freedom for optimisation is a crucial way of obtaining better solutions, and that invariable aeration is not generally suitable for ATAD systems.

It can be observed that, while the minimum requirement for the pasteurisation lethality is exceeded by over 50 times, stabilisation is limiting. It was found that in all optimal solutions stabilisation was limiting. This is consistent with the tendency found in the sensitivity analysis presented in the previous chapter (see section 5.4.2).

The optimal final time is 0.7 days, which corresponds to the lower boundary. It was found that the algorithm tends to favour shorter final times, which is also consistent with the aforementioned sensitivity analysis. Thus, the optimal value of the final time, being the value of the lower boundary, makes sense of the dependence of the energy requirement (objective functional) on the final time: shorter final times tend to result in lower energy requirements. Let us recall that conventional systems use a 1-day final time due to operational convenience, thus not exploiting this important degree of freedom.

The corresponding energy requirement is 0.55 kWh/kg, representing a reduction of 23%.

It was found that the objective functional $E_m$ is highly multimodal. When calling the local solver, the optimal solution would often depend on the starting point $\vec{u}_0$. This justifies the use of the eSS algorithm which alternates global and local search methods. The global optimality of the solution, however, cannot be guaranteed. As expected, the quality of the solution depended strongly on the discretization parameter $n_{q_a}$.

## 6.5 Optimisation results for CS2

The same problem formulation (equations 6.9 to 6.14), approach (CVP), and algorithm (eSS) were used to optimise the energy requirement of the two-stage system CS2.

In this case, the control variables are the aeration flowrate, the final time, and

the polymer concentration (see section 5.1.2 for an explanation). The polymer is added because the VS concentration after pre-thickening is generally 15 g/l; this is not sufficient to reach and maintain thermophilic operation. Adding the polymer ensures that the VS concentration consistently reaches 40 g/l, thus avoiding this problem with the operating temperature. However, the addition of polymer has a profound and negative impact on the energy requirement. Consequently, it is a natural choice to take it as control variable. The lower and upper boundaries for the aeration flowrate are 1 and 10 vvh, respectively. The boundaries for the final time are 0.7 and 1.5 days. The lower and upper boundaries chosen for the polymer concentration are respectively 0 and 25 g/l. It follows that the minimum and maximum VS concentration after polymer addition are 15 and 40 g/l, respectively. The volume changed after each batch was assumed to be 25 $m^3$.

In this case, the control vector $\vec{u}$ consists of the $2n_{q_a}$ discrete values for the aeration flowrate, the final time, and the polymer concentration: a total of $2n_{q_a} + 2$ components. The discretization parameter $n_{q_a}$ was given the value 10 for the two reactors. The periodicity parameter $n_b$ maintains here the previous value of 10.

As was seen in section 5.1.2, the usual final time of the two-stage system CS2 is $\sim$1 day, the aeration flowrate is 4 and 3 vvh for the first- and second-stage reactors, respectively, the volume replaced daily is 25 $m^3$, and the typical VS concentration after polymer addition is 40 g/l. The corresponding energy requirement is 1.22 kWh/kg.

Figure 6.6 shows the optimal profiles of the state and control variables for the two-stage system CS2. The conditions are oxygen-limited in the first-stage reactor and substrate-limited in the second-stage. This is generally the case in this kind of systems, and it is due to the fact that the first reactor is loaded with fresh sludge and the second with partially digested sludge. The behaviour of the concentrations is as usual.

The temperature in the first-stage is relatively low and in the second-stage it does not exceed 60 °C. The overall low temperatures are due to the low influent VS concentration of 21.7 g/l (optimal polymer concentration is 6.7 g/l), and to the low aeration flowrates. The temperatures are notwithstanding high enough to exceed

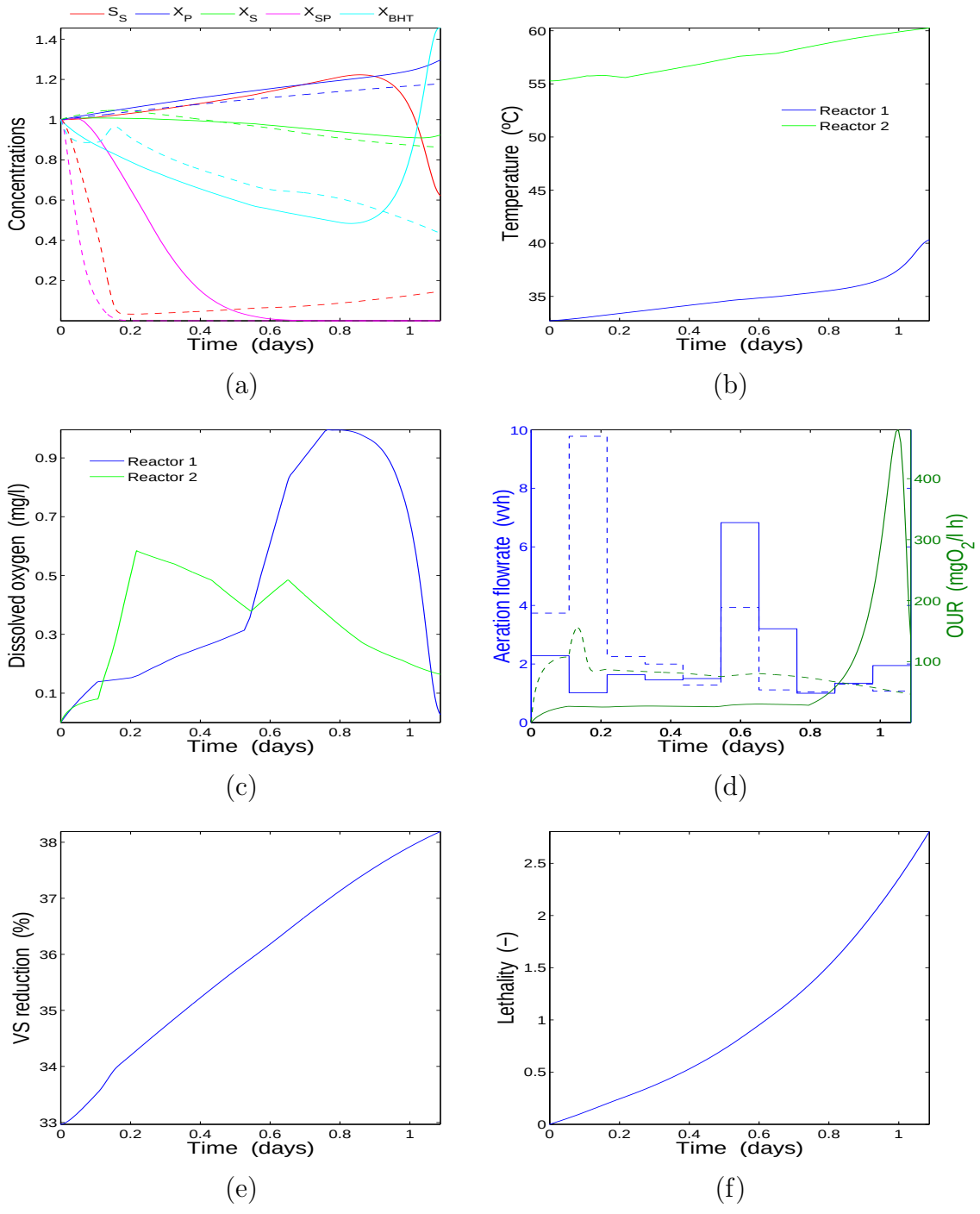


Figure 6.6: Optimisation results for CS2: optimal profiles of (a) concentrations (initial condition: $S_S^1 = 4$ g/l, $X_P^1 = 2$ g/l, $X_S^1 = 11$ g/l, $X_{SP}^1 = 0.01$ g/l, $X_{BHT}^1 = 1.8$ g/l,$S_S^2 = 1$ g/l, $X_P^2 = 6$ g/l, $X_S^2 = 7$ g/l, $X_{SP}^2 = 0$ g/l, $X_{BHT}^2 = 1$ g/l) (solid: reactor 1; dashed: reactor 2), (b) temperature, (c) DO, (d) aeration flowrate and OUR (solid: reactor 1; dashed: reactor 2), (e) VS reduction, and (f) lethality ($n_b = 10$, $n_{q_a} = 10$, polymer concentration: $\sim$6.7 g/l). The optimal energy requirement is 0.99 kWh/kg, corresponding to a reduction of 18%.

pasteurisation requirements by more than 2.5 times. Stabilisation is once more the limiting process.

The aeration flowrate of the first-stage reactor is relatively constant, apart from the 6th and 7th intervals, and its mean value is 2 vvh. This value is well below that usually implemented in the plant (4 vvh). As for the second-stage, the aeration flowrate starts at a higher value and gradually decreases until reaching the lower boundary. This latter behaviour is qualitatively the same as found for the CS1 system. However, it is not clear that the same biological plausibility applies here, as the level of readily biodegradable substrate is nearly zero throughout the reaction. The mean value of the aeration flowrate in the second reactor is lower than that of the plant (3 vvh). Thus, in both reactors the aeration flowrate is lower than in the default mode of operation. The possible meaning of this is that the manufacturers of this kind of plant oversized the aeration level in order to exceed stabilisation and pasteurisation requirements (even though in this particular case the influent VS concentration, and thus the oxygen demand, is lower than usual). As it was found in the previous case study, variable aeration provides here probably the most important degree of freedom for optimisation.

The optimal final time is 1.08 days which is very close to conventional plant operation of 1 day. The algorithm tended to find solutions close to this value, even when the starting point was far away from it (or when starting with a randomised matrix of starting points). It is not clear why in this particular case the algorithm did not seek to further shorten the final time.

The optimal polymer concentration is just 6.7 g/l, corresponding to a total influent VS concentration of 21.7 g/l. The latter value is well below the recommended minimum of 25 g/l to ensure thermophilic operation. Nevertheless, the temperatures in the second-stage reactor are consistently thermophilic, and pasteurisation requirements are exceeded. The optimal polymer concentration is obviously very low. This could be understood in the following manner: by lowering the polymer concentration, the influent VS concentration is also lowered, and this should (up to a point) decrease the reaction time; the reason being that the less VS undergo treatment, the shorter the time needed to stabilise the sludge. Shorter reaction times

result in turn in lower energy requirements. However, as can be seen, the optimal final time is actually higher than in conventional operation. What is then the reason for the reduction in the energy requirement? The answer is, of course, that the lower polymer concentration requires lower aeration flowrates to satisfy stabilisation, when compared to conventional operation. It is thus the interaction between the optimal (low) aeration profile and the optimal (low) polymer concentration that allows us to achieve such a low energy requirement.

The optimal value of the energy requirement is 0.99 kWh/kg, representing a reduction of 18%.

Another potential way to substantially reduce the energy requirement of CS2 is by pre-dewatering the influent sludge. Let us assume that there is a way to pre-dewater the influent sludge thereby reducing its volume by 50%. That is, the usual 25 $m^3$ of sludge with a VS concentration of 15 g/l would be reduced to 12.5 $m^3$ with an influent VS concentration of 30 g/l, thus avoiding the need for polymer. This amount of sludge can be treated in one single reactor, for it is less than 15% of the total reactor volume. Let us therefore consider the treatment of this amount of sludge (12.5 $m^3$ with 30 g/l) in the first-stage reactor. The control variables are the aeration flowrate with 0.8 and 15 vvh as lower and upper boundaries, and the final time with 0.7 and 1.5 days.

The optimal profiles of state and control variables for this scenario are displayed in Figure 6.7. As expected, under these conditions the reaction is substrate-limited. This is due to the relatively low VS content in the influent sludge. In spite of the low VS content, reactors' temperatures are consistently thermophilic and pasteurisation requirements are exceeded. DO concentration is slightly higher than in previous cases, probably due to the lower oxygen demand resulting from the lower VS concentration of the influent sludge.

The pasteurisation lethality exceeds requirements by more than 2.5 times, whereas stabilisation is again limiting with just over 38% of VS reduction.

As for the optimal aeration profile, its qualitative behaviour is a gradual decrease starting close to the upper boundary and finishing at the lower boundary. This behaviour is qualitatively the same as in the previous cases, and it reinforces the

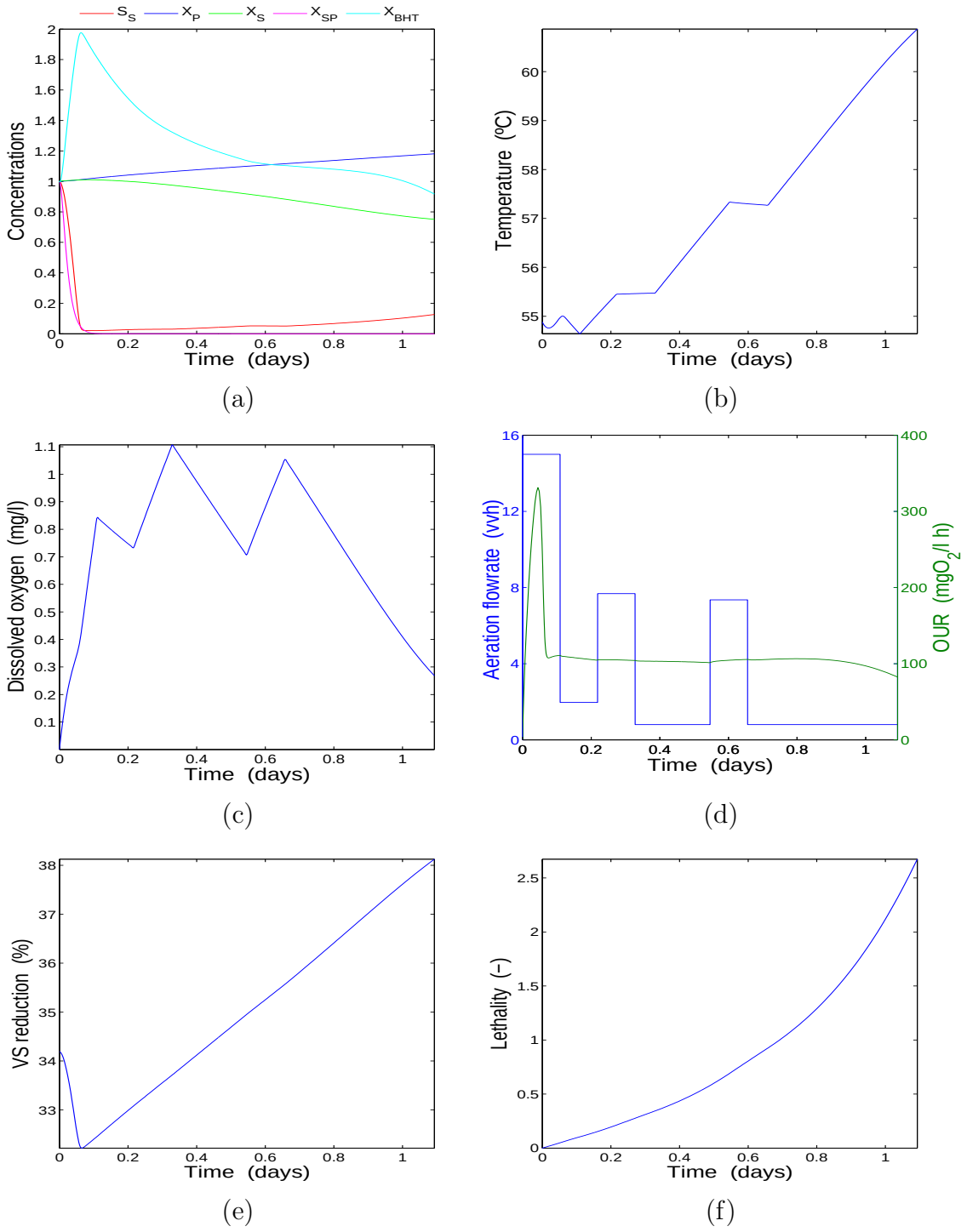


Figure 6.7: Optimisation results for CS2 using one single stage after pre-dewatering (12.5 $m^3$ of sludge with an influent VS concentration of 30 g/l; no addition of polymer): optimal profiles of (a) concentrations (initial condition: $S_S = 0.7$ g/l, $X_P = 7.5$ g/l, $X_S = 7.5$ g/l, $X_{SP} = 0.5$ g/l, $X_{BHT} = 0.8$ g/l), (b) temperature, (c) dissolved oxygen, (d) aeration flowrate and OUR, (e) VS reduction, and (f) lethality ($n_b = 10$, $n_{q_a} = 10$). The optimal energy requirement is 0.70 kWh/kg, corresponding to a reduction of 42%.

idea that the degree of freedom offered by variable air supply is central to advancing towards more efficient systems. The same biological plausibility discussed for the results of the CS1 system applies to this optimal profile.

Similar to the previous case, the optimal final time is 1.09 days which is very close to conventional operation. Again, it is not clear why the algorithm did not seek to further decrease this value given the first-order dependence between energy requirement and final time. The optimal value of the energy requirement is 0.70 kWh/kg, which represents a reduction of 42%.

What may be more important, though, is that by using one single stage, one entire reactor has been freed. Thus, plant capacity has been nearly doubled without expensive structural changes.

While in the short term it is more important to reduce the energy use of the facilities, in the long term (and in the light of rising population) the need to increase plant capacity is likely to become inevitable. With this in mind, process optimisation offers a solution to these two necessities. It should be noted that plant capacity improvements may, in the long term, lead to substantially higher savings than energy efficiency improvements do in the short term.

It should also be kept in mind that the base values used to calculate the reduction of the energy requirement of the optimal solutions are those pertaining to the actual plants (i.e., the experimental values). Thus, a point open to criticism is that the experimental base values and the calculated optimal values may not necessarily be comparable. Another approach would be to calculate the base values through simulations with the conventional operating conditions.

## 6.6 Tentative framework for dynamic optimisation of ATAD following the simultaneous approach

In this section, we will present a tentative framework for the dynamic optimisation of generic ATAD systems in accordance with the simultaneous approach. Such

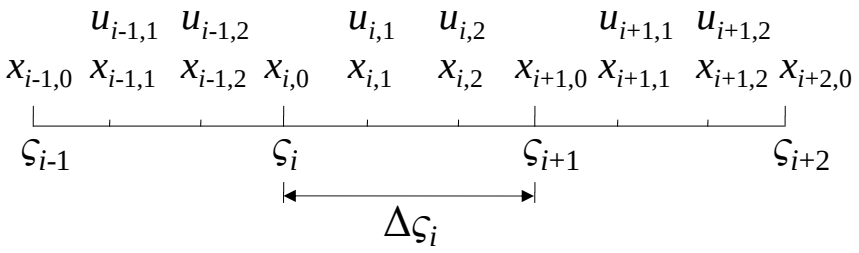


Figure 6.8: Time interval divided in three finite elements, each with two collocations points. Adapted from Cizniar et al. (2005).

framework shall prove very useful as a platform for further development toward the structural optimisation of ATAD systems.

### 6.6.1 Introduction[3]

In section 6.2.2, we reviewed the philosophy of the simultaneous approach, known as orthogonal collocation. A recent overview of this approach can be found in Biegler (2007). For a comprehensive treatment of the formalism, see Biegler (2010).

The salient feature of orthogonal collocation is that the process of optimisation is carried out in the full space of control and state variables. The solution of the differential-algebraic equation (DAE) system is coupled with that of the optimisation, and thus the DAE is satisfied only once, namely, at the optimal solution. Because intermediate solutions (that are often infeasible or far from the optimum) are avoided, this method is computationally more efficient than the sequential approach.

The principal idea behind the reformulation is to transform the DAE system (see equations 6.4 to 6.7) into a system of algebraic equations. This is done by approximating the solution of the DAE system through a series of polynomials (usually the Legendre polynomials), then selecting a finite number of points at which these polynomials are evaluated (called *collocation points*, and usually taken as the roots of the shifted Legendre or Radau polynomials), and, finally, finding the coefficients of the polynomials that satisfy the DAE system and solve the optimisation problem.

Let us consider the solution of the DAE system over the interval $[t_0, t_f]$. This

[3]This introductory section has been partly adapted from Cizniar et al. (2005).

time interval is then divided into a total of $N$ finite elements of length $\Delta\varsigma_i$, where $i = 1, ..., N$. Then, the approximation of the states $x_{K+1}(t)$ and controls $u_K(t)$ over the finite element $i$ of length $[\varsigma_i, \varsigma_{i+1}]$ (see Figure 6.8) given by the Legendre polynomials is

$$\vec{x}_{K+1}(t) = \sum_{j=0}^{K} \vec{x}_{ij}\phi_j(t), \text{ where } \phi_j(t) = \prod_{k=0,j}^{K} \frac{t - t_{ik}}{t_{ij} - t_{ik}} \text{ and } i = 1, ..., N, \tag{6.15}$$

$$\vec{u}_K(t) = \sum_{j=1}^{K} \vec{u}_{ij}\theta_j(t), \text{ where } \theta_j(t) = \prod_{k=1,j}^{K} \frac{t - t_{ik}}{t_{ij} - t_{ik}} \text{ and } i = 1, ..., N, \tag{6.16}$$

where $K$ is the number of collocation points, $\vec{x}_{ij}$ and $\vec{u}_{ij}$ are the sought state and control coefficients at time $t_{ij}$, respectively, and $\phi_j(t)$ and $\theta_j(t)$ are polynomials of order $K$. In this notation, $k = 0, j$ means that $k$ starts from 0 and does not take the current value of $j$. Note that while $\vec{x}_{K+1}(t)$ is a polynomial of order $K+1$, $\vec{u}_K(t)$ has order $K$. The difference in order is due to the fact that, in each finite element, the state coefficients are defined at the $K$ collocation points plus the initial condition, while the controls have only coefficients at the $K$ collocation points.

The connection between the DAE and the algebraic system is given by the so-called *residual equations*. If the polynomials $\phi_j(t)$ and $\theta_j(t)$ are defined in such a way that they are normalised over each finite element, the residual equations can then be stated as

$$\begin{aligned} \Delta\varsigma_i \vec{r}(t_{ik}) &= \sum_{j=0}^{K} \vec{x}_{ij}\dot{\phi}(\tau_k) - \Delta\varsigma_i \vec{F}(t_{ik}, \vec{x}_{ik}, \vec{u}_{ik}), \\ & \quad i = 1, ..., N, \ k = 1, ..., K, \end{aligned} \tag{6.17}$$

where $\vec{r}$ is the residual, $\tau$ the normalised time over the finite element $i$ (with $\tau\epsilon[0, 1]$), $\dot{\phi}(\tau_k) = d\phi_j/d\tau$, and $\vec{F}$ is the function on the right hand side of the differential equation $\dot{\vec{x}} = \vec{F}(\vec{x}, \vec{u}, t)$. The relation between the absolute time $t$ and the relative time $\tau$ is given by $t_{ik} = \varsigma_i + \Delta\varsigma_i\tau_k$. Note that in the more general formulation the element lengths $\Delta\varsigma_i$ are used as optimisation variables along with $\vec{x}_{ij}$ and $\vec{u}_{ij}$. This

additional degree of freedom is very important to find potential discontinuities in the optimal profile of control variables and to reach the desired degree of accuracy.

Another important element of this approach is that, while the control variables are allowed to display discontinuities, the continuity of state variables at the element boundaries (that is, at $\tau = 0$ and $\tau = 1$) has to be imposed. This is done by writing

$$\vec{x}^i_{K+1}(0) = \vec{x}^{i-1}_{K+1}(\varsigma_i),\ i = 2, ..., N, \tag{6.18}$$

which can be also written as

$$\vec{x}_{i0} = \sum_{j=0}^{K} \vec{x}_{i-1,j}\phi_j(\tau = 1),\ i = 2, ..., N,\ j = 0, ..., K. \tag{6.19}$$

These equalities effectively extrapolate $\vec{x}^{i-1}_{K+1}$ at $\tau = 1$, thus specifying an accurate initial point for the next polynomial $\vec{x}^i_{K+1}$ at $\tau = 0$ and enforcing continuity.

As for the control variables, it was mentioned above that they do not require continuity. They are, nonetheless, bound at the collocation points by means of the residual equation. Their control boundaries can be enforced by

$$\vec{u}^i_L \ \leq\ \vec{u}^i_K(\tau = 0) \ \leq\ \vec{u}^i_U, \tag{6.20}$$

$$\vec{u}^i_L \ \leq\ \vec{u}^i_K(\tau = 1) \ \leq\ \vec{u}^i_U, \tag{6.21}$$

where $\vec{u}^i_L$ and $\vec{u}^i_U$ are the lower and upper boundaries at element $i$, respectively. As the coefficients of the control variables are only defined at collocation points, the values of $\vec{u}^i_K(\tau = 0)$ and $\vec{u}^i_K(\tau = 1)$ have to be determined through extrapolation, as follows

$$\vec{u}^i_K(\tau = 0) \ =\ \sum_{j=1}^{K} \vec{u}_{ij}\theta_j(\tau = 0),\ i = 1, ..., N \tag{6.22}$$

$$\vec{u}^i_K(\tau = 1) \ =\ \sum_{j=1}^{K} \vec{u}_{ij}\theta_j(\tau = 1),\ i = 1, ..., N. \tag{6.23}$$

At this stage, the problem posed by equations 6.3 to 6.8 can be reformulated within the framework of orthogonal collocation as

$$\min_{\vec{x}_{ij},\vec{u}_{ij},\Delta\varsigma_i} J = \sum_{i=1}^{N}\sum_{j=1}^{K} w_{ij}\mathcal{L}(\vec{x}_{ij},\vec{u}_{ij},\Delta\varsigma_i) + \Phi(\vec{x}_f), \tag{6.24}$$

subject to

$$\vec{x}_{10} - \vec{x}_0 = \vec{0}, \tag{6.25}$$

$$\Delta\varsigma_i\dot{\vec{r}}_{ij} = \dot{\vec{x}}_{K+1}(\tau_j) - \Delta\varsigma_i\vec{F}(\vec{x}_{ij},\vec{u}_{ij}) = \vec{0}, \tag{6.26}$$

$$i = 1,...,N,\ j = 1,...,K,$$

$$\vec{x}_{i0} - \vec{x}^{i-1}_{K+1}(\tau = 1) = \vec{0}, \tag{6.27}$$

$$i = 2,...,N,$$

$$\vec{x}_f - \vec{x}^{N}_{K+1}(\varsigma_{N+1}) = \vec{0}, \tag{6.28}$$

$$\vec{u}^i_L \le \vec{u}^i_K(\tau = 0) \le \vec{u}^i_U, \tag{6.29}$$

$$i = 1,...,N,$$

$$\vec{u}^i_L \le \vec{u}^i_K(\tau = 1) \le \vec{u}^i_U, \tag{6.30}$$

$$i = 1,...,N,$$

$$\Delta\varsigma^L_i \le \Delta\varsigma_i \le \Delta\varsigma^U_i, \tag{6.31}$$

$$i = 1,...,N,$$

$$\vec{g}(\vec{x}_{ij},\vec{u}_{ij},\Delta\varsigma_i) = \vec{0}, \tag{6.32}$$

$$\vec{h}(\vec{x}_f) \le \vec{0}, \tag{6.33}$$

$$\vec{x}^L_{ij} \le \vec{x}_{K+1}(\tau_j) \le \vec{x}^U_{ij}, \tag{6.34}$$

$$i = 1,...,N,\ j = 0,...,K,$$

$$\vec{u}^L_{ij} \le \vec{u}_K(\tau_j) \le \vec{u}^U_{ij}, \tag{6.35}$$

$$i = 1,...,N,\ j = 1,...,K,$$

$$\sum_{i=1}^{N}\Delta\varsigma_i = t_f, \tag{6.36}$$

where $w_{ij}$ is the positive quadrature weight. Equation 6.24 is the optimisation criterion, 6.25 the initial condition of the system (if present), 6.26 the residual equation whose elements are forced to be zero, 6.27 the states continuity constraint, 6.28 the final condition of the system (if present), 6.29 and 6.30 the control boundary constraints at the element boundaries, 6.31 the boundary constraints for element lengths, 6.32 the path equality constraints (active along the entire path if present), 6.33 the path inequality constraints (active at terminal point if present), 6.34 the state boundaries, 6.35 the control boundaries at collocation points, and 6.36 the total time constraint.

Note that state variables, control variables, and element lengths are all used as optimisation variables in this formulation. This NLP problem can be solved by large nonlinear programming solvers.

### 6.6.2 Problem formulation for a generic ATAD system

According to the above formulation, the minimisation of the energy requirement of a generic ATAD system can be formulated as

$$\min_{\vec{x}_{ij},\vec{u}_{ij},\Delta\varsigma_i} E_m = \sum_{i=1}^{N}\sum_{j=1}^{K} \frac{E(\vec{u}_{ij}, t_{ij})}{m_{in}}, \tag{6.37}$$

subject to

$$\Delta\varsigma_i \vec{r}_{ij} = \dot{\vec{x}}_{K+1}(\tau_j) - \Delta\varsigma_i \vec{F}(\vec{x}_{ij}, \vec{u}_{ij}) = \vec{0}, \tag{6.38}$$

$$i = 1, ..., N,\ j = 1, ..., K,$$

$$\vec{x}_{i0} - \vec{x}^{i-1}_{K+1}(\tau = 1) = \vec{0}, \tag{6.39}$$

$$i = 2, ..., N,$$

$$\vec{x}_{10} - \vec{x}^{N}_{K+1}(\varsigma_{N+1}) = \vec{0}, \tag{6.40}$$

$$\vec{u}^i_L \leq \vec{u}^i_K(\tau = 0) \leq \vec{u}^i_U, \tag{6.41}$$

$$i = 1, ..., N,$$

$$\vec{u}^i_L \leq \vec{u}^i_K(\tau = 1) \leq \vec{u}^i_U, \tag{6.42}$$

$$i = 1, ..., N,$$

$$\Delta\varsigma^L_i \leq \Delta\varsigma_i \leq \Delta\varsigma^U_i, \tag{6.43}$$

$$i = 1, ..., N, 0.38 - r_{VS}(t_f) \leq 0,$$

$$1 - L(t_f) \leq 0, \tag{6.44}$$

$$\vec{x}^L_{ij} \leq \vec{x}_{K+1}(\tau_j) \leq \vec{x}^U_{ij}, \tag{6.45}$$

$$i = 1, ..., N,\ j = 0, ..., K,$$

$$\vec{u}^L_{ij} \leq \vec{u}_K(\tau_j) \leq \vec{u}^U_{ij}, \tag{6.46}$$

$$i = 1, ..., N,\ j = 1, ..., K,$$

$$\sum_{i=1}^{N} \Delta\varsigma_i = t_f, \tag{6.47}$$

where 6.37 states the optimisation criterion, 6.38 the residual constraint, 6.39 the states continuity constraint, 6.40 the states periodicity constraint, 6.41 and 6.42 the control boundary constraints at the element boundaries, 6.43 the boundary constraint for element lengths, 6.44 the stabilisation path constraint (active at terminal point), 6.44 the pasteurisation path constraint (also active at terminal point), 6.45 and 6.46 the states and control boundary constraint, respectively, and 6.47 the total time constraint.

An important difference between this formulation and the previous one is that no constraints are present for the initial and final conditions of the system. Nonetheless,

there is a periodicity constraint (Equation 6.40) that forces the equality between initial and final conditions, which are not fixed beforehand. What determines the particular initial and final condition for any given run is the control variable. This is due to the fact that the state variables are derived from the control variables, as has been seen in previous sections.

There is also no equality path constraints, as we saw in the case of the continuous formulation for the sequential approach (see equations 6.9 to 6.14).

Another important point in the framework of the simultaneous approach is that integrals in the continuous domain are generally calculated here following a Gauss quadrature. In the above formulation, two integrals were involved in the continuous problem: the energy requirement $E_m$ and the pasteurisation lethality $L$. These two magnitudes have now to be specified in terms of a Gauss quadrature.

To this end, we choose here a two-point Gauss quadrature. In the case of the energy requirement, the formula for the quadrature over a time period $[a, b]$ is

$$E_i(a,b) = \frac{b-a}{2} \sum_{i=1}^{2} P(\frac{b-a}{2} t_i + \frac{a+b}{2}),\ t_i = \pm \frac{1}{\sqrt{3}}, \tag{6.48}$$

where, in the case of CS1, $P(t) = 6q_a(t) + 28$, and $q_a$ can be evaluated at any given time $t$ using the Lagrange polynomial. Thus, the formula to determine the energy requirement over the entire time period $[\varsigma_1, \varsigma_{N+1}]$ is

$$E_m = \frac{1}{m_{in}} \sum_{i=1}^{N} E_i(\varsigma_i, \varsigma_{i+1}). \tag{6.49}$$

Similarly, the pasteurisation lethality over a certain period $[a, b]$ can be specified through a two-point Gauss quadrature following

$$L_i(a,b) = \frac{b-a}{2} \sum_{i=1}^{2} D(\frac{b-a}{2} t_i + \frac{a+b}{2}),\ t_i = \pm \frac{1}{\sqrt{3}}, \tag{6.50}$$

where $D = 50070000/10^{0.14T}$ is the contact time, and the temperature $T(t)$ can be computed for any time instant via the Legendre polynomial. To calculate the lethality over the whole period of interest $[\varsigma_1, \varsigma_{N+1}]$ we write then

$$L = \sum_{i=1}^{N} L_i(\varsigma_i, \varsigma_{i+1}). \tag{6.51}$$

In some instances, the Gauss quadrature may present difficulties when attempting to solve the problem. This is because sometimes the Legendre polynomials behave in an unexpected oscillatory manner. In such cases, it is possible to substitute the Gauss quadrature through the less accurate trapezoidal rule.

### 6.6.3 Simulation studies

The implementation of the optimisation problem posed by equations 6.24 to 6.36 is often very challenging. Thus, it is important to perform the implementation in a step-by-step manner that will prevent potential errors from going unnoticed. A way to do this is to implement first a simulation problem, instead of implementing directly the optimisation problem. By implementing a simulation problem, it can be easily detected whether or not solutions display infeasible behaviour arising from hidden implementation errors. But implementation errors are not the only source of infeasible solutions in the orthogonal collocation framework. Some of the parameters of the formalism itself have a strong influence on the accuracy of the solution. These are the number of finite elements $N$ and the number of collocation points $K$. Apart from these parameters, the length of the finite elements $\Delta\varsigma_i$ also plays a critical role in this regard.

Because no reference was found in the literature as for how simulations should be carried out within the framework of orthogonal collocation, we chose to formulate the simulation as a standard optimisation problem (see equations 6.24 to 6.36) in which the objective functional is the summation of the absolute values of the residual elements $r_{ij}$:

$$\min_{\vec{x}_{ij}, \vec{u}_{ij}, \Delta\varsigma_i} \sum_{i=1}^{N} \sum_{j=1}^{K} |r_{ij}|, \tag{6.52}$$

subject to equations 6.25 to 6.36.

The influence of $N$ and $K$ on the accuracy of the solutions can be easily seen

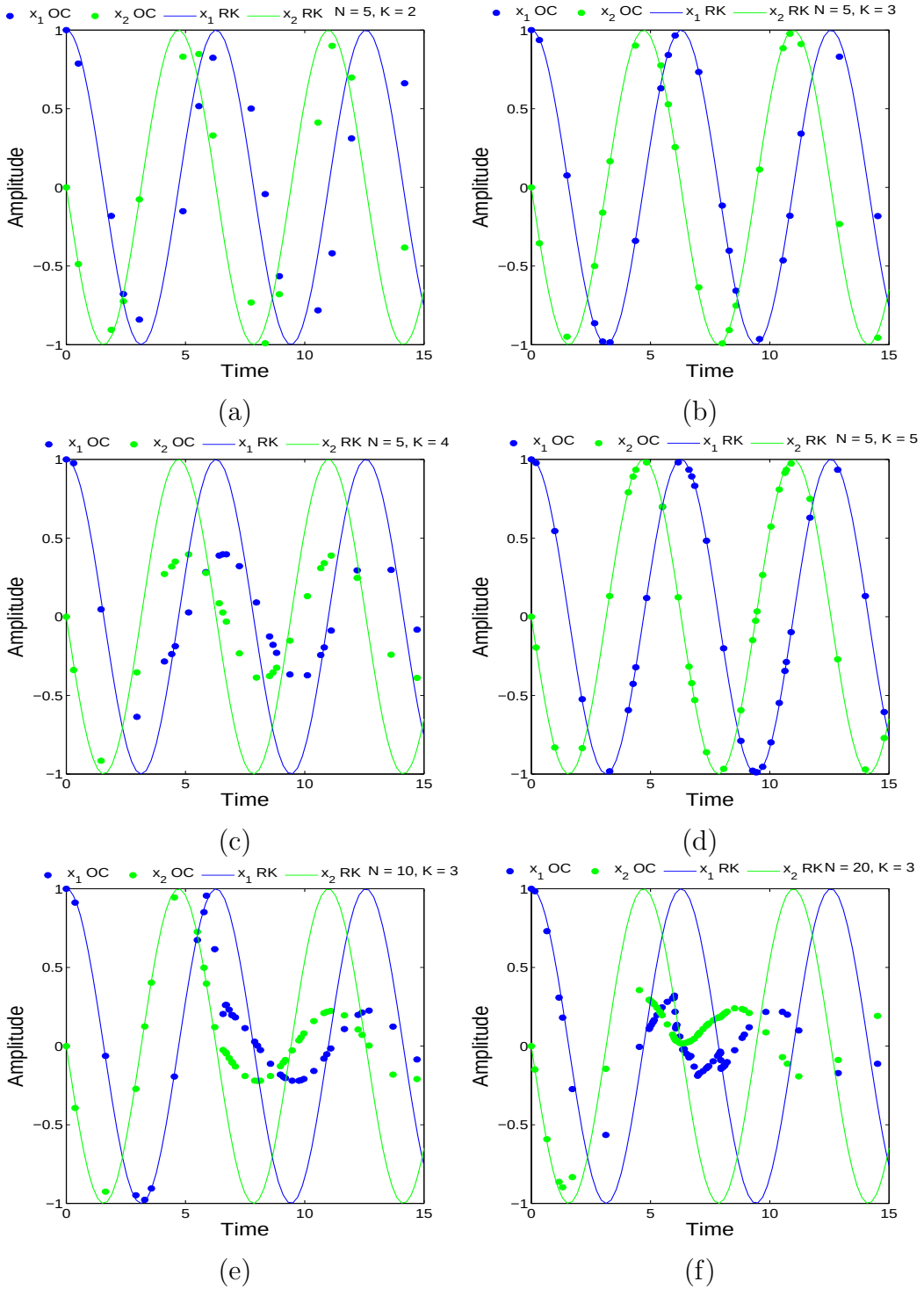


Figure 6.9: Effect of number of finite elements $N$ and number of collocation points $K$ on the solution of a two-dimensional harmonic oscillator: (a) $N = 5$ and $K = 2$, (b) $N = 5$ and $K = 3$, (c) $N = 5$ and $K = 4$, (d) $N = 5$ and $K = 5$, (e) $N = 10$ and $K = 3$, and (f) $N = 20$ and $K = 3$. Solid lines represent the "exact" solution obtained via Runge Kutta (RK) integration, while dots represent the solution obtained through orthogonal collocation (OC).

through a simple example. Figure 6.9 shows the effect of these parameters on the solution of a two-dimensional harmonic oscillator. This example illustrates well how most parameter combinations result in poor solutions, whereas some others (often few) result in reasonably accurate solutions. Thus, careful attention has to be given to the tuning of the parameters prior to the implementation of the optimisation problem. Otherwise, good[4] solutions may be obtained that are in fact spurious and even completely infeasible. This fine tuning of the algorithm and its parameters is generally performed manually for each individual implementation. There is, however, a more systematic, though rather arduous, way of determining the parameter values (see Biegler (2010)). In our work, we shall choose them manually.

In the simulation of the CS1 system, the Radau roots were chosen instead of the Legendre roots. To manually fine-tune the value of the parameters $N$ and $K$, a number of simulations were carried out for different parameter values. Figure 6.10 shows the simulation of the CS1 system for $N = 3$ and $K = 5$. It can be clearly seen that the match between the exact solution and the orthogonal collocation is fairly poor for this particular parameter combination.

Figure 6.11 displays the simulation of CS1 for the parameter combination $N = 1$ and $K = 5$. The match is still not complete but it is far more accurate. It was thus found that, for our particular problem, the simulations converged to the exact solution for $N = 1$ and $K \geq 4$. This approach (that is, fixing $N$ and achieving convergence by increasing the degree $K$ of the Radau polynomials) and its convergence properties have been recently studied by Garg et al. (2011). The opposite approach (fixing $K$ and increasing $N$) and its convergence properties have also been studied (Kameswaran and Biegler, 2008).

We found that Radau roots yield more accurate results than Legendre roots.[5] Our hypothesis is that this may be the case because the element boundaries are also collocation points. It was also found that Radau roots prevent the oscillatory behaviour often found in the solutions derived from Legendre roots. Again, the reason is likely to be the fact that element boundaries are also collocation points,

[4]Here, the word "good" is meant in terms of the objective functional.

[5]In a private communication, Prof. Lorenz T. Biegler (Carnegie Mellon University, US) confirmed that also according to his experience the Radau roots yield more accurate solutions.

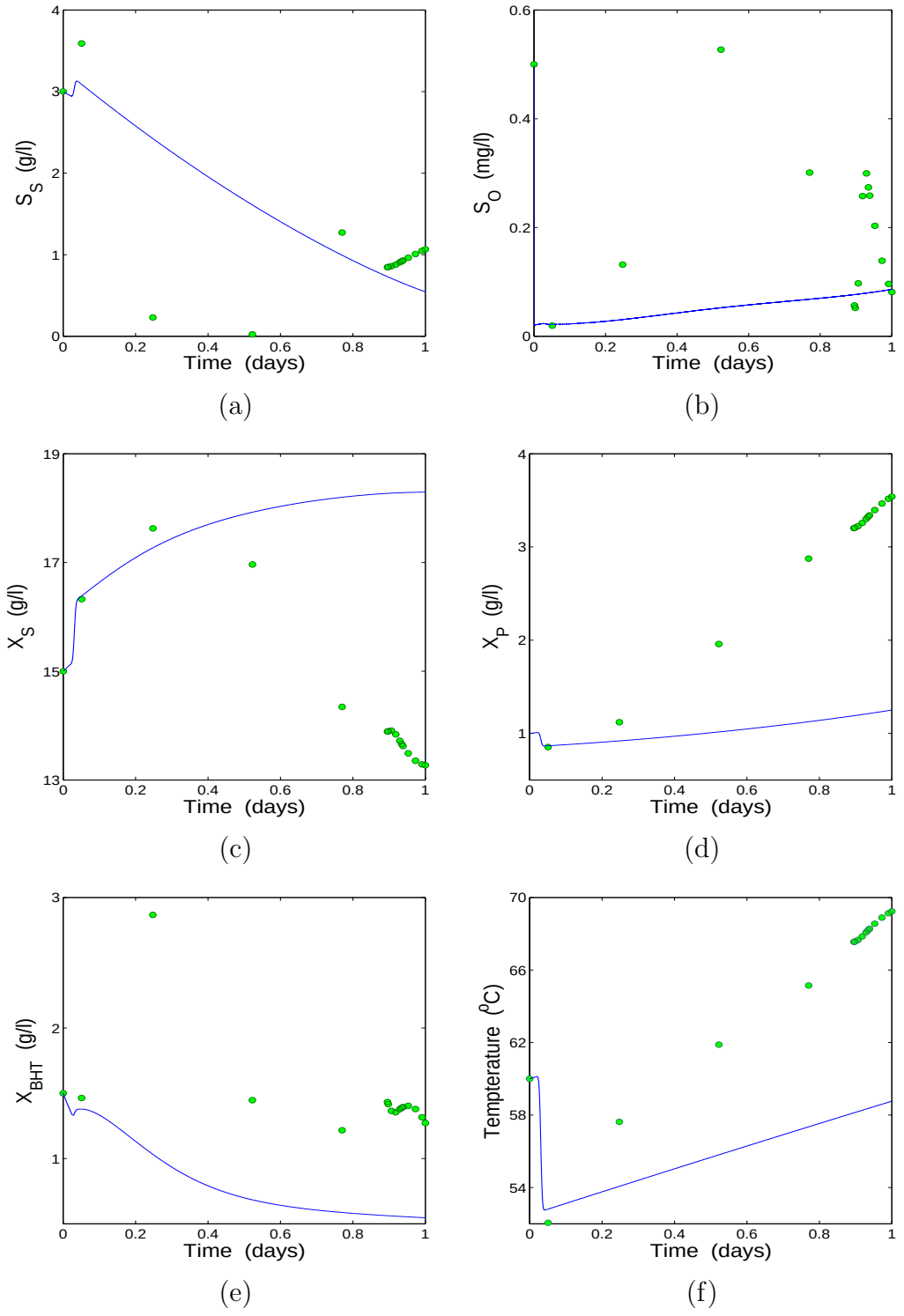


Figure 6.10: Simulation of CS1 via orthogonal collocation for $N = 3$ and $K = 5$: (a) readily biodegradable substrate, (b) DO, (c) slowly biodegradable substrate, (d) particulate products from decay, (e) thermophilic biomass, and (f) temperature. Solid lines represent the "exact" solution obtained via Runge Kutta integration, while dots represent the solution obtained through orthogonal collocation.

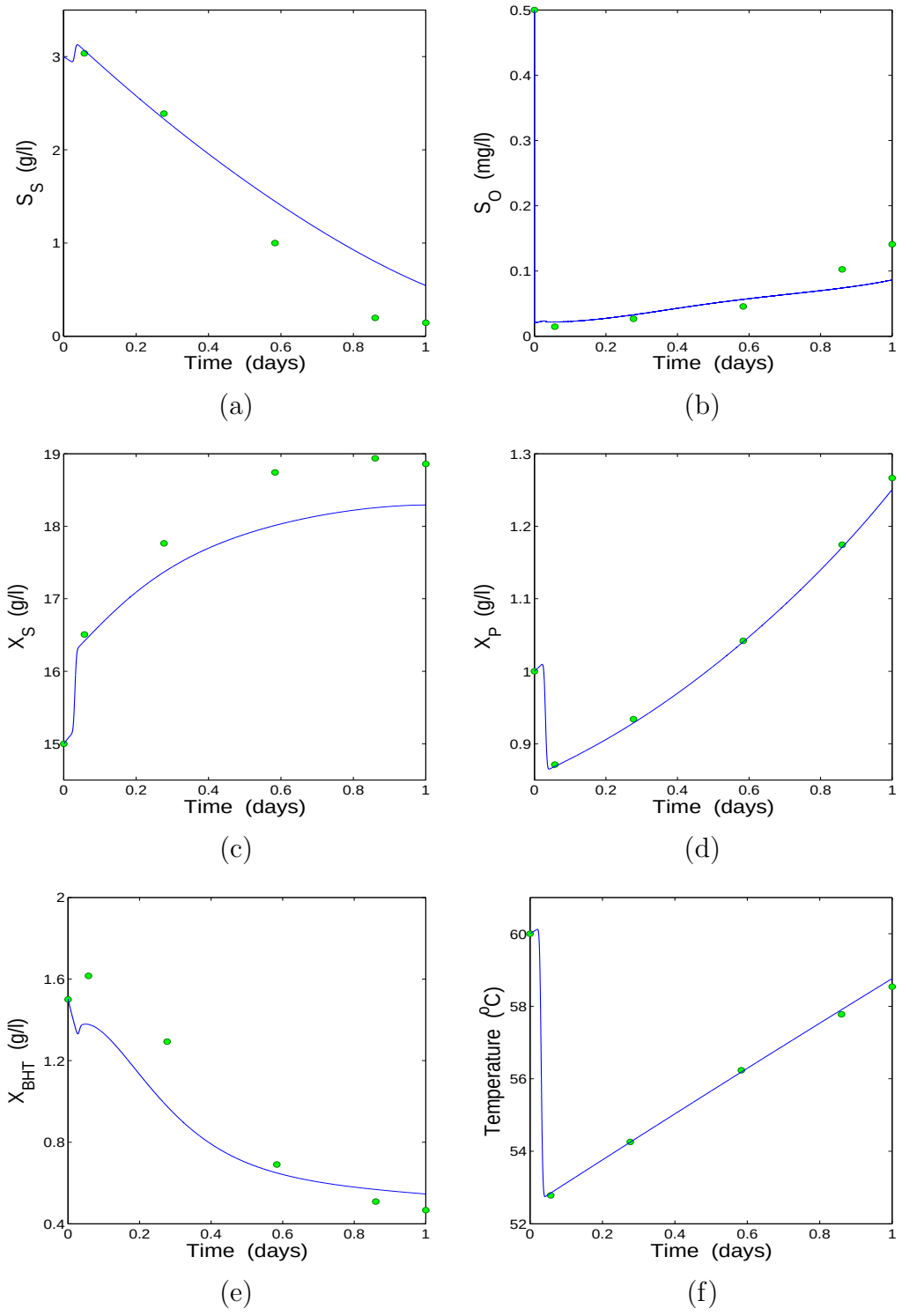


Figure 6.11: Simulation of CS1 via orthogonal collocation for $N = 1$ and $K = 5$: (a) readily biodegradable substrate, (b) DO, (c) slowly biodegradable substrate, (d) particulate products from decay, (e) thermophilic biomass, and (f) temperature. Solid lines represent the "exact" solution obtained via Runge Kutta integration, while dots represent the solution obtained through orthogonal collocation.

which forces higher accuracy on the element boundaries.

The optimisation problem posed by equations 6.37 to 6.47 was implemented for the CS1 system. The problem was solved with the eSS algorithm. So far, no positive results have been obtained. Optimal solutions are inaccurate and infeasible. This problem has been surmounted by including an additional accuracy constraint, which forces the summation of the absolute values of the residual elements to be smaller than a certain threshold value $\epsilon$ which has to be carefully chosen. The constraint is given by

$$\sum_{i=1}^{N}\sum_{j=1}^{K}|r_{ij}| - \epsilon \leq 0, \tag{6.53}$$

where $\epsilon$ is a threshold value that has to be chosen very carefully.

While this constraint does improve convergence to the exact solution, positive solutions have not yet been obtained. The introduction of this accuracy constraint is in line with the suggestion of Srinivasan et al. (1995).

It should be also noted that the two-point Gauss quadrature was partly responsible for the infeasible results, due to the fact that it makes use of the Legendre or Radau polynomials to approximate the aeration flowrate and the temperature profiles, even when these profiles display infeasible dynamics (such as adopting negative values). However, after substituting the Gauss quadrature with the trapezoidal rule, infeasible results were still obtained. This showed that there are other sources of error, yet undiscovered.

Due to time restrictions, the implementation of the simultaneous approach had to be interrupted and could not be further researched. However, the work performed to date lays the foundation for the optimisation (via orthogonal collocation) of ATAD systems in general, and their structural optimisation in particular. For the latter task, the approach investigated in this section shall prove very useful, due to its superior computational efficiency.

# Chapter 7

# Conclusions

The aim of the present investigation was to minimise the energy requirement of ATAD systems while complying with treatment objectives. To accomplish this aim, a number of tasks had first to be tackled. These include the development of a dynamic model of the ATAD reaction, the quantification of ATAD's treatment objectives, and the selection of control variables. Another important aspect of this research are the simulation studies that shed new light on the inner workings of the ATAD process and their implications. Following are the main conclusions pertaining to each of these facets of the investigation.

## 7.1 Modeling

In Chapter 4, two dynamic ATAD models were developed: ATM1, a model with 10 variables including nine mass balances and one energy balance, and ATM2, a reduced version of ATM1 incorporating three mass balances and one energy balance.

Even though the main model ATM1 was derived from models previously found in the literature, its energy balance contains an important qualitative modification that significantly simplifies the model: the gas phase was eliminated. This is based on the assumption that heat transfer between the gas and liquid phases takes place instantaneously. This assumption can be made on the grounds of two observations explained in section 4.2.2.

A novel and unique feature of the models presented herein is the quantification

of the treatment objectives (that is, stabilisation and pasteurisation), discussed in section 4.4. The authors of other models have not explicitly discussed the way to determine the degree of stabilisation or VS reduction, which has been discussed in the present work. As for the degree of pasteurisation or lethality, it was quantified for the first time in field of wastewater treatment in general and ATAD in particular. The importance of this novel feature cannot be overstated, for it allows the computation of the stabilisation and pasteurisation times. Moreover, it allows the determination of the reaction time, that is, the minimum time needed to satisfy legal requirements. This capability is unique to the models developed herein.

The quantification of the specific energy requirement and plant capacity was discussed in section 4.5. In this context, it is worth restating that the specific magnitude often used for this purpose by other authors is the volumetric one. However, we have given grounds that favour the use of the gravimetric magnitude as a more adequate measure for energy use. Through the computation of the reaction time mentioned above, the models presented herein have the unique capability to determine the minimum energy requirement of any given ATAD system.

Quantification of treatment objectives and energy requirement and plant capacity were central to the present work, and paved the way for the optimisation of ATAD systems.

## 7.2 Simulation studies

In Chapter 5, a number of numerical analyses were carried out, including simulation studies, an asymptotic analysis, a sensitivity analysis, and a model assessment and parameter estimation.

### Start-up and steady state simulations

The simulation studies in section 5.2 showed a sample of representative start-up and steady state simulations for the two case study plants under different operating conditions. In both cases, the systems behaved and responded to changes in operating conditions as expected from full-scale plant experience.

An important qualitative observation was made from the simulations that is in accord with experimental evidence: higher ambient temperatures and higher influent VS concentrations result in higher degrees of stabilisation and pasteurisation. In this regard, the influent VS concentration had a stronger influence than ambient temperature. The effect of ambient temperature and influent VS concentration on the degrees of stabilisation and pasteurisation could be explained as being due to an increase of bacterial activity: increasing ambient temperature and the influent VS concentration increased in turn the OUR of the microorganisms (though the combination of the effects was found to be asymmetrical).

It was shown that, opposed to a previously held assumption, single-stage systems can achieve the same degree of pasteurisation as multi-stage systems. It was also shown that, contrary to another previously held assumption, systems can operate with influent VS concentrations lower than 25 g/l, but only as long as ambient temperature is not too low.

## Asymptotic analysis

In section 5.3, an asymptotic analysis of a particular solution of the ATM1 model was carried out. This particular solution was chosen because it displays a qualitative structure which we believe to be general under most operating conditions and model inputs. In this way, the analysis provides an insight into the inner workings of the reaction. The solution is divided into a set of regions in which the reaction is limited by different factors. In the first region, the reaction rate is limited by the availability of oxygen and it lasts until the readily biodegradable substrate $S_S$ is depleted. After $S_S$ is depleted, dissolved oxygen becomes more plentiful and the reaction becomes substrate-limited, marking the beginning of the second region. During this period, the reaction rate is also limited by the hydrolysis rate. It is mainly over this time period that endogenous respiration takes place and sludge is stabilised. The concentration of $S_S$ does not increase over time because it is consumed faster by the biomass than it is generated via hydrolysis. After slowly biodegradable substrate $X_S$ is depleted, which marks the beginning of the next region, endogenous decay increases markedly. This solution and its structure can

explain the qualitative behaviour of respirometric curves typical of ATAD systems.

## Sensitivity analysis

In section 5.4, a global sensitivity analysis was performed to study the effect of all possible model inputs on the energy requirement, plant capacity, and reaction time.

The first part of the analysis concerned the effect of all model parameters. It was found that reactor volume, initial system enthalpy, aeration flowrate, conversion factor between COD and VS, and initial concentration of slowly biodegradable substrate were the most significant parameters. Overall, it was found that the type of correlations displayed by these parameters are intuitive, logical, and consistent with reported experimental evidence. Of special significance is the positive correlation between reactor volume and energy requirement. This correlation has implications that should be of special interest to manufacturers.

The second part of the sensitivity analysis concerned exclusively the effect of the operating conditions on model outputs. The considered operating conditions were the reaction time, loading time, aeration flowrate, influent temperature, and the amount of volume replaced. The three former correlated in a positive manner with the energy requirement, while the volume replaced did so in a negative manner. The influent sludge temperature displayed no significant effect on none of the model outputs. Most of these correlations could also be explained in an intuitive manner and were consistent with other studies. It was also found that in most scenarios the reaction was limited by stabilisation. This insight suggests that the ATAD reaction is generally limited by the stabilisation process. But most importantly, it was found that the energy requirement and plant capacity are inversely proportional. This correlation could be attributed to the very definition of these magnitudes. Highly significant is the generality of this correlation: as the same (or similar) definitions apply to energy requirement and plant capacity of most wastewater and sludge treatment processes, this inverse proportionality should also hold for them. Indeed, other authors have found that such relationship applies to other treatment processes. While it is not yet clear what the full implications of this relation are, more work should be carried out to unearth such implications and realise their potential.

### Model assessment and parameter estimation

In this section, the ATM1 model was assessed and the value of the reactor-specific parameter $K_a$ was estimated for the two case study plants. In both cases, a reasonable qualitative agreement was found between data and simulation, though there is room for improvement concerning the quantitative agreement.

It should be recalled that, unlike the ASM model family, all ATAD models (whether those presented here or elsewhere) are at a relatively early stage of development. Therefore, the process of model validation should be carried on. To this end, more quantity and higher quality data, at present extremely scarce, should be published.

## 7.3 Optimisation

### Sequential approach

The modeling and simulation work carried out in chapters 4 and 5 paved the way for the optimisation of ATAD systems by developing the ATM1 model, quantifying treatment objectives and energy requirement, and identifying the best choices as control variables.

All these elements converged in section 6.3 to formulate the minimisation problem of the energy requirement for a generic ATAD system following the direct sequential CVP approach.

Next, sections 6.4 and 6.5 presented the results of this optimisation problem for the CS1 and CS2 systems. After optimisation, the optimal energy requirement of CS1 and CS2 displayed a reduction of 23 and 18%, respectively. In the case of CS1, the optimal control consisted of a lower reaction time (located at lower boundary) and higher aeration flowrates, when compared to usual plant operation. The qualitative behaviour of the aeration profile is a gradual decrease starting at higher values and ending at the lower boundary. As for the solution of CS2, the optimal controls were made of a polymer concentration of 6.7 g/l (influent VS concentration of 21.7 g/l), a reaction time of 1.08 days, and overall lower aeration rates when compared

to conventional plant operation. However, a better solution was found for CS2 by assuming a pre-dewatering stage resulting in a 50% reduction of influent sludge with double VS concentration (with no polymer addition), which was treated in the first-stage reactor alone. The optimal energy requirement displayed a reduction of 42%. But more importantly, one entire reactor was freed, thus nearly doubling plant capacity. The optimal reaction time was 1.09 day. The qualitative behaviour of the optimal aeration profile was once more that of a decreasing line starting at higher values and ending at the lower boundary.

It is highly significant that in most optimisation results this kind of behaviour was found for the optimal aeration profile. The biological plausibility of this solution has been pointed out before. Experimental work should be carried out in order to validate this result. It should be recalled that most ATAD plants make use of invariable aeration during the reaction.

It should be pointed out that the objective functional was found to be highly multimodal. The global optimality of the solutions can thus not be guaranteed. Apart from this, the quality of the solutions was strongly dependent on control vector parameterization.

## Simultaneous approach

Finally, section 6.6 provided a tentative framework for the optimisation of ATAD systems through the simultaneous approach. The problem of the minimisation of the energy requirement for a generic ATAD system was formulated within the framework of orthogonal collocation. An approach was proposed to generate simulations via orthogonal collocation: the minimisation of the summation of the absolute values of the residual elements. This approach was tested and used to simulate the behaviour of the CS1 system. It could then be seen that some of the parameters of the formalism ($N$ and $K$) had a significant effect on the accuracy of the solution. It was found that the CS1 system could be simulated to a satisfactory degree of accuracy when choosing $N = 1$ and $K \geq 4$. When the optimisation problem was implemented, innacurate and even infeasible solutions were obtained. This problem was surmounted by including an additional accuracy constraint. It should also be

mentioned that the Radau polynomials yielded more accurate results than the Legendre polynomials. The two-point Gauss quadrature was partly responsible for the generation of infeasible results and it was replaced with the trapezoidal rule.

Though optimisation results were not presented in this section, it provides a platform for further development. This tentative framework for orthogonal collocation and the insights provided herein shall aid in the optimisation of ATAD systems in general and their structural optimisation in particular. For the latter task, this approach shall prove very useful, given its superior computational efficiency.

As a concluding remark, it should be noted that optimisation is still relatively rare in wastewater engineering. Given the high, rising cost of wastewater treatment, optimisation should become the norm when it comes to design and operation of wastewater treatment plants. We hope that the present work will contribute momentum to this line of research.

For a list of the publications that emanated from this research, see Appendix.

## 7.4 Future work

An open and ongoing task is that of model validation. Future efforts will have to be devoted to further validate and assess existing ATAD models. As pointed out before, all ATAD models existing at present are at an early stage of development (compared, for example, to the Activated Sludge Model family). There is still considerable uncertainty with regard to many of the model parameters. Thus, these models are only to be regarded as platforms for yet further development. Data of ATAD systems are currently very scarce. Higher quality and more quantity of data should be published if model validation is to be carried out to a satisfactory extent.

Another difficulty associated with modeling of ATAD systems is the fact that VS concentration (i.e., the indicator of sludge stabilisation) can only be measured at the end of the batch. Moreover, the measurement cannot be made online and takes a considerable time to be completed. What is more, this kind of measurement is often subject to a large margin of error. For all these reasons, it is being suggested here that the VS concentration is not a satisfactory indicator of sludge stabilisation. We

propose that an alternative indicator is adopted that can be measured online and to a reasonable degree of accuracy. Some plants measure the oxidation reduction potential (ORP) to determine the level of bacterial activity; this kind of indicator may go in the right direction. This would allow the development of new ATAD models that would be more accurate and it would aid in the task of model validation. Furthermore, for purposes of process optimisation it is important that the degree of stabilisation is measured online, so that the legal requirements are not exceeded (as is generally the case in current practice), for this is generally associated with an increase of energy consumption.

An interesting theoretical exercise would be to regard ATAD as a continuous process. In this way, the steady state of the system could be studied, simulated, and optimised. A continuous ATAD system may result in lower energy requirement and higher plant capacity, when compared to discontinuous, semi-batch systems. The reason for this is that a continuous system would not have the fluctuations of the operating conditions that appear in discontinuous systems, and this could have a positive effect on the stabilisation process (which is generally limiting). As for the pasteurisation of the sludge, the hot effluent could be stored in an insulated stirred tank long enough to achieve legal requirements (while cooling down).

Experiments have shown that anaerobic species of bacteria as well as methanogenic activity can be present in ATAD reactors (Ugwuanyi et al., 2005; Piterina et al., 2008). This raises the question of whether anaerobic species contribute to sludge stabilisation to a significant extent. If so, future models would then have to take into account anaerobic microorganisms and their metabolism. More work is needed to answer this open question.

Yet another important open task is the validation of the optimisation results presented in this work. In qualitative terms, it was found that a variable aeration profile starting at higher values and ending at a value close to zero minimises the energy requirement. One of our collaborators has expressed willingness to implement and validate these results in a pilot plant.

In future implementations of the optimisation problem posed in this work, it would be interesting to consider the reactor volume as state variable as well as the

loading time as control variable. As it was found that reactor volume has a significant influence on the energy requirement, it would be also interesting to investigate the optimal topology of ATAD systems, especially that of multi-stage systems.

Perhaps the most challenging open task is the structural optimisation of ATAD systems. For this purpose, the tentative framework of orthogonal collocation presented in this study could serve as a starting point.

It should be noted that the present study has been restricted to the optimisation of the energy requirement of ATAD systems. That by no means excludes the possibility of other important and relevant problems. Such a problem is the maximisation of plant capacity. Given the rising population of many urban areas, the need to increase plant capacity is likely to become a matter of urgency sooner or later. It was found in this study that plant capacity is strongly influenced by operating conditions. It thus becomes a natural choice that plant capacity should be maximised through process optimisation in a similar problem as those posed and solved in this work. In doing so, no expensive structural changes would have to be made in order to cope with increased load. As for the importance of improvements in energy efficiency and plant capacity, it may be said that energy efficiency improvements are perceived to be more urgent in the short term, as the authorities have to pay electricity bills regularly. However, plant capacity improvements often become inevitable and urgent in the long term due to population growth and increased load; such improvements are often very expensive because they involve structural changes. This is where process optimisation can make a substantial difference by increasing plant capacity without expensive structural changes, thus leading to savings far more important than those achieved through energy efficiency optimisation in the short term.

Let us conclude by paying attention to the fact that most of the energy consumed by aerobic wastewater and sludge treatment processes (about 50%) is used for aeration. Most of these systems use air aeration with oxygen as electron acceptor. Air, however, contains about 80% of nitrogen gas (which is not a reactant) and less than 20% of oxygen. This means that these systems literally waste most of the aeration energy by injecting nitrogen into the sludge. For this reason, it is being suggested here that air is likely to be a bad choice as a gas to drive the reaction. Our

proposal is that pure oxygen could be used as an alternative to air. Or, perhaps, alternating air and pure oxygen in periods of low and high OUR, respectively. As it is well known that pure oxygen is expensive, a recycling system for the oxygen-rich exhaust gas could be set up. This would decrease the need for pure oxygen and its associated cost. A notable advantage of pure oxygen is that it has a much higher partial pressure and a higher saturation concentration of $\sim 40$ mg/l (Barnes et al., 1986). The higher saturation concentration would lead to significantly higher levels of dissolved oxygen and this in turn would accelerate the reaction, decrease the reaction time, and lower energy requirements. There would be, nonetheless, a trade off between the reduced cost through saved energy and the cost of pure oxygen. This trade off would have to be determined. It is known that the American manufacturer $m^2ttech$ has developed and commercializes an oxygen-driven ATAD system called UNOX®, but the available data on such systems is extremely scarce, and, in any case, these systems have not yet been optimised (Warakomski et al., 2007). This new, as yet unstarted, line of research could prove very promising. The investigation of the impact of using pure oxygen on the energy requirement and plant capacity of ATAD systems could also bear significance and implications for other wastewater and sludge treatment processes.

# Appendix

In the course of this investigation, the following articles have been published in specialist, peer-reviewed journals (the third article is still under review):

Rojas, J., Zhelev, T., and Bojarski, A. D. (2010) Modelling and sensitivity analysis of ATAD, *Computers and Chemical Engineering* **34**(5): 802–811.

Rojas, J., Zhelev, T. et al. (2010) Modeling of autothermal thermophilic aerobic digestion, *Mathematics-in-Industry Case Studies (MICS) Journal* **2**: 34–63.

Rojas, J. and Zhelev, T. Energy efficiency optimisation of wastewater treatment: study of ATAD, Submitted to *Computers and Chemical Engineering*.

The first publication deals with the ATM1 model developed in Chapter 4, steady state simulations discussed in Chapter 5 section 5.2, and the sensitivity analysis presented in section 5.4. The second publication was the product of our joint work with mathematicians from the University of Limerick and Oxford University, and it deals with the ATM2 model developed in Chapter 4 and with the asymptotic analysis of the ATM1 model presented in Chapter 5 section 5.3. The last article deals with the optimisation problem posed in Chapter 6 in terms of the direct sequential CVP approach which is solved for the CS1 and CS2 systems.

The following publication emanated from the early stages of the present investigation, but its content has not been included in this thesis:

Vaklieva-Bancheva, N., Kirilova, E., Zhelev, T., and Rojas, J. (2010). Modeling of energy integrated ATAD system, *Journal of International Scientific Publications: Materials, Methods & Technology* **4**(1): 220–233.

APPENDIX

It is devoted to heat integration of ATAD systems. The emphasis is in the minimisation of the thermal shock by recovering heat from the effluent sludge to pre-heat the influent sludge via sludge-sludge heat exchangers. At that stage of the investigation, we believed that temperature was a critical parameter and we had reasons to think that it would be favourable for the reaction to increase the overall temperature profile by pre-heating the influent sludge.

This work has also been presented at several international conferences where it was delivered in the form of either oral or poster presentations. The following articles correspond to the oral presentations:

Rojas, J., Zhelev, T., Vaklieva-Bancheva, N. (2008) Enhancing energy efficiency of wastewater treatment - Study of autothermal thermophilic aerobic digestion, *18th International Conference of Chemical and Process Engineering*, Prague, 24-28 August, pp. 1162–1163.

Rojas, J., Zhelev, T., Bojarski, A. (2009) Optimizing the energy efficiency of wastewater treatment - Study of autothermal thermophilic aerobic digestion, *3rd International Conference on Sustainable Energy & Environmental Protection*, Dublin, 12–15 August, pp. 357–361.

Rojas, J., Zhelev, T. et al. (2009) Improvement of energy efficiency for wastewater treatment, *70th European Study Group with Industry*, Limerick, Ireland, June 28 – July 3, pp. 107–140.

Zhelev, T. and Rojas, J. (2010) Efficient use of energy in wastewater treatment, *2nd International Symposium on Sustainable Chemical Product and Process Design*, Hangzhou, 9–12 May.

Rojas, J. and Zhelev, T. (2010) Taylor-made energy efficiency optimization of an ATAD plant, *23rd International Conference on Efficiency, Cost, Optimization, Simulation and Environmental Impact of Energy Systems*, Lausanne, 14–17 June, pp. 748–753.

Capon-Garcia, E., Rojas, J., Zhelev, T., Graells, M. (2010) Operation scheduling of batch autothermal thermophilic aerobic digestion processes, *20th European Symposium of Computer Aided Process Engineering*, Ischia, 6–9 June, pp. 1177–1182.

The following articles correspond to poster presentations:

Rojas, J., Zhelev, T., Vaklieva-Bancheva, N. (2008) On the improvement of energy efficiency of wastewater treatment - Case study: autothermal thermophilic aerobic digestion, *18th Irish Environmental Researcher's Colloquium*, Dundalk, 1–3 February, pp. 101–102.

Rojas, J., Zhelev, T. (2009) Maximizing the capacity of wastewater treatment - Study of autothermal thermophilic aerobic digestion, *Chemical Engineering Transactions* **18**: 881–886.

Rojas, J., Zhelev, T. (2009) Energy efficiency advancements in wastewater treatment – Study of autothermal thermophilic aerobic digestion, *19th European Symposium on Computer Aided Process Engineering*, Cracow, 14-17 June, pp. 1269–1273.

Zhelev, T., Vaklieva-Banchevab, N., Rojas, J., Pembroke, T. (2009) "Smelly" Pinch, *Computer Aided Chemical Engineering* **27**: 933–938.

Rojas, J., Zhelev, T., Graells, M. (2010) Energy efficiency optimization of wastewater treatment: study of ATAD, *20th European Symposium of Computer Aided Process Engineering*, Ischia, 6–9 June, pp. 967–972.

# Bibliography


Banga, J. R., Balsa-Canto, E. and Moles, C. G. (2003). Dynamic optimization of bioreactors: a review, *Proc. Ind. Natl. Sci. Acad.*, Vol. 69A, pp. 257–265.

Banga, J. R., Balsa-Canto, E., Moles, C. G. and Alonso, A. A. (2005). Dynamic optimization of bioprocesses: Efficient and robust numerical strategies, *Journal of Biotechnology* **117**: 407–419.

Barnes, D., Bliss, P. J., Gould, B. W. and Vallentine, H. R. (1986). *Water and Wastewater Engineering Systems*, Longman Scientific & Technical.

Batts, C. W., Burton, F. L. and Jone, M. (1993). Demand side management opportunities in the wastewater industry, *Proceedings of the 66th Annual Conference & Exposition*, Water Environment Federation.

Biegler, L. (1984). Solution of dynamic optimization problems by successive quadratic programming and orthogonal collocation, *Computers and Chemical Engineering* **8**: 243–248.

Biegler, L. T. (2007). An overview of simultaneous strategies for dynamic optimization, *Chemical Engineering and Processing* **46**: 1043–1053.

Biegler, L. T. (2010). *Nonlinear Programming: Concepts, Algorithms, and Applications to Chemical Processes*, SIAM-Society for Industrial and Applied Mathematics.

Biegler, L. T., Cervantes, A. M. and Wachter, M. A. (2002). Advances in sumultaneous strategies for dynamic process optimization, *Chemical Engineering Science* **57**: 575–593.

Blottner, F. G. (1990). Accurate navier-stokes results for the hypersonic flow over a spherical nosetip, *AIAA Journal of spacecraft and Rockets* **27**(2): 113–122.

Boehm, B. W. (1981). *Software engineering economics*, Prentice-Hall.

Bojarski, A. D. (2010). *Life cycle thinking and general modelling contribution to chemical process sustainable design and operation*, PhD thesis, Universitat Politectinca de Catalunya.

Bonvin, D., Palanki, S. and Srinivasan, B. (2003). Dynamic optimization of batch processes: I. characterization of the nominal solution, *Computers and Chemical Engineering* **27**: 1–26.

Burton, F. L. (1996). Water and wastewater industries: Characteristics and energy management opportunities, *Technical Report CR-10691*, Electric Power research Institute, St. Louis, MO.

Cervantes, A. and Biegler, L. T. (1998). Large-scale dae optimization using a simultaneous nlp formulation, *American Institute of Chemical Engineers Journal* **44**(5): 1038–1050.

Chiang, A. C. (1992). *Elements of dynamic optimisation*, McGraw-Hill, New York.

Chu, A. and Mavinic, D. S. (1998). The effects of macromolecular substrates and a metablic inhibitor on volatile fatty acid metabolism in thermophilic aerobic digestion, *Water Science Technology* **38**(55).

Cizniar, M., Salhi, D., Fikar, M. and Latifi, M. A. (2005). A matlab package for orthogonal collocations on finite elements in dynamic optimization, *15th Conference Process Control*, Strbske Pleso, Slovakia, pp. 058.1–058.7.

Crabb, J. W., Murdock, A. L. and Amenlunxen, R. E. (1975). A proposed mechanism of thermophily in facultative thermophiles, *Biochem. Biophys. Res. Commun.* **62**(3): 627–633.

Csikor, Z., Mihaltz, P., Hanifa, A., Kovacs, R. and Dahab, M. F. (2002). Identification of factors contributing to degradation in autothermal thermophilic sludge digestion, *Water Science and Technology* **46**(10): 131–8.

Cuthrell, J. E. and Biegler, L. T. (1989). Simultaneous optimization and solution methods for batch reactor control profiles, *Computers and Chemical Engineering* **13**: 49–62.

Deeny, K., Hahn, H., Leonard, D. and Heidman, J. (1991). Autoheated thermophilic aerobic digestion, *Water Environ. Technol.* **3**: 65–72.

Descoins, N., Stephane, D., Remi, L. and Marechal, F. (2010). Energetic efficiency in waste water treatments plants: Optimization of activated sludge process coupled with anaerobic digestion, *Proc. of the 23rd International Conference on Efficiency, Cost, Optimization, Simulation and Environmental Impact of Energy Systems*, Lausanne, pp. 1062–1069.

Dold, P. L., Ekama, G. A. and Marais, G. v. R. (1980). A general model for the activated sludge process, *Prog. Wat. Technol.* **12**: 42–77.

Edgar, T. F. and Himmelblau, D. M. (1988). *Optimisation of chemical processes*, McGraw-Hill, New York.

Egea, J. A., Balsa-Canto, E., Garcia, M. S. G. and Banga, J. R. (2009). Dynamic optimization of nonlinear processes with an enhanced scatter search method, *Industrial & Engineering Chemistry Research* **48**(9): 4388–4401.

Egea, J. A., Marti, R. and Banga, J. R. (2010). An evolutionary method for complex-process optimization, *Computers & Operations Research* **37**: 315–324.

Ehrenreich, A. (2011). Sporulating cell of *B. licheniformis*.[image online], *available:http://wwwuser.gwdg.de/~appmibio/research_ehrenreich.html* . [accessed 3 Aug 2011].

European Commission (2000). Working document on sludge - 3rd draft, *Technical report*, European Commission, Brussels. reference ENV.E.3/LM.

European Commission (2006). Action plan for energy efficiency: Realising the potential, *Technical Report COM(2006)545 final*, European Commission, Brussels.

Fikar, M., Chachuat, B. and Latifi, M. A. (2005). Optimal operation of alternating activated sludge processes, *Control Engineering Practice* **13**(7): 853–861.

Flores, A., Biegler, L. T. and Saldivar-Guerra, E. (2005). Dynamic optimization of hips open-loop unstable polymerization reactors, *Industrial & Engineering Chemistry Research* **44**(8): 2659–2674.

Focus on Energy (2006). Water and wastewater energy best practice guidebook, *Technical report*, Prepared for Wisconsin Department of Administration by the Focus on Energy Program, Madison, WI, US.

FUCHS (2011). Scheme of the fuchs spiral aerator.[image online], *available:http://fuchs-en.mindwerk.info/frames.php?ziel=%2Fstaticsite%2Fstaticsite.php%3Fmenuid%3D34%26topmenu%3D3* . [accessed 4 Aug 2011].

Furlonge, H. I., Pantelides, C. C. and Sorensen, E. (1999). Optimal operation of multivessel batch distillation columns, *American Institute of Chemical Engineers Journal* **45**(4): 781–800.

Garg, D., Patterson, M. A., Francolin, C., L., D. C., Huntington, G. T., W., H. W. and Rao, A. V. (2011). Direct trajectory optimization and costate estimation of finite-horizon and infinite-horizon optimal control problems using a radau pseudospectral method, *Computational Optimization and Applications* **49**: 335–358.

Gellings, C. W. (1996). Electrotechnology cleans up, *IEEE Spectrum* **34**: 46–50.

Gomez, J. (2007). *Digestion Aerobica Termofila Autosostenida (ATAD) de fangos. Estudio experimental a escala real y modelizacion matematica del reactor*, PhD thesis, Universidad de Navarra, San Sebastian, Spain.

Gomez, J., de Gracia, M., Ayesa, E. and Garcia-Heras, J. L. (2007). Mathematical modelling of autothermal thermophilic aerobic digesters, *Water Research* **41**(5): 959–968.

Gould, M. S. and Drnevich, R. F. (1978). Autothermal thermophilic aerobic digestion, *J. Envir. Engrg. Div.* **104**: 259–270.

Grau, P., Sutton, P. M., Henze, M., Elmaleh, S., Grady, C. P. L. J., Gujer, W. and Koller, J. (1982). Recommended notation for use in the description of biological wastewater treatment processes, *Water Research* **16**: 1501–1505.

Gyger, R. F., McWhirter, J. R. and Balan, P. (2007). Continuous multi-stage autothermal aerobic digestion process, *WEF/AWWA Joint Residuals and Biosolids Management Conference 2007*, Water Environment Federation.

Haardle, W. and Hlavka, Z. (2007). *Multivariate statistics: exercises and solutions*, Springer.

Heijungs, R. and Klejin, R. (2001). Numerical approaches towards life cycle interpretation: five examples, *The Internation Journal of Life Cycle Assessment* **6**: 141–148.

Henze, M., Gujer, W., Grady, C. P. L., Marais, W. and Matsuo, T. (1987). *Activated Sludge Model No. 1*, IAWPRC, London.

Henze, M., Gujer, W., Mino, T. and van Loosdrecht, M. (2000). *Activated Sludge Models ASM1, ASM2, ASM2d and ASM3. Scientific and Technical Report No. 9*, IWA Publishing, London.

Henze, M., Harremoes, P., (la Cour Jansen), J. and Arvin, E. (1990). *Wastewater treatment - Biological and chemical processes*, Springer.

Holenda, B., Domokos, E., Redey, A. and Fazakas, J. (2007). Aeration optimization of a wastewater treatment plant using genetic algorithm, *Optimal Control Applications and Methods* **28**: 191–208.

Holowko, P. (2011). *Bacillus stearothermiphilis.*[image online], *available:http://home.comcast.net/~pholowko/OnLineShows/Soil/MicroBio/BioBacteriaDescription.html* . [accessed 3 Aug 2011].

Hoover, S. R. and Porges, N. (1952). Assimilation of dairy wastes by activated sludge ii: The equations of synthesis and oxygen utilization, *Sewage and Industrial Wastes* .

Horan, N. J. (1990). *Biological wastewater treatment systems: theory and operation*, John Wiley & Sons Ltd.

ISMA (2011). photo2.jpg.[image online], *available:http://isma.pagesperso-orange.fr/en_sat-documentation.html* . [accessed 4 Aug 2011].

Jamniczky-Kaszas, D. (2010). *Energy efficiency improvement of wastewater treatment case study of an autothermal thermophilic aerobic digestion process*, PhD thesis, University of Limerick.

Jang, S. S. and Lin, P. H. (1991). Discontinuous minimum end-time temperature/ initiator policies for batch emulsion polymerization of vinyl acetate, *Chemical Engineering Science* **46**(12): 3153–3163.

Jewell, W. J. and Kabrick, R. M. (1978). Autoeated aerobic thermophilic digestion with air aeration, *51st Annual Water pollution Control Federation Conference*, Anaheim, California.

Jewell, W. J. and Kabrick, R. M. (1980). Autoheated aerobic thermophilic digestion with aeration, *Pollut. Control Fed.* **52**: 512–523.

Jones, M. (1991). Demand side management: Opportunities in water and sewage treatment, *IEEE Power Engineering Review* pp. 8–9.

Juteau, P. (2006). Review of the use of aerobic thermophilic bioprocesses for the treatment of swine waste, *Livestock Science* **102**(3): 187–196.

Kambhu, K. and Andrews, J. F. (1969). Aerobic thermophilic process for the biological treatment of wastes - simulation studies, *Journal - Water Pollution Control Federation* **41**: 127–143.

Kameswaran, S. and Biegler, L. T. (2008). Convergence rates for direct transcription of optimal control problems using collocation at radau points, *Comput. Optim. Appl.* **41**(1): 81–126.

Kelly, H. G. (1999). Comparing biosolids treatment of thermophiic digestion, thermal-chemical and heat drying technologies, *Proceedings of the 4th European Biosolids and Organic Residuals Conference*, Chartered Institution of Water and Environmental Management, Wakefield, UK, pp. 1–13.

Kelly, H. G. and Mavinic, D. S. (2003). Autothermal thermophilic aerobic digestion research, application and operational experience, *WEFTEC 2003 Workshop W104*, Los Angeles, CA.

Kelly, H. G. and Warren, R. (1997). Autothermal thermophilic aerobic digestion design, *Proceedings ASCE/CSCE Joint Environmental Engineering Conference*, Edmonton, Alberta, Canada.

Kovacs, R. (2007). *Az aerob termofil szennyviziszap-kezeles kinetikajanak leirasa*, PhD thesis, University of Budapest, Budapest, Hungary.

Kovacs, R., Csikor, Z., Hazi, F. and Mihaltz, P. (2007b). Application of activated sludge model no. 3 for the modeling of organic matter biodegradation at thermophilic temperatures, *Water Environment Research* **79**(5): 554–560.

Kovacs, R., Mihaltz, P. and Csikor, Z. (2007a). Kinetics of autothermal thermophilic aerobic digestion - application and extension of activated sludge model no. 1 at thermophilic temperatures, *Water Sci. Technol.* **56**(9): 137–145.

Lang, Y. D., Cervantes, A. and T., B. L. (1998). Dynamic optimization of a batch crystallization process, *Industrial & Engineering Chemistry Research* .

LaPara, T. M. and Alleman, J. E. (1999). Thermophilic aerobic biological wastewater treatment, *Water Research* **33**(4): 895–908.

Law, A. and Kelton, W. (1999). *Simulation modeling and analysis*, 3rd edn, McGraw-Hill - Boston.

Layden, N. M., Kelly, H. G., Mavinic, D. S., Moles, R. and Barlet, J. (2007a). Autothermal thermophilic aerobic digestion (atad) – part i: Review of origins, design, and process operation, *Journal of Environmental Engineering and Science* **6**(6): 665–678.

Layden, N. M., Kelly, H. G., Mavinic, D. S., Moles, R. and Barlet, J. (2007b). Autothermal thermophilic aerobic digestion (atad) – part ii: Review of research and full-scale operating experiences, *Journal of Environmental Engineering and Science* **6**(6): 679–690.

Le, S. M. (2006). Thermophilic biological pre-treatments for mads, *AquaEnviro Workshop: Advances in Technology for the Anaerobic Digestion of Municipal Sludge*, Manchester, UK.

Li, X. S., Ma, H. Z., Wang, Q. H., Matsumoto, S., Maeda, T. and Ogawa, H. I. (2009). Isolation, identification of sludge-lysing strain and its utilization in thermophilic aerobic digestion for waste activated sludge, *Bioresour. Technol* **100**: 24752481.

Liu, S., Song, F., Zhu, N., Yuan, H. and Cheng, J. (2010). Chemical and microbial changes during autothermal thermophilic aerobic digestion (atad) of sewage sludge, *Bioresource Technology* **101**: 94389444.

Loll, U. (1977). Treatment of thermally-conditioned sludge liquors, *Water Research* **11**: 869–872.

Matsch, L. C. and Drnevich, R. F. (1977). Autothermal aerobic digetion, *J. Water Pollut. Control Fed.* **49**: 296–310.

Mehta, U. B. (1995). Guide to credible computational fluid dynamics simulations, *26th AIAA Fluid Dynamics Conference*, number 95, San Diego, CA, p. 2225.

Messenger, J. R., de Villiers, H. A. and Ekama, G. A. (1990). Oxygen utilization as a control parameter for the aerobic stage in dual digestion, *Wat. Sci. Technol.* **22**(12): 217–227.

Metcalf & Eddy (2003). *Wastewater Engineering: Treatment and Reuse*, 4th edn, McGraw-Hill, New York.

M/J Industrial Solutions (2003). Municipal wastewater treatment plant energy baseline study, *Technical report*, Pacific Gas and Electric Company, San Francisco CA.

Moles, C. G., Gutierrez, G., Alonso, A. A. and Banga, J. R. (2003). Integrated process design and control via global optimization: a wastewater treatment plant case study, *Chem. Eng. Res. Des.* **81**: 507–517.

Mujtaba, M. and Macchietto, S. (1997). Efficient optimization of batch distillation with chemical reaction using polynomial curve fitting technique, *Industrial & Engineering Chemistry Research* **36**(6): 2287–2295.

Muller, R., Antrakian, G., Maloney, S. and Sharp, R. (1998). Thermophilic degradation of environmental pollutants, *Advances in Biochemical Engineering/Biotechnology* **61**: 155–169.

Olsson, G. and Newell, B. (1999). *Wastewater Treatment Systems: Modelling, Diagnosis and Control*, IWA Publishing, London, UK.

Petersen, E. E. (1965). *Chemical Reaction Analysis*, Prentice-Hall, Englewood Cliffs, NJ.

Piterina, A., Barlett, J. and Pembroke, T. (2011). Morphological characterisation of atad thermophilic sludge; sludge ecology and settleability, *Water Research* **45**(11): 3427–3438.

Piterina, A., MacCusland, C., Bartlett, J. and Pembroke, T. (2008). *Multidisciplinary Applied Microbiology: Understanding and Exploiting Microbes and Their Interactions. Biological, Physical, Chemical and Engineering Aspects*, Wiley-VCH, Weinheim, chapter Microbial Ecology of Authothermal Aerobic Digestion (ATAD): Diversity, Dynamics and Activity of Bacterial Communities Involved in Treatment of a Municipal Wastewater. (in press).

Ponti, C., Sonnleitner, B. and Fiechter, A. (1995a). Aerobic thermophilic treatment of sewage sludge at pilot plant scale. 1. operating conditions, *Journal of Biotechnology* **38**(2): 173–182.

Ponti, C., Sonnleitner, B. and Fiechter, A. (1995b). Aerobic thermophilic treatment of sewage sludge at pilot plant scale. 2. technical solutions and process design, *Journal of Biotechnology* **38**(2): 183–192.

Pontryagin, L. S. (1964). *Mathematische Theorie Optimaler Prozesse*, Oldenbourg Verlag, Wien.

Ray, W. H. (1981). *Advanced process control*, McGraw-Hill, New York.

Renfro, I. G., Morshedi, A. M. and Asbjornsen, O. A. (1987). Simultaneous optimization and solutions of systems described by differential-algebraic equations, *Computers and Chemical Engineering* **11**(5): 503–517.

Riascos, C. A. M. and Pinto, J. M. (2004). Optimal control of bioreactors: a simultaneous approach for complex systems, *Chemical Engineering Journal* **99**(1): 23–34.

Riley, D. W. and Forster, C. F. (2002). An evaluation of an autothermal aerobic digestion system, *Process Safety and Environmental Protection* **80**(B2): 100–104.

Roache, P. J. (1998). *Verification and validation in computational science and engineering*, Hermosa Publishers.

Saltelli, A., Tarantola, S., Campolongo, F. and Ratto, M. (2004). *Sensitivity analysis in practice: a guide to assessing scientific models*, Wiley & Sons.

Sargent, R. W. H. and Sullivan, G. R. (1979). Development of feed change-over policies for refinery distillation units, *Industrial & Engineering Chemistry Process Design and Development* **18**: 113–124.

Scisson, J. P. J. (2003). Atad, the next generation: Design, construction, start-up and operation of the first municipal 2nd generation atad, *Joint Residuals and Biosolids Managament Conference and Exhibition 2003*, Baltimore, MD.

Sonnleitner, B. and Fiechter, A. (1983). Bacterial diversity in thermophilic aerobic sewage sludge (ii) types of organisms and their capacities, *Appl. Microbiol. Biotechnol.* **18**: 174–180.

Sorensen, E., Macchietto, S., Stuart, G. and Skogestad, S. (1996). Optimal control and online operation of reactive batch distillation, *Computers and Chemical Engineering* **20**(12): 1491–1498.

Srinivasan, B., Myszkorowski, P. and Bonvin, D. (1995). A multicriteria approach to dynamic optimization, *American control conference*, Seattle, WA, pp. 1767–1771.

Staton, K. L., Alleman, J. E., Pressley, R. L. and Eloff, J. (2001). 2nd generation autothermal thermophilic aerobic digestion: Conceptual issues and process advancements, *WEF/AWWA/CWEA Joint Residuals and Biosolids Management Conference Biosolids 2001*, San Diego, CA.

Stensel, H. D. and Coleman, T. E. (2000). Assessment of innovative technologies for wastewater treatment: Autothermal aerobic digestion (atad), *Technical report*, International Water Association. Preliminary report, Project 96-CTS-1.

Strogatz, S. H. (2001). *Nonlinear Dynamics And Chaos: With Applications To Physics, Biology, Chemistry, And Engineering (Studies in Nonlinearity)*, Westview Press.

Takacs, I. and Patry, G. G. (2002). The dynamic solids residence time, *Proceedings of the 3rd International Water Association World Water Congress*, International Water Association: London, Melbourne, Australia.

Todar, K. (2011). Figure 5. sem of a thermophilic bacillus species isolated from a compost pile at 55 c.[image online], *available:http://www.textbookofbacteriology.net/nutgro_5.html* . [accessed 3 Aug 2011].

Toledo, R. T. (1994). *Fundamentals of Food Process Engineering*, 2nd edn, Chapman and Hall, New York.

Topiwala, H. and Sinclair, C. G. (1971). Temperature relationship in continuous culture, *Biotechnol. Bioeng.* **13**: 795–813.

Tsang, C. F. (1991). The modeling process and model validation, *Ground Water* pp. 825–831.

Ugwuanyi, J. O., Harvey, L. M. and McNeil, B. (2005). Effect of digestion temperature and ph on treatment efficiency and evolution of volatile fatty acids during thermophilic aerobic digestion of model high strength agricultural waste, *Bioresource Technology* **96**: 707–719.

Ugwuanyi, J. O., Harvey, L. M. and McNeil, B. (2008). Diversity of thermophilic populations during thermophilic aerobic digestion of potato peel slurry, *J. Appl. Microbiol.* **104**: 7990.

USEPA (1990). Environmental regulations and technology: Autothermal thermophilic aerobic digestion of municipal wastewater sludge, *Technical report*, United States Environmental Protection Agency, Office of Research and Development, Washington, D.C.

USEPA (1993). Standards for the use or disposal of sewage sludge, *Technical report*, United States Environmental Protection Agency, Washington, D.C.

Vismara, R. (1985). A model for autothermic aerobic digestion, *Wat. Res.* **19**: 441–447.

Vogelaar, J. C. T., Klapwijkm, A., Van-Lierm, J. B. and Rulkens, W. H. (2000). Temperature effects on the oxygen transfer rate between 20 and 55 °c, *Wat. Res.* **34**(3): 1037–1041.

Warakomski, A., McWhirter, J., Balan, P., Swope, B. and Gyger, R. (2007). Evolution of atad/dual digestion and recent process developments, *IWA Specialist Conference: Moving Forward Wastewater Biosolids Sustainability: Technical, Managerial, and Public Synergy*, Moncton, New Brunswick, Canada.

Yonkin, M., Clubine, K. and O'Connor, K. (2008). Importance of energy efficiency to the water and wastewater sector, *Clear Waters* **38**: 12–13.